

Department of Chemical Engineering
June 2001

**VISCOSITY STUDY OF HYDROCARBON
FLUIDS AT RESERVOIR CONDITIONS
MODELING AND MEASUREMENTS**

Claus K. Zéberg-Mikkelsen

Ph.D. Thesis, Technical University of Denmark

Preface

This thesis is submitted as partial fulfillment of the requirements for obtaining the Ph.D. degree in chemical engineering at the Technical University of Denmark, Lyngby, Denmark. The work presented in this thesis has been carried out from April 1998 to May 2001 in the research group Center for Phase Equilibria and Separation Processes (IVCSEP) at the Department of Chemical Engineering, Technical University of Denmark. The work has been supervised by Associate Professor Sergio E. Quiñones-Cisneros and Professor Erling H. Stenby and founded by the European Project EVIDENT. I would like to express my gratitude and thank my supervisors for their inspiration and fruitful discussions of topics related to the viscosity behavior of fluids and modeling, resulting in a very successful and productive collaboration, in particular to Associate Professor Sergio E. Quiñones-Cisneros for proposing of the friction theory for viscosity modeling, which was jointly developed. Further, I would also like to thank Dr. You-Xiang Zuo, who I worked together with in the beginning of the EVIDENT project.

Further, I am very grateful to Professor Christian Boned and Associate Professor Antoine Baylaucq, both at Groupe Haute Pression, Laboratoire des Fluides Complexes, Université de Pau, Pau, France, for giving me the opportunity of working in their group for 6 months in order to gain experience working with high pressure equipments by carrying out density and viscosity measurements. In addition, I would like to thank them together with Ph.D. student Xavier Canet for a very good collaboration and discussion of the experimental results. Further, I would also thank Groupe Haute Pression for a nice and pleasant time during my stay in France.

Claus K. Zéberg-Mikkelsen

Abstract

The viscosity is an important property in many engineering disciplines such as the design of transport equipments or the simulation of production profiles for petroleum reservoirs. Due to this, reliable and accurate viscosity models, which can be applied over wide ranges of temperature, pressure, and composition, are required. An evaluation of five currently used viscosity models applicable to hydrocarbon and petroleum fluids has been performed using a database containing 35 pure hydrocarbons, carbon dioxide, nitrogen, and 39 well-defined hydrocarbon mixtures, being very simple representations of petroleum and reservoir fluids. This evaluation showed that a more accurate and reliable viscosity model has to be developed in order to be able to predict the viscosity accurately over wide ranges of temperature, pressure, and composition.

Recently, starting from basic principle of mechanics and thermodynamics Quiñones-Cisneros et al. (2000) developed the friction theory (*f-theory*) for viscosity modeling. In the *f-theory*, the viscosity of dense fluids is approached as a mechanical property rather than a transport property. Thus by linking the Amontons-Coulomb friction law to the van der Waals attractive and repulsive pressure terms of a simple cubic EOS, such as the SRK or the PR EOS, highly accurate viscosity modeling has been obtained for n-alkanes over wide ranges of temperature and up to high pressure. The *f-theory* has been further developed into a general model based on a corresponding states behavior and with only one adjustable parameter – a characteristic critical viscosity. The general one-parameter *f-theory* models have been derived using a database containing smoothed tabulations of the viscosity versus temperature and pressure for n-alkanes, ranging from methane to n-octadecane. These smoothed viscosity data have been estimated by modeling experimental viscosities using the *f-theory*.

The general one-parameter *f-theory* model has been extended to the viscosity prediction and modeling of real reservoir fluids. In case of light reservoir oils the general one-parameter *f-theory* can predict the fluid viscosity with good accuracy. However, for reservoir oils in general, a more accurate modeling can be obtained by means of a simple tuning procedure. A tuned general *f-theory* model can deliver highly accurate viscosity modeling above the saturation pressure and good predictions of the

liquid phase viscosity at pressures below the saturation pressure. The tuning of the general *f-theory* models requires the solving of a simple linear equation. Thus, the simplicity and stability of the general *f-theory* models make them a powerful tool for applications such as reservoir simulations, between other. Further, the concepts of the *f-theory* have also been applied to the viscosity prediction of natural gases, mixtures composed of hydrogen and natural gas (hythane), and the accurate modeling of light gases at supercritical conditions, such as argon, hydrogen, nitrogen, and oxygen.

In addition, since experimental data are required in order to evaluate and test viscosity models, a comprehensive experimental study has been carried out for 21 ternary mixtures composed of 1-methylnaphthalene + n-tridecane + 2,2,4,4,6,8,8-heptamethylnonane in the temperature range 293.15 K to 353.15 K and up to 1000 bar. These ternary mixtures should represent some simple petroleum distillation cuts at 510 K. The viscosity measurements have been performed using a falling body viscometer, except at atmospheric pressure, where an Ubbelohde viscometer has been used. Since the working equations for these viscometers require the density of the studied fluids, density measurements have also been carried out at the same conditions as for the viscosity measurements. The measured viscosities of the ternary mixtures along with the already reported experimental values for the pure compounds and their binary mixtures of this ternary system have been used in order to evaluate the performance of different viscosity models, ranging from empirical expressions to models with a physical and theoretical background. These models have all been derived for hydrocarbon fluids. The best performance is obtained by the free-volume model and the friction theory, which have a physical and theoretical background. For these two viscosity approaches, the AAD is within or close to the experimental uncertainty (2%), whereas the LBC model, which is widely used in the oil industry, does not give very satisfactory viscosity predictions.

Abstract in Danish

Viskositeten af væsker og gasser er af stor betydning indenfor mange ingeniørmæssige discipliner, som f.eks. design af transportudstyr eller simulering af produktionsprofiler for oile- og gasreservoirier. Derfor er det nødvendigt at have pålidelige og akkurate viskositetsmodeller, der kan bruges både til væsker og gasser over store temperatur- og trykintervaller. En evaluering af fem eksisterende viskositetsmodeller, der ofte benyttes til beregning af viskositeten af kulbrinter og reservoirolier, viste, at det er nødvendigt at udvikle en mere nøjagtig og akkurat viskositetsmodel til beregning af viskositeten som funktion af temperaturen, trykket, og sammensætningen. Evalueringen er blevet foretaget på basis af viskositetsdata for 35 rene kulbrinter, kuldioxide, kvælstof og 39 veldefinerede kulbrinteblandninger.

Med udgangspunkt i klassisk mekanik og termodynamik udviklede og introducerede Quiñones-Cisneros et al. (2000) friktionsteorien (*f-teorien*) for viskositetsmodellering. I *f-teorien* betragtes viskositeten af en fluid som en mekanisk egenskab, i stedet for en transportegenskab. En meget præcis viskositetsmodellering af n-alkaner over store temperatur- og trykintervaller kan opnås med *f-teorien* ved at sammenkæde Amontons-Coulomb's friktionslov med van der Waal's attraktive og repulsive trykled, der kan fås fra en simpel kubisk tilstandsligning som f.eks. SRK eller PR tilstandsligningen. *f-teorien* er yderligere blevet videreudviklet til en generel model baseret på de korresponderende tilstandes principper og med en parameter – en karakteristisk kritisk viskositet. Modellen er blevet udviklet ved at bruge en database med anbefalede viskositetsværdier som funktion af temperaturen og trykket for n-alkaner, fra methane til n-octadecane. Disse anbefalede viskositeter er blevet estimeret ved at modellere eksperimentelle værdier ved hjælp af *f-teorien*.

Den generelle en-parameter *f-teori* model er blevet anvendt til viskositetsberegning og modellering af reservoirolier. For lette olier kan den generelle *f-teori* model beregne viskositeten med god nøjagtighed. Men for tunge olier kan en nøjagtig modellering opnås ved en meget simple tuningsprocedure. En tunet *f-teori* model kan give meget nøjagtige viskositetsberegninger over damptrykket, mens en god beregningsnøjagtighed opnås for væskefasen under damptrykket af olien. En tuning af *f-teori* modellen kræver kun, at en lineær ligning løses. SimPLICITETEN og stabiliteten af de

generelle *f-teori* modeller gør, at disse modeller kan blive et stærkt redskab indenfor f.eks. reservoirsimulering. Endvidere er konceptet i *f-teorien* blevet anvendt til viskositetsberegning af naturgas, blandinger af hydrogen og naturgas (hythane), samt til en meget nøjagtig viskositetsmodellering af gasser, som f.eks. argon, hydrogen, kvælstof og ilt, ved superkritiske temperaturer og op til høje tryk.

Endvidere, da eksperimentelle målinger er nødvendige for at udvikle og teste viskositetsmodeller, er et meget stort eksperimentelt studie af 21 ternære blandinger af 1-methylnaphthalene + n-tridecane + 2,2,4,4,6,8,8-heptamethylnonane blevet udført ved at måle viskositeten op til 1000 bar i temperaturintervallet 293.15 K – 353.15 K. Disse ternære blandinger skulle repræsentere nogle simple petroleumdestillationsfraktioner ved 510 K. Viskositetsmålingerne er blevet udført med et faldlegemeviskosimeter, undtagen ved 1 atm, hvor et Ubbelohde viskosimeter er blevet benyttet. Da arbejdsligningerne for de benyttede viskosimetre er funktioner af densiteten af den studerede blanding, er densitetsmålinger også blevet udført. De målte viskositeter for de ternære blandinger er sammen med de allerede målte viskositeter for de rene stoffer og de binære blandinger blevet brugt til at evaluere forskellige viskositetsmodeller. De evaluerede modeller spænder lige fra empiriske ligninger til modeller med en fysisk og teoretisk baggrund. De bedste resultater opnås med viskositetsmodellerne baseret på det fri volumen og *f-teorien*, der begge har en fysisk og teoretisk baggrund. For disse to modeller er den absolute gennemsnitlige afvigelse (AAD) tæt på den eksperimentelle usikkerhed (2%), hvorimod LBC modellen, der er en meget brugt viskositetsmodel indenfor olieindustrien, ikke giver særligt tilfredsstillende viskositetsberegninger.

Table of Contents

Introduction	1
Part I: Viscosity Modeling and Prediction	
I.1 Viscosity Definitions	5
I.1.1 Viscosity Behavior Versus Temperature, Pressure, and Composition	7
I.2 Viscosity Models	13
I.2.1 The Dilute Gas Viscosity.....	14
I.2.2 The Residual Viscosity Concept.....	17
I.2.2.1 The LBC model.....	17
I.2.2.2 The LABO Model	19
I.2.3 The Corresponding States Models	21
I.2.3.1 The Corresponding States Model with One Reference Fluid	22
I.2.3.2 The Corresponding States Model with Two Reference Fluids	26
I.2.4 Viscosity Models Based on Cubic EOS	28
I.2.5 Critical Viscosity.....	31
I.3 Density Models.....	32
I.3.1 Cubic EOS	33
I.3.1.1 The SRK and PR EOS	34
I.3.1.2 The Peneloux Correction	37
I.3.1.3 Density Estimation of the Reference Fluids in the CS2 Model	38
I.3.2 Non-cubic EOS	40
I.3.2.1 The Lee-Kesler Method.....	41
I.3.2.2 The SBWR EOS.....	43
I.3.3 Comparison of Different EOSs.....	47

I.4 Characterization of Petroleum Reservoir Fluids	51
I.5 Evaluation of Existing Viscosity Models.....	54
I.5.1 Evaluation Procedure	54
I.5.2 Results and Discussion.....	56
I.5.3 The Dilute Gas Viscosity.....	74
I.5.4 Conclusion	76
I.6 Modified CS2 Model	80
I.6.1 The Interpolation Parameter	80
I.6.2 The Reference Fluids	82
I.6.3 Results	84
I.7 The Friction Theory	89
I.7.1 Basic Ideas of the Friction Theory	90
I.7.1.1 Illustration of the Friction Theory	93
I.7.1.2 Modeling of Pure n-Alkanes.....	100
I.7.1.3 Application of the Friction Theory to Mixtures.....	101
I.7.2 Viscosity Prediction of Hydrocarbon Mixtures	102
I.7.3 Recommended Viscosities.....	107
I.7.3.1 Estimating Recommended Viscosities	108
I.7.3.2 Tabulations and Discussion	111
I.7.3.3 Overall Representation	113
I.7.4 General One-Parameter Friction Theory Models	116
I.7.4.1 General Concepts	118
I.7.4.2 The Critical Isotherm.....	119
I.7.4.3 The Residual Friction Functions	120
I.7.4.4 Application of the General One-Parameter Models to n-Alkane Mixtures	125
I.7.4.5 Modeling of Other Pure Fluids	127
I.7.5 Viscosity Modeling of Light Gases at Supercritical Conditions	127
I.7.5.1 Data Sources	129

I.7.5.2 The Dilute Gas Limit	129
I.7.5.3 Use of Cubic EOS in the Supercritical Region	131
I.7.5.4 Friction Theory Modeling of Light Gases	134
I.7.5.5 Concluding Remarks	141
I.7.6 Conclusion	141
I.8 Application of the Friction Theory to Industrial Processes	143
I.8.1 Viscosity Prediction of Carbon Dioxide + Hydrocarbon Mixtures	143
I.8.1.1 Data Sources for Carbon Dioxide + Hydrocarbon Mixtures	144
I.8.1.2 Results and Discussion	145
I.8.1.3 Concluding Remarks	151
I.8.2 Viscosity Prediction of Reservoir Oils	152
I.8.2.1 Calculation Procedure and Results	153
I.8.2.2 Tuning of the General <i>f-theory</i> Model	158
I.8.2.3 Concluding Remarks	161
I.8.3 Viscosity Prediction of Natural Gas	162
I.8.3.1 Calculation Procedure	163
I.8.3.2 Results and Discussion	164
I.8.3.3 Concluding Remarks	168
I.8.4 Viscosity Prediction of Hydrogen + Natural Gas Mixtures (Hythane)	170
I.8.4.1 Viscosity Prediction Procedure for Hythane	170
I.8.4.2 Results and Discussion	172
I.8.4.3 Concluding Remarks	176
I.9 Conclusion	177
I.10 List of Symbols	180
I.11 References	182

Part II: Viscosity Measurements and Modeling

II.1 Introduction	197
II.2 Experimental Techniques and Procedures	203
II.2.1 Falling Body Viscometer	203
II.2.2 Ubbelohde Viscometer.....	207
II.2.3 Densimeter.....	210
II.2.4 Characteristics of the Samples.....	214
II.3 Results of Viscosity and Density Measurements	216
II.4 Modeling of the Viscosity.....	223
II.4.1 Classical Mixing Laws.....	223
II.4.1.1 Modified Grunberg-Nissan Mixing Laws	225
II.4.1.2 The Excess Activation Energy of Viscous Flow	226
II.4.2 The Hard-Sphere Viscosity Scheme	228
II.4.3 The Free-Volume Viscosity Model	233
II.4.4 The Friction Theory	237
II.4.5 The LBC Model.....	242
II.4.6 The Self-Reference Model	244
II.4.7 Corresponding States Model	247
II.4.8 The PRVIS Model	248
II.4.9 Comparison of Models.....	249
II.5 Conclusion	255
II.6 List of Symbols	257
II.7 References.....	259

Part III: Concluding Remarks

III.1 Concluding Overview.....	269
III.1.1 Future Work	270

Introduction

Since petroleum and reservoir fluids, such as crude oils and natural gases, are of significant importance, accurate and reliable fluid properties are required. One of these properties is the viscosity, which is an important property required in many engineering disciplines ranging from the design of transport equipments, such as pipelines or compressors, to the simulation of production profiles of oil and gas reservoirs, enhance oil recovery, or the storage of natural gas. The reason is that flow models, such as the Navier-Stoke's model or Darcy's law, require the viscosity, since it is related to the mobility of the fluid. In spite of this importance, the general understanding of the viscosity along with the other transport properties (the thermal conductivity and the diffusion coefficient) is inferior to that of thermodynamic and equilibrium properties, because transport properties are non-equilibrium properties.

The viscosity of a fluid can be obtained in two ways, either by carrying out experimental measurements or estimated by a proper model. However, it is impossible to measure the viscosity of all fluids at all temperatures, pressures, and compositions, because it is very expensive and time consuming to carry out viscosity measurements. This has led to the requirement of accurate and reliable models.

In case of petroleum and reservoir fluids, which are multicomponent fluids mainly consisting of hydrocarbons, compositional and phase changes can undergo in the reservoir or through the transportation system and in the process equipments in the refinery. Therefore, the petroleum and oil industry requires reliable and accurate viscosity models, applicable to both liquids and gases over wide ranges of temperature, pressure, and composition. Although that a tremendous number of viscosity models have been derived for the viscosity prediction of hydrocarbon fluids, these models are mainly only suitable at low to moderate pressures, up to a few hundred bar, corresponding to normal reservoir conditions. However, new offshore reservoirs are located at higher depths, where the pressure and the temperature are significantly higher than at normal reservoir conditions (150 – 250 bar). In these deep-water reservoirs the temperature can reach 500 K and the pressure can be higher than 1000 bar, see Ungerer et al. (1995). Because of this, a demand for a new and accurate viscosity model applicable to high pressure and able to describe compositional changes over wide ranges

of temperature has risen. This has been the subject of the European project *Extended Viscosity and Density Technology* (EVIDENT), which this ph.d. project has been a part of. The objective of the EVIDENT project has been to develop predictive models for the viscosity of reservoir fluids at high pressure and high temperature (HP/HT) conditions.

Thus, since reservoir fluids are not suitable in order to derive compositional dependent viscosity models, experimental viscosity measurements of well-defined mixtures, being simple representations of petroleum and reservoir fluids, are required covering wide ranges of temperature and pressure. In spite that these systems are only simple representations of real reservoir fluids, they can be used to evaluate the performance of viscosity models for the potential extension to real reservoir fluids and the application within the oil industry. However, it should be stressed that most of the reported viscosity measurements in the literature are for pure compounds and binary mixtures versus temperature, whereas measurements versus pressure are less frequent. Thus, viscosity studies of binary mixtures have been carried out versus pressure, but for multicomponent mixtures being simple representations of reservoir and petroleum fluids particularly no systematic study of the viscosity versus pressure has been carried out.

In general, the viscosity is a very important fluid property within the oil as well as other industries, but less frequently studied compared to thermodynamics properties. Because of this, the main object and aim of this project has been to study the viscosity of hydrocarbon fluids versus temperature, pressure, and composition in order to develop a new and accurate viscosity model applicable to high-pressure reservoir fluids. In addition, since there is a lack of experimental studies of the viscosity of well-defined mixtures versus temperature, pressure, and composition, a comprehensive experimental study of the viscosity and density on ternary mixtures composed of 1-methylnaphthalene + n-tridecane + 2,2,4,4,6,8,8-heptamethylnonane up to 1000 bar and in the temperature range 293.15 K – 353.15 K has been carried out. These ternary mixtures should represent some simple petroleum distillation cuts at 510 K. Since the techniques used in order to measure the viscosity require the knowledge of the density of the fluid, density measurements have also been carried out at the same conditions as the viscosity measurements. This thesis has been divided into a modeling part (Part I) and an experimental part (Part II). These parts can be read independently of each other.

PART I

VISCOSITY MODELING AND PREDICTION

I.1 Viscosity Definitions

In this chapter, some general viscosity definitions and concepts are reviewed. The viscosity of a fluid is related to the internal resistance or friction and is therefore related to the mobility of the fluid. The most common way to introduce the fluid property *viscosity* is by considering a fluid placed between two large parallel plates of area A with a distance h between them, see Figure I.1. At a given time $t = 0$ a force F is applied to the upper plate, and a shear stress $\tau = F/A$ is exerted on the fluid. The upper plate will start moving until it reaches a steady state velocity U . The fluid in direct contact with the upper plate will have the velocity U , whereas the velocity of the fluid in immediate contact with the lower plate will be zero. If the distance h is very small, experiments show that the velocity distribution from the lower to the upper plate will increase linearly from zero to U , as illustrated in Figure I.1. The velocity at a given distance y from the lower plate is given by $u(y) = Uy/h$. Thus, for many fluids the force F required in order to maintain the motion of the upper plate is proportional to the area A and the velocity U and inversely proportional to the thickness h , resulting in the following expression

$$\tau = \frac{F}{A} = \eta \frac{U}{h} \quad (\text{I.1.1})$$

where η is the dynamic viscosity. Further, it is assumed that the flow of the fluid is laminar and free of turbulence. In a more explicit way Eq.(I.1.1) can be expressed as

$$\tau = \eta \frac{du}{dy} \quad (\text{I.1.2})$$

which is Newton's law of viscosity and where du/dy is the local velocity gradient orthogonal to the direction of flow or the shear rate $\dot{\gamma}$. Fluids, which obey Newton's

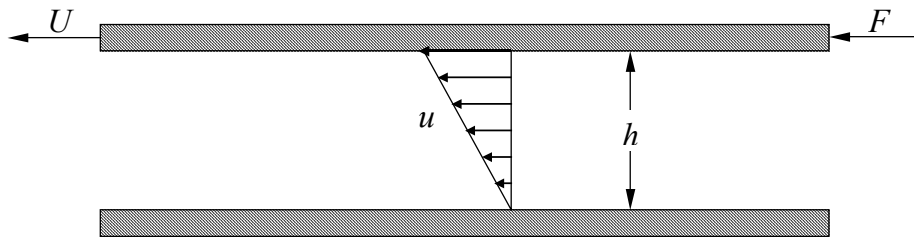


Figure I.1 A fluid between two plates under shear stress. F is the force acting on the upper plate, U the speed at which the upper plate moves, h the thickness between the plates, and u the velocity of the fluid.

law, are called Newtonian fluids. To these fluids belong all gases and many simple liquids such as water and hydrocarbons. The viscosity of these fluids is independent of the shear stress and the velocity gradient (shear rate), but depends on conditions of state (pressure P , volume v , and temperature T). However, some fluids called non-Newtonian do not obey Newton's law, and the viscosity depends on the shear stress and the shear rate. Non-Newtonian fluids may be classified as Bingham plastic, dilatant, and pseudo-plastic fluids. Bingham plastic fluids such as drilling mud and tooth pasta require a punch in order to move, because the shear stress needs to exceed a certain minimum value. Pseudo-plastic fluids such as polymer melts, gelatine, and mayonnaise become less viscous with increasing shear rate and shear stress. The reason is that long molecules become better oriented at high shear rates, resulting in a reduction of the viscosity (higher mobility). For dilatant fluids the opposite happens – the fluid becomes more viscous with increasing shear rate. Slurries and suspensions with a high concentration of particles belong to the dilatant fluids. For dilatant fluids, at low shear rates the liquid will have a lubricating effect between the particles, but at high shear rates this effect is reduced and the internal friction between the particles is increased. The behavior of the shear stress as a function of the shear rate (velocity gradient) is shown in Figure I.2 for both Newtonian and non-Newtonian fluids. However, in spite

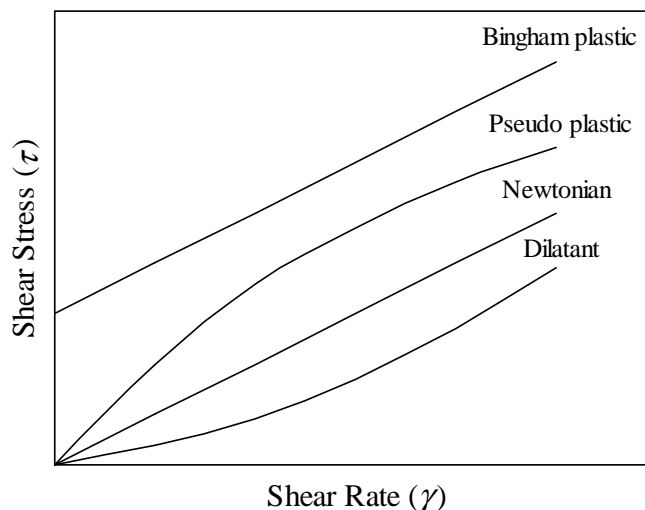


Figure I.2 Shear stress versus shear rate (velocity gradient) for Newtonian and non-Newtonian fluids.

non-Newtonian fluids are also of great interest for many industrial applications, they will not be discussed further, since the fluids considered in this work are assumed to behave as ideal Newtonian fluids. Further, the dynamic viscosity η will in the rest of the text be referred to as the viscosity. It has the scientific unit [Pa s] but the engineering unit [P] (Poise) is also used commonly; e.g. 1 mPa s \cong 1 cP. In addition, the kinematic viscosity ν with the unit [St] (Stoke) is defined as $\nu = \eta/\rho$ where ρ is the density.

I.1.1 Viscosity Behavior Versus Temperature, Pressure, and Composition

The viscosity of a fluid changes with temperature, pressure and composition. In the gaseous state the viscosity is much lower than in the liquid state. The reason is that the distance between the molecules in the gas phase is greater than in the liquid phase. In the liquid phase, the transfer of momentum is mainly due to intermolecular effects between the dense packed molecules, whereas in the gaseous phase the momentum is transferred by collisions of the freely moving molecules.

Figure I.3 shows a qualitative representation of the viscosity behavior of pure fluids as a function of the reduced pressure for various isotherms. At the saturation pressure, a jump in the viscosity is observed for reduced temperatures below 1.0, when going from the vapor phase to the liquid phase. Further, when the pressure approaches zero for a given temperature, the viscosity approaches the dilute gas limit. In general, the viscosity of a fluid in the gaseous phase increases with increasing temperature, whereas the viscosity of liquids decreases with increasing temperature. In all cases, the viscosity increases with increasing pressure. However, for dense supercritical fluids at a constant reduced pressure above 1.0, the viscosity decreases with increasing temperature down to a minimum and then increases with the temperature, see Figure I.3. As the pressure is increased this minimum is shifted towards higher temperatures. At very high temperatures, the viscosity of dense supercritical fluids will only be slightly higher than the value at the dilute gas limit. Further, when the critical point is approached the derivative of the viscosity with respect to the pressure diverges. In addition, it should be mentioned that in the vicinity of the critical point an abnormal viscosity behavior is observed, when the viscosity is plotted against the density for different isotherms very close to the critical temperature. This is illustrated in Figure I.4

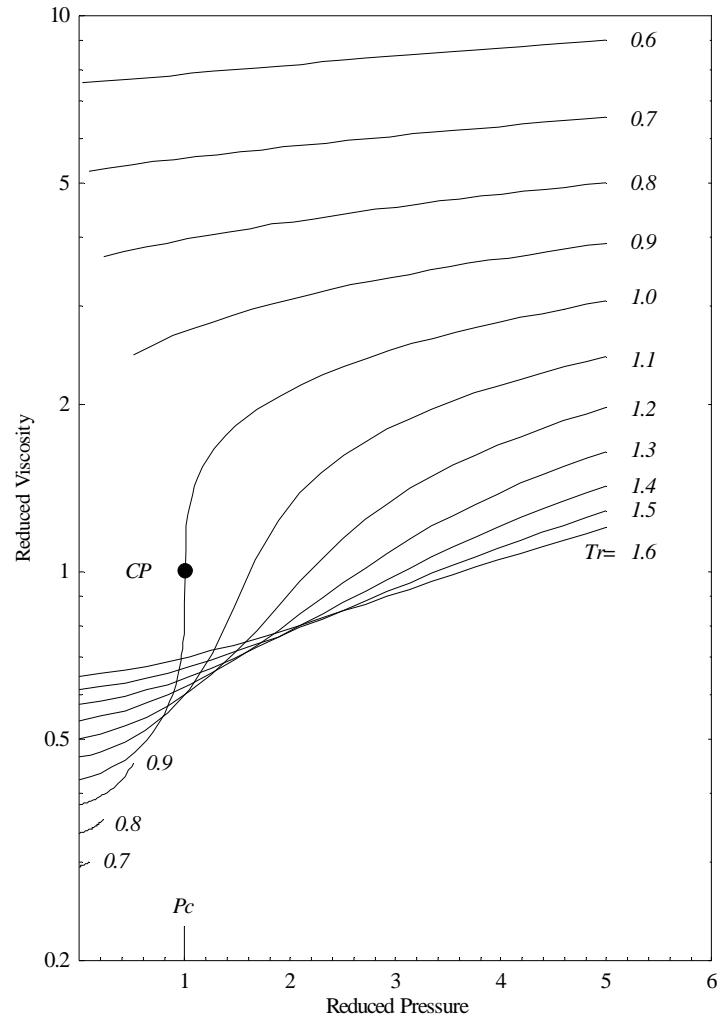


Figure I.3 General illustration of the reduced viscosity $\eta_r = \eta/\eta_c$ versus reduced pressure $P_r = P/P_c$ for various reduced temperatures $T_r = T/T_c$. CP is the critical point.

for ethane (Iwasaki and Takahashi 1981) and the similar behavior has been found and observed for nitrous oxide (Yokoyama et al. 1994), carbon dioxide (Iwasaki and Takahashi 1981), nitrogen (Zozulya and Blagoi 1975), and xenon (Strumpf et al. 1974). The abnormal viscosity behavior disappears with increasing temperature and it is only important very close to the critical isotherm. Thus, it should be mentioned that for the thermal conductivity, this abnormal critical behavior is much more pronounced than for the viscosity.

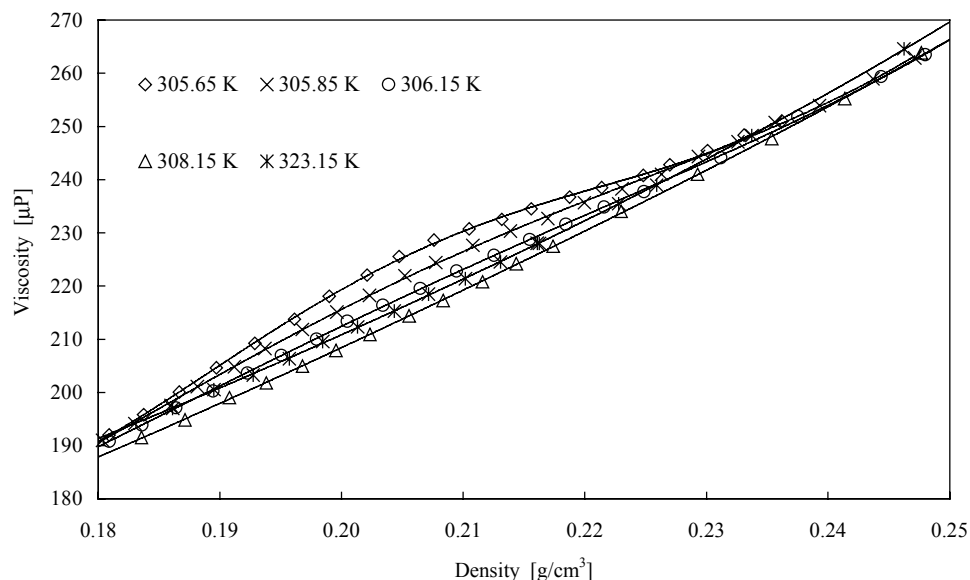


Figure I.4 Viscosity behavior of ethane in the vicinity of the critical point for different isotherms very close to the critical isotherm $T_c = 305.43$ K. Points represent experimental data taken from Iwasaki and Takahashi (1981).

For mixtures the viscosity behavior versus temperature, pressure, and composition is more complex than for pure fluids. Generally, the viscosity of mixtures does not vary linearly with composition at constant temperature and pressure. For gaseous mixtures composed of very dissimilar molecules, such as hydrogen and hydrocarbons, a maximum is observed at low pressures, when the viscosity is plotted as a function of the composition at constant temperature. This is illustrated in Figure I.5a, where the dilute gas viscosity of the binary mixture composed of hydrogen and methane is shown as a function of the composition. Generally, the maximum disappears with increasing temperature and pressure. However for gaseous mixtures composed of very similar compounds, such as hydrocarbons, a monotonical viscosity behavior is observed versus the composition, as illustrated in Figure I.5b. In this figure, the dilute gas viscosity is shown for the binary mixture composed of methane and n-butane.

Non-monotonical viscosity behaviors may also be observed for liquid mixtures, when the viscosity is plotted versus the composition at constant temperature and pressure. This is the case for liquid mixtures composed of polar and associating fluids. For such mixtures a maximum is observed, as shown in Figure I.6 for the binary

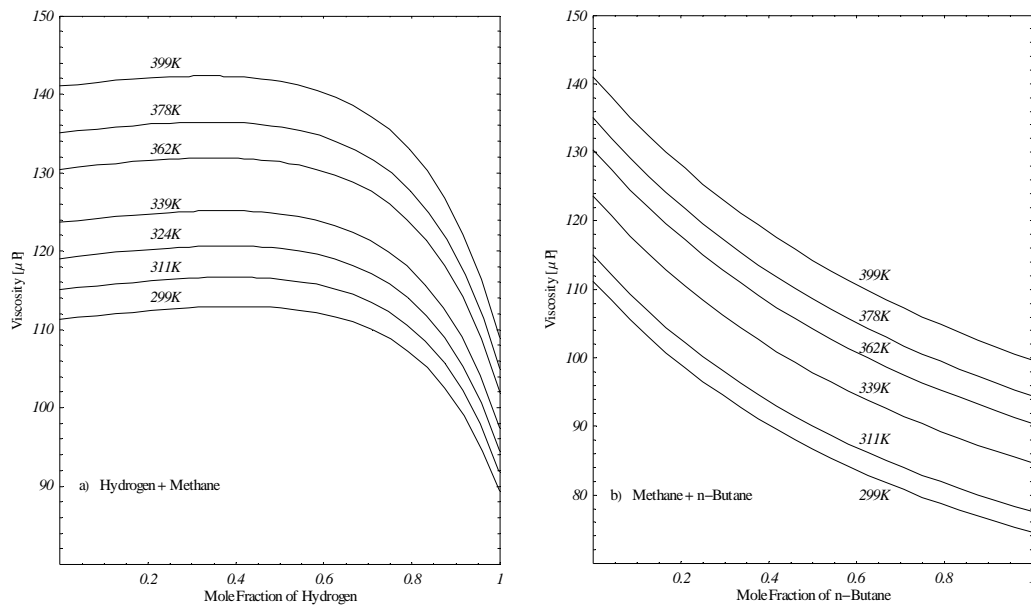


Figure I.5 Illustration of the dilute gas viscosity behavior for two binary mixtures versus composition for various temperatures. a) hydrogen + methane, and b) methane + n-butane.

mixture water + 2-propanol. The reason for this non-monotonical behavior is due to the intermolecular and associating effects between polar and associating molecules. The maximum decreases with increasing temperature, but the maximum can still be observed at high pressure, see Figure I.6b. Also for non-polar liquid mixtures it is possible to observe non-monotonical viscosity behaviors versus composition, but it is not very common. Generally, this non-monotonical viscosity behavior versus composition is observed as a minimum at 1 bar and may be the effect of repulsive interactions or structural effects. This is shown in Figure I.7 for the non-polar binary system 1-methylnaphthalene + 2,2,4,4,6,8,8-heptamethylnonane (Canet et al. 2001). A similar behavior has been observed by Zhang and Liu (1991) for the binary system benzene + cyclohexane and by Zéberg-Mikkelsen et al. (2001) for the ternary system 1-methylnaphthalene + n-tridecane + 2,2,4,4,6,8,8-heptamethylnonane. However, for non-polar mixtures the minimum disappears with increasing temperature and pressure, see e.g. Figures I.7a and I.7b.

Figure I.8 shows the viscosity behavior of a reservoir oil with compositional changes as a function of the pressure at constant temperature. In principle, Figure I.8

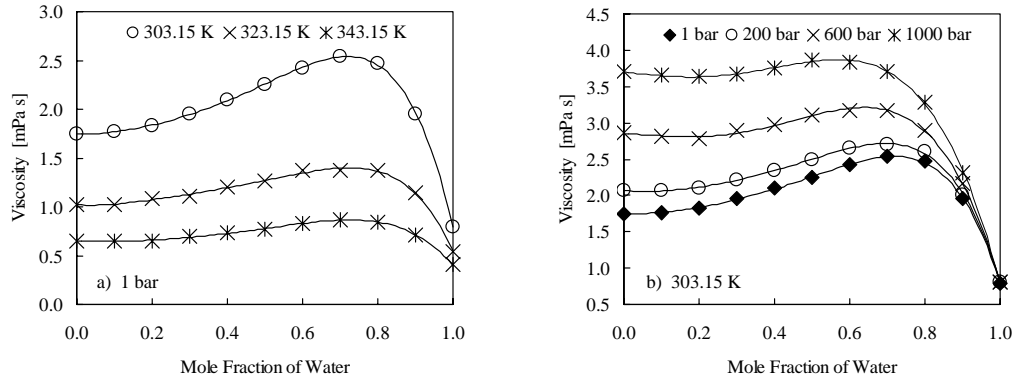


Figure I.6 Viscosity versus composition for the binary mixture water + 2-propanol (Moha-Ouchane et al. 1998) at a) 1 bar and b) 303.15 K.

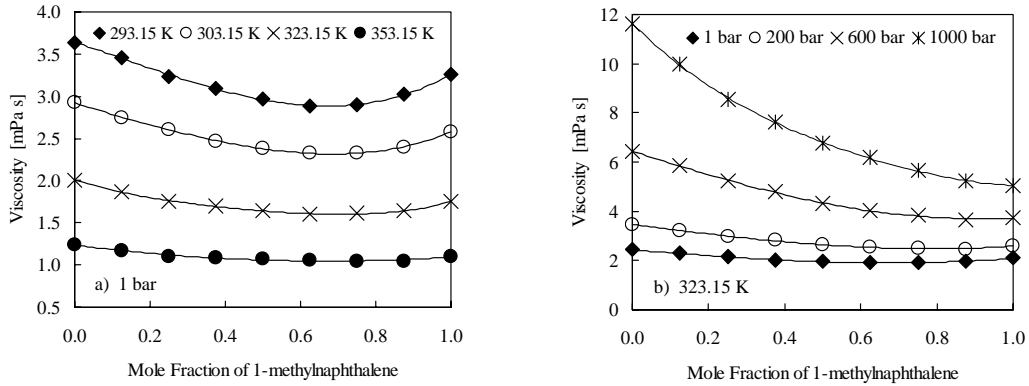


Figure I.7 Viscosity versus composition for the binary system 1-methylnaphthalene + 2,2,4,4,6,8,8-heptamethylnonane (Canet et al. 2001) at a) 1 bar and b) 323.15 K.

illustrates what will happen with the viscosity of the oil when the pressure in the reservoir decreases due to the depletion of the oil reservoir. Generally, the temperature of the reservoir is approximately constant during the depletion. The production of the oil reservoir is started at the initial reservoir pressure P^{res} , and as the pressure is reduced the viscosity decreases until the saturation pressure is reached. In case the pressure in the oil reservoir drops below the saturation pressure, the viscosity of the oil (liquid phase) is increased (lower mobility), resulting in a lower production. The reason is that the oil separates into a liquid phase and a gaseous phase below the saturation pressure. This phase split will result in changes in the composition of both the gas and the liquid as the pressure is further reduced, because the volatile or light hydrocarbons go into the gaseous phase, whereas the heavy hydrocarbons are left behind in the liquid phase,

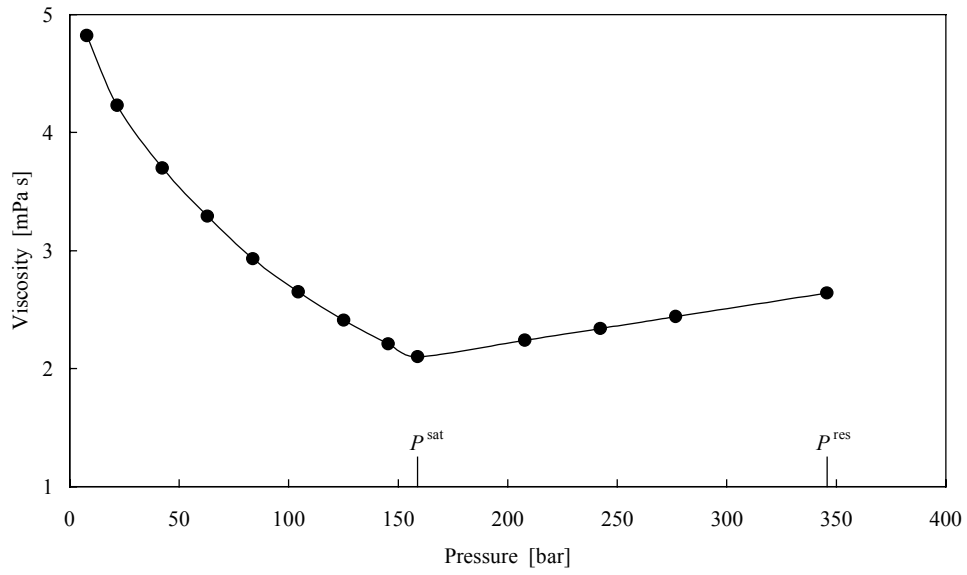


Figure I.8 Viscosity of an oil as a function of pressure at 344.15 K. P^{sat} is the saturation pressure and P^{res} the initial reservoir pressure. (•) experimental data (Pedersen et al. 1989).

leading to an increase in the viscosity of the liquid as the pressure is reduced, see Figure I.8. Therefore, it is important to keep the pressure in the reservoir above the saturation pressure of the oil. Even if the oil is produced from the reservoir as a single phase, the oil will undergo compositional changes during the pressure and temperature reductions occurring through the required transport and separation equipments from the wellhead to the refinery.

I.2 Viscosity Models

Viscosity models are important tools in order to describe the viscosity of a fluid as a function of temperature, pressure, and composition. The literature contains many different viscosity models and every year new models or modifications of existing models are derived and proposed. A critical review of existing viscosity models suitable for practical engineering applications can be found in Monnery et al. (1995), Mehrotra et al. (1996), and Reid et al. (1987). The available viscosity models range from highly theoretical models to simple empirical correlations. Many of these models are only suitable for predicting either the liquid or the gas phase viscosity. The kinetic theory of gases and the Chapman-Enskog theory have formed the basis of achieving accurate semi-theoretical models for predicting the viscosity of gases at low pressure. Thus, for dense fluids the complexity of the intermolecular forces resulting from short range forces, such as repulsion and hydrogen bonding, wide range electrostatic effects, and long range attractive forces makes a semi-theoretical description based on concepts of statistical mechanics extremely difficult. According to Monnery et al. (1995) the only methods, which can be applied to both liquids and gases, are semi-theoretical methods based on either the corresponding states principle, the hard-sphere theory, the modified Chapman-Enskog theory, or the empirical residual concept. Viscosity models based on cubic equations of state (EOS), see e.g. Guo et al. (1997) have also been introduced. These models are also suitable for estimating the viscosity of gases and liquids.

Most of the viscosity models presented in the literature have been derived for hydrocarbon fluids due to their importance in the petroleum industry. The viscosity models and methods considered and discussed in this work are those currently used by the petroleum industry and applicable to both the gaseous and liquid phases. Thus, the models should also be applicable to wide ranges of temperature T , pressure P , and composition x . The reason is that production processes related to the petroleum industry are carried out at different T,P conditions for fluids having different compositions. Further, it would be preferred to evaluate the performance of existing viscosity models related to petroleum engineering, since a fragmental part of the EVIDENT project is related to the development of a new viscosity model suitable for hydrocarbon and reservoir fluids. Currently, the models used in petroleum engineering are based on

either the corresponding states principle or the empirical residual concept such as the well-known Lohrenz-Bray-Clark (LBC) model (Lohrenz et al. 1964). These models have been implemented into reservoir simulators. Thus, viscosity models based on cubic EOS are currently been implemented in reservoir simulators. Based on the above-mentioned remarks, the viscosity models considered in this work are based on the empirical residual concepts of Lohrenz et al. (1964), the corresponding states principle with one reference fluid (Pedersen and Fredenslund 1987) and with two reference fluids (Aasberg-Petersen et al. 1991), and the viscosity model based on a cubic EOS (Guo et al. 1997). In addition, the estimation of the dilute gas viscosity is also discussed.

I.2.1 The Dilute Gas Viscosity

The dilute gas viscosity is defined as the viscosity at the zero density limit and is related to the kinetic theory of gases and the Chapman-Enskog theory. These theories have been described in details by e.g. Hirschfelder et al. (1967) and Chapman et al. (1970). Thus, it should be stressed that the dilute gas viscosity contribution to the total viscosity of a fluid will only be important, when predicting the viscosity of vapors or dense fluids at high temperatures, see Figure I.3.

By considering a low-density gas consisting of rigid, non-interacting spherical molecules with a diameter d and a mass m , the simplest viscosity model based on the kinetic gas theory can be derived, see e.g. Hirschfelder et al. (1964) or Bird et al. (1960)

$$\eta_0 = \frac{2}{3\pi^{3/2}} \frac{\sqrt{m k_B T}}{d^2} \quad (\text{I.2.1})$$

using the additional assumptions that the motion of the molecules is randomly directed with a mean velocity $\bar{u} = (8 k_B T / (\pi m))^{1/2}$, obtained from kinetic theory, and that the collisions between molecules occur after they have moved a distance defined as the mean free path. Here, k_B is Boltzmann's constant and T the temperature.

Independently of each other Chapman and Enskog extended the simple kinetic gas theory for transport properties by considering the potential energy of interaction between pairs of molecules, which is related to the attractive and repulsive interaction forces. The Chapman-Enskog expression for the dilute gas viscosity of monatomic molecules is given by

$$\eta_0 = \frac{5}{16\pi^{1/2}} \frac{\sqrt{m k_B T}}{\sigma^2 \Omega^*} \quad (\text{I.2.2})$$

where σ is a characteristic collision diameter defined as the distance where the energy potential between two molecules is zero. The reduced collision integral Ω^* is related to a potential energy function. A fairly good empirical potential energy function is the Lennard-Jones (12-6) potential, which Neufeld et al. (1972) used to derive an empirical expression for the reduced collision integral. Based on the Chapman-Enskog theory and the empirical expression for the reduced collision integral (Neufeld et al. 1972), Chung et al. (1984, 1988) derived an empirical dilute gas viscosity model incorporating structural effects in order to apply the model to polyatomic, polar, and hydrogen bonding fluids over wide ranges of temperature. This model is applicable of predicting the dilute gas viscosity of several polar and non-polar fluids within an uncertainty of 1.5%. The model is given by

$$\eta_0 = 40.785 \frac{\sqrt{M_w T}}{v_c^{2/3} \Omega^*} F_c \quad (\text{I.2.3})$$

where the reduced collision integral Ω^* corresponds to

$$\begin{aligned} \Omega^* = & \frac{1.16145}{T^*} + \frac{0.52487}{\exp(0.77320 T^*)} + \frac{2.16178}{\exp(2.43787 T^*)} \\ & - 6.435 \cdot 10^{-4} T^{*0.14874} \sin\left(18.0323 T^{*-0.76830} - 7.27371\right) \end{aligned} \quad (\text{I.2.4})$$

with

$$T^* = \frac{1.2593 T}{T_c} \quad (\text{I.2.5})$$

The dilute gas viscosity obtained by Eq.(I.2.3) has units of microPoise [μP], when the temperature T is in [K] and the critical volume v_c in [cm^3/mole]. M_w is the molecular weight and T_c the critical temperature. The best performance of this model is obtained when the real critical volume of the fluid v_c is used. The empirical expression for the F_c factor is defined as

$$F_c = 1 - 0.2756 \omega + 0.059035 \mu_r^4 + \chi \quad (\text{I.2.6})$$

where ω is the acentric factor, μ_r a dimensionless dipole moment, and χ a correction factor for the hydrogen bonding effects in associating substances, such as alcohols. However, since the fluids considered in this work are non-polar hydrocarbons Eq.(I.2.6) reduces to

$$F_c = 1 - 0.2756 \omega \quad (\text{I.2.7})$$

Curtiss and Hirschfelder (1949) extended the Chapman-Enskog theory to multi component gas mixtures at low densities. Thus, the final expressions are quite complex and rarely used to calculate the viscosity of mixtures. However, simple and adequate models exist for estimating the dilute gas viscosity of multicomponent mixtures. Wilke (1950) derived the following mixing rule based on the kinetic gas theory with several simplifications in order to estimate the dilute gas viscosity of a mixture

$$\eta_{0,mix} = \frac{\sum_{i=1}^n x_i \eta_{0,i}}{\sum_{j=1}^n x_j \phi_{ij}} \quad (\text{I.2.8})$$

with

$$\phi_{i,j} = \frac{\left[1 + \left(\frac{\eta_{0,i}}{\eta_{0,j}} \right)^{0.5} \left(\frac{M_{w,j}}{M_{w,i}} \right)^{0.25} \right]^2}{\frac{4}{\sqrt{2}} \left(1 + \frac{M_{w,i}}{M_{w,j}} \right)^{0.5}} \quad (\text{I.2.9})$$

This mixing rule is totally predictive in the sense that it only requires the molecular weight, the dilute gas viscosity, and the mole fraction of the pure compounds. Further, it should be mentioned that the Wilke mixing rule is capable of describing the right viscosity behavior of gas mixtures showing a nonlinear and non-monotonical behavior or attaining a maximum, see Figure I.5, when the viscosity is plotted versus the composition at constant temperature. This kind of viscosity behavior is common for gas mixtures composed of compounds with large differences in size and shape, such as mixtures composed of hydrogen and hydrocarbons, see Nabizadeh and Mayinger (1999), or a polar and a non-polar compound.

Another, simple mixing rule is the calculation procedure proposed by Herning and Zipperer (1936)

$$\eta_{0,mix} = \frac{\sum_{i=1}^n x_i \eta_{0,i} \sqrt{M_{w,i}}}{\sum_{i=1}^n x_i \sqrt{M_{w,i}}} \quad (I.2.10)$$

which has been found suitable for estimating the dilute gas viscosity of hydrocarbon mixtures.

I.2.2 The Residual Viscosity Concept

By subtracting the dilute gas viscosity η_0 from the total viscosity of a fluid η the residual viscosity term η_{res} is obtained

$$\eta_{res} = \eta - \eta_0 \quad (I.2.11)$$

The residual viscosity is defined as the viscosity in excess of the dilute gas viscosity. This concept is common both for empirical models and models considered to have a theoretical background. Normally, the dilute gas viscosity contribution first becomes important, when the zero density limit is approached, unless the studied fluid is a supercritical fluid at a relative high reduced temperature.

I.2.2.1 The LBC model

Within the petroleum industry a widely used empirical viscosity correlation based on the residual viscosity concept is the correlation of Jossi et al. (1962), because it can be applied to both gases and liquids. This correlation is used in many compositional reservoir simulators and is generally referred to as the Lohrenz-Bray-Clark (LBC) model (Lohrenz et al. 1964) due to the fact that Lohrenz et al. (1964) introduced a procedure for calculating the viscosity of hydrocarbon mixtures and reservoir fluids using the same equation derived by Jossi et al. (1962) for pure fluids. This equation is a sixteenth degree polynomial in the reduced density and is shown below

$$\left[(\eta - \eta_0) \zeta + 10^{-4} \right]^{1/4} = d_0 + d_1 \rho_r + d_2 \rho_r^2 + d_3 \rho_r^3 + d_4 \rho_r^4 \quad (I.2.12)$$

where η_0 is the dilute gas viscosity, ζ the viscosity reducing parameter, and ρ_r the reduced density of the fluid defined as

$$\rho_r = \frac{\rho}{\rho_c} \quad (I.2.13)$$

where ρ_c is the critical density of the fluid. The d_i coefficients in Eq.(I.2.12) are

$$\begin{aligned} d_0 &= 0.1023 & d_3 &= -0.040758 \\ d_1 &= 0.023364 & d_4 &= 0.0093324 \\ d_2 &= 0.058533 \end{aligned}$$

These coefficients were adjusted by Jossi et al. (1962) by applying Eq.(I.2.12) to the following 11 pure compounds: argon, nitrogen, oxygen, carbon dioxide, sulfur dioxide, methane, ethane, propane, i-butane, n-butane, and n-pentane, for reduced densities between 0.02 and 3.0.

In order to apply the method of Jossi et al. (1962) to mixtures, Lohrenz et al. (1964) introduced the following mixing rules in order to estimate the dilute gas viscosity and the viscosity reducing parameter of the mixture

$$\zeta = \frac{\left(\sum_{i=1}^n x_i T_{c,i} \right)^{1/6}}{\left(\sum_{i=1}^n x_i M_{w,i} \right)^{1/2} \left(\sum_{i=1}^n x_i P_{c,i} \right)^{2/3}} \quad (\text{I.2.14})$$

$$\eta_0 = \frac{\sum_{i=1}^n x_i \eta_{0,i} \sqrt{M_{w,i}}}{\sum_{i=1}^n x_i \sqrt{M_{w,i}}} \quad (\text{I.2.15})$$

where $T_{c,i}$ is the critical temperature, $P_{c,i}$ the critical pressure, $M_{w,i}$ the molecular weight, and x_i the mole fraction of component i in the mixture. The mixing rule for the dilute gas viscosity is the mixing rule proposed by Herning and Zipperer (1936), see Eq.(I.2.10). The dilute gas viscosity of the pure components is obtained with the following expressions proposed by Stiel and Thodos (1961) and adapted by Jossi et al. (1962)

$$\eta_{0,i} \zeta_i = 34.0 \cdot 10^{-5} T_{r,i}^{0.94} \quad \text{for } T_{r,i} \leq 1.5 \quad (\text{I.2.16})$$

$$\eta_{0,i} \zeta_i = 17.78 \cdot 10^{-5} (4.58 T_{r,i} - 1.67)^{5/8} \quad \text{for } T_{r,i} > 1.5 \quad (\text{I.2.17})$$

$$\zeta_i = \frac{T_{c,i}^{1/6}}{M_{w,i}^{1/2} P_{c,i}^{2/3}} \quad (\text{I.2.18})$$

where $T_{r,i}$ is the reduced temperature, and ζ_i is the viscosity reducing parameter of component i . The calculated viscosity will have the unit [cP], if the pressure is in [atm]

and the temperature in [K]. The general expression proposed by Lohrenz et al. (1964) for estimating the critical density of a well-defined mixture or a reservoir fluid is

$$\frac{1}{\rho_c} = \sum_{\substack{i=1 \\ i \neq C_{7+}}}^n x_i v_{c,i} + x_{C_{7+}} v_{c,C_{7+}} \quad (\text{I.2.19})$$

where $v_{c,i}$ is the real critical molar volume of component i and subscript C_{7+} refers to the heptane plus fraction of the reservoir fluid. The critical volume of the C_{7+} fraction in [ft³/lb mole] is obtained from the expression

$$\begin{aligned} v_{c,C_{7+}} = & 21.573 + 0.015122 M_{w,C_{7+}} - 27.656 SG_{C_{7+}} \\ & + 0.070615 M_{w,C_{7+}} SG_{C_{7+}} \end{aligned} \quad (\text{I.2.20})$$

where $SG_{C_{7+}}$ is the specific gravity of the C_{7+} fraction.

In addition, it should be stressed that the viscosity calculations with the LBC model are very sensitive to the estimated densities, since the model is a sixteenth degree polynomial in the reduced density. This can lead to large errors for highly viscous fluids, but also because the adjustment of the d_i coefficients was based on light hydrocarbons, normally found in natural gas mixtures. A common procedure, when the LBC model is applied to real reservoir fluids, is to optimize the critical volume of the plus fraction in order to improve the viscosity calculations. The calculation procedure presented here is the procedure originally suggested by Lohrenz et al. (1964). Further, the residual viscosity term is expected to be only a function of the reduced density. This is also correct for low and moderate reduced densities, but for reduced densities above 3 a temperature dependency is observed, as shown for propane in Figure I.9. It should be stressed that a similar behavior has been observed for methane, n-hexane, and n-decane.

I.2.2.2 The LABO Model

Et-Tahir (1993) readjusted the d_i coefficients in the LBC model, Eq.(I.2.11), using experimental viscosity and density data in the temperature range 150 K – 520 K and up to 1000 bar for methane, ethane, propane, i-butane, n-pentane, n-octane, n-decane, toluene, benzene, o-xylene, and 2,2-dimethylpropane in order to improve the viscosity calculations of hydrocarbon fluids. This model is referred to as the LABO model, and

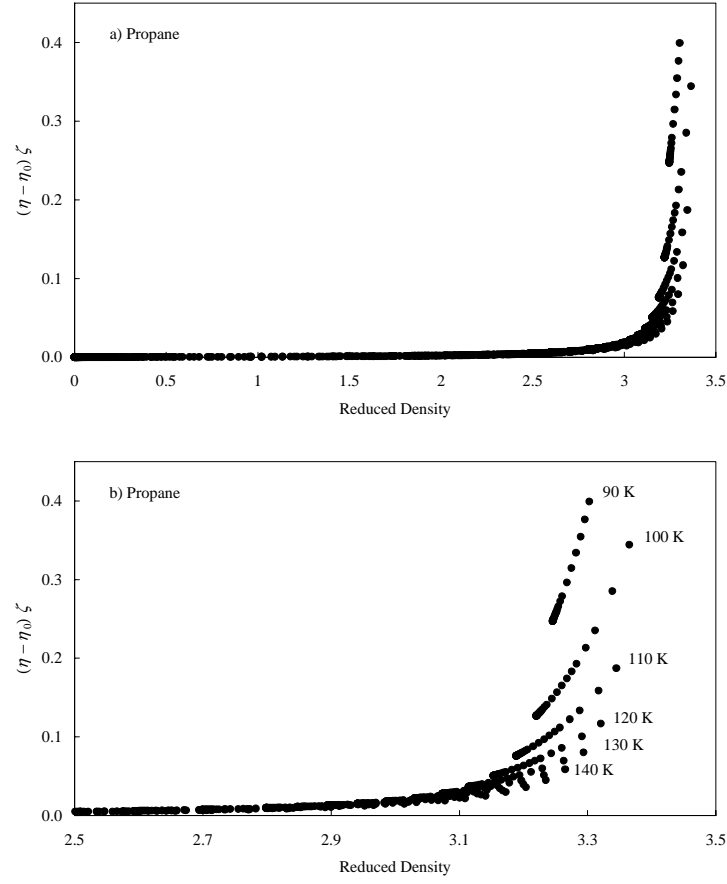


Figure I.9 The reduced residual viscosity $(\eta - \eta_0)\zeta$ defined in the LBC model versus the reduced density for propane; a) includes all data taken from Vogel et al. (1998) ranging from 90 K – 600 K and up to 1000 bar, b) shows the temperature dependency at high reduced densities.

the calculation procedure is similar to the procedure outlined for the original LBC model, described in Section I.2.2.1. The d_i coefficients in the LABO model are

$$\begin{aligned} d_0 &= 0.1019346 & d_3 &= -0.0326267 \\ d_1 &= 0.024885 & d_4 &= 0.00758663 \\ d_2 &= 0.0507222 \end{aligned}$$

In case, experimental densities are not available, Et-Tahir (1993) and Alliez et al. (1998) investigated the performance of the LABO model by comparing the experimental viscosity values with the calculated values, when the densities are estimated by four different EOSs. They found that the best results are obtained when the density is estimated with the method of Lee-Kesler (1975), whereas the use of the cubic

EOS by Peng and Robinson (1976) is not recommended. Further, they also investigated ten different mixing rules in order to obtain the critical temperature and critical pressure of mixtures. A detailed description of this study is given by Et-Tahir (1993). In case the experimental density is known, the best viscosity predictions with the LABO model are obtained when the calculation procedure described for the LBC model is used, see Section I.2.2.1. Otherwise, the mixing rules proposed by Pedersen et al. (1984a) can be applied among others. These mixing rules are used in the corresponding states models by Pedersen and Fredenslund (1987) and Aasberg-Petersen et al. (1991) and they are presented in connection with these models, see Section I.2.3.1

I.2.3 The Corresponding States Models

Viscosity models based on the corresponding states principle are common and generally either based on one to three reference fluids. The basic idea of the corresponding states principle is that the same functional behavior for a given reduced property e.g. the reduced viscosity, expressed in terms of other reduced properties, is obtained for a group of fluids. This means that at the same reduced conditions the same reduced viscosity value is obtained for any of the fluids in the group. When the corresponding states principle is applied to the reduced viscosity η_r , it can be related to two of the following reduced properties: T_r (reduced temperature), P_r (reduced pressure), ρ_r (reduced density) and v_r (reduced volume). The functional dependency of the reduced viscosity can for example be expressed as

$$\eta_r(\rho, T) = f(\rho_r, T_r) \quad \text{or} \quad \eta_r(P, T) = f(P_r, T_r) \quad (\text{I.2.21})$$

When a group of fluids obeys the corresponding states principle, only comprehensive viscosity data are required for some of the fluids in the group. These fluids or compounds are then used as reference fluids. The general expression for estimating the viscosity of a fluid by the corresponding states principle is shown below.

$$\eta_x(P, T) = \frac{K_x}{K_{ref}} \eta_{ref}(P, T) \quad (\text{I.2.22})$$

where subscripts x and ref refer to the considered fluid and the reference fluid, respectively. The K factors are related to the “critical viscosity”.

I.2.3.1 The Corresponding States Model with One Reference Fluid

The corresponding states viscosity model with one reference fluid specifically derived for hydrocarbon fluids by Pedersen et al. (1984a) is based on the approach of Christensen and Fredenslund (1980). The reference fluid is methane and was chosen because methane is one of the most studied fluids with respect to viscosity and density in the liquid and the gaseous phases. In order to improve the viscosity prediction of fluids with a reduced temperature below 0.4 (the freezing point of methane) Pedersen and Fredenslund (1987) modified the approach by Pedersen et al. (1984a). This modified approach by Pedersen and Fredenslund (1987) is referred to as the CS1 model in this work and presented below for an n component mixture

$$\eta_{mix} = \left(\frac{T_{c,mix}}{T_{c,ref}} \right)^{-1/6} \left(\frac{P_{c,mix}}{P_{c,ref}} \right)^{2/3} \left(\frac{M_{w,mix}}{M_{w,ref}} \right)^{1/2} \frac{\alpha_{mix}}{\alpha_{ref}} \eta_{ref}[P', T'] \quad (I.2.23)$$

where

$$P' = \frac{P P_{c,ref} \alpha_{ref}}{P_{c,mix} \alpha_{mix}} \quad \text{and} \quad T' = \frac{T T_{c,ref} \alpha_{ref}}{T_{c,mix} \alpha_{mix}} \quad (I.2.24)$$

The structure of this model is similar to that proposed by Ely and Hanley (1981), who used the reduced density as one of the corresponding states parameters instead of the reduced pressure. The advantage of using the pressure instead of the density is that the density of the considered fluid does not have to be estimated. Thus, at the saturation line problems may be encountered due to the discontinuity in the viscosity.

In the CS1 model the critical properties of the considered mixture are estimated with the following mixing rules

$$T_{c,mix} = \frac{\sum_i^n \sum_j^n x_i x_j \left[\left(\frac{T_{c,i}}{P_{c,i}} \right)^{1/3} + \left(\frac{T_{c,j}}{P_{c,j}} \right)^{1/3} \right]^3 (T_{c,i} T_{c,j})^{1/2}}{\sum_i^n \sum_j^n x_i x_j \left[\left(\frac{T_{c,i}}{P_{c,i}} \right)^{1/3} + \left(\frac{T_{c,j}}{P_{c,j}} \right)^{1/3} \right]^3} \quad (I.2.25)$$

$$P_{c,mix} = \frac{8 \sum_i^n \sum_j^n x_i x_j \left[\left(\frac{T_{c,i}}{P_{c,i}} \right)^{1/3} + \left(\frac{T_{c,j}}{P_{c,j}} \right)^{1/3} \right]^3 (T_{c,i} T_{c,j})^{1/2}}{\left[\sum_i^n \sum_j^n x_i x_j \left[\left(\frac{T_{c,i}}{P_{c,i}} \right)^{1/3} + \left(\frac{T_{c,j}}{P_{c,j}} \right)^{1/3} \right]^3 \right]^2} \quad (I.2.26)$$

These mixing rules are the van der Waals one-fluid approximations (Leland et al. 1968). The molecular weight of the mixture is estimated with the empirical expression

$$M_{w,mix} = 1.304 \cdot 10^{-4} \left(M_{ww}^{2.303} - M_{wn}^{2.303} \right) + M_{wn} \quad (I.2.27)$$

with

$$M_{ww} = \frac{\sum_i^n x_i M_{w,i}^2}{\sum_i^n x_i M_{w,i}} \quad (I.2.28)$$

$$M_{wn} = \sum_i^n x_i M_{w,i} \quad (I.2.29)$$

where M_{ww} is the weight average molecular weight and M_{wn} is the number average molecular weight. The reason for using this expression in order to estimate the molecular weight of a mixture is related to the fact that the heavier compounds have a larger influence on the mixture viscosity than the lighter compounds (Pedersen et al. 1984a).

The α parameters are given by

$$\alpha_{mix} = 1 + 7.378 \cdot 10^{-3} \rho_r^{1.847} M_{w,mix}^{0.5173} \quad (I.2.30)$$

$$\alpha_{ref} = 1 + 0.031 \rho_r^{1.847} \quad (I.2.31)$$

where ρ_r is the reduced density of methane defined by

$$\rho_r = \frac{\rho_{ref} \left(\frac{P P_{c,ref}}{P_{c,mix}}, \frac{T T_{c,ref}}{T_{c,mix}} \right)}{\rho_{c,ref}} \quad (I.2.32)$$

The density of methane ρ_{ref} is estimated by the modified Benedict-Webb-Rubin (BWR)-EOS proposed by McCathy (1974).

In order to ensure continuity in the viscosity estimations of the reference viscosity η_{ref} above and below the freezing point of methane ($T_F = 95.0$ K) corresponding to a reduced temperature of 0.4, Pedersen and Fredenslund (1987) modified the viscosity expression derived for methane by Hanley et al. (1975) by introducing a fourth viscosity term. The expression is

$$\eta_{ref} = \eta_0 + \eta_1 \rho_{ref} + F_1 \Delta\eta' + F_2 \Delta\eta'' \quad (I.2.33)$$

where

$$F_1 = \frac{HTAN + 1}{2} \quad \text{and} \quad F_2 = \frac{1 - HTAN}{2} \quad (I.2.34)$$

$$HTAN = \frac{\exp(\Delta T) - \exp(-\Delta T)}{\exp(\Delta T) + \exp(-\Delta T)} \quad (I.2.35)$$

with

$$\Delta T = T - T_F \quad (I.2.36)$$

The dilute gas viscosity expression $\eta_0(T)$ for methane shown in Eq.(I.2.37) has been derived by Hanley et al. (1975) using values derived from the kinetic theory of gases

$$\eta_0 = \sum_{i=1}^9 GV_i T^{\frac{i-3}{4}} \quad (I.2.37)$$

and the GV_i coefficients are given in Table I.1.

The first density correlation term above the dilute gas viscosity $\eta_1(T)$ is given by

$$\eta_1 = 1.696985927 - 0.133372346 \left(1.4 - \ln \frac{T}{168.0} \right)^2 \quad (I.2.38)$$

In the dense liquid region Eq.(I.2.33) is mainly governed by the term $\Delta\eta'(\rho, T)$ expressed as

$$\Delta\eta' = \exp \left[j_1 + \frac{j_4}{T} \right] \left(\exp \left[\rho^{0.1} \left(j_2 + \frac{j_3}{T^{3/2}} \right) + \theta \rho^{0.5} \left(j_5 + \frac{j_6}{T} + \frac{j_7}{T^2} \right) \right] - 1.0 \right) \quad (I.2.39)$$

and where

$$\theta = \frac{\rho - \rho_c}{\rho_c} \quad (I.2.40)$$

The j_i coefficients are reported in Table I.2 and have been determined by Hanley et al. (1975).

$GV_1 =$	$-2.090975 \cdot 10^5$	$GV_4 =$	$4.716740 \cdot 10^4$	$GV_7 =$	$-9.627993 \cdot 10^1$
$GV_2 =$	$2.647269 \cdot 10^5$	$GV_5 =$	$-9.491872 \cdot 10^3$	$GV_8 =$	$4.274152 \cdot 10^0$
$GV_3 =$	$-1.472818 \cdot 10^5$	$GV_6 =$	$1.219979 \cdot 10^3$	$GV_9 =$	$-8.141531 \cdot 10^{-2}$

Table I.1 Coefficients used in Eq.(I.2.37) for estimating the dilute gas viscosity of methane.

$j_1 =$	-10.35060586	$k_1 =$	-9.74602
$j_2 =$	17.571599671	$k_2 =$	18.0834
$j_3 =$	-3019.3918656	$k_3 =$	-4126.66
$j_4 =$	188.73011594	$k_4 =$	44.6055
$j_5 =$	0.042903609488	$k_5 =$	0.976544
$j_6 =$	145.29023444	$k_6 =$	81.8134
$j_7 =$	6127.6818706	$k_7 =$	15649.9

Table I.2 Coefficients for methane used in the CS1 model, Eqs.(I.2.39) and (I.2.41).

For reduced temperatures below 0.4, the term $\Delta\eta''(\rho, T)$ secures continuity between viscosities above and below the freezing point of methane, and it is given by

$$\Delta\eta'' = \exp\left[k_1 + \frac{k_4}{T}\right] \left(\exp\left[\rho^{0.1} \left(k_2 + \frac{k_3}{T^{2/3}}\right) + \theta \rho^{0.5} \left(k_5 + \frac{k_6}{T} + \frac{k_7}{T^2}\right)\right] - 1.0 \right) \quad (\text{I.2.41})$$

The k_i coefficients are given in Table I.2 and have been determined by Pedersen and Fredenslund (1987).

The unit of the reference viscosity is $[\mu\text{P}]$, when the density is in $[\text{g}/\text{cm}^3]$, the temperature in $[\text{K}]$ along with the reported coefficients for the CS1 model. When the viscosity of an unknown fluid is calculated by the CS1 model, the required density of methane is estimated at two different sets of T, P conditions. The density required in Eq.(I.2.33) is estimated at the T, P conditions defined in Eq.(I.2.24), whereas the T, P conditions used in order to estimate the density in Eqs.(I.2.30) and (I.2.31) are defined in Eq.(I.2.32). This has also been stressed by Aasberg-Petersen (1991), who concluded that this might be inconvenient and a short-come of the CS1 model. Further, according to Aasberg-Petersen et al. (1991), the CS1-model will yield reliable viscosity predictions for reservoir fluids, but the CS1-model may overestimate the viscosities of pure hydrocarbons and well-defined hydrocarbon mixtures.

I.2.3.2 The Corresponding States Model with Two Reference Fluids

Aasberg-Petersen et al. (1991) proposed a viscosity model based on the corresponding states principle with two reference fluids (CS2) applicable to hydrocarbon fluids in the liquid and gaseous phases. The reference fluids are methane and n-decane. They choose n-decane as the second reference compound, because it is the largest alkane for which sufficient amount of experimental viscosity data is known. The CS2 model is described below for an n component mixture

$$\eta_{mix} = \frac{\eta_{c,mix} \eta_1(T_1, P_1)}{\eta_{c,1}} \left(\frac{\eta_2(T_2, P_2) \eta_{c,1}}{\eta_1(T_1, P_1) \eta_{c,2}} \right)^{K_{CS}} \quad (I.2.42)$$

where K_{CS} is an interpolation parameter related to the molecular weight

$$K_{CS} = \frac{M_{w,mix} - M_{w,1}}{M_{w,2} - M_{w,1}} \quad (I.2.43)$$

Subscript mix refers to the mixture, while subscripts 1 and 2 refer to the reference fluids methane and n-decane, respectively. The functional structure of the CS2 model was originally introduced by Teja and Rice (1981) for viscosity calculations of liquids. Teja and Rice (1981) used the acentric factor in the interpolation parameter.

The critical viscosity of either the considered fluid or the two reference fluids is estimated with the following equation

$$\eta_c = C' M_w^{1/2} P_c^{2/3} T_c^{-1/6} \quad (I.2.44)$$

where C' is a constant, which cancels out, when the critical viscosities are inserted in Eq.(I.2.42). The structure of the critical viscosity equation is similar to that introduced by Uyehara and Watson (1944). The critical temperature and the critical pressure of the mixture are estimating with the same mixing rules used in the CS1 model, see Eqs.(I.2.25) and (I.2.26). The molecular weight of the mixture is obtained using Eq.(I.2.45), which has the same structure as the equation used in the CS1 model, see Eq.(I.2.27).

$$M_{w,mix} = M_{wn} + 0.00867358 \left(M_{ww}^{1.56079} - M_{wn}^{1.56079} \right) \quad (I.2.45)$$

where M_{ww} and M_{wn} are calculated according to Eqs.(I.2.28) and (I.2.29).

The viscosity of the two reference fluids (η_1 and η_2) is evaluated at T, P conditions corresponding to the reduced temperature and reduced pressure of the

mixture

$$T_i = \frac{T T_{c,i}}{T_{c,mix}} \quad i = 1,2 \quad (I.2.46)$$

$$P_i = \frac{P P_{c,i}}{P_{c,mix}} \quad i = 1,2 \quad (I.2.47)$$

using the following expression

$$\eta_i(\rho, T) = \eta_0(T) + \rho \eta_1(T) + \eta_2(\rho, T) \quad (I.2.48)$$

where

$$\eta_0 = \sum_{i=1}^9 G V_i T^{\frac{i-4}{3}} \quad (I.2.49)$$

$$\eta_1 = A + B \left(D - \ln \left(\frac{T}{F} \right) \right)^2 \quad (I.2.50)$$

$$\eta_2 = H_2 \exp \left(j_1 + \frac{j_4}{T} \right) \quad (I.2.51)$$

$$H_2 = -1 + \exp \left[\rho^{0.1} \left(j_2 + \frac{j_3}{T^{3/2}} \right) + \theta \rho^{0.5} \left(j_5 + \frac{j_6}{T} + \frac{j_7}{T^2} \right) \right] \quad (I.2.52)$$

$$\theta = \frac{\rho - \rho_c}{\rho_c} \quad (I.2.53)$$

The coefficients in Eqs.(I.2.49) – (I.2.53) are reported in Table I.3 for each reference fluid. The coefficients for n-decane were determined using viscosity data in the temperature range 240 K to 478 K and up to 1000 bar. For methane the coefficients were determined using viscosity data in the temperature range 91 K to 523 K and up to 690 bar, except the GV_i coefficients, which were determined by Hanley et al. (1975). Using these coefficients along with the density in $[\text{g}/\text{cm}^3]$ and the temperature in $[\text{K}]$ the reference viscosity has the unit $[\mu\text{P}]$. The density of each reference fluid is calculated by the procedure proposed by Knudsen (1992) based on the Jensen (1987) modification of the Adachi-Lu-Sugie (ALS) EOS Adachi et al. (1983).

However, Aasberg-Petersen et al. (1991) mentioned in their paper that the CS2 model is not suitable for mixtures with large concentrations of naphthenic compounds.

Methane			
$GV_1 =$	-209097	$B =$	343.79
$GV_2 =$	264727	$C =$	0.4487
$GV_3 =$	-147282	$F =$	168.0
$GV_4 =$	47167	$j_1 =$	-22.768
$GV_5 =$	-9491.9	$j_2 =$	30.574
$GV_6 =$	1220.0	$j_3 =$	-14929
$GV_7 =$	-96.28	$j_4 =$	1061.5
$GV_8 =$	4.274	$j_5 =$	-1.4748
$GV_9 =$	-0.0814	$j_6 =$	290.62
$A_{100} =$	23946	$j_7 =$	30396
n-Decane			
$GV_1 =$	0.2640	$B =$	81.35
$GV_2 =$	0.9487	$C =$	5.9583
$GV_3 =$	71.0	$F =$	490.0
$GV_4 =$	0.0	$j_1 =$	-11.739
$GV_5 =$	0.0	$j_2 =$	16.092
$GV_6 =$	0.0	$j_3 =$	-18464
$GV_7 =$	0.0	$j_4 =$	-811.3
$GV_8 =$	0.0	$j_5 =$	1.9745
$GV_9 =$	0.0	$j_6 =$	898.45
$A_{100} =$	0.00248	$j_7 =$	119620

Table I.3 Coefficients for the reference fluids in the CS2 model, Eqs.(I.2.49) – (I.2.53).

I.2.4 Viscosity Models Based on Cubic EOS

By plotting the temperature T versus the viscosity η for different isobars, as shown in Figure I.10 for propane, a similarity to the PvT relationship is found. This similarity was observed by Phillips (1912). Based on this similarity, Little and Kennedy (1968) derived the first EOS based viscosity model from the van der Waals EOS by interchanging P and T , replacing v with η , and the gas constant R along with the a and b parameters were replaced by empirical constants for each pure compound. Recently, Guo et al. (1997) used the same procedure in order to derive two new viscosity models based on cubic EOSs; one model is based on the Patel-Teja EOS (Patel and Teja 1982) and the other is based on the Peng-Robinson (PR) EOS (Peng and Robinson 1976). In this work the modified PR viscosity model by T.-M. Guo (1998) is presented and will

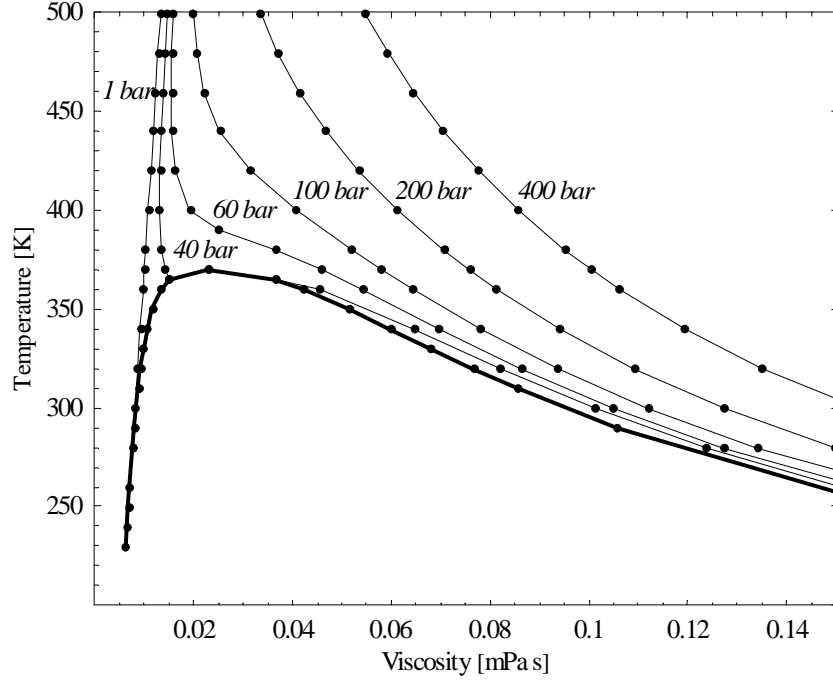


Figure I.10 Temperature versus viscosity at various isobars (—) and at the saturation line (—) for propane. Data (•) taken from Vogel et al. (1998).

be referred to as the PRVIS model. For an n component mixture the PRVIS model is given by

$$T = \frac{r(T)_{mix} P}{\eta_{mix} - b(T)_{mix}} - \frac{a_{mix}}{\eta_{mix}(\eta_{mix} + b_{mix}) + b_{mix}(\eta_{mix} - b_{mix})} \quad (\text{I.2.54})$$

where subscript mix refers to the mixture. The a_{mix} , b_{mix} , $b(T)_{mix}$, and $r(T)_{mix}$ parameters are determined using the following mixing rules:

$$a_{mix} = \sum_{i=1}^n x_i a_i \quad (\text{I.2.55})$$

$$b_{mix} = \sum_{i=1}^n x_i b_i \quad (\text{I.2.56})$$

$$b(T)_{mix} = \sum_{i=1}^n \sum_{j=1}^n x_i x_j \sqrt{b_i(T) b_j(T)} (1 - k_{ij}) \quad (\text{I.2.57})$$

$$r(T)_{mix} = \sum_{i=1}^n x_i r_i(T) \quad (\text{I.2.58})$$

where

$$a_i = 0.45724 \frac{r_{c,i}^2 P_{c,i}^2}{T_{c,i}} \quad (\text{I.2.59})$$

$$b_i = 0.07780 \frac{r_{c,i} P_{c,i}}{T_{c,i}} \quad (\text{I.2.60})$$

$$r_i(T) = r_{c,i} \tau_i(T_{r,i}, P_{r,i}) \quad (\text{I.2.61})$$

$$b_i(T) = b_i \phi_i(T_{r,i}, P_{r,i}) \quad (\text{I.2.62})$$

with

$$r_{c,i} = \frac{\eta_{c,i} T_{c,i}}{P_{c,i} Z_{c,i}} \quad (\text{I.2.63})$$

where $T_{c,i}$, $P_{c,i}$, and $Z_{c,i}$ are respectively the critical temperature, the critical pressure, and the critical compressibility factor of the pure compounds. The critical viscosity $\eta_{c,i}$ is obtained by the Uyehara and Watson equation (Uyehara and Watson 1944)

$$\eta_{c,i} = 7.7 \cdot 10^{-7} T_{c,i}^{-1/6} M_{w,i}^{1/2} P_{c,i}^{2/3} \quad (\text{I.2.64})$$

The unit of $\eta_{c,i}$ is [Pa s], when the temperature is in [K] and the pressure in [atm]. The τ_i and the ϕ_i parameters are estimated using the following expressions

$$\tau_i(T_{r,i}, P_{r,i}) = \left(1 + Q_{1,i} \left(\sqrt{P_{r,i} T_{r,i}} - 1\right)\right)^{-2} \quad (\text{I.2.65})$$

$$\phi_i(T_{r,i}, P_{r,i}) = \exp\left[Q_{2,i} \left(\sqrt{T_{r,i}} - 1\right) + Q_{3,i} \left(\sqrt{P_{r,i}} - 1\right)^2\right] \quad (\text{I.2.66})$$

and the Q parameters are determined in the following way:

For $\omega_i < 0.3$

$$\begin{aligned} Q_{1,i} &= 0.829599 + 0.350857\omega_i - 0.747680\omega_i^2 \\ Q_{2,i} &= 1.94546 - 3.19777\omega_i + 2.80193\omega_i^2 \\ Q_{3,i} &= 0.299757 + 2.20855\omega_i - 6.64959\omega_i^2 \end{aligned} \quad (\text{I.2.67})$$

For $\omega_i \geq 0.3$

$$\begin{aligned} Q_{1,i} &= 0.956763 + 0.192829\omega_i - 0.303189\omega_i^2 \\ Q_{2,i} &= -0.258789 - 37.1071\omega_i + 20.5510\omega_i^2 \\ Q_{3,i} &= 5.16307 - 12.8207\omega_i + 11.0109\omega_i^2 \end{aligned} \quad (\text{I.2.68})$$

where ω_i is the acentric factor of component i .

The calculated viscosity by the PRVIS model will have the unit [Pa s], when the pressure and the critical pressure are in [Pa], except in the estimation of the critical viscosity by Eq.(I.2.64). An advantage of the PRVIS model is that the density of the considered fluid is not required in order to perform viscosity calculations. The only required data are the composition of the mixture, the pressure, the temperature, along with the acentric factor and the critical properties of the pure compounds. The PRVIS model has been derived for viscosity predictions of hydrocarbon fluids at high pressures.

I.2.5 Critical Viscosity

By considering the viscosity at the critical point from a kinetic gas theory point of view Uyehara and Watson (1944) suggested the following expression

$$\eta_c = k' \frac{\sqrt{M_w T_c}}{v_c^{2/3}} \quad (\text{I.2.69})$$

where η_c is the critical viscosity, k' a constant, and v_c the molar volume. By combining Eq.(I.2.69) with the gas law Uyehara and Watson (1944) obtained

$$\eta_c = \frac{k'}{(Z_c R)^{2/3}} \frac{M_w^{1/2} P_c^{2/3}}{T_c^{1/6}} \quad (\text{I.2.70})$$

Using the critical compressibility factor $Z_c = 0.275$, and based on experimental viscosity data for 60 compounds Uyehara and Watson (1944) determined an average value of $k' = 61.2$, when the viscosity is in [μP], the temperature in [K], and the pressure in [atm], leading to

$$\eta_c = 7.7 \frac{M_w^{1/2} P_c^{2/3}}{T_c^{1/6}} \quad (\text{I.2.71})$$

This equation is commonly used to estimate the critical viscosity of fluids and it is e.g. used in the corresponding states model with two reference fluids (CS2) by Aasberg-Petersen et al. (1991), the viscosity model based on the PR EOS (PRVIS) by Guo et al. (1997) and Guo (1998), and as the viscosity reducing parameter ζ in the LBC model (Lohrenz et al. 1964).

I.3 Density Models

In spite that the viscosity is normally required for a given temperature T and pressure P , most viscosity models are instead related to the density or molar volume, see e.g. Monnery et al. (1995). However in most cases the density (molar volume) of the considered fluid is not known for a given T, P condition and therefore reliable and accurate PvT models are required, applicable to both liquids, gases and dense fluids over wide ranges of temperature, pressure, and composition. Figure I.11 shows the PvT behavior of a pure fluid. At the critical point (P_c, v_c) the critical isotherm exhibits a horizontal inflection, resulting in the following mathematical conditions

$$\left(\frac{\partial P}{\partial v}\right)_{T,CP} = 0 \quad ; \quad \left(\frac{\partial^2 P}{\partial v^2}\right)_{T,CP} = 0 \quad (\text{I.3.1})$$

where CP refers to the critical point. In Figure I.11, the full line to the left of the critical point represents saturated liquid, whereas the full line to the right of the critical point represents saturated vapor. The area lying inside the full lines is the two phase region, whereas only one phase, liquid or gas, exists outside for a given temperature and pressure. As the pressure goes to infinity the isotherms approach an asymptotic value, which can be interpreted as the hard-core volume. Further, it can be seen from Figure I.11 that liquids are almost incompressible for temperatures below the critical temperature. The ideal gas state is approached for temperatures significantly higher than

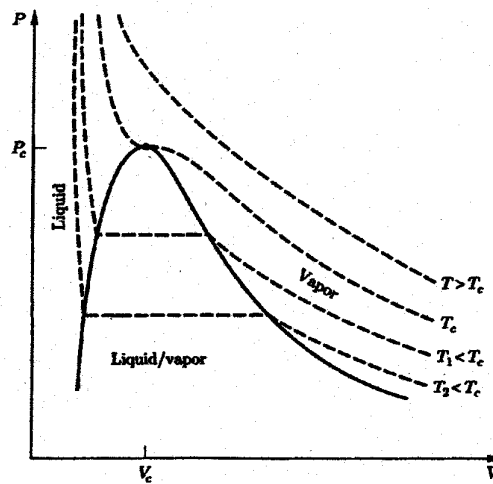


Figure I.11 Pressure P versus volume V of a pure fluid at different temperatures.

the critical temperature and at low pressures.

PvT models, which in addition also can represent the thermodynamic functions derived from integration and differentiation of the PvT relation, are referred to as equations of state (EOS) (Jensen 1987). The literature contains many different types of EOSs. In the remaining of this chapter, the EOSs used in this work for estimating the molar volume (density) are presented. These EOSs are all pressure explicit and can be separated into two categories:

- Cubic EOS.
- Non-cubic EOS of the Benedict-Webb-Rubin (BWR) type.

In spite that the more complex BWR type of EOSs have been found to deliver more accurate density estimations, especially for pure compounds, cubic EOSs are the most popular and commonly used models in compositional simulators within the chemical and petroleum industry. This is due to their simplicity and that they can be solved easily. Further, cubic EOSs can also easily be applied for accurate estimations of vapor/liquid equilibria of pure fluids and mixtures. This is generally not the case for the BWR models due to the empirical mixing rules associated with the different parameters.

I.3.1 Cubic EOS

In 1873 van der Waals introduced the first cubic EOS

$$P = \frac{RT}{v-b} - \frac{a}{v^2} \quad (\text{I.3.2})$$

where v is the molar volume, b the covolume or the hard core volume, and a the intermolecular attraction parameter. The first term in Eq.(I.3.2) is defined as the repulsive pressure, while the last term is the attractive pressure term also referred to as the internal pressure. The first accepted modification of the van der Waals EOS for engineering applications was the Redlich-Kwong (RK) EOS by Redlich and Kwong (1949), who multiplied the attractive part by $v(v+b)^{-1}T^{-0.5}$, but still kept the a parameter constant. Since the RK EOS was introduced, a tremendous number of cubic EOSs have been derived and every year new cubic EOSs or modifications of existing cubic EOSs are proposed. Thus, for most of the derived cubic EOSs the main modifications have been performed on the attractive pressure contribution. In spite new

cubic EOSs are proposed, the simple and well-known Soave-Redlich-Kwong (SRK) EOS (Soave 1972) or the Peng-Robinson (PR) EOS (Peng and Robinson 1976) are still very common and widely used within the chemical and petroleum industry.

I.3.1.1 The SRK and PR EOS

The SRK and PR EOS are referred to as two-parametric cubic EOSs and the general expression for both EOSs can be written as

$$P = \frac{RT}{v-b} - \frac{a(T)}{v^2 + ubv + wv^2} \quad (\text{I.3.3})$$

where u and w are integers dependent on the cubic EOS, see Table I.4. The b and $a(T)$ parameters are defined as

$$b = \frac{\Omega_b R T_c}{P_c} \quad (\text{I.3.4})$$

$$a(T) = \frac{\Omega_a R T_c^2}{P_c} \alpha(T) \quad (\text{I.3.5})$$

with

$$\alpha(T) = \left(1 + m \left(1 - T_r^{0.5} \right) \right)^2 \quad (\text{I.3.6})$$

where T_r is the reduced temperature defined as T/T_c . This alpha function was proposed by Soave (1972) for the SRK EOS in order to improve the vapor/liquid equilibrium pressure compared to the original RK EOS (Redlich and Kwong 1949). Peng and Robinson (1976) adapted the structure of the Soave alpha function for the PR EOS.

For the SRK EOS

$$m = 0.48 + 1.574\omega - 0.176\omega^2 \quad (\text{I.3.7})$$

	u	w	Ω_a	Ω_b	Z_c
SRK	1	0	0.427480	0.086640	1/3
PR	2	-1	0.457236	0.077796	0.307401

Table I.4 Parameters for the SRK and PR EOS.

while for the PR EOS

$$m = 0.37464 + 1.54226\omega - 0.26992\omega^2 \quad (\text{I.3.8})$$

where ω is the acentric factor. Further improvements of the alpha function have extended the application of cubic EOSs to many polar and nonpolar fluids, as it is the case with e.g. the Mathias (1983) modification of the SRK EOS (SRKM) or the Stryjek and Vera (1986) modification of the PR EOS (PRSV). For the SRKM EOS

$$m = 0.48508 + 1.555191\omega - 0.156136\omega^2 \quad \text{for } T_r \leq 1 \quad (\text{I.3.9})$$

whereas at supercritical temperatures the expression proposed by Boston and Mathias (1980) is used

$$\alpha = \left(\exp \left[c(1 - T_r)^d \right] \right)^2 \quad (\text{I.3.10})$$

with

$$\begin{aligned} c &= 1 + \frac{m}{2} + 0.3p \\ d &= \frac{c-1}{c} \end{aligned} \quad (\text{I.3.11})$$

and where p is a characteristic parameter related to each polar fluid. In Eq.(I.3.11) m is obtained by Eq.(I.3.9).

For the PRSV EOS

$$\begin{aligned} m &= \kappa_0 + \kappa_1(1 + T_r^{0.5})(0.7 - T_r) \quad \text{for } T_r < 1 \\ m &= \kappa_0 \quad \text{for } T_r \geq 1 \end{aligned} \quad (\text{I.3.12})$$

with

$$\kappa_0 = 0.378893 + 1.4897153\omega - 0.17131848\omega^2 + 0.0196554\omega^3 \quad (\text{I.3.13})$$

and κ_1 is an adjustable parameter characteristic of each pure compound reported by Stryjek and Vera (1986).

However, since the Soave alpha function Eq.(I.3.6) was originally intended for improving vapor/liquid equilibrium calculations some remarks should be stressed, when this function is applied at supercritical temperatures. At high reduced temperatures, cubic EOSs should approach the ideal gas limit. However, neither the alpha function in the PR or the SRK EOS does decrease monotonically to zero, but instead the alpha function passes through a minimum located at

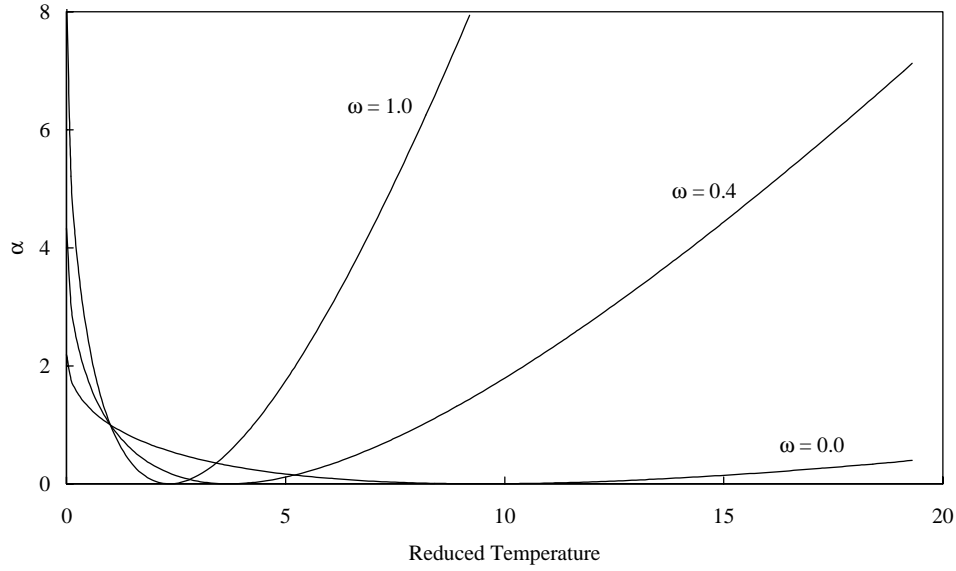


Figure I.12 Behavior of the alpha function in the SRK EOS as a function of the reduced temperature for various acentric factors ω .

$$T_r = \left(1 + \frac{1}{m}\right)^2 \quad (\text{I.3.14})$$

followed by an increase with T_r^2 , as shown in Figure I.12. In this figure the behavior of the alpha function in the SRK EOS is shown as a function of the reduced temperature for positive acentric factors ω . For fluids, which have an acentric factor close to zero such as methane ($T_c \cong 190.6$ K) or nitrogen ($T_c \cong 126.1$ K) the alpha function decreases monotonically up to around 1800 K for methane and 1200 K for nitrogen. For n-octane ($\omega \approx 0.40$ and $T_c \cong 568.7$ K) the monotonical decrease of the alpha function continues up to around 2100 K. So generally for all possible temperature ranges of industrial interest, the performance of the Soave alpha function for hydrocarbon fluids will be adequate. However, for some fluids such as neon, helium, and hydrogen the Soave alpha function may not be adequate. One way to correct this problem is to use a different alpha function for the supercritical region, as e.g. the alpha function suggested by Boston and Mathias (1980).

For the two-parametric cubic EOSs, the prefactors Ω_a and Ω_b along with the critical compressibility Z_c have been determined using the critical point criteria given in

Eq.(I.3.1). These values are reported in Table I.4 for the SRK and the PR EOS, respectively. It should be stressed that the EOS determined Z_c is not equal to the value obtained from experimental measurements.

In order to apply the SRK and the PR EOS to mixtures, the required a and b parameters of the mixture have to be estimated. In this work, in order to keep the EOS as simple as possible, the regular van der Waals mixing rules are used. These mixing rules are given by

$$a_{mix} = \sum_{i=1}^n \sum_{j=1}^n x_i x_j \left(\sqrt{a_i a_j} \right) (1 - k_{ij}) \quad (\text{I.3.15})$$

$$b_{mix} = \sum_{i=1}^n x_i b_i \quad (\text{I.3.16})$$

where k_{ij} is the binary interaction parameter between compound i and compound j in the mixture. These binary interaction parameters k_{ij} are determined by optimizing the performance of the EOS to experimental VLE measurements, and values have been reported by Knapp et al. (1982) for the SRK and the PR EOS, respectively.

I.3.1.2 The Peneloux Correction

Peneloux et al. (1982) introduced a simple method based on the volume translation principles in order to improve the estimation of the liquid molar volume by cubic EOSs. With this procedure the volumes of the liquid and the gas phase are changed, but the phase equilibrium conditions are preserved according to the unmodified EOS, as shown by Knudsen (1992). The volume correction by Peneloux (1982) was introduced for the SRK EOS by using the following relation between the SRK volume \tilde{v} and the Peneloux volume v

$$v = \tilde{v} - c \quad (\text{I.3.17})$$

By inserting Eq.(I.3.17) into the SRK EOS leads to

$$P = \frac{RT}{v + c - b} - \frac{a(T)}{(v + c)(v + b + c)} \quad (\text{I.3.18})$$

For an n compound mixture the c parameter is obtained using a linear mixing rule

$$c = \sum_{i=1}^n x_i c_i \quad (\text{I.3.19})$$

with

$$c_i = 0.40768 \frac{R T_{c,i}}{P_{c,i}} (0.29441 - Z_{RA,i}) \quad (\text{I.3.20})$$

and where Z_{RA} is the Rackett compressibility factor. An approximate value for Z_{RA} can be obtained by

$$Z_{RA,i} = 0.29056 - 0.08775 \omega_i \quad (\text{I.3.21})$$

The Peneloux correction improves the estimated liquid volumes, except in the vicinity of the critical point and at very high pressures (Peneloux et al. 1982). Further, it should be stressed that the principles of the volume translation can also be applied to other cubic EOSs, if the constants in Eq.(I.3.20) are readjusted.

I.3.1.3 Density Estimation of the Reference Fluids in the CS2 Model

The general method used to estimate the density (molar volume) of the reference fluids (methane and n-decane) in the CS2 model (Aasberg-Petersen et al. 1991) is described below. Knudsen (1992) found that the optimal expression for estimating the molar volume of the reference fluids is given by

$$v = v_{ALS} - c - \frac{D_c d_3 k_1 k_2}{(k_1 + d_1)(k_2 + d_2)} \quad (\text{I.3.22})$$

with

$$D_c = v_{c,ALS} - c - v_{c,\text{exp}} \quad (\text{I.3.23})$$

and where $v_{c,\text{exp}}$ is the real critical molar volume. The molar volume v_{ALS} and the critical molar volume $v_{c,ALS}$ are determined by the Jensen (1987) modification of the Adachi-Lu-Sugie (ALS) EOS (Adachi et al. 1983). The ALS EOS is given by

$$P = \frac{RT}{v - b_1} - \frac{a(T)}{(v - b_2)(v + b_3)} \quad (\text{I.3.24})$$

where

$$b_k = \frac{\Omega_{b,k} R T_c}{P_c} \quad \text{for} \quad k = 1, 2, 3 \quad (\text{I.3.25})$$

$$a(T) = \frac{\Omega_a R T_c^2}{P_c} \alpha(T) \quad (\text{I.3.26})$$

The perfactors Ω have been determined by applying the critical point criteria

$$\begin{aligned} \Omega_a &= 0.44869 + 0.04024\omega + 0.01111\omega^2 - 0.00576\omega^3 \\ \Omega_{b1} &= 0.08974 - 0.03452\omega + 0.0033\omega^2 \\ \Omega_{b2} &= 0.5 \left[2(1 + \Omega_{b1}) - 3\Omega_a^{1/3} + d^{1/2} \right] \\ \Omega_{b3} &= 0.5 \left[-2(1 + \Omega_{b1}) - 3\Omega_a^{1/3} + d^{1/2} \right] \end{aligned} \quad (\text{I.3.27})$$

and where

$$d = 4\Omega_a - 3\Omega_a^{2/3} \quad (\text{I.3.28})$$

The $\alpha(T)$ function in Eq.(I.3.26) is equal to the Soave alpha function presented in Eq.(I.3.6), but with

$$m = 0.4070 + 1.3787\omega - 0.2933\omega^2 \quad (\text{I.3.29})$$

The c parameter in Eq.(I.3.23) is a Peneloux type correction defined as

$$c = \frac{\Omega_c R T_c}{P_c} \quad (\text{I.3.30})$$

The d_1 parameter is evaluated at the saturated liquid condition for subcritical temperatures, and for supercritical temperatures at the critical isochore, as suggested by Chou and Prausnitz (1989)

$$d_1 = \frac{1}{R T_c} \left(\frac{\partial P}{\partial \rho} \right)_T \quad (\text{I.3.31})$$

whereas the d_2 and d_3 parameters are evaluated at the actual temperature and pressure with the aid of the following expressions

$$DP1 = \frac{1}{R T_c} \left(\frac{\partial P}{\partial \rho} \right)_T \quad ; \quad DP2 = \frac{1}{R T_c} \left(\frac{\partial^2 P}{\partial \rho^2} \right)_T \quad (\text{I.3.32})$$

and using the following criteria:

$$\begin{aligned} d_2 &= DP1 & \text{and} & & d_3 &= 1 & \text{for } DP2 \geq 0 \\ d_2 &= DP1^{1/4} & \text{and} & & d_3 &= -DP1^{1/2} & \text{for } DP2 < 0 \end{aligned} \quad (\text{I.3.33})$$

	Methane	n-Decane
k_1	0.3695	0.0001665
k_2	0.4669	0.6376
Ω_c	-0.000122	0.000970

Table I.5 Constants in Eqs.(I.3.22) and (I.3.30) for methane and n-decane, respectively.

The fluid constants in Eqs.(I.3.22) and (I.3.30) are given in Table I.5 for both methane and n-decane, respectively. In order to estimate the coefficients for methane, Knudsen (1992) used calculated densities obtained by the 33-parameter modified BWR EOS derived for methane by McCarty (1974) as “experimental” density data. In addition, the n-decane coefficients were estimated using experimental densities in the temperature range 283 K to 673 K and up to 1000 bar.

I.3.2 Non-cubic EOS

In addition to the cubic EOSs, the literature also contains many non-cubic EOSs. One family of these non-cubic EOS is the BWR type. As previously mentioned, the BWR type of EOSs calculates the density of especially pure fluids better than cubic EOSs. The BWR EOS

$$\begin{aligned}
 P = \rho RT + \left(B_0 RT - A_0 - \frac{C_0}{T^2} \right) \rho^2 + (bRT - a) \rho^3 + (\alpha a) \rho^6 \\
 + \frac{(c\rho^3)}{T^2} (1 + \gamma \rho^2) \exp(-\gamma \rho^2)
 \end{aligned}
 \tag{I.3.34}$$

was introduced by Benedict et al. (1940) and is an extension of the virial equation. In order to apply the BWR EOS, the eight coefficients have to be estimated for each fluid. Since the BWR EOS was introduced, many different modifications have been proposed mainly focusing on the parametric expressions or the mixing rules. One of these models is the 33 parameter modification of the BWR EOS (MBWR) derived by McCarty (1974) for very accurate density calculations of methane. This equation is used in the CS1 viscosity model (Pedersen and Fredenslund 1987) in order to estimate the density

of the methane reference fluid. In addition, the concepts of the MBWR EOS have also been applied by Younglove and Ely (1987) in order to estimate recommended densities for methane, ethane, propane, n-butane, and isobutane over wide ranges of temperature and pressure. However for most fluids it is impossible to determine all 33 parameters due to few experimental PvT data covering wide ranges of temperature and pressure. This obstacle has led to the development of BWR models based on the corresponding states principle, such as the well-known Lee-Kesler method (Lee and Kesler 1975), but also to the development of more general models, such as the Soave (1995) modification of the BWR EOS (SBWR). However, before continuing describing the BWR based EOSs used in this work, it should be stressed that the exponential term in the BWR based EOSs is active at intermediate densities and it improves the prediction of the critical isotherm of pure compounds compared to cubic EOSs.

I.3.2.1 The Lee-Kesler Method

In the 1950s Pitzer and coworkers found that for a constant reduced temperature and pressure, the compressibility Z of a fluid could be adequately represented by a linear function of the acentric factor ω

$$Z = Z^{(0)} + \omega Z^{(1)} \quad (\text{I.3.35})$$

Here $Z^{(0)}$ is the compressibility factor of a simple fluid ($\omega = 0$) and $\omega Z^{(1)}$ is the deviation of the compressibility factor from $Z^{(0)}$. By applying the corresponding states principle and the context of the Pitzer's three parameter correlation for the compressibility factor, Lee and Kesler (1975) suggested to express the compressibility factor Z of a real fluid as

$$Z = Z^{(0)} + \frac{\omega}{\omega^{(r)}} (Z^{(r)} - Z^{(0)}) \quad (\text{I.3.36})$$

where superscript (0) and (r) refer to the two reference fluids, and ω is the acentric factor of the real fluid. The first reference fluid denoted with superscript (0) is the simple fluid, while the second reference fluid is n-octane for which $\omega^{(r)} = 0.3978$.

For a given temperature T and pressure P , the compressibility factor of a considered fluid is calculated by estimating the compressibility factors of the two

reference fluids at the corresponding reduced temperature ($T_r = T/T_c$) and reduced pressure conditions ($P_r = P/P_c$), where T_c and P_c are related to the properties of the considered fluid. Generally, the compressibility factor can be expressed as

$$Z = \frac{P_r v_r}{T_r} \quad (\text{I.3.37})$$

when reduced properties are used.

The compressibility factor of each reference fluid is estimated by Eq.(I.3.37), when the following reduced form of the Lee and Kesler (1975) modification of the BWR based EOS is solved with respect to the reduced molar volume v_r .

$$\frac{P_r v_r}{T_r} = 1 + \frac{B}{v_r} + \frac{C}{v_r^2} + \frac{D}{v_r^5} + \frac{c_4}{T_r^3 v_r^2} \left(\beta + \frac{\gamma}{v_r^2} \right) \exp \left(-\frac{\gamma}{v_r^2} \right) \quad (\text{I.3.38})$$

with

$$\begin{aligned} B &= b_1 - \frac{b_2}{T_r} - \frac{b_3}{T_r^2} - \frac{b_4}{T_r^3} \\ C &= c_1 - \frac{c_2}{T_r} + \frac{c_3}{T_r^3} \\ D &= d_1 + \frac{d_2}{T_r} \end{aligned} \quad (\text{I.3.39})$$

The constants in Eqs.(I.3.38) and (I.3.39) are reported in Table I.6 for the simple reference fluid and the second reference fluid, n-octane.

Generally, the Lee-Kesler method has been found to deliver accurate density calculations within 2% for hydrocarbons in the liquid and the gaseous phases (Reid et al. 1987). The method has been derived for reduced temperatures ranging from 0.3 to 4.0 and reduced pressures ranging from 0 to 10.

In addition, it should be mentioned that mixing rules have been proposed by Lee and Kesler (1975) in order to estimate the critical properties of mixtures. However, these mixing rules are not used in this work, because the Lee-Kesler method is only used to estimate the densities of fluids in the LABO viscosity model. The reason is that Et-Tahir (1993) and Alliez et al. (1998) found that the best viscosity estimations are obtained with the LABO model, when the Lee-Kesler method is used compared with other EOSs. In addition, they also found that the Pedersen et al. (1984a) mixing rules

	Simple Fluid	n-Octane
b_1	0.1181193	0.2026579
b_2	0.2657280	0.3315110
b_3	0.1547900	0.0276550
b_4	0.0303230	0.0313385
c_1	0.0236744	0.0313385
c_2	0.0186984	0.0503618
c_3	0.0000000	0.0169010
c_4	0.0427240	0.0415770
$d_1 10^4$	0.1554880	0.4873600
$d_2 10^4$	0.6236890	0.0740336
β	0.6539200	1.2260000
γ	0.0601670	0.0375400

Table I.6 Constants for Eqs.(I.3.38) and (I.3.39) in the Lee-Kesler method.

(Eqs.(I.2.25) and (I.2.26)) are adequate for estimating the critical temperature and critical pressure of mixtures.

I.3.2.2 The SBWR EOS

Recently, based on the BWR EOS, Soave (1995) and (1996) derived a new general model (SBWR) for the accurate estimation of the densities of pure non-polar fluids, primarily hydrocarbons, and their mixtures. In addition, it should be stressed that the SBWR EOS also reproduces VLE data accurately. The only properties required in order to calculate the density of a fluid for a given temperature and pressure are the critical temperature, the critical pressure, and the acentric factor of the pure compounds, along with the composition. The general expression for the SBWR EOS is

$$Z = \frac{P v}{R T} = 1 + B \rho + C \rho^2 + D \rho^4 + E \rho^2 (1 + F \rho^2) \exp(-F \rho^2) \quad (\text{I.3.40})$$

The structure of this expression is similar to that of Lee-Kesler (Eq.I.3.38)), except that exponent 5 has been changed to 4 in Eq.(I.3.40). The reason is that the densities at the critical isotherm are reproduced more accurately (Soave 1995).

However, Soave (1995) found it more convenient to transform Eq.(I.3.40) into adimensional quantities

$$Z = \frac{P_r}{T_r \psi} = 1 + \beta \psi + \gamma \psi^2 + \delta \psi^4 + \varepsilon \psi^2 (1 + \phi \psi^2) \exp(-\phi \psi^2) \quad (\text{I.3.41})$$

with

$$\psi = \frac{R T_c}{P_c v} \quad (\text{I.3.42})$$

The parameters in Eq.(I.3.41) are defined as

$$\begin{aligned} \beta &= \beta_c + b_1 \left(1 - \frac{1}{T_r^{1.6}} \right) + b_2 \left(1 - \frac{1}{T_r^{3.2}} \right) \omega \\ \gamma &= \gamma_c + c_1 \left(\frac{1}{T_r} - 1 \right) + c_2 \left(\frac{1}{T_r} - 1 \right)^2 + c_3 \left(\frac{1}{T_r} - 1 \right)^3 \\ \delta &= \frac{\delta_c}{T_r} \\ \varepsilon &= \varepsilon_c + e_1 \left(\frac{1}{T_r} - 1 \right) + e_2 \left(\frac{1}{T_r} - 1 \right)^2 + e_3 \left(\frac{1}{T_r} - 1 \right)^3 \end{aligned} \quad (\text{I.3.43})$$

where subscript c refers to the critical point. Generally, the b_i , c_i , and e_i parameters in Eq.(I.3.43) can be expressed by the following equation:

$$\zeta_i = \zeta_{i,1} + \xi_{i,2} \omega + \xi_{i,3} \omega^2 \quad (\text{I.3.44})$$

The $\zeta_{i,j}$ parameters used to obtain the b_i , c_i , and e_i parameters by Eq.(I.3.44) are given in Table I.7.

The critical parameters have been determined by using the critical constraints (forcing the critical isotherm through the critical point with zero slope and zero

i,j	$b_{i,j}$	$c_{i,j}$	$e_{i,j}$
1,1	0.4220	-0.02663	0.1087
1,2	0	0.06170	0.2154
1,3	0	0.00779	-0.0591
2,1	0.2971	0.00605	0.0705
2,2	0	0.07544	0.3007
2,3	0	-0.06134	0.4948
3,1	0	0.1087	-0.0068
3,2	0	0.2154	0.1858
3,3	0	0.01191	-0.1157

Table I.7 Constants for estimating b_i , c_i , and e_i using Eq.(I.3.44).

curvature, see e.g. Figure I.11). The critical parameters are given by

$$\begin{aligned}
 \beta_c &= b Z_c \\
 \gamma_c &= c Z_c^2 \\
 \delta_c &= d Z_c^4 \\
 \varepsilon_c &= e Z_c^2 \\
 \phi_c &= f Z_c^2
 \end{aligned} \tag{I.3.45}$$

where the b , c and d parameters are defined in Eq(I.3.46).

$$\begin{aligned}
 b &= \frac{1}{3} \left(-8 + 15Z_c - 4f^2 e(-1+f) \exp(-f) \right) \\
 c &= 2 - 5Z_c + e(-1+f(-1+f(-3+2f))) \exp(-f) \\
 d &= -\frac{1}{3} + Z_c - \frac{1}{3} e f^2 (-5+2f) \exp(-f)
 \end{aligned} \tag{I.3.46}$$

By modeling the critical isotherm Soave (1995) found that it was appropriate to set

$$e = 0.5 \quad \text{and} \quad f = \frac{0.06}{Z_c^2} \tag{I.3.47}$$

The critical compressibility factor Z_c used in the SBWR model is related to the Rackett compressibility factor Z_{RA} , which was calculated by the Rackett equation (Rackett 1970)

$$v_L^{sat} = \frac{RT_c}{P_c} (Z_{RA})^{1+(1-T_r)^{2/7}} \tag{I.3.48}$$

using the critical properties and saturated liquid densities, v_L^{sat} . The estimated values for Z_{RA} were correlated against the acentric factor obtaining the following expression

$$Z_c = Z_{RA} = 0.2908 - 0.099\omega + 0.04\omega^2 \tag{I.3.49}$$

When the SBWR EOS is applied to mixtures, the critical temperature, critical pressure, and the acentric factor of the mixture are required. In order to determine these mixture properties Soave (1995) derived the following mixing rules for the SBWR EOS based on an analogy with the usually applied regular van der Waals mixing rules of cubic EOSs for the a and b parameters of the mixture, see Eqs.(I.3.15) and (I.3.16).

For a cubic EOS

$$a_{mix} = \sum_{i=1}^n \sum_{j=1}^n x_i x_j \left(\sqrt{a_i a_j} \right) (1 - k_{ij}) \tag{I.3.50}$$

where

$$a(T) = \frac{\Omega_a R T_c^2}{P_c} \alpha(T) \quad (\text{I.3.51})$$

with

$$\alpha(T) = \left(1 + m \left(1 - T_r^{0.5} \right) \right)^2 \quad (\text{I.3.52})$$

and where m is a function of the acentric factor. By combining Eqs.(I.3.50) – (I.3.52) leads to

$$\frac{T_{c,mix}^2}{P_{c,mix}} \alpha_{mix} = \sum_{i=1}^n \sum_{j=1}^n x_i x_j (1 - k_{ij}) \frac{T_{c,i} T_{c,j}}{\sqrt{P_{c,i} P_{c,j}}} \sqrt{\alpha_i \alpha_j} \quad (\text{I.3.53})$$

Since this equation should be valid for all temperatures, the following equations can be derived

$$\frac{T_{c,mix}^2}{P_{c,mix}} (1 + m_{mix})^2 = \sum_{i=1}^n \sum_{j=1}^n x_i x_j (1 - k_{ij}) \frac{T_{c,i} T_{c,j}}{\sqrt{P_{c,i} P_{c,j}}} (1 + m_i) (1 + m_j) \equiv S_1 \quad (\text{I.3.54})$$

$$\frac{T_{c,mix}}{P_{c,mix}} m_{mix}^2 = \sum_{i=1}^n \sum_{j=1}^n x_i x_j (1 - k_{ij}) \sqrt{\frac{T_{c,i} T_{c,j}}{P_{c,i} P_{c,j}}} m_i m_j \equiv S_2 \quad (\text{I.3.55})$$

Further for a cubic EOS

$$b_{mix} = \sum_{i=1}^n x_i b_i \quad (\text{I.3.56})$$

with

$$b = \frac{\Omega_b R T_c}{P_c} \quad (\text{I.3.57})$$

and by combining Eqs.(I.3.56) and (I.3.57) leads to

$$\frac{T_{c,mix}}{P_{c,mix}} = \sum_{i=1}^n x_i \frac{T_{c,i}}{P_{c,i}} \equiv S_3 \quad (\text{I.3.58})$$

The following mixing rules are obtained for the critical parameters of the mixture, when Eqs.(I.3.54), (I.3.55), and (I.3.58) are combined

$$T_{c,mix} = \frac{S_1}{\left(\sqrt{S_2} + \sqrt{S_3} \right)^2} \quad (\text{I.3.59})$$

$$P_{c,mix} = \frac{T_{c,mix}}{S_3} \quad (I.3.60)$$

$$m_{mix} = \sqrt{\frac{S_2}{S_3}} \quad (I.3.61)$$

Thus, these mixing rules do not lead to the acentric factor of the mixture, but to m_{mix} , which is a function of the acentric factor. Based on VLE data for alkane systems Soave (1995) obtained the following relationship between m and the acentric factor ω .

$$m = 1.4\omega \quad (I.3.62)$$

which is valid for both pure compounds and mixtures. This leads to

$$\omega_{mix} = \frac{m_{mix}}{1.4} \quad (I.3.63)$$

In addition, Soave (1995) also found that it is appropriate to set the binary interaction parameters $k_{ij} = 0$ for alkane systems. For other systems, the binary interaction parameters determined for cubic EOSs can be applied, but care must be taken, since binary interaction parameters are generally related to a specific EOS model.

I.3.3 Comparison of Different EOSs

The performance of the SBWR EOS has been evaluated by comparing calculated densities with experimental values reported in the literature. In addition, the performance of commonly used cubic EOSs has also been evaluated. The investigated cubic EOSs are the PR, the SRK, and the PRSV along with the SRK using a Peneloux correction. The evaluation has been performed on three fluids for which sufficient experimental data exist over wide ranges of temperature and pressure. The three fluids are methane, n-hexane, and n-decane, since this work is related to hydrocarbon fluids, but also because these fluids may be of interest for corresponding states models for viscosity estimations. For each fluid the references are given in Appendix A1 along with the number of points (NP), the temperature and pressure ranges. It should be mentioned that some of the references for methane contain measurements of liquid and gaseous densities close to saturation conditions and in the vicinity of the critical point.

In order to evaluate the performance of the investigated density models, the quantities defined in Appendix A2 are used. The calculation of the densities has been

performed using the critical properties and constants reported by Stryjek and Vera (1986). The obtained absolute average deviation (AAD) and absolute maximum deviation (MxD) are given in Table I.8. A comparison of the deviations obtained by the five density models shows that the SBWR model predicts the density of the investigated fluids significantly better than the four cubic EOSs, also close to the saturated conditions studied for methane. For the SBWR EOS the MxD for methane and n-hexane is around 10%, while the MxD is around 20% for the four cubic EOSs. The largest deviations are obtained in the critical region. For n-decane a closer look showed that the largest deviations (25%) obtained with the SBWR EOS are coming from the isochore $V_0 = 723.67 \text{ cm}^3/\text{mole}$ corresponding to a density of 0.1966 g/cm^3 (Gehrig and Lentz 1983) (6 points). The temperature and pressure ranges for this isochore are respectively $623.15 - 673.15 \text{ K}$ and $22.7 - 35.8 \text{ bar}$. These large deviations obtained for this isochore are not in agreement with the deviations obtained for the other data given by Gehrig and Lentz (1983) or the rest of the evaluated data for n-decane, see

		Methane	n-Hexane	n-Decane
<i>T</i> -range [K]		91 – 623	298 – 548	283 – 673
<i>P</i> -range [bar]		0 – 1111	1 – 5640	1 – 3021
NP		1353	387	563
SBWR	AAD%	0.76	1.23	1.75
	MxD%	12.0	7.45	25.1
PR	AAD%	3.78	2.65	5.42
	MxD%	23.8	18.7	16.8
PRSV	AAD%	3.25	2.63	5.40
	MxD%	23.8	18.4	16.6
SRK	AAD%	3.89	9.87	14.46
	MxD%	23.9	25.4	22.9
SRK-Peneloux	AAD%	3.65	3.61	6.04
	MxD%	23.4	21.7	18.3

Table I.8 Performance of five density models.

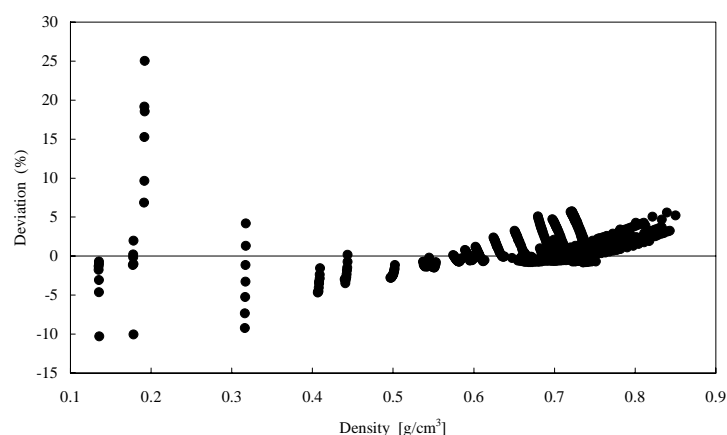


Figure I.13 Deviations between calculated densities by the SBWR EOS for n-decane and experimental values, references reported in Appendix A1, Table A1.3.

Figure I.13. By neglecting this isochore the maximum deviation for the SBWR EOS reduces to 10.3% at 613.15 K and 19.4 bar. This point lies in the critical region and the MxD is of the same order as the MxD obtained for methane and n-hexane.

Figure I.14 shows how the SBWR and the PRSV EOS predict the critical isotherm of methane ($T_c = 190.555$ K). The critical isotherm is satisfactorily predicted by the SBWR EOS, while the PRSV EOS has some problems predicting the dense site close to the critical point. This has also been observed for the other cubic EOSs. For the evaluated cubic EOSs it has been observed that the gas phase density is predicted better than the liquid density. In order to improve the density prediction of liquids a Peneloux correction can be introduced without changing the VLE performance of the EOS. By introducing the Peneloux correction in the SRK EOS much better liquid density predictions are obtained compared with the original SRK EOS, resulting in a lower AAD, see Table I.8. This is especially the case for n-hexane and n-decane, since the evaluated T, P conditions for these compounds correspond primarily to the liquid phase or the dense region. For methane, the introduction of the Peneloux correction is not so pronounced due to the fact that a large number of the evaluated data points are located either near saturation conditions or in the vicinity of the critical point.

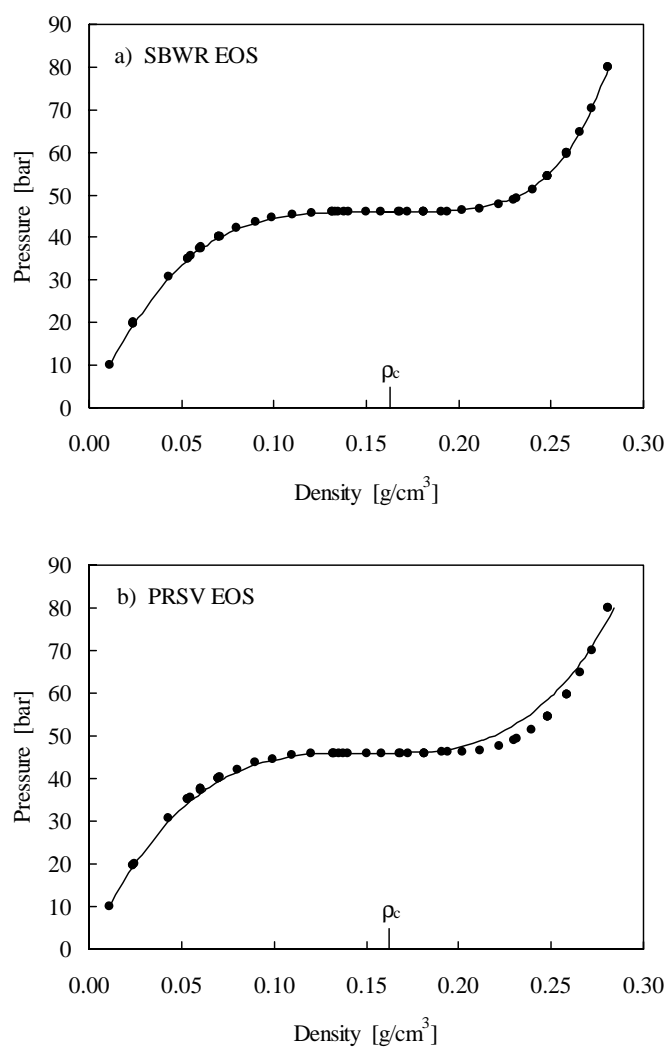


Figure I.14 Comparison of predicted (—) densities of methane at the critical isotherm ($T_c = 190.555$ K) using a) the SBWR EOS and b) the PRSV EOS with experimental values (●) by Kleinrahn et al. (1986) and Händel et al. (1992). ρ_c is the critical density of methane (0.16266 g/cm³).

I.4 Characterization of Petroleum Reservoir Fluids

For compositional dependent viscosity and density models, such as those presented in Chapters I.2 and I.3, it is necessary to know the composition of each compound along with the critical temperature, the critical pressure, the acentric factor, and the molecular weight. However, for petroleum and reservoir fluids it is impossible to determine the exact composition of all compounds in these fluids, since petroleum and reservoir fluids are multicomponent mixtures composed of hydrocarbons, carbon dioxide, nitrogen, and hydrogen sulfide and sometime small amount of helium. It is only the composition of the light components up to C_7 in petroleum and reservoir fluids, which are determined exactly. This is done by a gas chromatographic analysis. For these compounds the properties are well-defined. Generally, the C_6 paraffins are lumped into a C_6 fraction. The heavy hydrocarbon fraction of the mixture is fractionated by distillation into different cuts based on their true boiling point (TBP). The TBP fractions are then related to different carbon numbers and the amount of each fraction is determined. Thus due to cracking of the heavy molecules, it is impossible to distil the entire heavy fraction into TBP fractions. The distillation residue is referred to as the plus fraction. For each of the TBP fractions and the plus fraction the average molecular weight and the specific gravity are determined. These properties have become very important in the numerical characterization of the residue and the calculation of the critical temperature, the critical pressure, and the acentric fraction of each carbon fraction. A more detailed description of the procedure and the equipments used in the compositional analysis of petroleum reservoir fluids is given by Pedersen et al. (1989).

Generally depending on the used TBP distillation equipment, the plus fraction may contain hydrocarbons from C_{11} or C_{20} and up. In order to achieve a more proper description of the fluid for calculation purposes, such as PvT behavior, the plus fraction is separated into additional carbon groups or subgroups. In order to estimate the composition of these subfractions Pedersen et al. (1984b) proposed a procedure based on a logarithmic distribution of the mole fraction x versus the carbon number C , leading to the following expression

$$\ln x_i = A_1 + A_2 C_i \quad (I.4.1)$$

where A_1 and A_2 are adjustable constants related to the considered fluid. These constants can be determined from the mole fraction and the molecular weight of the plus fraction, assuming that the plus fraction can contain subfractions up to C_{80} . The molecular weight of each subfraction is given by

$$M_{w,i} = 14C_i - 4 \quad (I.4.2)$$

In addition, the specific gravity (SG) of each subfraction is given by

$$SG_i = B_1 + B_2 \ln C_i \quad (I.4.3)$$

where B_1 and B_2 are adjustable constants related to the considered fluid. These constants can be determined from the measured specific gravity of the plus fraction and the last defined TBP fraction.

Since, the EOSs and viscosity models require the critical temperature, the critical pressure, and the acentric factor of each compound, different methods have been proposed for obtaining these properties, see e.g. Pedersen et al. (1989). In this work, the method proposed by Aasberg-Petersen and Stenby (1991) is used in order to obtain the critical temperature, the critical pressure, and the acentric factor of each carbon fraction

$$T_{c,i} = d_1 SG_i + d_2 \ln M_{w,i} + d_3 M_{w,i} + \frac{d_4}{M_{w,i}} \quad (I.4.4)$$

$$\ln P_{c,i} = d_5 + d_6 SG_i + \frac{d_7}{M_{w,i}} + \frac{d_8}{M_{w,i}^2} \quad (I.4.5)$$

$$\omega_i = d_9 + d_{10} M_{w,i} + d_{11} SG_i + \frac{d_{12}}{M_{w,i}^2} \quad (I.4.6)$$

The values of these twelve parameters depend on the EOS, which has been chosen for the PvT calculations.

However, the characterized reservoir fluid will then contain more than 80 components, when the above-mentioned characterization procedure is used. This will in generally be too many. Therefore a lumping procedure is introduced in which the carbon fractions are divided into groups having approximately the same weight in order to ensure that each group contribute equally in the PvT calculations. Generally, this procedure is applied to the TBP fractions and the plus fraction. The critical temperature, the critical pressure, and the acentric factor of these groups are obtained by

$$T_{c,j} = \frac{\sum_i x_i M_{w,i} T_{c,i}}{\sum_i x_i M_{w,i}} \quad (\text{I.4.7})$$

$$P_{c,j} = \frac{\sum_i x_i M_{w,i} P_{c,i}}{\sum_i x_i M_{w,i}} \quad (\text{I.4.8})$$

$$\omega_j = \frac{\sum_i x_i M_{w,i} \omega_i}{\sum_i x_i M_{w,i}} \quad (\text{I.4.9})$$

The characterization and lumping procedures described above are the procedures used in the in-house software program SPECS, and which will be used in this work in order to characterize petroleum and reservoir fluids. The required twelve parameters in Eqs.(I.4.4) – (I.4.6) are given for the ALS, the SRK, and the PR EOS in the software program SPECS.

I.5 Evaluation of Existing Viscosity Models

The performance of the compositional dependent viscosity models presented in Chapter I.2, which have all been derived for hydrocarbon fluids, have been evaluated using viscosity data of pure compounds and well-defined mixtures covering wide ranges of temperature and pressure. In this way, it is possible to investigate the performance of the models and their mixing rules on well-defined fluids in order for the possible extension to real reservoir fluids. This will not be the case, if real reservoir fluids are used, because their composition of the different compounds are not exactly known. Therefore, the characterization of the fluid will have an important dependency on the density and viscosity results obtained. Further, it will also be impossible to investigate the performance of the mixing rules in the compositional dependent viscosity models. In addition, it should also be stressed that generally for reported viscosity data of reservoir fluids in the open literature not enough information is given in order to perform a proper characterization.

I.5.1 Evaluation Procedure

A database has been established in order to evaluate the different viscosity models. For this purpose tabulations of recommended viscosities versus temperature and pressure have been found to be very useful. In this way, a more equal distribution of the data points is obtained over wide ranges of temperature and pressure compared with experimental data taken from different sources. Due to their importance in the petrochemical industry some of the better-investigated fluids in terms of viscosity versus temperature and pressure are the hydrocarbon fluids, along with nitrogen, carbon dioxide, and water. By smoothing experimental viscosity measurements, temperature and pressure tabulations of recommended viscosities have been obtained. Stephan and Lucas (1979) presented tabulations of the viscosity versus pressure and temperature for approximately 50 different pure fluids, primarily hydrocarbons. But, because of new measurements, especially up to high pressures, new tabulations of recommended viscosities have been reported for e.g. methane (Younglove and Ely 1987), ethane (Friend et al. 1991), propane (Vogel et al. 1998), nitrogen (Stephan et al. 1987), carbon dioxide (Fenghour et al. 1998), and water (Wagner and Kruse 1998). However,

tabulations of recommended viscosities generally only exist for pure fluids, and therefore experimental data for well-defined hydrocarbon mixtures have been implemented in the database. The database contains viscosity data for 35 pure hydrocarbons, hydrogen sulfide, nitrogen, carbon dioxide, and water along with viscosity data for 39 well-defined mixtures over wide ranges of temperature and pressure. Since most industrial processes are carried out for pressures below 1000 bar, only data up to 1000 bar have been used, although that some references contain data up to very high pressures. In addition, also data below 200 K have not been used. Thus, it should be mentioned that viscosity data up to 1400 bar have been included for the two binary mixtures methane + toluene (Canet 2001), and methane + methylcyclohexane (Tohidi et al. 2001), which have been measured within the framework of the EVIDENT project.

Since the LBC model (Lohrenz et al. 1964) is a sixteenth degree polynomial in the reduced density, an accurate calculation of the viscosity depends strongly on the accuracy of the models used for the density estimations. For the required density estimations in the LBC model the SRK EOS (Soave 1972) with a Peneloux correction (Peneloux et al. 1982), described in Section (I.3.1.2), has been used in order to obtain the LBC-SRK results. However, to improve the predictions the actual critical molar volume reported by Reid et al. (1987) has been used in order to estimate the reduced densities. In case of mixtures, the regular van der Waals mixing rules, Eqs.(I.3.15) and (I.3.16), have been used. In addition, in order to obtain an optimal performance of the LBC model and for comparison reasons, the highly accurate noncubic SBWR EOS (Soave 1995) has been used to obtain the LBC-SBWR results. Since the SBWR EOS also predicts the critical molar volume accurately, the reduced densities used in the LBC-SBWR model have entirely been predicted by the SBWR EOS. In case of mixtures, the density predictions have been performed using the mixing rules derived by Soave (1995) for the SBWR EOS. These mixing rules are described in Section I.3.2.2.

The LABO model (Alliez et al. 1998) has the same structure as the LBC model. In the viscosity calculations with the LABO model, the density of the considered fluids has been estimated by the Lee-Kesler method (Lee and Kesler 1975), as recommended by Alliez et al. (1998). For mixtures, the required critical temperature and critical

pressure have been estimated by Eqs.(I.2.25) and Eq.(I.2.26), which are also used in the CS1 model (Pedersen and Fredenslund 1987) and the CS2 model (Aasberg-Petersen et al. 1991). For the two corresponding states models, CS1 and CS2, their respective original procedure, described by Pedersen and Fredenslund (1987) and Aasberg-Petersen et al. (1991), have been used. This is also the case for the PRVIS model (Guo 1998). For all viscosity and density calculations, the required pure compound properties have been taken from Reid et al. (1987), and no binary interaction parameters have been used in the density estimations of the mixtures.

I.5.2 Results and Discussion

The calculated viscosities have been compared with the reported values in the literature and the obtained average absolute deviation (AAD) and maximum absolute deviation (MxD) are given in Table I.9 for the pure compounds and in Table I.10 for the mixtures. In addition and for comparison purposes, Figures I.15 to I.24 show the performance of the evaluated viscosity models for different pure compounds and mixtures.

As mentioned previously, the calculated viscosities with the LBC model will strongly depend on how accurate the density is estimated. The reason is that the parameters in the LBC model have been derived using experimental viscosity and density data. In Table I.9 and I.10 it can be seen by comparing the LBC-SRK and the LBC-SBWR results that much better viscosity predictions are obtained with the LBC model, when a highly accurate density model, such as the SBWR EOS, is used. With the LBC-SBWR model, the best results for pure fluids are obtained for light hydrocarbons, carbon dioxide, and nitrogen, see e.g. Figures I.15 and I.20. But the LBC-SBWR model also gives satisfactory results for heavy hydrocarbons up to high pressure taking into account that the LBC model was not derived using heavy hydrocarbons, see Figure I.16 and I.17. This is also the case for olefinic compounds. However for naphthenic compounds, the viscosity is not properly and satisfactorily predicted with the LBC-SBWR model. This is also the case for 1-methylnaphthalene, see Figure I.19, but for the rest of the aromatic hydrocarbons used in the evaluation, the resultant deviations can be considered satisfactorily, taken into account that the LBC model has not been derived for such fluids. In case of mixtures, the LBC-SBWR model

	Ref.	NP	T-range [K]	P-range [bar]	LBC-SRK		LBC-SBWR		LABO	
					AAD%	MxD%	AAD%	MxD%	AAD%	MxD%
Methane	1	2112	200 - 600	1 - 1000	2.45	43.7	2.71	29.5	3.19	31.8
Ethane	2	341	200 - 500	1 - 600	6.66	50.2	4.01	11.5	5.13	26.7
Propane	3	682	200 - 600	1 - 1000	9.10	61.4	6.63	15.7	5.41	22.0
i-Butane	4	416	310 - 850	1 - 500	10.1	29.3	12.5	29.9	4.37	19.3
n-Butane	1	1561	200 - 600	1 - 700	6.30	47.2	5.24	18.0	2.76	36.5
i-Pentane	4	354	320 - 750	1 - 600	15.4	34.4	14.3	30.8	7.23	30.8
neo-Pentane	5	46	311 - 444	7 - 552	36.9	49.6	37.0	45.2	32.9	46.1
n-Pentane	4	322	320 - 850	1 - 500	13.2	42.3	10.2	34.6	8.52	28.6
n-Hexane	6	265	289 - 548	1 - 507	16.3	50.7	12.0	34.3	6.01	35.3
n-Heptane	4	357	300 - 620	1 - 500	19.0	73.1	12.8	27.9	5.98	29.4
i-Octane	4	258	290 - 540	1 - 500	17.8	41.3	24.6	32.9	15.5	29.0
n-Octane	4	228	320 - 670	1 - 500	21.8	73.4	13.1	23.7	4.75	17.9
n-Nonane	4	281	300 - 470	1 - 500	34.2	81.1	7.71	26.6	4.29	13.5
n-Decane	7	136	311 - 511	14 - 551	24.7	74.9	10.3	27.5	7.45	16.0
n-Undecane	4	206	300 - 520	1 - 500	31.3	91.3	6.97	24.1	5.55	20.2
n-Dodecane	4	206	300 - 520	1 - 500	17.7	64.8	8.36	22.4	20.8	40.2
n-Tetradecane	8	28	293 - 373	1 - 1000	51.7	113	20.9	54.9	16.7	42.8
n-Pentadecane	8	24	313 - 373	1 - 1000	29.1	68.8	17.2	48.8	18.5	44.2
n-Hexadecane	8	24	313 - 373	1 - 1000	21.7	53.3	19.6	53.2	39.8	64.1
n-Octadecane	8	24	313 - 373	1 - 1000	79.9	89.5	21.3	52.1	83.2	91.4
Cyclohexane	4	283	290 - 520	1 - 500	41.7	57.6	49.6	65.0	43.4	62.9
Methylcyclohexane	4,9	290	290 - 530	1 - 1000	32.9	50.0	38.0	42.2	33.1	45.3
Ethylcyclohexane	4	252	290 - 530	1 - 500	21.3	37.9	31.4	41.5	24.9	37.8
Benzene	4	258	290 - 550	1 - 400	13.3	26.8	19.1	34.7	11.4	31.5
Toluene	4	268	295 - 550	1 - 400	8.59	27.3	5.97	15.0	4.47	14.2
Ethylbenzene	4	188	300 - 560	1 - 400	12.1	38.6	10.4	25.9	4.98	16.8
Butylbenzene	8	30	293 - 373	1 - 1000	42.4	98.0	10.9	29.9	16.8	38.8
Naphthalene	10	23	375 - 454	1 - 1013	42.4	65.9	5.34	13.3	15.9	30.2
1-Methylnaphthalene	9	18	303 - 343	1 - 1000	68.6	82.9	45.9	65.4	68.2	81.2
Phenanthrene	10	19	396 - 573	1 - 1013	99.5	187	13.7	33.9	50.4	81.3
Ethylene	4	380	300 - 700	1 - 800	4.31	16.9	2.79	7.89	2.85	10.1
Propylene	4	575	290 - 650	1 - 900	10.8	39.3	9.98	36.5	4.74	37.9
1-Hexene	4	149	280 - 375	1 - 450	19.4	60.0	12.6	47.5	9.29	30.6
1-Heptene	4	200	300 - 490	1 - 500	127	228	9.15	21.7	72.3	117
1-Octene	4	202	300 - 490	1 - 500	16.0	44.0	10.2	36.0	30.1	9.54
Carbon Dioxide	11	1000	200 - 1000	1 - 1000	5.05	24.7	4.95	24.4	3.13	9.42
Nitrogen	12	1287	200 - 1000	1 - 1000	2.84	7.10	2.23	7.95	3.00	9.18
Hydrogen Sulfide	13	33	388 - 413	100 - 500	45.3	69.9	42.6	69.1	36.1	69.6
Water	14	6885	273 - 1073	1 - 1000	21.5	71.0	35.2	137	22.2	80.6

Table I.9 Performance of viscosity models for pure compounds. NP is the number of data points.

1) Younglove and Ely (1987), 2) Friend et al. (1991), 3) Vogel et al. (1998), 4) Stephan and Lucas (1979), 5) Gonzales and Lee (1968), 6) Agaev and Golubev (1963), 7) Lee and Ellington (1965), 8) Ducuolombier et al. (1986), 9) Baylaucq et al. (1997a), 10) Roetling et al. (1987), 11) Fenghour et al. (1998), 12) Stephan et al. (1987), 13) Monteil et al. (1969), and 14) Wagner and Kruse (1998).

	Ref.	NP	T-range [K]	P-range [bar]	CS1		CS2		PRVIS	
					AAD%	MxD%	AAD%	MxD%	AAD%	MxD%
Methane	1	2112	200 - 600	1 - 1000	0.61	5.40	1.45	13.7	7.07	41.1
Ethane	2	341	200 - 500	1 - 600	3.24	77.3	8.67	84.6	5.82	60.8
Propane	3	682	200 - 600	1 - 1000	5.82	71.5	16.9	91.6	10.1	73.3
i-Butane	4	416	310 - 850	1 - 500	13.2	78.2	18.9	80.1	8.90	43.9
n-Butane	1	1561	200 - 600	1 - 700	16.9	86.9	24.0	79.8	11.6	75.8
i-Pentane	4	354	320 - 750	1 - 600	16.5	79.6	15.1	73.7	8.24	56.9
neo-Pentane	5	46	311 - 444	7 - 552	19.2	78.8	24.7	42.9	30.7	67.5
n-Pentane	4	322	320 - 850	1 - 500	14.1	80.8	16.7	77.1	6.34	48.6
n-Hexane	6	265	289 - 548	1 - 507	21.4	81.0	17.8	77.0	23.0	96.4
n-Heptane	4	357	300 - 620	1 - 500	25.5	79.2	22.6	76.7	25.8	104
i-Octane	4	258	290 - 540	1 - 500	16.1	80.7	9.74	70.8	15.4	63.7
n-Octane	4	228	320 - 670	1 - 500	26.7	79.1	23.0	82.0	14.5	84.2
n-Nonane	4	281	300 - 470	1 - 500	29.0	73.7	3.55	9.30	5.20	24.6
n-Decane	7	136	311 - 511	14 - 551	27.9	70.2	5.51	23.2	6.22	30.1
n-Undecane	4	206	300 - 520	1 - 500	31.9	84.7	5.90	23.2	7.06	28.3
n-Dodecane	4	206	300 - 520	1 - 500	33.0	89.1	6.88	23.7	7.27	28.5
n-Tetradecane	8	28	293 - 373	1 - 1000	46.2	76.9	24.4	31.1	15.5	37.8
n-Pentadecane	8	24	313 - 373	1 - 1000	45.9	70.9	24.9	30.9	15.9	45.7
n-Hexadecane	8	24	313 - 373	1 - 1000	49.2	76.3	30.2	38.9	16.4	49.7
n-Octadecane	8	24	313 - 373	1 - 1000	60.9	85.5	47.2	70.3	16.3	36.3
Cyclohexane	4	283	290 - 520	1 - 500	29.2	48.4	41.0	59.7	50.0	74.0
Methylcyclohexane	4,9	290	290 - 530	1 - 1000	7.74	17.6	21.6	35.7	42.2	68.3
Ethylcyclohexane	4	252	290 - 530	1 - 500	10.2	38.7	9.92	19.4	37.6	68.8
Benzene	4	258	290 - 550	1 - 400	13.2	38.1	15.2	33.9	20.0	57.4
Toluene	4	268	295 - 550	1 - 400	32.5	61.6	11.2	31.8	11.8	44.7
Ethylbenzene	4	188	300 - 560	1 - 400	30.6	59.2	10.7	24.5	8.87	46.1
Butylbenzene	8	30	293 - 373	1 - 1000	45.6	82.9	17.4	29.4	20.6	53.6
Naphthalene	10	23	375 - 454	1 - 1013	58.2	78.5	21.4	40.5	11.4	28.6
1-Methylnaphthalene	9	18	303 - 343	1 - 1000	30.2	37.7	24.0	39.8	53.1	73.8
Phenanthrene	10	19	396 - 573	1 - 1013	98.3	125	54.1	75.0	21.4	48.6
Ethylene	4	380	300 - 700	1 - 800	1.51	7.90	5.12	27.3	4.83	26.8
Propylene	4	575	290 - 650	1 - 900	3.61	74.2	8.26	79.2	6.49	37.0
1-Hexene	4	149	280 - 375	1 - 450	41.6	103	13.1	45.0	6.85	36.2
1-Heptene	4	200	300 - 490	1 - 500	41.1	77.7	13.2	31.0	14.3	61.2
1-Octene	4	202	300 - 490	1 - 500	37.1	74.6	7.34	24.2	11.9	52.0
Carbon Dioxide	11	1000	200 - 1000	1 - 1000	9.44	50.2	17.3	56.7	11.2	44.8
Nitrogen	12	1287	200 - 1000	1 - 1000	27.2	17.2	18.8	53.8	51.8	271
Hydrogen Sulfide	13	33	388 - 413	100 - 500	36.4	69.0	37.8	66.1	36.5	65.5
Water	14	6885	273 - 1073	1 - 1000	21.7	87.3	20.9	85.5	-----	-----

Table I.9 *Continued.*

1) Younglove and Ely (1987), 2) Friend et al. (1991), 3) Vogel et al. (1998), 4) Stephan and Lucas (1979), 5) Gonzales and Lee (1968), 6) Agaev and Golubev (1963), 7) Lee and Ellington (1965), 8) Ducuolombier et al. (1986), 9) Baylaucq et al. (1997a), 10) Roetling et al. (1987), 11) Fenghour et al. (1998), 12) Stephan et al. (1987), 13) Monteil et al. (1969), and 14) Wagner and Kruse (1998).

	Ref.	NP	T-range [K]	P-range [bar]	LBC-SRK		LBC-SBWR		LABO	
					AAD%	MxD%	AAD%	MxD%	AAD%	MxD%
Methane + Ethane	1	250	120 - 300	15 - 349	11.0	34.6	2.87	11.9	17.8	40.8
Methane + Propane	2	282	311 - 411	1 - 552	3.55	20.3	3.51	16.7	4.01	28.2
Methane + n-Butane	3	104	278 - 478	1 - 358	8.53	20.7	9.58	16.0	8.68	18.1
Methane + n-Hexane	4	53	295 - 451	150 - 428	8.49	33.7	10.9	18.6	20.9	31.8
Methane + n-Decane	5	96	292 - 431	98 - 419	11.3	46.7	17.8	25.9	25.5	40.0
n-Pentane + n-Octane	6	295	298 - 373	1 - 250	16.0	53.9	8.85	23.1	6.39	17.4
n-Pentane + n-Decane	7	312	298 - 373	1 - 250	11.8	62.1	9.70	23.7	9.82	20.1
n-Hexane + n-Heptane	8	53	303 - 323	1 - 717	44.1	67.9	5.98	16.7	13.0	19.2
n-Hexane + n-Hexadecane	9	93	298 - 373	1 - 1039	20.0	74.3	13.4	46.9	30.5	59.9
n-Heptane + n-Octane	10	172	293 - 471	1 - 491	41.0	86.1	9.32	26.7	11.2	28.2
n-Heptane + n-Nonane	8	57	303 - 323	1 - 718	46.6	79.0	5.42	14.9	11.6	18.7
n-Heptane + n-Decane	11	12	293 - 313	1 - 1000	51.8	72.6	14.7	31.7	17.3	24.9
n-Heptane + n-Undecane	12	27	303 - 323	1 - 719	40.6	66.5	4.49	13.1	5.94	14.9
n-Octane + n-Decane	13	324	298 - 373	1 - 250	23.4	47.1	6.18	14.9	3.95	15.4
Isooctane + Ethylene	14	28	298 - 453	500 - 800	17.2	40.3	15.6	27.5	11.5	31.4
n-Decane + n-Hexadecane	11	54	313 - 353	1 - 1000	17.6	49.7	10.5	30.5	26.5	51.5
n-Pentane + n-Octane + n-Decane	15	530	298 - 373	1 - 250	19.3	47.3	4.93	13.9	3.09	13.5
n-Decane + n-Dodecane + n-Tetradecane + n-Hexadecane	11	18	313 - 353	1 - 1000	16.4	40.0	10.5	28.3	23.3	36.8
Methane + Carbon Dioxide	16	132	323 - 474	34 - 692	2.79	12.7	3.59	12.5	4.46	16.9
Ethane + Carbon Dioxide	17+18	362	210 - 500	17 - 614	10.4	58.9	8.89	59.7	20.2	56.6
n-Decane + Carbon Dioxide	19	57	311 - 403	67 - 347	37.3	67.1	5.38	17.3	36.9	69.2
n-Pentane + n-Decane + CO ₂	20	10	354 - 401	25 - 49	4.19	7.14	10.6	15.8	12.9	23.1
n-C4 + n-C6 + n-C10 + CO ₂	20	10	324 - 395	25 - 49	13.3	32.6	9.32	23.4	25.0	56.0
n-C5+n-C6+n-C7+n-C10+CO ₂	20	8	360 - 395	25 - 49	4.58	8.99	12.1	16.6	14.5	28.2
Methane + Benzene	4	102	293 - 433	125 - 475	4.83	18.9	13.9	24.5	11.4	29.2
Methane + Cyclohexane	4	57	295 - 443	102 - 407	22.8	39.0	32.2	49.4	12.4	35.2
Methane + Methylcyclohexane	21	101	323 - 423	207 - 1393	6.78	25.2	8.01	26.2	10.9	21.7
Methane + Toluene	22	280	293 - 373	200 - 1400	19.0	44.0	6.57	17.1	20.8	41.2
Ethylene + Ethylbenzene	14	26	298 - 453	500 - 800	26.3	56.4	9.67	23.6	19.6	43.2
n-Hexane + Cyclohexane	23	47	298 - 373	1 - 1000	24.0	66.3	20.8	49.5	18.6	50.8
n-Hexane + Toluene	24	60	298 - 373	1 - 1019	28.9	72.0	7.73	27.6	6.55	17.5
n-Heptane + Methylcyclohexane	25	126	303 - 343	1 - 1000	26.0	88.4	14.5	33.9	13.9	35.6
n-Heptane + 1-Methylnaphthalene	25	126	303 - 343	1 - 1000	31.5	75.2	14.4	49.2	24.9	70.1
n-Octane + Cyclohexane	26	86	298 - 348	1 - 1039	22.3	69.6	21.7	49.4	16.4	48.0
n-Dodecane + Cyclohexane	26	65	298 - 348	1 - 1020	22.5	44.3	27.8	53.5	38.5	53.9
n-Hexadecane + Cyclohexane	26	55	298 - 348	1 - 1017	31.0	49.9	33.9	56.7	54.8	67.9
Me-cyclohexane + 1-Me-naphthalene	25	126	303 - 343	1 - 1000	41.6	76.8	28.7	56.5	45.4	74.8
Toluene + 1-Methylnaphthalene	27	90	298 - 363	1 - 1000	29.4	69.9	15.5	46.7	31.7	66.9
n-Heptane + Methylcyclohexane + 1-Methylnaphthalene	28	378	303 - 343	1 - 1000	20.3	65.4	12.3	42.1	22.4	63.8

Table I.10 Performance of viscosity models for mixtures. NP is the number of data points.

1) Diller (1984), 2) Giddings et al. (1966), 3) Carmichael et al. (1967), 4) Berstad (1989), 5) Knapstad et al. (1990), 6) Barrufet et al. (1999), 7) Estrada-Baltazar et al. (1998b), 8) Assael et al. (1992), 9) Dymond et al. (1980), 10) Aleskerov et al. (1979), 11) Ducoulombier et al. (1986), 12) Assael et al. (1991), 13) Estrada-Baltazar et al. (1998a), 14) Krahn and Luft (1994), 15) Iglesias-Silva et al (1999), 16) de Witt and Thodos (1977), 17) Diller et al. (1988), 18) Diller and Ely (1989), 19) Cullick and Mathis (1984), 20) Barrufet et al. (1996), 21) Tohidi et al. (2001), 22) Canet et al. (2001), 23) Isdale et al. (1979), 24) Dymond et al. (1991), 25) Baylaucq et al. (1997a), 26) Tanaka et al. (1991), 27) Et-Tahir et al. (1995), 28) Baylaucq et al. (1997b).

	Ref.	NP	T-range [K]	P-range [bar]	CS1		CS2		PRVIS	
					AAD%	MxD%	AAD%	MxD%	AAD%	MxD%
Methane + Ethane	1	250	120 - 300	15 - 349	8.72	87.2	4.35	17.7	22.1	76.9
Methane + Propane	2	282	311 - 411	1 - 552	6.96	78.8	6.53	32.9	20.6	67.4
Methane + n-Butane	3	104	278 - 478	1 - 358	5.65	21.6	8.22	38.9	16.6	50.9
Methane + n-Hexane	4	53	295 - 451	150 - 428	11.5	23.2	9.27	24.8	35.5	80.0
Methane + n-Decane	5	96	292 - 431	98 - 419	6.83	32.2	9.51	23.4	14.0	41.1
n-Pentane + n-Octane	6	295	298 - 373	1 - 250	16.6	46.2	7.73	18.2	9.80	66.7
n-Pentane + n-Decane	7	312	298 - 373	1 - 250	14.2	36.7	9.51	18.3	12.7	59.5
n-Hexane + n-Heptane	8	53	303 - 323	1 - 717	39.1	63.6	3.76	11.1	3.11	12.5
n-Hexane + n-Hexadecane	9	93	298 - 373	1 - 1039	22.0	58.5	7.50	18.9	8.95	36.0
n-Heptane + n-Octane	10	172	293 - 471	1 - 491	30.3	72.1	5.91	16.0	11.0	49.6
n-Heptane + n-Nonane	8	57	303 - 323	1 - 718	36.1	57.3	3.98	11.2	7.03	16.8
n-Heptane + n-Decane	11	12	293 - 313	1 - 1000	45.5	65.2	9.16	14.6	7.00	21.6
n-Heptane + n-Undecane	12	27	303 - 323	1 - 719	32.0	53.1	3.65	11.9	8.05	21.6
n-Octane + n-Decane	13	324	298 - 373	1 - 250	18.0	42.3	6.47	12.8	5.69	8.06
Isooctane + Ethylene	14	28	298 - 453	500 - 800	7.16	23.2	12.2	19.7	12.9	38.3
n-Decane + n-Hexadecane	11	54	313 - 353	1 - 1000	33.0	57.7	8.16	19.3	15.3	43.2
n-Pentane + n-Octane + n-Decane	15	530	298 - 373	1 - 250	21.4	48.1	5.20	12.4	7.41	40.6
n-Decane + n-Dodecane + n-Tetradecane + n-Hexadecane	11	18	313 - 353	1 - 1000	31.8	55.2	7.83	14.0	17.2	41.8
Methane + Carbon Dioxide	16	132	323 - 474	34 - 692	7.13	19.1	10.5	22.6	3.80	18.6
Ethane + Carbon Dioxide	17+18	362	210 - 500	17 - 614	15.8	81.0	14.4	64.9	12.9	48.2
n-Decane + Carbon Dioxide	19	57	311 - 403	67 - 347	24.5	51.0	4.76	12.9	5.37	17.8
n-Pentane + n-Decane + CO ₂	20	10	354 - 401	25 - 49	15.1	20.5	5.73	10.8	2.52	6.57
n-C4 + n-C6 + n-C10 + CO ₂	20	10	324 - 395	25 - 49	17.8	29.8	5.61	12.9	7.68	13.8
n-C5+n-C6+n-C7+n-C10+CO ₂	20	8	360 - 395	25 - 49	15.3	25.7	6.27	11.2	4.36	12.4
Methane + Benzene	4	102	293 - 433	125 - 475	9.76	25.4	8.77	26.3	24.5	58.4
Methane + Cyclohexane	4	57	295 - 443	102 - 407	11.7	33.2	18.7	44.7	18.9	51.2
Methane + Methylcyclohexane	21	101	323 - 423	207 - 1393	7.87	88.6	7.57	21.5	18.1	51.8
Methane + Toluene	22	280	293 - 373	200 - 1400	12.5	31.2	4.39	16.5	15.2	47.6
Ethylene + Ethylbenzene	14	26	298 - 453	500 - 800	28.8	86.9	11.2	19.6	21.9	55.5
n-Hexane + Cyclohexane	23	47	298 - 373	1 - 1000	16.0	43.5	22.3	50.7	31.8	69.2
n-Hexane + Toluene	24	60	298 - 373	1 - 1019	38.7	71.7	3.80	9.51	18.6	61.2
n-Heptane + Methylcyclohexane	25	126	303 - 343	1 - 1000	28.5	70.3	10.9	27.9	30.8	69.4
n-Heptane + 1-Methylnaphthalene	25	126	303 - 343	1 - 1000	53.6	81.4	25.8	42.0	16.2	61.5
n-Octane + Cyclohexane	26	86	298 - 348	1 - 1039	17.4	50.6	22.3	47.8	38.4	69.1
n-Dodecane + Cyclohexane	26	65	298 - 348	1 - 1020	16.6	36.9	24.6	49.1	48.2	70.1
n-Hexadecane + Cyclohexane	26	55	298 - 348	1 - 1017	19.7	42.0	26.1	52.7	49.3	77.9
Me-cyclohexane + 1-Me-naphthalene	25	126	303 - 343	1 - 1000	24.5	50.8	14.1	34.4	46.2	78.8
Toluene + 1-Methylnaphthalene	27	90	298 - 363	1 - 1000	41.0	75.5	17.1	42.0	37.2	70.9
n-Heptane + Methylcyclohexane + 1-Methylnaphthalene	28	378	303 - 343	1 - 1000	38.0	70.7	11.8	35.9	26.3	71.6

Table I.10 *Continued.*

1) Diller (1984), 2) Giddings et al. (1966), 3) Carmichael et al. (1967), 4) Berstad (1989), 5) Knapstad et al. (1990), 6) Barrufet et al. (1999), 7) Estrada-Baltazar et al. (1998b), 8) Assael et al. (1992), 9) Dymond et al. (1980), 10) Aleskerov et al. (1979), 11) Ducoulombier et al. (1986), 12) Assael et al. (1991), 13) Estrada-Baltazar et al. (1998a), 14) Krahn and Luft (1994), 15) Iglesias-Silva et al (1999), 16) de Witt and Thodos (1977), 17) Diller et al. (1988), 18) Diller and Ely (1989), 19) Cullick and Mathis (1984), 20) Barrufet et al. (1996), 21) Tohidi et al. (2001), 22) Canet et al. (2001), 23) Isdale et al. (1979), 24) Dymond et al. (1991), 25) Baylaucq et al. (1997a), 26) Tanaka et al. (1991), 27) Et-Tahir et al. (1995), 28) Baylaucq et al. (1997b).

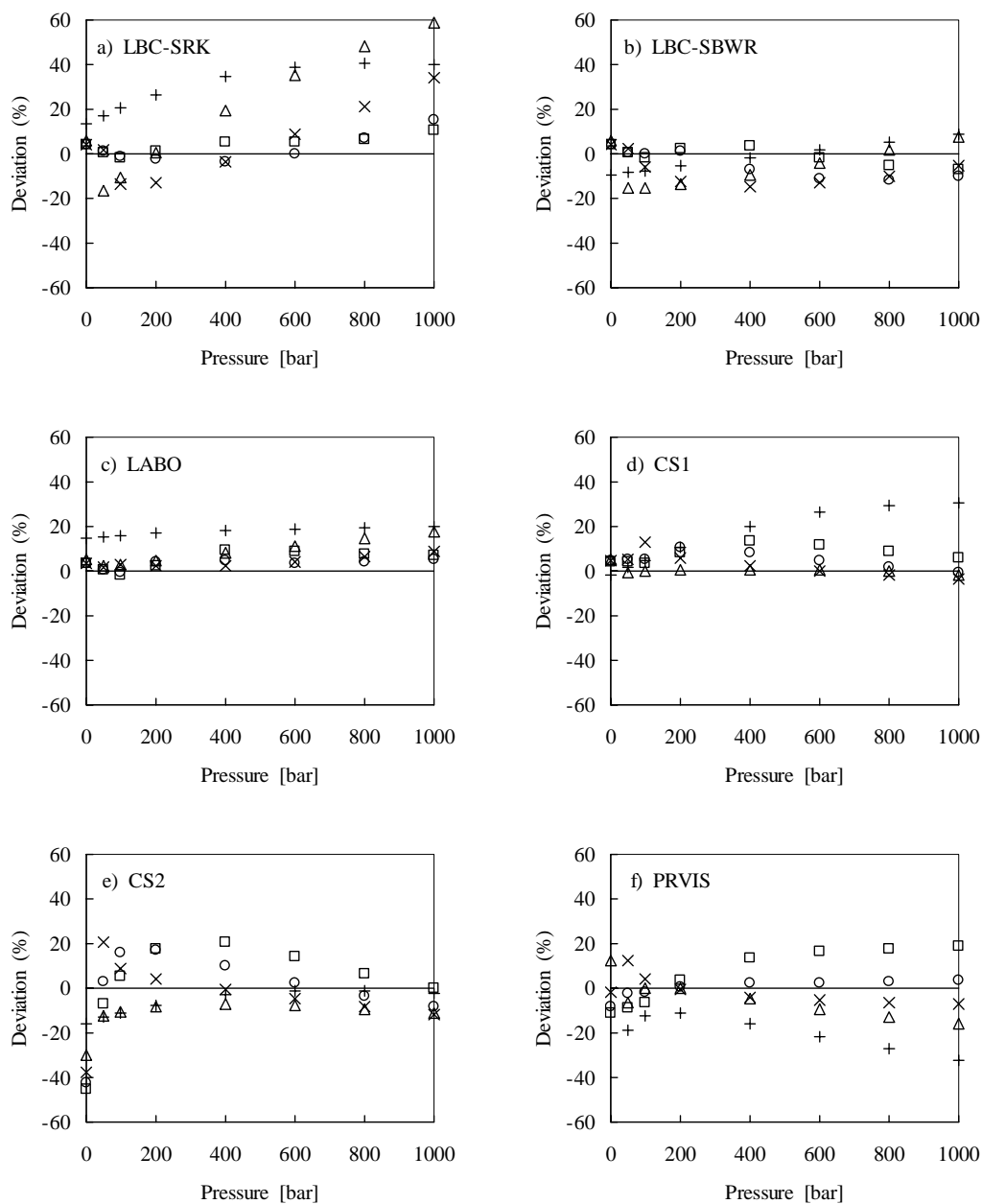


Figure I.15 Deviations in viscosity predictions for propane using different viscosity models compared with literature data (Vogel et al. 1998) versus pressure at 200 K (+), 300 K (Δ), 400 K (×), 500 K (○), and 600 K (□).

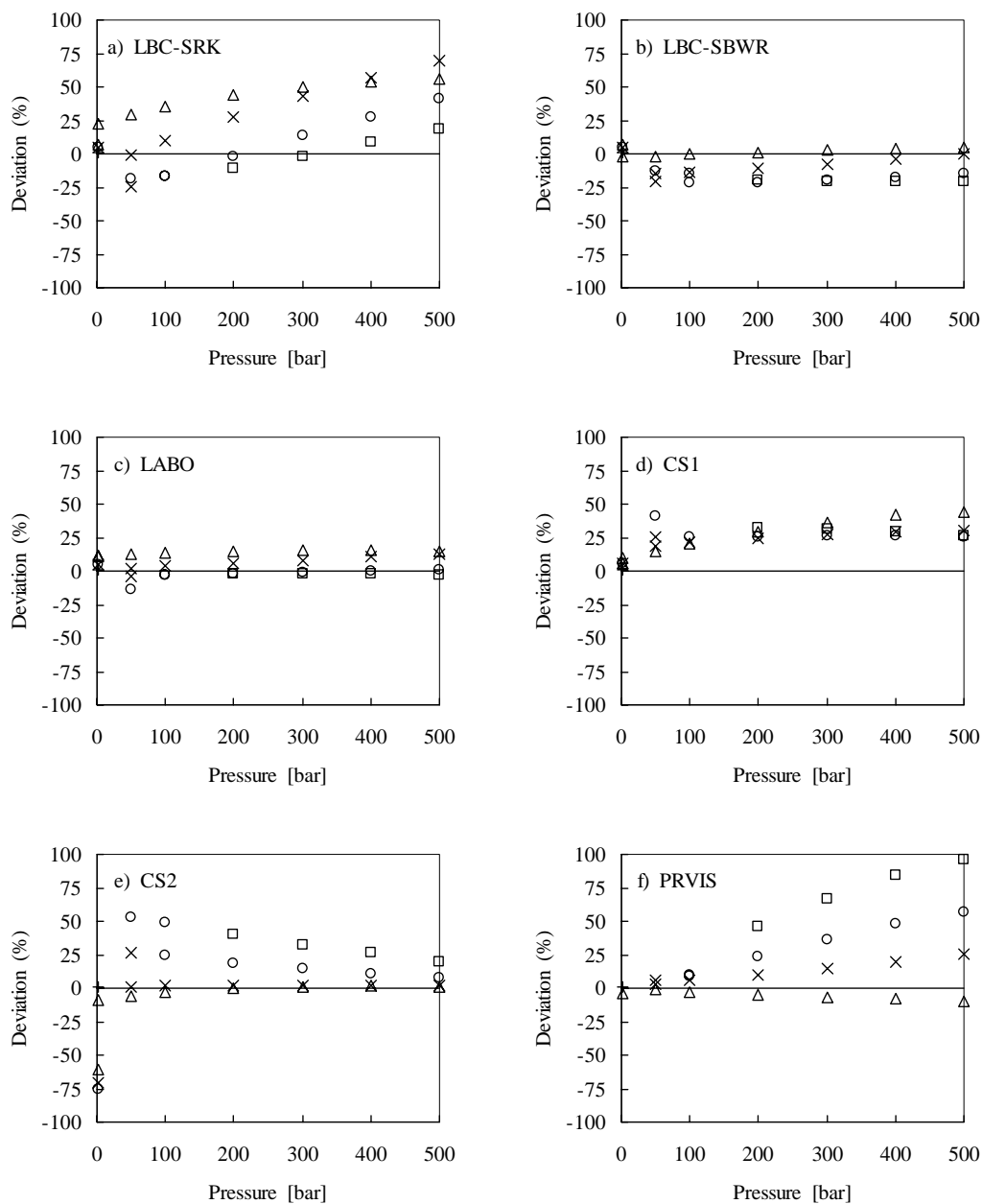


Figure I.16 Deviations in viscosity predictions for n-heptane using different viscosity models compared with literature data (Stephan and Lucas 1979) versus pressure at 300 K (Δ), 400 K (×), 500 K (○), and 600 K (□).

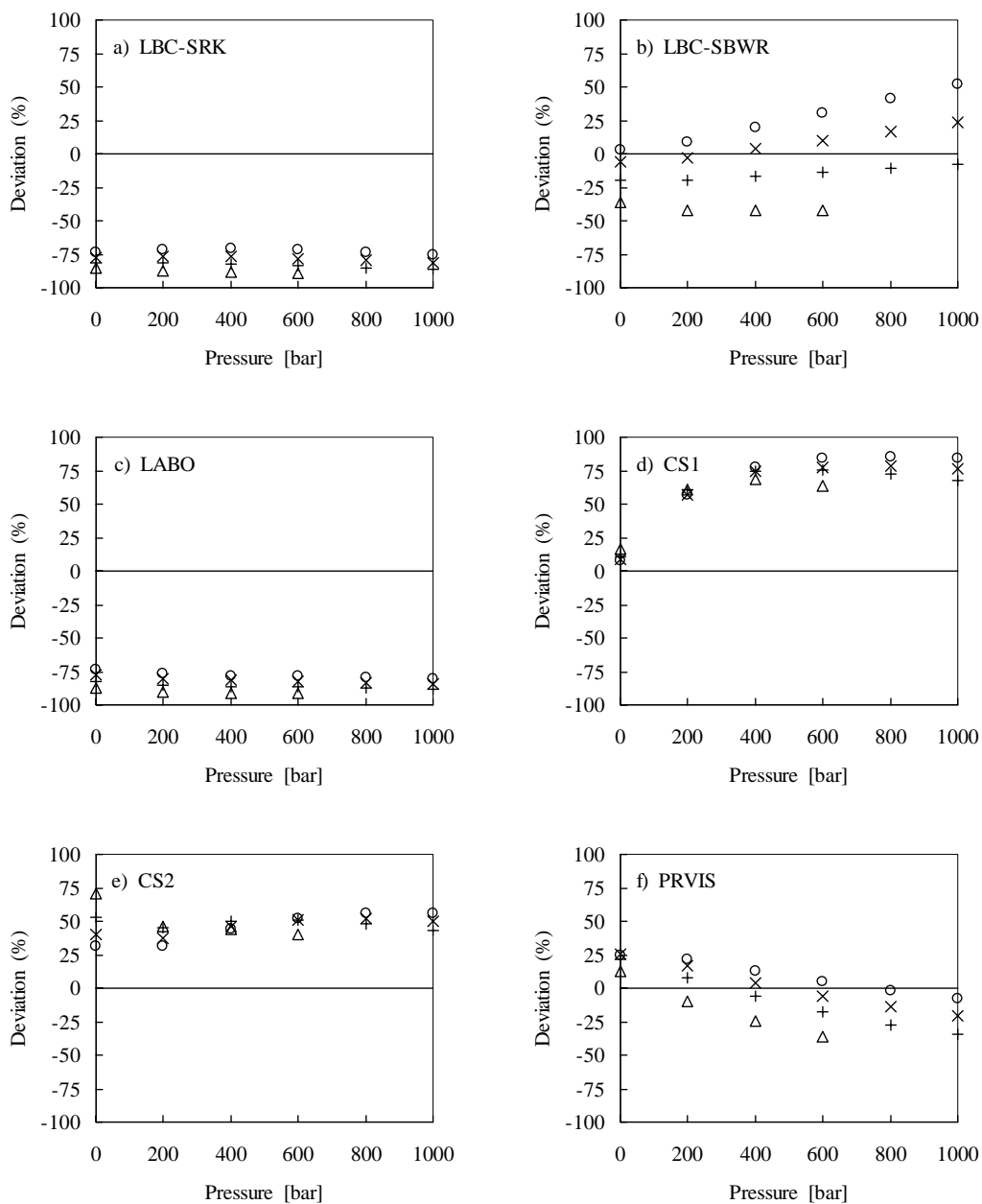


Figure I.17 Deviations in viscosity predictions for n-octadecane using different viscosity models compared with literature data (Ducoulombier et al. 1986) versus pressure at 313.15 K (Δ), 333.15 K (+), 353.15 K (\times), and 373.15 K (\circ).

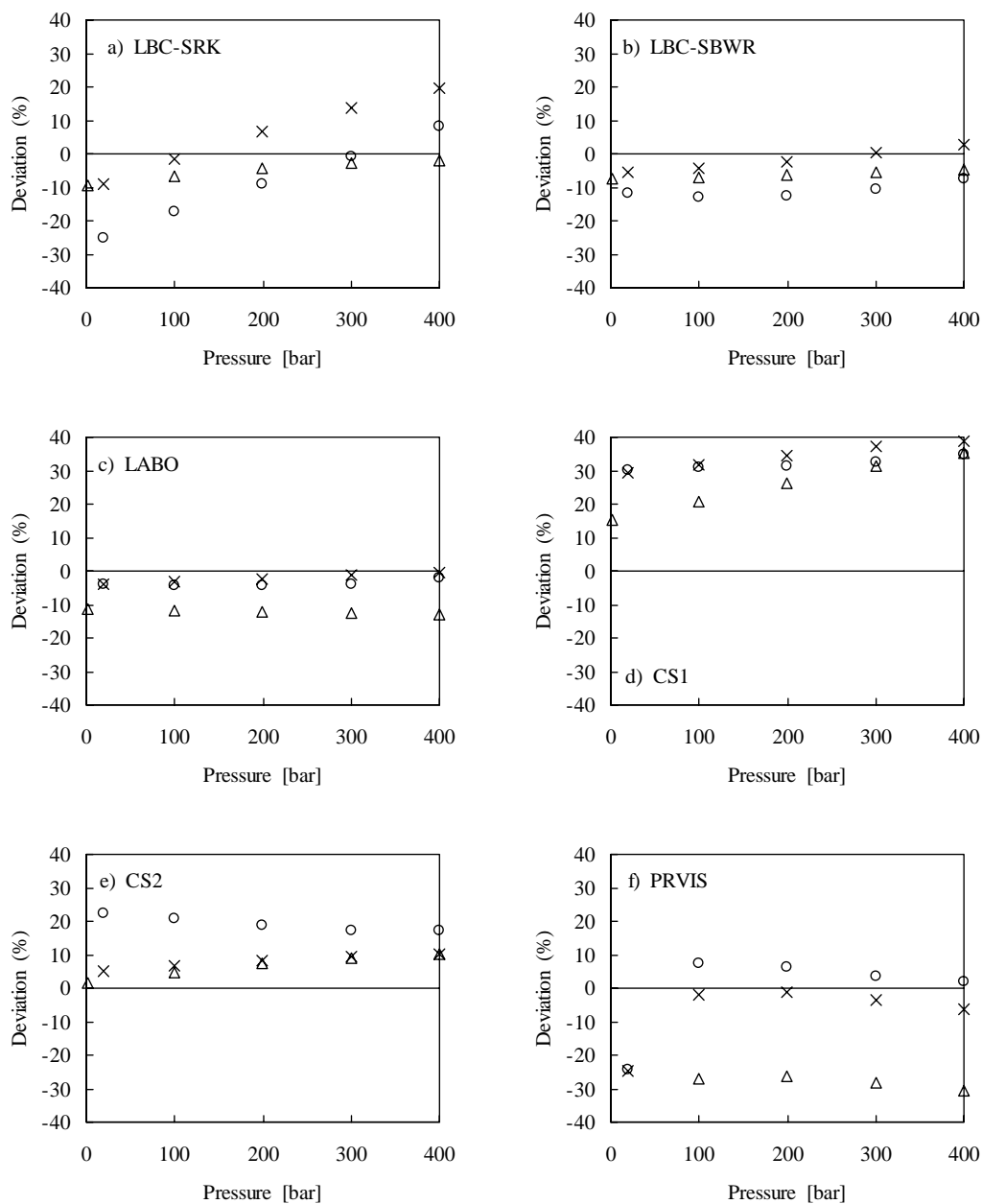


Figure I.18 Deviations in viscosity predictions for toluene using different viscosity models compared with literature data (Stephan and Lucas 1979) versus pressure at 300 K (Δ), 400 K (\times), and 500 K (\circ).

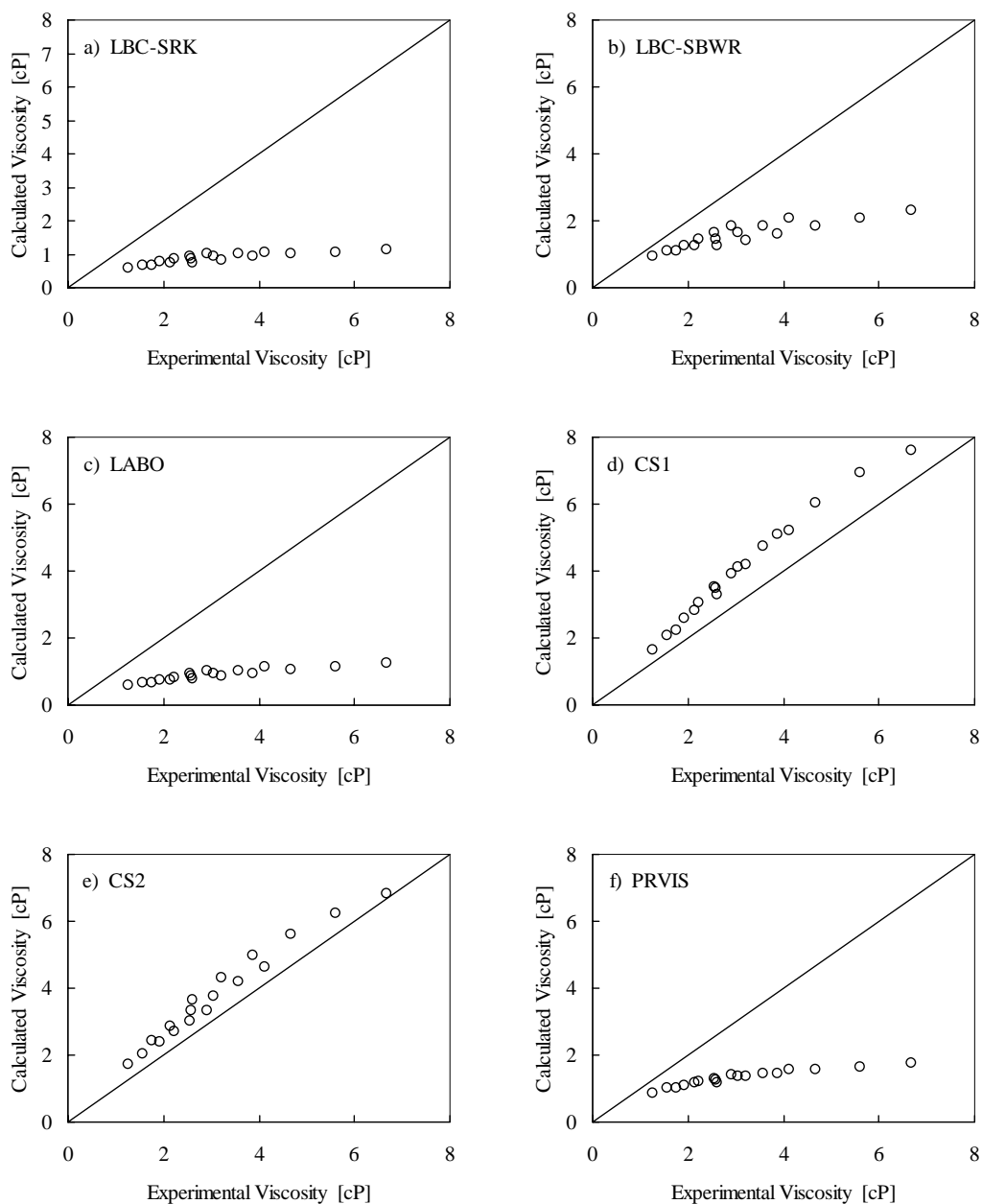


Figure I.19 Comparison of experimental viscosities of 1-methylnaphthalene (Baylaucq et al. 1997a) with viscosities calculated by different models in the temperature range 303 – 343 K and for pressures ranging from 1 to 1000 bar.

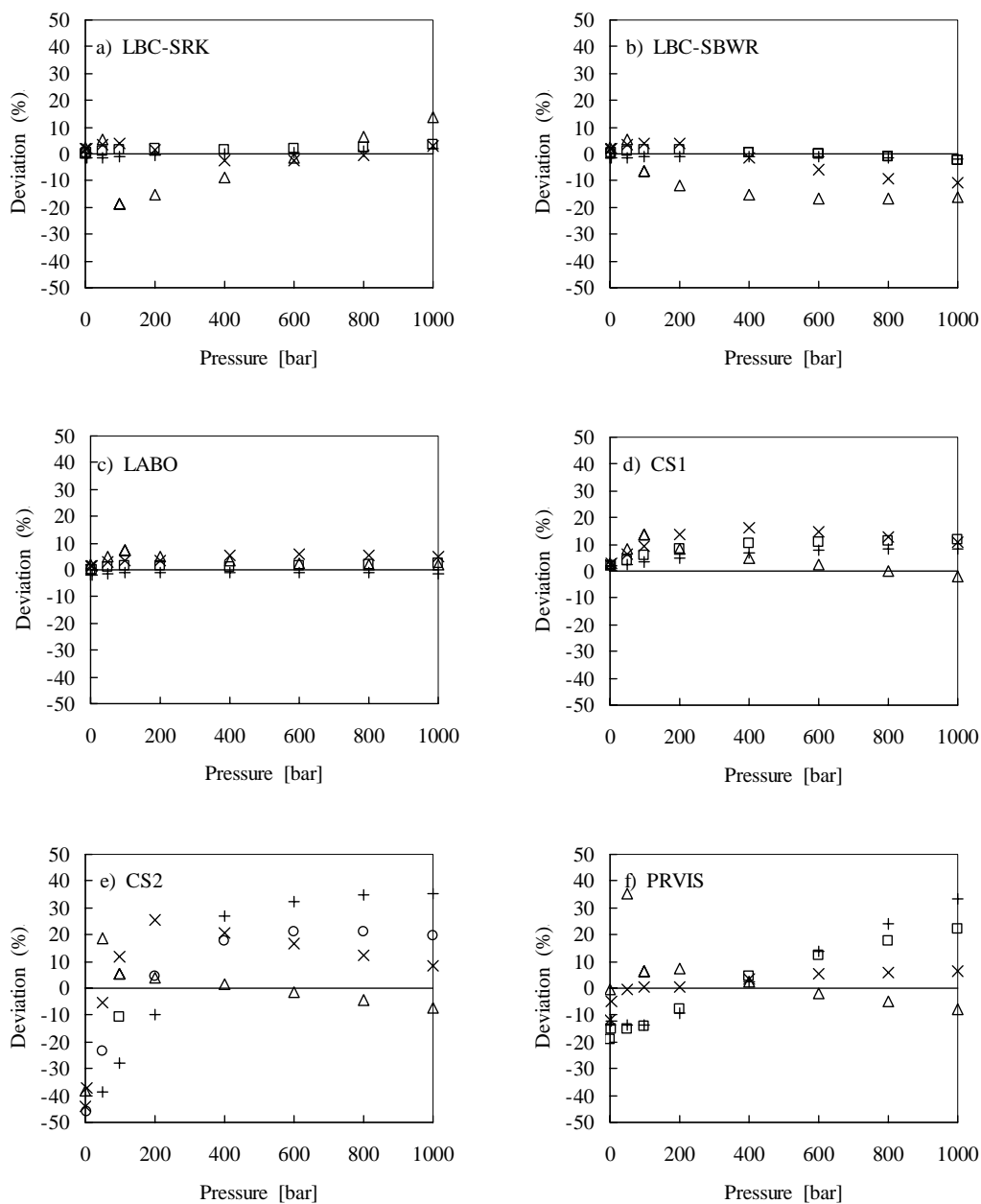


Figure I.20 Deviations in viscosity predictions for carbon dioxide using different viscosity models compared with literature data (Fenghour 1998) versus pressure at 300 K (Δ), 400 K (×), 600 K (□), and 1000 K (+).

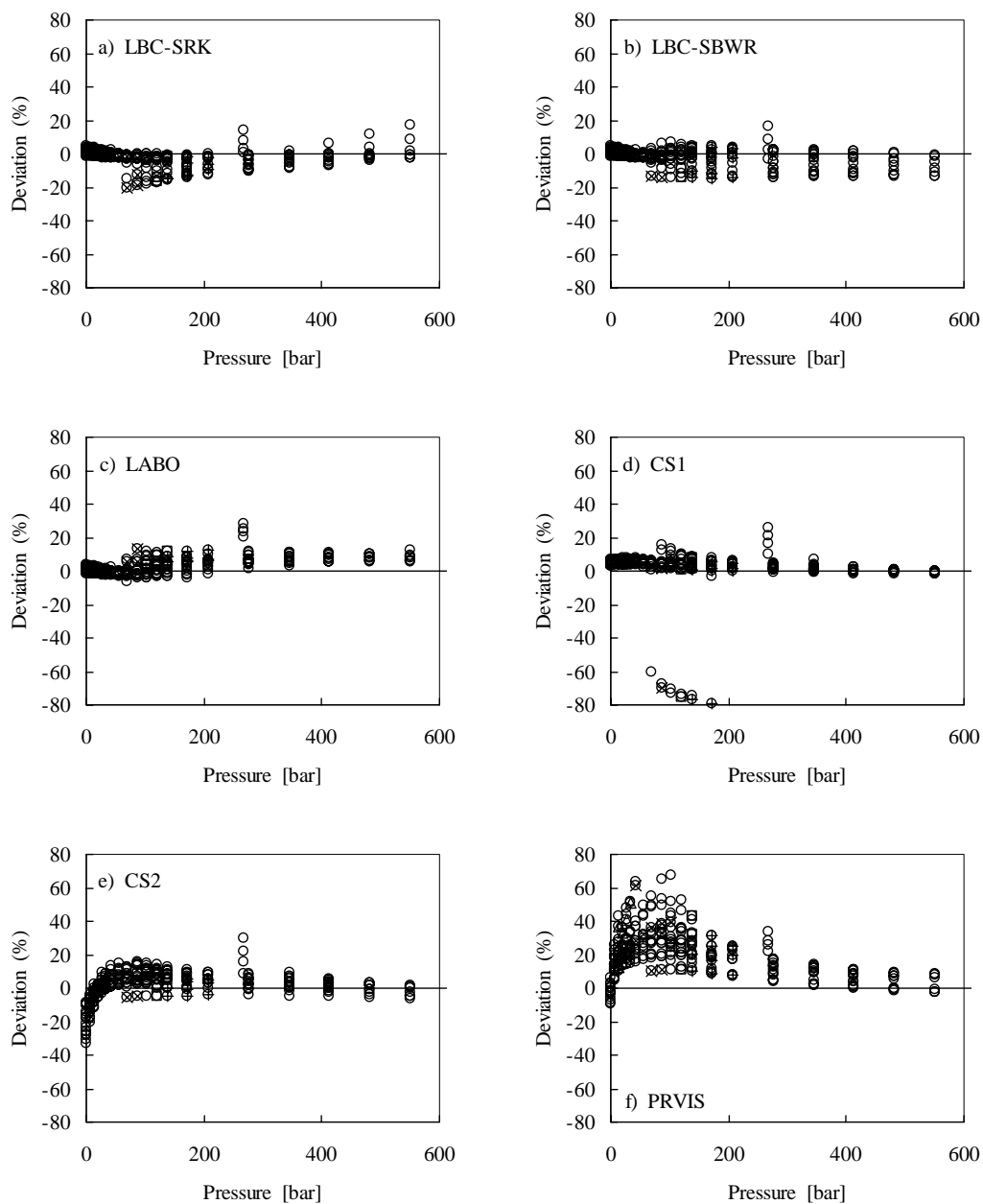


Figure I.21 Deviations in viscosity predictions for binary mixtures composed of methane + propane using different viscosity models compared with all 282 literature data (Giddings et al. 1966) in the temperature range 311 – 411 K and for pressures ranging from 1 – 552 bar..

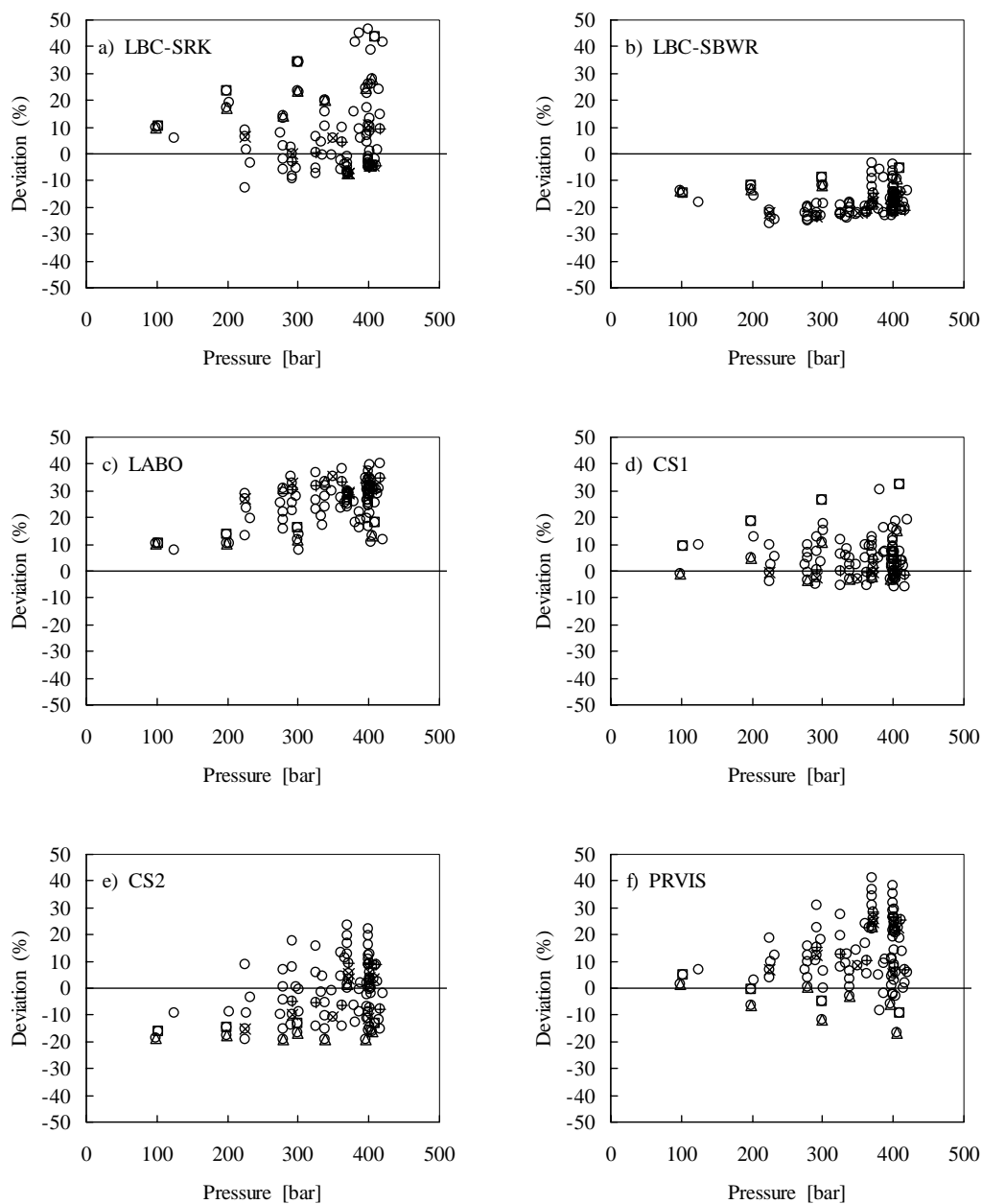


Figure I.22 Deviations in viscosity predictions for binary mixtures composed of methane + n-decane using different viscosity models compared with all 96 literature data (Knapstad et al. 1990) in the temperature range 292 – 431 K and for pressures ranging from 98 – 419 bar.

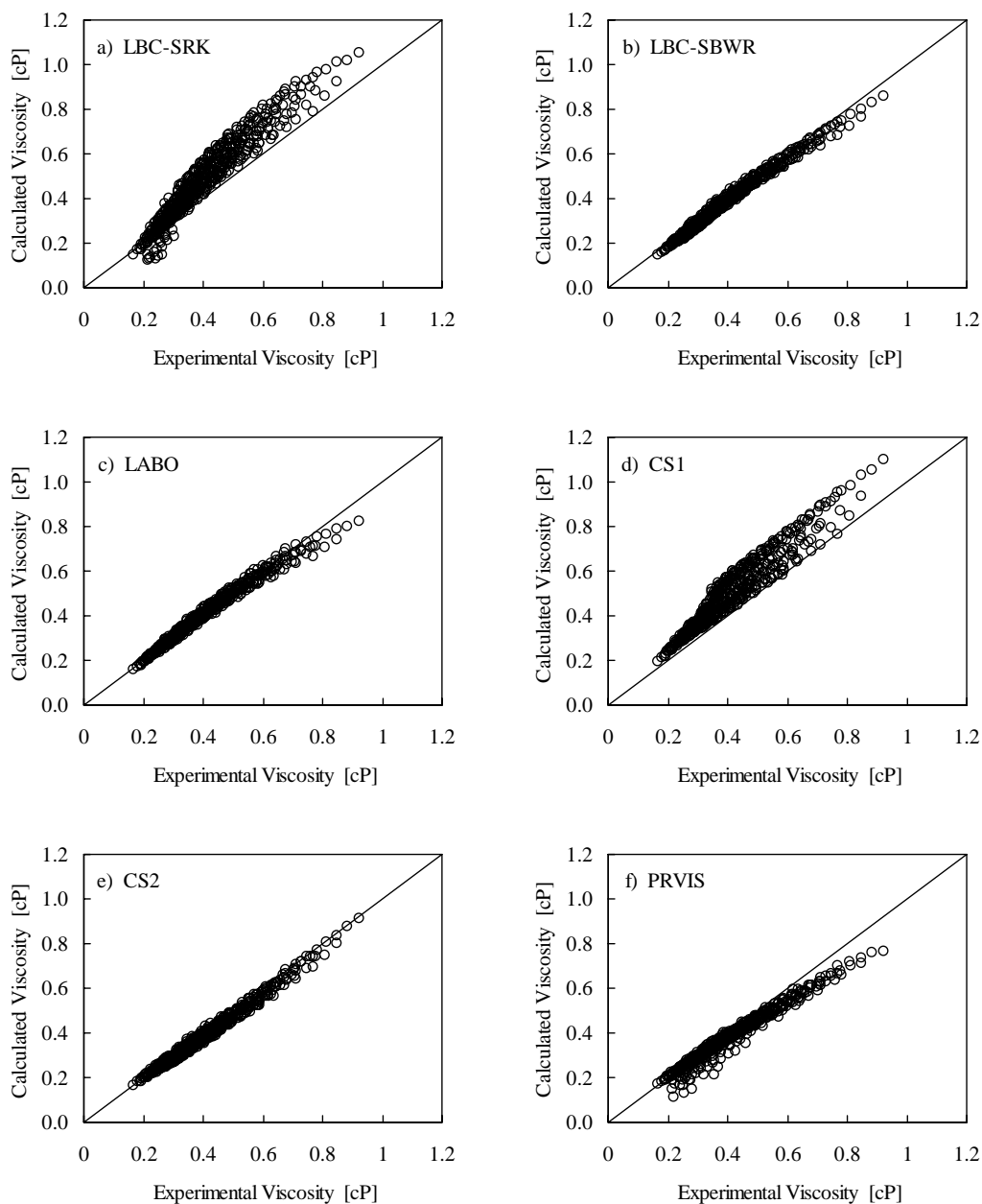


Figure I.23 Comparison of experimental viscosities (530 data points) for the ternary mixtures composed of n-pentane + n-octane + n-decane (Iglesias-Silva et al. 1999) with viscosities calculated by different models in the temperature range 298 – 373 K and for pressures ranging from 1 to 250 bar.

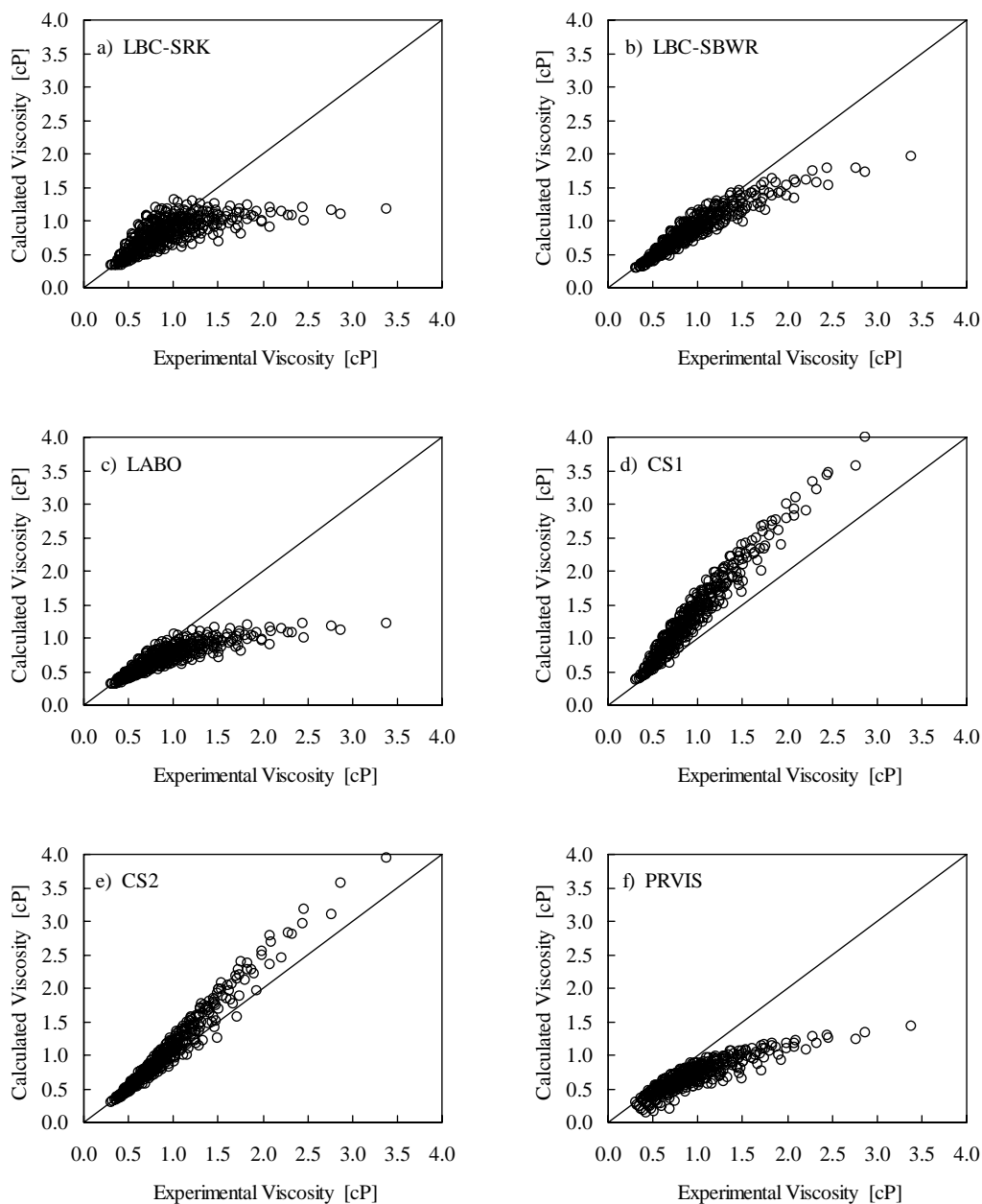


Figure I.24 Comparison of experimental viscosities (378 data points) for the ternary mixtures composed of n-heptane + methylcyclohexane + 1-methylnaphthalene (Baylaucq et al. 1997b) with viscosities calculated by different models in the temperature range 298 – 373 K and for pressures ranging from 1 to 1000 bar.

also gives the best results for mixtures composed of light compounds, see Table I.10 and Figures I.21 – I.24, because the constants in the LBC model have been derived using only light compounds. But also satisfactory overall results are obtained for mixtures being simple representations of petroleum fluids, such as the ternary system n-pentane + n-octane + n-decane or the ternary n-heptane + methylcyclohexane + 1-methylnaphthalene system, with the LBC model when the accurate SBWR EOS is used. However, in spite that the overall results obtained with the LBC model for the ternary mixtures composed of n-heptane + methylcyclohexane + 1-methylnaphthalene can be considered satisfactory, it can be seen from Figure I.24 that as the viscosity exceeds ~ 1.5 cP, the LBC model starts to underestimate the viscosity and the deviations increase with increasing viscosity. Similar tendencies have been observed for other fluids (pure and well-defined hydrocarbon mixtures) having viscosities higher than 1 – 1.5 cP.

For the LABO model, which has a similar structure as the LBC model, very satisfactory results are obtained for pure fluids such as carbon dioxide, nitrogen, and primarily paraffinic hydrocarbons up to C_{11} , except neopentane, see e.g. Figures I.15, I.16, and I.20. Above C_{11} the LABO model gives similar results, as those obtained with the LBC-SRK model, see Table I.9 and Figure I.17 and I.19. The reason for these large deviations obtained with the LABO model for heavy hydrocarbons, in spite that the constants in the LABO model have been readjusted using heavier hydrocarbons than in the original LBC model, is due to the less accurate density estimations of heavy hydrocarbons with the Lee-Kesler model. This density model is based on the corresponding states principle and it uses a simple fluid (acentric factor equal to zero) and n-octane as reference fluids. If, the SBWR EOS had been used instead, similar results for heavy hydrocarbons as those obtained with the LBC-SBWR model would be expected. It may even be the fact that the LABO model would give better results, since the constants have been adjusted using heavier hydrocarbons. By comparing the AAD obtained for mixtures (Table I.10) by the LABO model and the LBC-SBWR model, it can be seen that the performance of the LBC-SBWR model is better than for the LABO model, see also Figures I.21 – I.24. But as mentioned above, if the same density model and mixing rules had been used, similar results would have been obtained with the two viscosity models.

The performance of the CS1 model for viscosity estimations of pure fluids is only satisfactory for very light hydrocarbon fluids, such as methane and ethylene. As the compounds become heavier the deviations obtained with the CS1 model increase. The CS1 model over predicts the viscosity of pure compounds, see Figure I.15 to I.20. This has also been stressed by Aasberg-Petersen et al. (1991). Generally, as it can be seen from Figure I.15 to I.20, the deviations in the viscosity calculations with the CS1 model increase with increasing pressure. Also around saturation conditions large deviations have been found. This may be linked to the fact that the CS1 model Eq.(I.2.23) is related to the pressure instead of the density. Because of this, a discontinuity in the viscosity can be obtained at the saturation line, as mentioned in Section I.2.3.1. But the large deviations can also be a result of the fact that the required density in order to determine the reference viscosity in the CS1 model is estimated at two different T,P conditions, as pointed out by Aasberg-Petersen et al. (1991) and mentioned in Section I.2.3.1. For mixtures, the performance of the LBC-SBWR model is significantly better than the performance of the CS1 model, see Table I.10 and Figures I.21 to I.24. For some of the binary mixtures containing methane + propane (Giddings et al. 1966) experimental values have been reported at T,P conditions corresponding to the vicinity of the critical point of the mixtures. At these conditions large deviations are obtained between the calculated viscosities with the CS1 model and the reported values for the binary system methane + propane, see Figure I.21d. Outside the critical region the CS1 model gives similar deviations as those obtained by the other evaluated models. Thus generally, the viscosity of the tested well-defined hydrocarbon mixtures is over predicted by the CS1 model and the deviations increase with pressure.

For the pure fluids, the best results with the CS2 model are obtained for methane and n-alkanes ranging from $C_9 - C_{12}$. This is not strange, since the CS2 model uses methane and n-decane as reference fluids. Generally, the viscosity of pure compounds is over predicted with the CS2 model, see e.g. Figures I.15 to I.20, but as the pressure increases the performance of the CS2 model becomes better. In spite of the less satisfactory performance of the CS2 model for pure fluids compared with the LBC-SBWR model, better results are obtained with the CS2 model for the well-defined mixtures compared with the LBC-SBWR model, especially for mixtures with high

viscosities, see Table I.10 and Figures I.21 – I.24. Also for mixtures composed of hydrocarbons and carbon dioxide the obtained deviations with the CS2 model are satisfactorily. The good overall performance obtained with the CS2 model for well-defined mixtures, being very simple representations of petroleum and reservoir fluids, shows the potential of extending this model to real reservoir fluids.

The PRVIS model is the viscosity model giving the best predictions for heavy hydrocarbons, see Figures I.17 and I.19. However, for n-hexane and n-heptane the performance of the PRVIS model is not very satisfactory, as shown in Figure I.16. For these compounds the deviations increase with increasing pressure. Also for nitrogen at high temperatures and high pressures the performance of the PRVIS model is not very satisfactory. In case of mixtures, relative large deviations are obtained with the PRVIS model for methane containing mixtures at low to moderate pressures compared with the other evaluated models, see Figure I.21 and Table I.10. However, for mixtures composed of heavier hydrocarbons the performance of the PRVIS model is of the same order of magnitude as for the LBC-SBWR model and the CS2 model, but generally larger deviations are obtained with the PRVIS model for mixtures composed of alkanes and aromatic hydrocarbons or naphthenic hydrocarbons. For hydrocarbon + carbon dioxide mixtures, the viscosity predictions with the PRVIS model is very satisfactory and better than the results obtained for the other evaluated models. This shows the potential application to viscosity predictions of carbon dioxide enhance oil recovery. Thus, it should be stressed that for fluids having viscosities above 1 – 1.5 cP, the PRVIS model under predicts the viscosity and the deviations increase with increasing viscosity. This tendency is similar to that observed for the LBC model.

Generally, in case of naphthenic fluids all of the evaluated models have problems predicting the viscosity. For the two binary systems methane + toluene (Canet 2001) and methane + methylcyclohexane (Tohidi et al. 2001) the best performance is obtained by the CS2 model and the LBC-SBWR model. The AAD and MxD with the CS2 model is 4.39% and 16.5% for the binary system methane + toluene, whereas for the binary system methane + methylcyclohexane the AAD and MxD are 7.57% and 21.5%, respectively. For the binary system methane + toluene an AAD of 6.57% and an MxD of 17.1% are obtained with the LBC-SBWR model. The AAD and MxD are

8.01% and 26.2%, respectively for the binary system methane + methylcyclohexane using the LBC-SBWR model.

In addition and in spite none of the evaluated viscosity models have been derived for the accurate viscosity prediction of water, the overall AAD obtained with the LBC-SRK, LABO, CS1 and CS2 models is around 21 – 22%, whereas an AAD = 36% is obtained for the LBC-SBWR model. No AAD and MxD are reported in Table I.9 for the PRVIS model. The reason is that this model does not predict the viscosity of water properly, because very large deviations are obtained compared with the other models. In general, it can not be recommended to use any of the evaluated models to calculate the viscosity of water, since the models have not been derived for associating and polar fluids. Water has only been included in the database in order to see the performance of the evaluated viscosity models on a strong polar compound.

I.5.3 The Dilute Gas Viscosity

In addition, the performance of the dilute gas viscosity model by Chung et al. (1988), Eq.(I.2.3), has been evaluated by comparing the calculated dilute gas viscosities with values reported in the literature for alkanes ranging from methane through n-hexane, cyclohexane, benzene, toluene, p-xylene, ethylene, carbon dioxide, and nitrogen over wide ranges of temperature - all these compounds are found in petroleum fluids. The required properties in Eq.(I.2.3) have been taken from the DIPPR Data Compilation (Daubert and Danner 1989). The obtained AAD and MxD, together with the temperature range and the uncertainty in the reported literature values are given in Table I.11. Further, the percentage deviation of the predicted dilute gas viscosities for each fluid as a function of the reduced temperature between 0.5 and 3.0 is shown in Figure I.25 and I.26. Comparing the uncertainty of the reported literature values with the AAD given in Table I.11 and the percentage deviation shown in Figures I.25 and I.26, a good agreement between the Chung et al. dilute gas viscosity model and the reported literature values is found, except for neopentane. Overall, the obtained results are satisfactory for a general model developed for calculations of dilute gas viscosities of different fluids over wide temperature ranges, where a difference of 1 μP can easily correspond to a deviation of 1 – 1.5% due to the low value of the dilute gas viscosity.

	Ref.	NP	T -range [K]	AAD%	MxD%	Reported uncertainty
Methane	a	31	100 – 400	0.56	2.97	3.0% $T < 270$ K
	b	95	110 – 600	1.00	3.02	0.5% $270\text{K} < T < 400$ K 2.0%
Ethane	c	41	100 – 500	1.54	6.21	5.0% $100\text{K} < T < 250$ K
	d	12	293 – 633	0.74	1.39	1.5% $250\text{K} < T < 300$ K 1.0% $300\text{K} < T < 375$ K 0.3%
Propane	e	14	297 – 625	1.29	1.53	0.3%
i-Butane	f	10	298 – 627	1.35	1.89	0.4%
n-Butane	g	14	298 – 626	0.76	1.25	0.4%
n-Pentane	h	7	323 – 623	0.65	0.93	0.3%
neo-Pentane	i	10	298 – 633	8.10	10.0	0.3%
n-Hexane	j	9	363 – 623	0.52	0.72	0.3%
n-Heptane	h	7	353 – 623	0.19	0.63	0.3%
Ethylene	k	51	180 – 680	1.71	3.27	2.0%
Cyclohexane	i	11	323 – 623	2.87	4.93	0.3%
Benzene	l	9	333 – 623	1.52	2.75	0.3%
Toluene	m	11	353 – 633	1.63	3.08	0.3%
p-Xylene	m	10	383 – 633	3.13	4.12	0.3%
Carbon Dioxide	b	71	200 – 600	1.67	2.41	2.0%
Nitrogen	n	87	120 – 600	1.41	2.90	2.0%

Table I.11 Performance of the dilute gas viscosity model, Eq.(I.2.3) (Chung et al. 1988).

a) Friend et al. (1989); b) Trengove and Wakeham (1987); c) Friend et al. (1991); d) Hendl and Vogel (1992); e) Vogel (1995); f) Küchenmeister and Vogel (1998), g) Küchenmeister and Vogel (2000); h) Vogel and Holdt (1991); i) Vogel et al. (1988); j) Vogel and Strehlow (1988); k) Holland et al. (1983); l) Vogel et al. (1986); m) Vogel and Hendl (1992); n) Cole and Wakeham (1985).

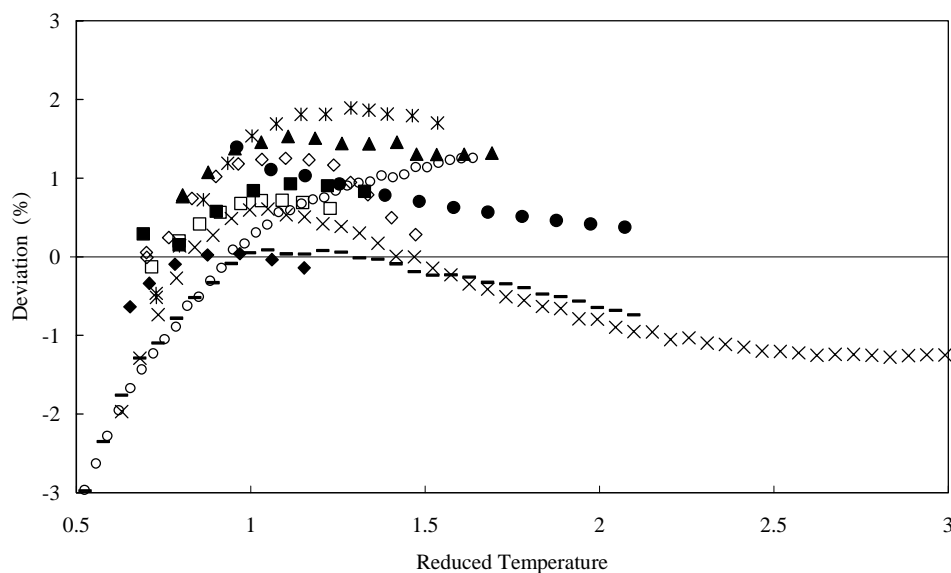


Figure I.25 Deviation of the predicted dilute gas viscosities by Eq.(I.2.3) (Chung et al. 1988) from reported values in the literature. (x) methane (Tremgove and Wakehame 1987); (–) methane (Friend et al 1989); (o) ethane (Friend et al. 1991); (●) ethane (Hendl and Vogel 1992); (▲) propane (Vogel 1995); (*) i-butane (Küchenmeister and Vogel 1998); (◇) n-butane (Küchenmeister and Vogel 2000); (■) n-pentane (Vogel and Holdt 1991); (□) n-hexane (Vogel and Strehlow 1988); (◆) n-heptane (Vogel and Holdt 1991).

Further, it shall be mentioned that the only way to obtain “experimental” dilute gas viscosities is by extrapolating experimental viscosity measurements at low densities to the zero density limit.

I.5.4 Conclusion

An evaluation of the performance of five compositional dependent viscosity models, applicable to hydrocarbon fluids, has been performed over wide ranges of temperature and pressure. The evaluated models are currently being used within the oil and gas industry or are of interest for the possible extension to petroleum reservoir fluids. The five evaluated models are the LBC model, the LABO model (a model similar to the LBC model), the two corresponding states models CS1 and CS2 with respectively one and two reference fluids, and the PRVIS model, which is a model based on the PR EOS due to the similarity between the PvT and $T\eta P$ relationships. These five models have

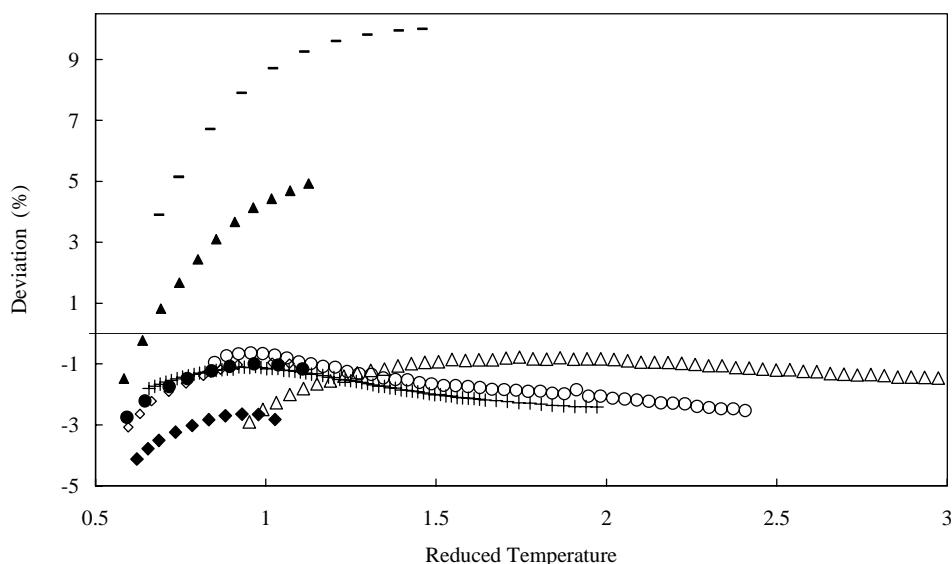


Figure I.26 Deviation of the predicted dilute gas viscosities by Eq.(I.2.3) (Chung et al. 1988) from reported values in the literature. (—) neopentane (Vogel et al. 1988); (o) ethylene (Holland et al. 1983); (•) benzene (Vogel et al. 1986); (▲) cyclohexane (Vogel et al. 1988); (◊) toluene (Vogel and Hendl 1992); (◆) p-xylene (Vogel and Hendl 1992), (+) carbon dioxide (Tremgove and Wakeham 1987), (Δ) nitrogen (Cole and Wakeham 1985).

been tested on 35 pure hydrocarbon fluids, nitrogen, carbon dioxide, and 39 well-defined hydrocarbon systems, which may be considered as being representative of very simple petroleum and reservoir fluids. To summarize the comparison of the deviations obtained by the five models, it has been found that the LBC model gives appropriate results for light fluids, if in addition also accurate density estimations are obtained by using a proper density model, such as the SBWR EOS. The reason for the good LBC results for pure, light fluids is due to the fact that the LBC model has been derived using light compound density and viscosity data. The viscosity calculations with the LABO model also depend on how well the density is estimated. In this work, the LABO model in connection with the Lee-Kesler density model predicts the viscosity of pure hydrocarbons up to C_{11} satisfactorily. If the SBWR EOS model had been used, the viscosity predictions with the LABO model would have been similar or even better than those obtained by the LBC-SBWR model for heavy hydrocarbons. In addition, the PRVIS model gives the best results for pure hydrocarbons above n-nonane. In cases of

mixtures composed of carbon dioxide and hydrocarbons the results obtained by the PRVIS model are very satisfactory, showing its potential for extension to enhance oil recovery of reservoir fluids. Also the CS2 model gives satisfactory results for hydrocarbon + carbon dioxide mixtures. However, in spite that the CS2 model does not give the best results for pure hydrocarbons, the best performance for the well-defined hydrocarbon mixtures is obtained with the CS2 model, showing its potential extension to real reservoir fluids. In addition, the results obtained with the CS1 model are not very satisfactorily compared with the other models, especially not at high pressures. For the studied fluids, the CS1 model generally overestimate the viscosity. Further, it should be stressed that none of the evaluated models predict the viscosity of fluids containing naphthenic compounds properly.

The evaluation of the five viscosity models has been performed in order to investigate their capabilities of predicting the viscosity accurately over wide ranges of temperature and pressure for pure and well-defined hydrocarbon fluids, which may be seen as very simple representations of petroleum and reservoir fluids. However, as it can be seen from Figures I.15 through I.24 along with Tables I.9 and I.10, this evaluation shows the requirement for a more reliable and accurate viscosity model, applicable to both the liquid, the gaseous, and the dense regions over wide ranges of temperature, pressure, and composition. The reason is that the viscosity is an important property required in flow models, such as the Navier-Stoke's model or Darcy's law, which are used e.g. in the design of transport equipments or in the simulation of the production profiles of oil and gas reservoirs. A more reliable and accurate viscosity model can either be derived by improving and modifying the existing models or by developing a totally new viscosity model. The modeling work described in the rest of Part I is related to the improving modeling and prediction of the viscosity of hydrocarbon fluids over wide ranges of temperature, pressure, and composition.

In addition, an analysis of the dilute gas viscosity model by Chung et al. (1988) has also been carried out, showing that this model is capable of predicting the dilute gas viscosity of pure compounds found in reservoir fluids within an overall uncertainty of the order of 1.5%, which is in agreement with the uncertainty of the reported dilute gas viscosities, except neopentane. However, the uncertainty in the dilute gas viscosity is

only important for fluids in the vapor phase or at high reduced temperatures as mentioned in Section I.1.1, see Figure I.3. For liquids and dense fluids, an uncertainty of 1.5% in the dilute gas viscosity will be negligible compared to the value of the viscosity in excess of the dilute gas viscosity.

I.6 Modified CS2 Model

Since the CS2 model is the viscosity model given the best results for the well-defined hydrocarbon mixtures, compared with the other evaluated models, but the less accurate results for pure hydrocarbons ranging from C₃ to C₈ or heavy hydrocarbons, an investigation has been performed in order to improve the viscosity predictions of these compounds with a modified CS2 model. The modeling work has mainly been performed in order to modify the CS2 model in a simple way either by changing the interpolation parameter K_{CS} or by introducing a second reference fluid.

I.6.1 The Interpolation Parameter

The general structure of the CS2 model in reduced terms is shown below

$$\ln \eta_{r,x} = \ln \eta_{r,1} + K_{CS} (\ln \eta_{r,2} - \ln \eta_{r,1}) \quad (I.6.1)$$

where subscript x refers to the real fluid, and subscripts 1 and 2 refer to the reference fluids. K_{CS} is the interpolation parameter. In the CS2 model by Aasberg-Petersen et al. (1991) the interpolation parameter is related to the molecular weight

$$K_{CS} = \frac{M_{w,x} - M_{w,1}}{M_{w,2} - M_{w,1}} \quad (I.6.2)$$

Et-Tahir (1993) investigated the influence of the interpolation parameter on the predicted viscosities with the CS2 model. This investigation was carried out by comparing the results obtained using the interpolation parameter originally defined for the CS2 model with results obtained using interpolation parameters based on the acentric factor, the critical temperature, the critical pressure, and a combination of the different interpolation parameters. Et-Tahir (1993) found that the following interpolation parameter

$$K_{CS} = \frac{1}{4} \left(\frac{M_{w,x} - M_{w,1}}{M_{w,2} - M_{w,1}} + \frac{\omega_x - \omega_1}{\omega_2 - \omega_1} + \frac{P_{c,x} - P_{c,1}}{P_{c,2} - P_{c,1}} + \frac{T_{c,x} - T_{c,1}}{T_{c,2} - T_{c,1}} \right) \quad (I.6.3)$$

significantly improved the viscosity predictions of heavy hydrocarbons, as shown for n-tetradecane, n-octadecane, and 1-methylnaphthalene in Figures I.27, I.28, and I.29. For the lighter hydrocarbons no improvements in the viscosity calculations are achieved by changing the interpolation parameter from the interpolation parameter defined in Eq.(I.6.2).

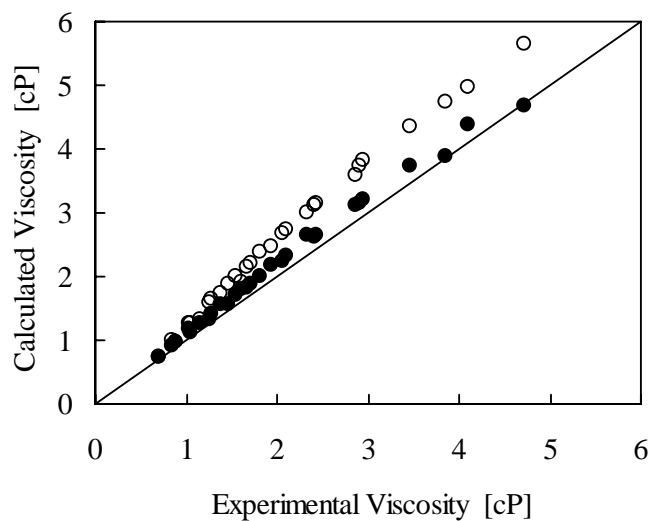


Figure I.27 Comparison of experimental viscosities for n-tetradecane from 1 to 1000 bar in the temperature range 313 – 373 K (Ducoulombier et al. 1986) with values calculated by the CS2 model using the interpolation parameter defined in Eq.(I.6.2) (o) and defined in Eq.(I.6.3) (•).

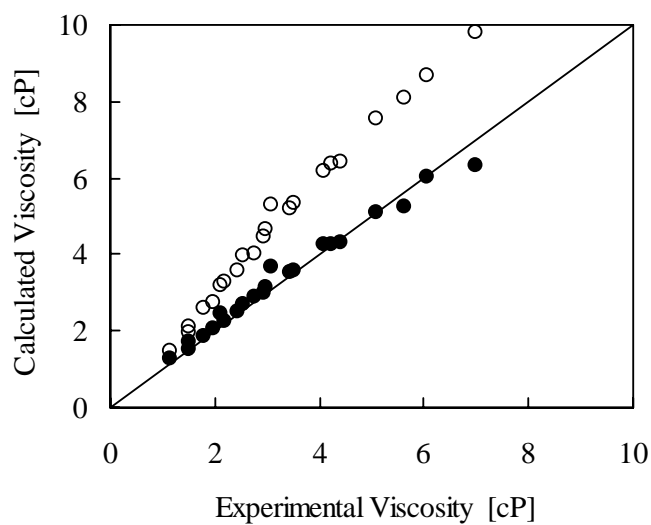


Figure I.28 Comparison of experimental viscosities for n-octadecane from 1 to 1000 bar in the temperature range 313 – 373 K (Ducoulombier et al. 1986) with values calculated by the CS2 model using the interpolation parameter defined in Eq.(I.6.2) (o) and defined in Eq.(I.6.3) (•).

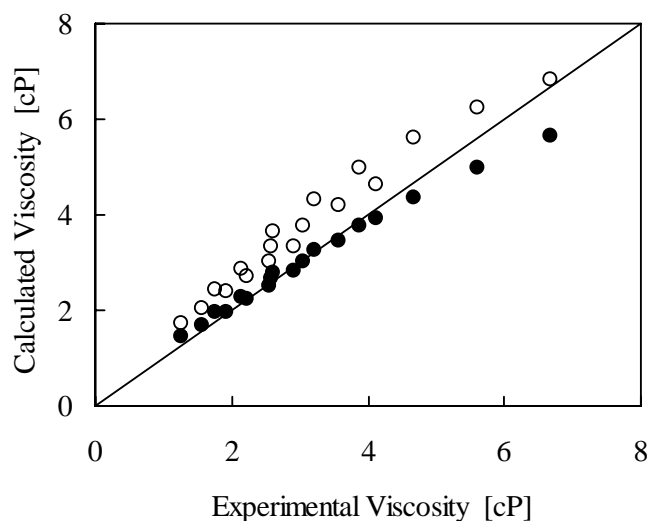


Figure I.29 Comparison of experimental viscosities for 1-methylnaphthalene from 1 to 1000 bar in the temperature range 303 – 343 K (Baylaucq et al. 1997a) with values calculated by the CS2 model using the interpolation parameter defined in Eq.(I.6.2) (o) and defined in Eq.(I.6.3) (•).

I.6.2 The Reference Fluids

Since relative large deviations are obtained with the CS2 model for pure hydrocarbons between propane and n-nonane, see Table I.9, a study of the choice of the second reference fluid has been carried out in order to improve the viscosity calculations of the lighter hydrocarbons. For this purpose, n-hexane has been chosen as the second reference fluid instead of n-decane. The reason for choosing n-hexane as the reference fluid is because it is one of the last paraffinic hydrocarbons for which experimental viscosity data exist in both the gaseous and the liquid regions.

The basic equations used to estimate the reference viscosities are the same as those used in the CS2 model, see Section I.2.3.2, and they are given below

$$\eta_i(\rho, T) = \eta_0(T) + \rho \eta_1(T) + \eta_2(\rho, T) \quad (\text{I.6.4})$$

Here η_0 is the dilute gas viscosity, η_1 the first density correlation and η_2 the correlation term for high densities. η_1 and η_2 are defined by the following equations

$$\eta_1 = A + B \left(D - \ln \left(\frac{T}{F} \right) \right)^2 \quad (\text{I.6.5})$$

$$\eta_2 = H_2 \exp\left(j_1 + \frac{j_4}{T}\right) \quad (\text{I.6.6})$$

with

$$H_2 = -1 + \exp\left[\rho^{0.1}\left(j_2 + \frac{j_3}{T^{3/2}}\right) + \theta \rho^{0.5}\left(j_5 + \frac{j_6}{T} + \frac{j_7}{T^2}\right)\right] \quad (\text{I.6.7})$$

and where

$$\theta = \frac{\rho - \rho_c}{\rho_c} \quad (\text{I.6.8})$$

However, compared with the original CS2 model (Aasberg-Petersen et al. (1991)) some modifications have been introduced for the estimation of the dilute gas viscosity and the density of the reference fluids. The dilute gas viscosity η_0 in Eq.(I.6.4) is estimated by the model derived by Chung et al. (1988), Eq.(I.2.3). This general dilute gas viscosity model has been shown in Section I.5.3 to predict the dilute gas viscosity accurately of methane and n-hexane along with other non-polar fluids over wide ranges of temperature. In addition, the required density of the reference fluids used in Eqs.(I.6.4) – (I.6.8) is estimated with the highly accurate SBWR EOS. The SBWR EOS has in Section I.3.3 been shown to predict the density accurately of methane, n-hexane, and n-decane over wide ranges of temperature and pressure, also in the vicinity of the critical point. The required critical density of each fluid in Eq.(I.6.8) has been estimated by the SBWR EOS, since it also calculates the critical density accurately.

The parameters in Eqs.(I.6.5) - (I.6.7) have been estimated for methane, n-hexane, and n-decane by a least squares minimization using only experimental viscosity data, no extrapolated values have been used. The references for the viscosity data of methane, n-hexane, and n-decane, which have been used in the parameter estimations, are given in Appendix A3, Table A3.1, A3.6, and A3.9 along with the number of points, the temperature and pressure ranges. In spite some of the references for n-hexane and n-decane contain viscosity data up to very high pressures, it has been decided only to use data up to 1000 bar. The reason is that most industrial applications are carried out at pressures below 1000 bar, but also because the pressure in most oil and gas reservoirs is less than 1000 bar, generally around 150 – 200 bar.

The estimated parameters are given in Table I.12 and the obtained AAD for

	Methane	n-Hexane	n-Decane
<i>A</i>	5.117292274	-3927.003214	8.261971446
<i>B</i>	205.4216898	44.14835846	-1.494367684
<i>D</i>	3.272931486	7.574428927	5.591740308
<i>F</i>	23.78006132	2387.565163	205.9568774
<i>j₁</i>	-9.964775064	-8.763923332	-9.057496998
<i>j₂</i>	17.72167106	16.21397400	18.54020709
<i>j₃</i>	-2177.051453	-30767.16154	-13987.91212
<i>j₄</i>	-92.52944093	1222.025332	-467.2595074
<i>j₅</i>	-0.055509863	-0.020954437	-0.253312117
<i>j₆</i>	256.5569447	232.0455992	410.2627493
<i>j₇</i>	5696.470962	101090.9658	113919.8280

Table I.12 Estimated parameters for Eqs.(I.6.5) – (I.6.7).

each fluid is given in Table I.13. Outside the critical region, the MxD is less than 10%. The modeling of these three compounds using Eqs.(I.6.4) – (I.6.8) is within the uncertainty reported for the experimental viscosity data. The estimated reference viscosity will have the unit [μP], when the parameters in Table I.12 are used along with the density in [g/cm^3] and the temperature in [K].

I.6.3 Results

By using methane and n-hexane as reference fluids in the CS2 model along with the interpolation parameter based on the molecular weight, Eq.(I.6.2), significantly better calculations are obtained for the lighter pure hydrocarbons between ethane and n-

	Methane	n-Hexane	n-Decane
NP	768	477	212
<i>T</i> -range [K]	97 – 478	273 – 548	278 – 478
<i>P</i> -range [bar]	0.5 – 1032	1.0 – 1022	0.1 – 1019
AAD%	1.69	1.83	1.94

Table I.13 Modeling results for each reference fluid in the modified CS2 model.

nonane compared with the original CS2 model. However, for the heavy hydrocarbons (above n-nonane) the best results are obtained using methane and n-decane as the reference fluids along with the interpolation parameter defined in Eq.(I.6.3) (Et-Tahir 1993).

Based on these results and observations mentioned above, a modification of the CS2 model has been suggested. This model is referred to as MCS2. The criterion set up for MCS2 is:

- For hydrocarbons with a molecular weight $M_w < 115$, methane and n-hexane are used as reference fluids. The interpolation parameter K_{CS} is based on the molecular weight and defined in Eq.(I.6.2).
- For hydrocarbons with a molecular weight $M_w \geq 115$, methane and n-decane are used as reference fluids. The interpolation parameter K_{CS} is defined in Eq.(I.6.3).

The viscosities of the reference fluids are estimated by Eqs.(I.6.4) – (I.6.8) using the parameters given in Table I.12, and the dilute gas viscosity by Eq.(I.2.3). The required densities are estimated by the SBWR EOS.

In order to evaluate the performance of the MCS2 model, a comparison with the reported viscosities for 35 pure hydrocarbons, carbon dioxide, nitrogen, and hydrogen sulfide over wide ranges of pressure and temperature has been performed. These fluids have previously been used in the evaluation of existing viscosity models, see Chapter I.5. The obtained AAD for each fluid with the MCS2 model is shown in Figure I.30 along with the AAD obtained by the original CS2 model, reported in Table I.9. From Figure I.30, it can be seen that by using methane and n-hexane as reference fluids, which is the case in the MCS2 model, much lower AADs are obtained for light paraffinic hydrocarbons up to n-octane, except for neopentane, compared to the CS2 model, which uses methane and n-decane as reference fluids. For the heavy hydrocarbons the introduction of the interpolation parameter K_{CS} defined in Eq.(I.6.3) significantly improves the prediction of the viscosity compared to the original CS2 model. For the viscosity prediction of heavy hydrocarbons methane and n-decane are used as reference fluids in both the MCS2 model and the original CS2 model. Also for carbon dioxide and nitrogen significant improvements are achieved with the MCS2

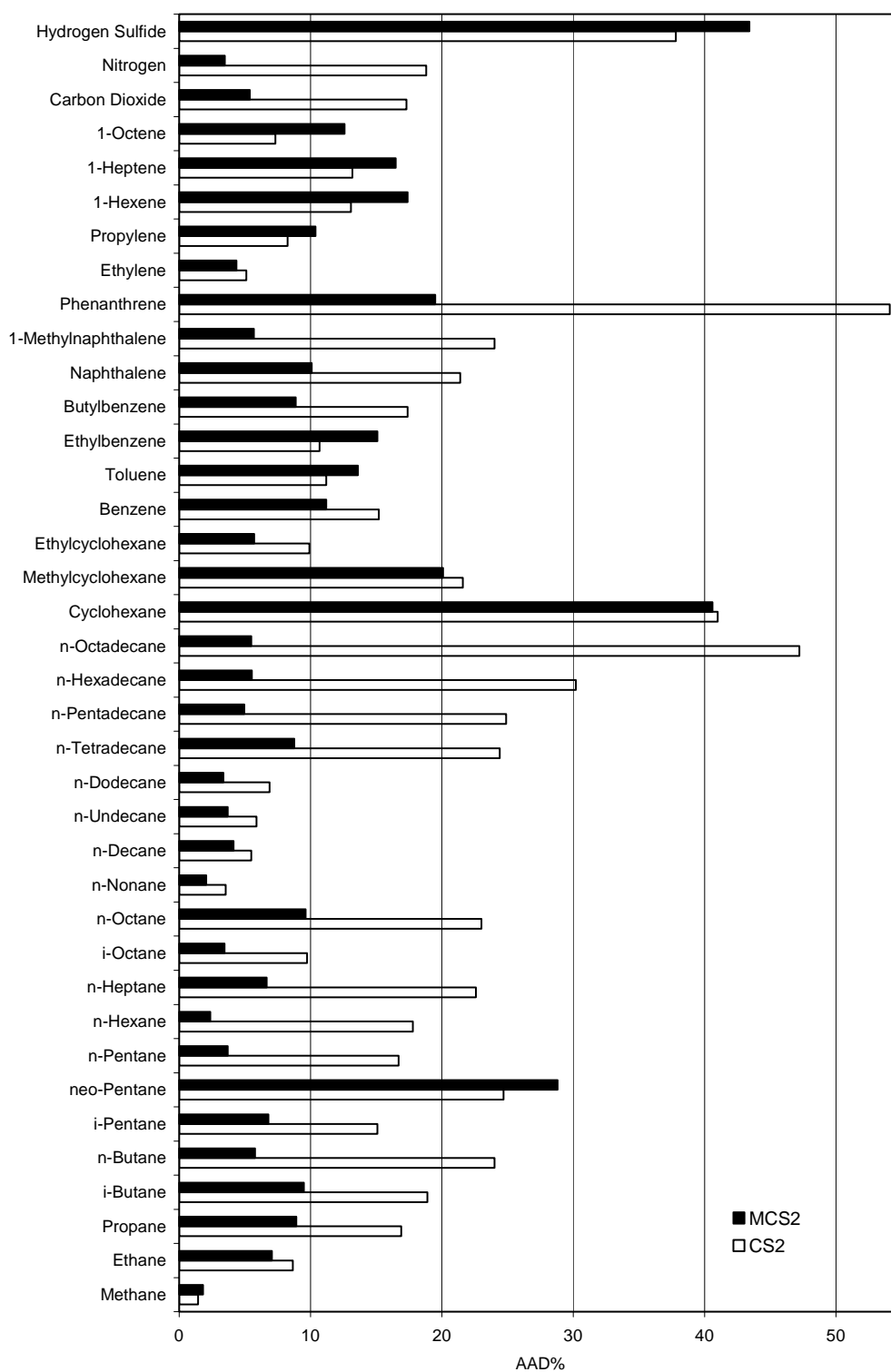


Figure I.30 Comparison of the modified CS2 (MCS2) model with the CS2 model by Aasberg-Petersen et al. (1991).

model. However, for olefinic compounds the CS2 model gives better results than the MCS2 model, except for ethylene. Approximately similar AADs are obtained for naphthenic hydrocarbons, but for these compounds none of the models predict the viscosity satisfactorily. In case of aromatic hydrocarbons the MCS2 model gives the best results for heavy aromatic hydrocarbons, such as 1-methylnaphthalene.

In addition and for comparison reasons, the viscosity of the 39 well-defined hydrocarbon mixtures in the database, which have been used in the evaluation of existing models (Chapter I.5), have also been used in order to evaluate the performance of the MCS2 model. The necessary properties of the mixtures have been estimated using the same mixing rules as in the original CS2 model. These mixing rules are described in Section I.2.3.2. A comparison of the obtained AADs with the MCS2 model and the original CS2 model is shown in Figure I.31. The overall conclusion of the comparison of the AADs obtained for the well-defined hydrocarbon mixtures by the MCS2 model and the CS2 model is that the performance of the two models is nearly the same. For some mixtures the MCS2 model improves the viscosity prediction, whereas the CS2 model gives better results for other mixtures, especially for mixtures containing n-alkanes and cyclohexane or with very different compounds such as n-decane + methane or carbon dioxide. So in order to obtain better results with the MCS2 model, a study of the mixing rules should be carried out. A possibility could be to use the mixing rules derived for the SBWR EOS by Soave (1995) and presented in Eqs.(I.3.59), (I.3.60), and (I.3.63) in order to estimate the required critical properties of mixtures.

However, in addition to the viscosity modeling carried out with the MCS2 model, other models have been derived and studied. One of these models was the friction theory for viscosity modeling, introduced by Quinones-Cisneros et al. (2000). With this model accurate viscosity modeling of n-alkanes is obtained over wide ranges of pressure and temperature using simple cubic EOSs, commonly used by the petroleum and oil industry. Due to this and the very good modeling results obtained with the friction theory, no further modeling of mixtures has been carried out with the MCS2 model.

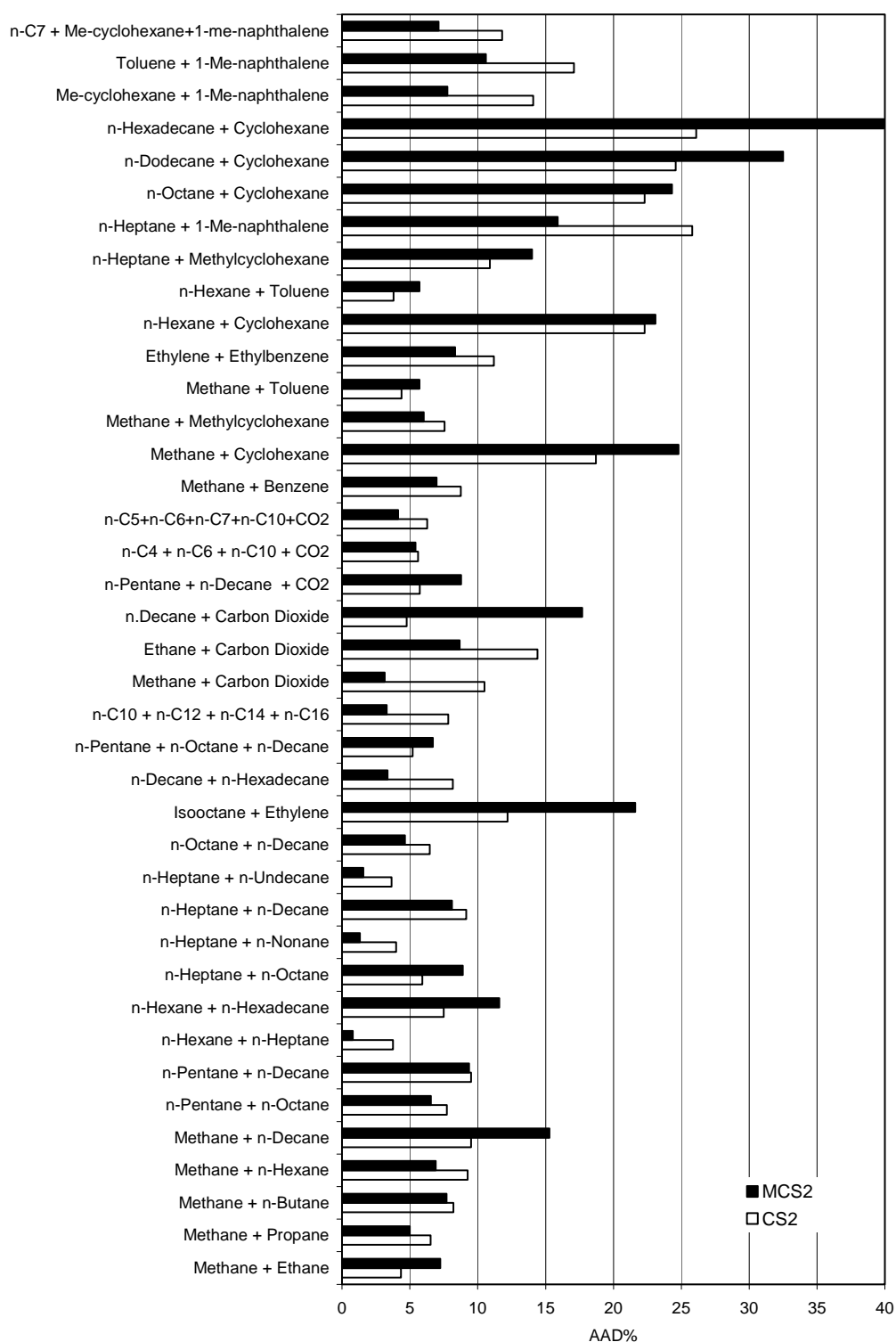


Figure I.31 Comparison of AAD% for well-defined mixtures obtained by MCS2 and CS2 (Aasbeg-Petersen et al. 1991).

I.7 The Friction Theory

Starting from basic principle of classical mechanics and thermodynamics, the friction theory (*f-theory*) for viscosity modeling has been introduced by Quiñones-Cisneros et al. (2000). The fundamental difference between the *f-theory* and other available approaches for viscosity modeling is that the viscosity in excess of the dilute gas viscosity is approached as a mechanical rather than a transport property. In the *f-theory*, the viscosity is linked to the pressure, which is the main mechanical variable, and by use of a simple cubic EOS highly accurate viscosity estimations can be obtained, from low to extremely high pressures. This is based on the fact that cubic EOSs are optimized for good pressure-temperature performance, and therefore good viscosity-pressure performance can also be obtained, as illustrated by Quiñones-Cisneros et al. (2000). This is achieved regardless of the accuracy of the estimated density.

In the *f-theory* the total viscosity, η , is separated into a dilute gas viscosity term η_0 and a residual friction term η_f ,

$$\eta = \eta_0 + \eta_f \quad (\text{I.7.1})$$

The dilute gas viscosity η_0 is defined as the viscosity at the zero density limit, while the residual friction term η_f is related to a connection between the van der Waals repulsive and attractive pressure terms and the Amontons-Coulomb friction law. The residual friction term may be expressed by the following quadratic model

$$\eta_f = \kappa_r p_r + \kappa_a p_a + \kappa_{rr} p_r^2 \quad (\text{I.7.2})$$

where κ_r , κ_a and κ_{rr} are temperature dependent friction coefficients, and p_r and p_a are the van der Waals repulsive and attractive pressure contributions, respectively. These repulsive and attractive pressure contributions can be obtained with the aid of a simple cubic EOS, such as the SRK or the PR EOS. The capability of the *f-theory* has been illustrated by (Quiñones-Cisneros et al. 2000) with the accurate modeling of the viscosity of n-alkanes and their mixtures from low to extremely high pressures over wide ranges of temperature going from near the triple point to light supercritical gas conditions.

In the following sections the basic ideas behind the *f-theory* are described along with the main *f-theory* models developed during this work.

I.7.1 Basic Ideas of the Friction Theory

From classical mechanics it is known that when two bodies in contact are moving relative to each other, contact forces will act between them. In order to maintain the motion, a force F parallel to the contact surface has to be applied. This force is opposite to the kinetic friction F_k , as illustrated in Figure I.32. Experimentally, the kinetic friction has been found to be constant for wide ranges of speed. Further, the two bodies will be pressed together by the normal force N acting perpendicular to the contact surface. According to the classical mechanics Amontons-Coulomb friction law, the ratio between the kinetic friction and the normal force is given by

$$\mu_k = \frac{F_k}{N} = \frac{A \tau}{A \sigma} = \frac{\tau}{\sigma} \quad (\text{I.7.3})$$

where μ_k is known as the kinetic friction coefficient, which is assumed to depend only on the smoothness of the surfaces of the materials and not the surface area A . Also in Eq.(I.7.3) the kinetic friction F_k can be expressed in terms of the shear stress τ , and the normal force N in terms of the pressure or normal stress σ acting on the contact surface area A .

For a fluid under shear made up of parallel layers, which move relatively to each

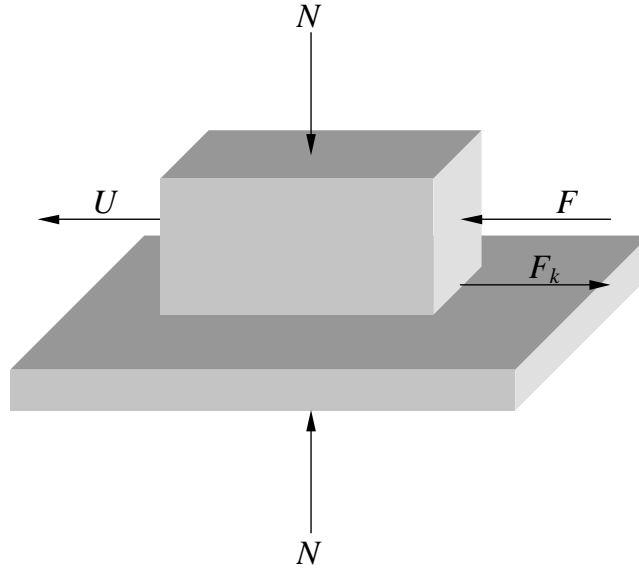


Figure I.32 Basic forces acting in the case of a block moving during friction contact. N is the pressure normal force, F the pushing force responsible for the movement, F_k the opposing friction force, and U the resulting velocity.

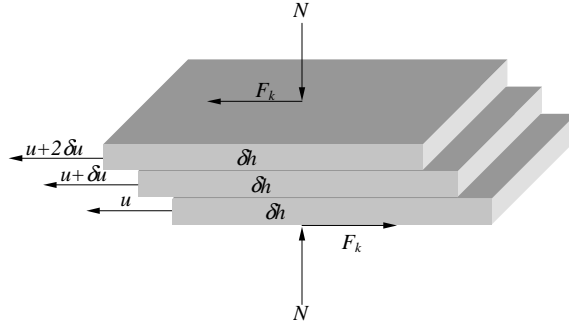


Figure I.33 Multilayer model for laminar shear flow. N is the normal force, F_k the dragging force, u the reference velocity, δu the relative velocity difference, and δh the distance of the layers

other at a constant rate of shear $\delta u / \delta h$, a similarity between the forces acting between the layers and those acting between two solid bodies can be established, see Figure I.33.

For a fluid at rest, the normal stress N can be related to the isotropic total pressure P , which according to the van der Waals theory of fluids can be separated into a repulsive and an attractive pressure term as follows

$$P = p_r + p_a \quad (\text{I.7.4})$$

where p_r and p_a are the contributions to the pressure coming from the short-range repulsive intermolecular forces and the long-range attractive intermolecular forces, respectively.

In the case of a fluid under shear motion, the shear stress τ (i.e. the dragging force) acting between the moving layers can be separated into a dilute gas collision term τ_0 and a residual friction term τ_f ,

$$\tau = \tau_0 + \tau_f \quad (\text{I.7.5})$$

Here, the dilute gas term will only be important at the ideal gas limit where the friction term must vanish. Thus, when a fluid is brought under shear motion, the attractive and repulsive intermolecular forces will contribute to enhance or diminish the mechanical properties of the fluid. Due to this, the residual friction shear stress term τ_f can be considered to consist of an attractive friction shear contribution τ_a and a repulsive friction shear contribution τ_r .

$$\tau_f = \tau_r + \tau_a \quad (\text{I.7.6})$$

By analogy with the Amontons-Coulomb friction law, Quiñones-Cisneros et al. (2000)

assumed that the attractive dragging force τ_a and the repulsive dragging force τ_r are analytical functions of the attractive pressure term p_a and the repulsive pressure term p_r , respectively. Thus, writing τ_a and τ_r as an n -th order Taylor series from the origin (i.e. the dilute gas limit where $p = p_a = p_r = 0$), it follows that

$$\tau_a = \sum_{i=1}^n \tau_{a,i} p_a^i \quad (\text{I.7.7})$$

and

$$\tau_r = \sum_{i=1}^n \tau_{r,i} p_r^i \quad (\text{I.7.8})$$

where the zero order terms in Eqs.(I.7.7) and (I.7.8) have been eliminated under the assumption that at the dilute gas limit the fluid layers are so far apart that they would not feel any kind of frictional dragging force. When Eqs.(I.7.7) and (I.7.8) are truncated after the first order, an equivalence to the Amontons-Coulomb friction law is obtained

$$\tau_a = \mu_a p_a \quad (\text{I.7.9})$$

and

$$\tau_r = \mu_r p_r \quad (\text{I.7.10})$$

where $\mu_a = \tau_{a,1}$ and $\mu_r = \tau_{r,1}$ are analogous to the Amontons-Coulomb coefficients of kinetic friction. It follows from this that the repulsive contribution to the shear stress is of a short-range nature and it will become the dominant term for dense fluids. On the other hand, the attractive part is a long-range property that will prevail in the case of light fluids. However when a fluid is brought under high pressure, the intermolecular distance between the moving layers reduces. This results in the fact that the short-range repulsive forces prevail over the long-range attractive forces. Due to this, Quiñones-Cisneros et al. (2000) suggested a second order truncation of the repulsive shear stress term, Eq.(I.7.8) for fluids under high pressure, whereas the high order contributions coming from attractive forces are neglected. This leads to the following expression for the friction shear stress τ_f term

$$\tau_f = \mu_r p_r + \mu_a p_a + \mu_{rr} p_r^2 \quad (\text{I.7.11})$$

Thus, from the definition of viscosity (Section I.1), the friction viscosity contribution η_f can be written as

$$\eta_f = \frac{\mu_r p_r + \mu_a p_a + \mu_{rr} p_r^2}{du/dh} \quad (\text{I.7.12})$$

resulting in

$$\eta_f = \kappa_r p_r + \kappa_a p_a + \kappa_{rr} p_r^2 \quad (\text{I.7.13})$$

where the repulsive and attractive viscous friction coefficients κ_r , κ_a , and κ_{rr} are defined by the ratios between the Amontons-Coulomb coefficients of kinetic friction and the shear rate du/dh . These viscous friction coefficients will depend only on the temperature. Eq.(I.7.13) will be referred to as the quadratic *f-theory* model. Clearly, when the dilute gas limit ($\rho = 0$) is approached the van der Waals repulsive and attractive forces vanish, resulting in

$$\lim_{\rho \rightarrow 0} [\eta_f] = 0 \quad (\text{I.7.14})$$

Thus, the total fluid viscosity can be expressed as

$$\eta = \eta_0 + \eta_f \quad (\text{I.7.15})$$

where η_f may be given by Eq.(I.7.13) and η_0 is the dilute gas viscosity. The dilute gas viscosity can be obtained by Eq.(I.2.3) (Chung et al. 1988), which is an empirical model related to kinetic theory of gases. This model has in Section I.5.3 been shown to satisfactorily predict the dilute gas viscosity of various hydrocarbon fluids over wide ranges of temperature.

If the second order repulsive pressure term is neglected, Eq.(I.7.13) reduces to a linear model

$$\eta_f = \kappa_r p_r + \kappa_a p_a \quad (\text{I.7.16})$$

which is analogous to the Amontons-Coulomb friction law. The linear model is referred to as the linear *f-theory* model.

I.7.1.1 Illustration of the Friction Theory

In order to illustrate the application of the *f-theory* to real fluids Quiñones-Cisneros et al. (2000) used the SRK EOS (Soave 1972) and the PRSV EOS (Stryjek and Vera 1986), which are two of the more widely used cubic EOSs of the van der Waals family, containing a repulsive pressure term p_r and an attractive pressure term p_a . For

consistency with the modeling results, the required critical constants and parameters in the SRK and the PRSV EOS are those recommended by Stryjek and Vera (1986). The critical volumes and the molecular weights required in Eq.(I.2.3) for the dilute gas viscosity calculations have been taken from Reid et al. (1987).

The performance of the linear and quadratic *f-theory* models with the SRK EOS has been investigated from low to very high pressures using isothermal viscosity data of methane at 273.1 K and 298.15 K (van der Gulik et al. 1988 and 1992). The application of the linear *f-theory* with the SRK EOS is shown in Figure I.34 for the 273.1 K and the 298.15 K isotherms of methane for pressures up to 10000 bar. From the results presented in this figure it can be seen that when the linear *f-theory* model is only fitted to pressures up to 1000 bar, monotonically increasing deviations are obtained as the model is extrapolated to higher pressures. By using all of the data for the fitting of the linear *f-theory* model a significant improvement of the modeling results are obtained compared with the results obtained using only data up to 1000 bar. However, although better modeling results are obtained, it can be seen from Figure I.34 that there are regions where some clear deviations are encountered. On the other hand, by fitting the

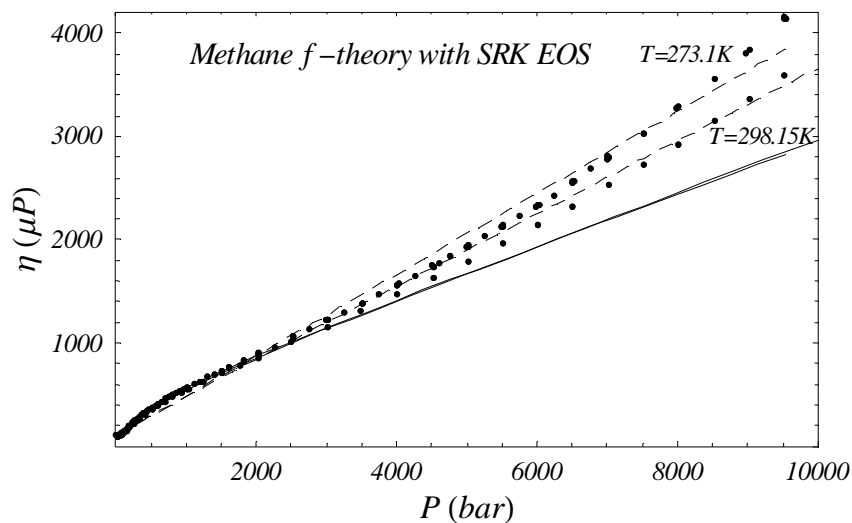


Figure I.34 Results for modeling the 273.1 K and the 298.15 K methane isotherms (van der Gulik et al. 1988 and 1992) by use of the linear *f-theory* with the SRK EOS for pressures up to 10000 bar. (—) shows the results of fitting the model to the data up to 1000 bar, (---) shows the results when all the data have been used for fitting the model.

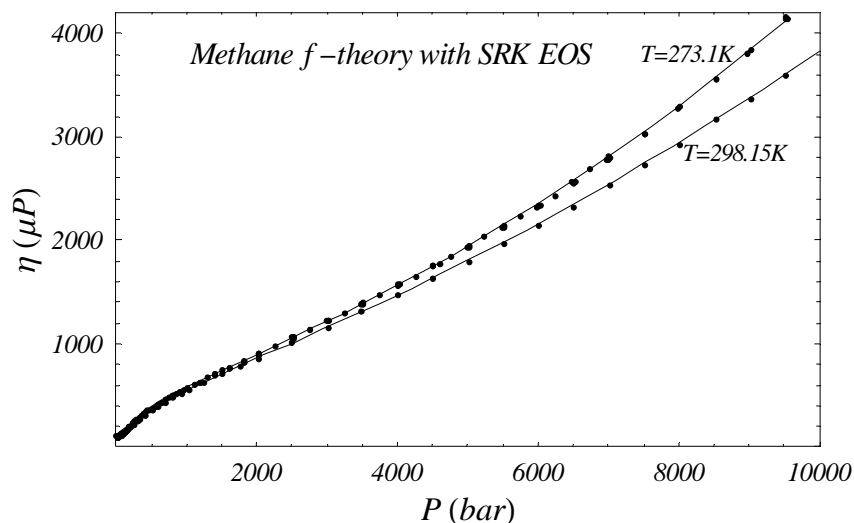


Figure I.35 Results for modeling the 273.1 K and the 298.15 K methane isotherms (van der Gulik et al. (1988 and 1992) by use of the quadratic *f-theory* with the SRK EOS for pressures up to 10000 bar.

quadratic *f-theory* model to the entire pressure range very accurate modeling results are obtained, see Figure I.35. In this case, the deviations are within the experimental uncertainty.

The different friction contributions in the quadratic *f-theory* model have been analyzed in order to get an understanding of the high-pressure viscosity results. Figure I.36 shows the friction contributions to the viscosity given by the linear repulsive term $\eta_{f,r}$, the linear attractive term $\eta_{f,a}$, and the quadratic repulsive term $\eta_{f,rr}$ for methane at 273.1 K. These results clearly show that from low pressure to pressures up to 1000 bar, both of the linear terms are the dominating terms, whereas the quadratic term may be neglected. However, as the pressure increases, far beyond 1000 bar, the attractive term appears to converge to a constant while the linear and the quadratic repulsive terms become the dominating terms.

Based on the accurate modeling of single isotherms up to high pressures using the quadratic *f-theory* model, the temperature dependency of the friction coefficients κ_r , κ_a , and κ_{rr} can be established. Thus, the temperature dependency of the friction coefficients has been studied by Quiñones-Cisneros et al. (2000) using the recommended viscosity data for propane by Vogel et al. (1998) in the temperature range 100 – 600 K and from 1 to 1000 bar. In Figure I.37 and I.38 the behavior of the friction

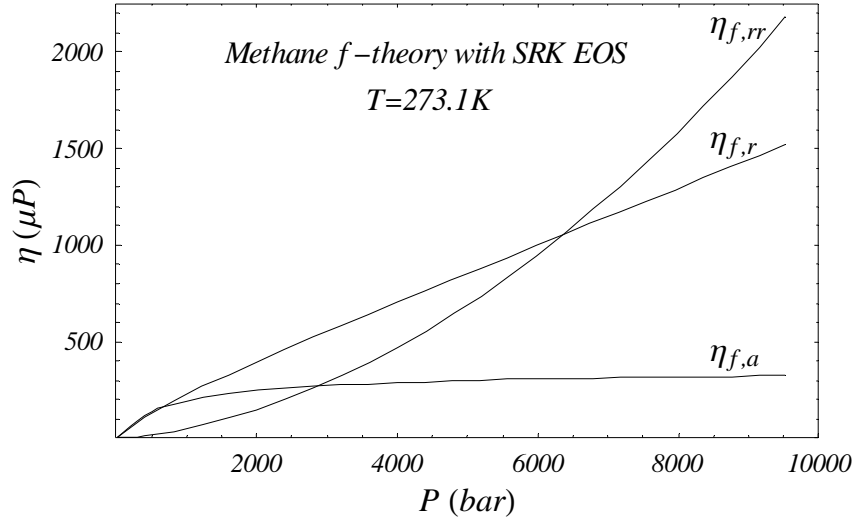


Figure I.36 Contribution of the different friction terms in the case of modeling methane at 273.1 K (van der Gulik et al. 1992) using the quadratic *f-theory* with the SRK EOS for pressures up to 10000 bar.

coefficients obtained for propane with the aid of the quadratic *f-theory* in connection with the SRK EOS for pressures up to 1000 bar is shown as a function of the inverse reduced temperature, T_r^{-1} . Based on these figures, it can be seen that the linear attractive and the quadratic repulsive contributions to the total viscosity, $\kappa_a p_a$ and $\kappa_{rr} p_r^2$ are always positive, since the van der Waals repulsive pressure term p_r is always positive and the attractive pressure term p_a is always negative. The positive values of these two friction contributions indicate that they act as dragging forces. In case of the linear repulsive viscosity term $\kappa_r p_r$ a more complex behavior is found, since the linear repulsive friction coefficients κ_r switches from a positive value to a negative value for reduced temperatures $T_r < 0.5$, see Figure I.37. This indicates that the linear repulsive viscosity term switches from a dragging force to an enhancing force for the fluid mobility. Due to this, the linear repulsion friction contribution at low reduced temperatures and high densities will then try to keep apart the neighboring fluid layers, whereas the quadratic repulsive friction contribution coming from layers other than the neighboring layers has a strong dragging force contribution, as shown in Figure I.39 for the 150 K isotherm of propane (Vogel et al. 1998).

Further, it can be seen from Figure I.37 that the linear friction coefficients

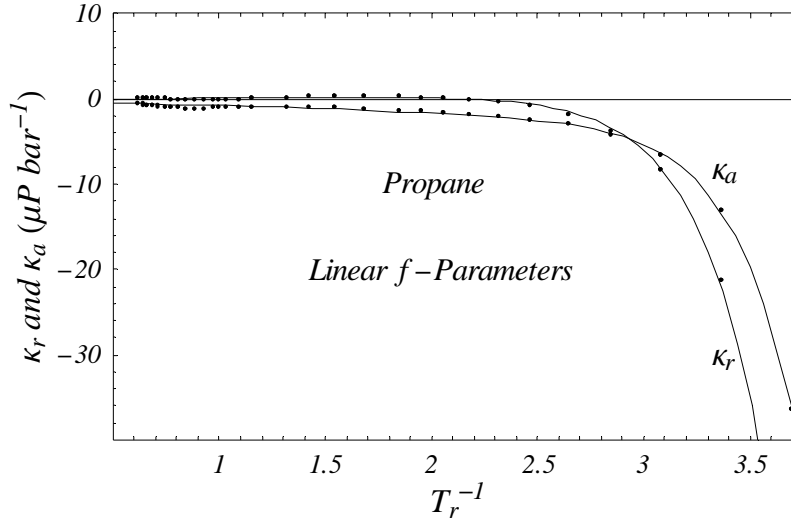


Figure I.37 Temperature behavior of the linear attractive and repulsive friction coefficients for propane modeled by the quadratic *f-theory* with the SRK EOS for pressures up to 1000 bar.

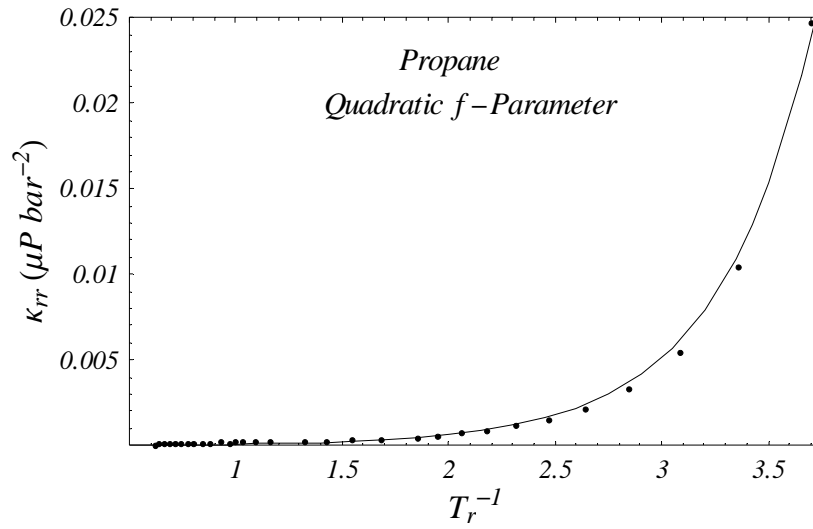


Figure I.38 Temperature behavior of the quadratic repulsive friction coefficient for propane modeled by the quadratic *f-theory* with the SRK EOS for pressures up to 1000 bar.

approach a constant value as the temperature goes to infinity, $T_r^{-1} \rightarrow 0$, whereas the quadratic repulsive friction term approaches zero, see Figure I.38. In case of low temperatures a strong exponential behavior is observed for both the linear attractive and repulsive friction coefficients as well as the quadratic repulsive friction coefficient.

Based on these observations with respect to the temperature dependencies of the

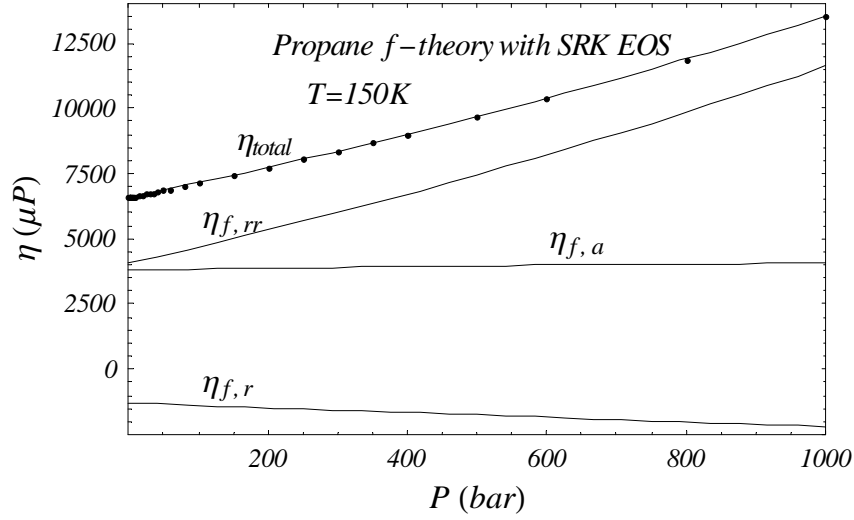


Figure I.39 Contribution of the different friction terms in the case of propane modeled at 150 K by the quadratic *f-theory* with the SRK EOS for pressures up to 1000 bar.

different friction coefficients Quiñones-Cisneros et al. (2000) derived the following parametric laws

$$\kappa_r = a_0 + \sum_{i=1}^n a_i (\exp[i(\Gamma - 1)] - 1) \quad (\text{I.7.17})$$

$$\kappa_a = b_0 + \sum_{i=1}^n b_i (\exp[i(\Gamma - 1)] - 1) \quad (\text{I.7.18})$$

and

$$\kappa_{rr} = \sum_{i=2}^n c_i (\exp[i\Gamma] - 1) \quad (\text{I.7.19})$$

where

$$\Gamma = \frac{T_c}{T} \quad (\text{I.7.20})$$

The a_0 and b_0 constants in Eqs.(I.7.17) and (I.7.18) are important for the modeling of the viscosity in the high temperature region, whereas the high order exponential terms become relevant at low temperatures. The reason, why the series for the quadratic term in Eq.(I.7.19) first starts with the second order term is because it has been forced to vanish as the temperature goes to infinity. In addition, for numerical convenience, the origin of the series for κ_r and κ_a has been shifted to the critical point.

The recommended viscosity data for propane by Vogel et al. (1998) from 100 K

to 600 K and up to 1000 bar have been modeled in order to illustrate the capability of the *f-theory* for accurate viscosity modeling. The modeling has been performed by a least squares fit of the propane data to the quadratic *f-theory* with the SRK EOS. For the κ_r , κ_a , and κ_{rr} friction coefficients, the series have been cut-off in Eqs.(I.7.17) – (I.7.19) at $n = 2$. In this way, the quadratic SRK *f-theory* model has only 7 adjustable constants. The modeling results are shown in Figure I.40, and, as it can be seen, the model performance over the entire temperature and pressure ranges is good. The obtained AAD is 1.68%, which is within the reported uncertainty of the recommended data. Even for the 370 K isotherm, which is close to the critical isotherm, the performance of the *f-theory* model is also very satisfactory, see Figure I.40.

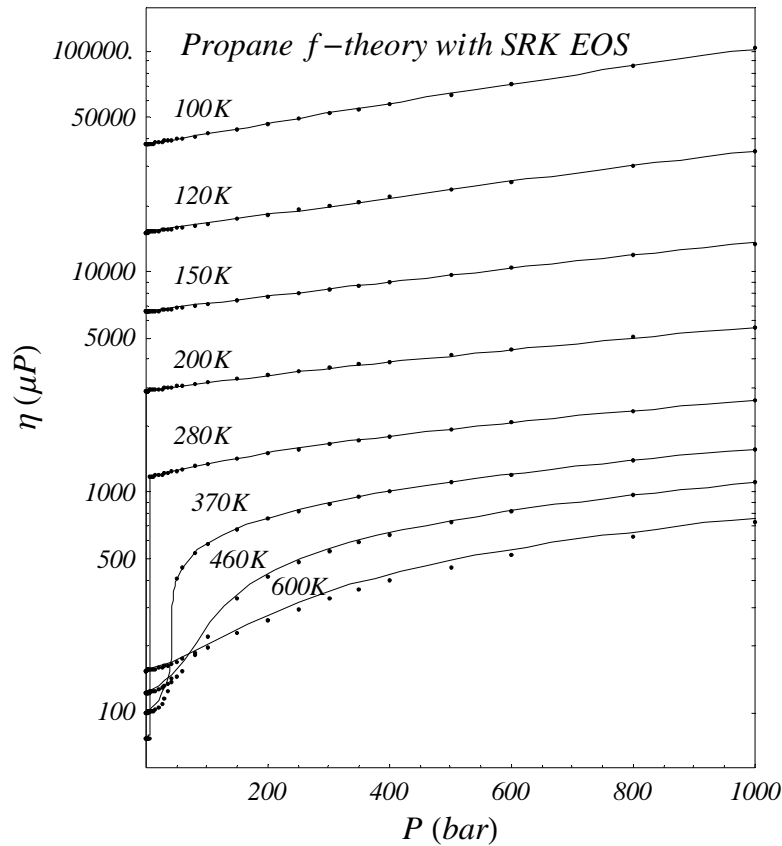


Figure I.40 Modeling of propane using a 7 constants *f-theory* model in conjunction with the SRK EOS (—), experimental data (•) taken from Vogel et al. (1998)

I.7.1.2 Modeling of Pure n-Alkanes

Quiñones-Cisneros et al. (2000) further illustrated the application of the *f-theory* for the accurate viscosity modeling of n-alkanes ranging from methane to n-decane using the SRK and the PRSV EOS in connection with the *f-theory*. However, instead of using the 7 constants *f-theory* model that has been used in the previous section to model the viscosity of propane, Quiñones-Cisneros et al. (2000) derived the following parametric laws for the friction coefficients containing only 5 adjustable constants.

$$\kappa_r = a_1 \exp[\Gamma - 1] + a_2 (\exp[2(\Gamma - 1)] - 1) \quad (\text{I.7.21})$$

$$\kappa_a = b_1 \exp[\Gamma - 1] + b_2 (\exp[2(\Gamma - 1)] - 1) \quad (\text{I.7.22})$$

and

$$\kappa_{rr} = c_2 (\exp[2\Gamma] - 1) \quad (\text{I.7.23})$$

where Γ is defined in Eq.(I.7.20).

The parameters obtained for the studied n-alkanes are given in Table I.14 for the SRK EOS and in Table I.15 for the PRSV EOS.

<i>f-theory</i> with the SRK EOS					
	a_1 [μP/bar]	a_2 [μP/bar]	b_1 [μP/bar]	b_2 [μP/bar]	c_2 [μP/bar ²]
Methane	0.0954878	-0.0983074	-0.424734	0.0598492	1.34730 10 ⁻⁵
Ethane	0.0404072	-0.2491910	-0.745442	0.0144118	1.53201 10 ⁻⁵
Propane	0.322169	-0.104459	-0.692914	0.0515112	1.08144 10 ⁻⁵
n-Butane	0.554315	-0.0334891	-0.577284	0.066969	1.03272 10 ⁻⁵
n-Pentane	0.556934	-0.143105	-0.825295	0.0812198	1.67262 10 ⁻⁵
n-Hexane	0.529445	-0.262603	-1.00295	-0.00765227	2.76425 10 ⁻⁵
n-Heptane	0.656480	-0.0643520	-0.964719	0.0485736	2.33140 10 ⁻⁵
n-Octane	0.503808	-0.114929	-1.29910	0.0479385	3.88652 10 ⁻⁵
n-Nonane	0.599863	-0.0625962	-1.40430	0.0220808	4.08108 10 ⁻⁵
n-Decane	0.396401	-0.345116	-1.73836	-0.178929	6.85603 10 ⁻⁵

Table I.14 Parameters for the *f-theory* with the SRK EOS (5 constants model).

	<i>f-theory</i> with the PRSV EOS				
	a_1 [μP/bar]	a_2 [μP/bar]	b_1 [μP/bar]	b_2 [μP/bar]	c_2 [μP/bar ²]
Methane	0.0978603	-0.0947431	-0.347478	0.060992	1.09269 10 ⁻⁵
Ethane	0.126032	-0.180542	-0.54886	0.033303	9.64845 10 ⁻⁶
Propane	0.245709	-0.164913	-0.630638	0.0339251	1.13654 10 ⁻⁵
n-Butane	0.478611	-0.0819001	-0.495743	0.0652985	1.07941 10 ⁻⁵
n-Pentane	0.439938	-0.232544	-0.753537	0.0584165	1.82595 10 ⁻⁵
n-Hexane	0.426605	-0.335750	-0.895709	-0.00664088	2.69972 10 ⁻⁵
n-Heptane	0.561799	-0.137427	-0.834083	0.0613722	2.33423 10 ⁻⁵
n-Octane	0.406290	-0.258599	-1.14826	0.0283937	3.88084 10 ⁻⁵
n-Nonane	0.484008	-0.256690	-1.24586	-0.00934743	4.30254 10 ⁻⁵
n-Decane	0.244111	-0.760327	-1.63800	-0.311341	7.49667 10 ⁻⁵

Table I.15 Parameters for the *f-theory* with the PRSV EOS (5 constants model).

I.7.1.3 Application of the Friction Theory to Mixtures

In order to apply the *f-theory* model to mixtures Quiñones-Cisneros et al. (2000) derived a simple mixing rule for the κ_r , κ_a , and κ_{rr} friction coefficients, but preserving the basic *f-theory* structure. For the derived quadratic *f-theory* models, the mixture viscosity is given by

$$\eta_{mx} = \eta_{0,mx} + \eta_{f,mx} \quad (\text{I.7.24})$$

where the subscript *mx* indicates the corresponding mixture property. The dilute gas viscosity of the mixture is calculated by

$$\eta_{0,mx} = \exp \left[\sum_{i=1}^n x_i \ln(\eta_{0,i}) \right] \quad (\text{I.7.25})$$

In all cases, the subscript *i* refers to the corresponding pure component of an *n* component mixture. The dilute gas viscosity of the pure compounds can be estimated by Eq.(I.2.3). The mixture friction contribution term is given by

$$\eta_{f,mx} = \kappa_{r,mx} p_{r,mx} + \kappa_{a,mx} p_{a,mx} + \kappa_{rr,mx} p_{r,mx}^2 \quad (\text{I.7.26})$$

where $p_{a,mx}$ and $p_{r,mx}$ are the attractive and repulsive pressure contributions of the mixture and the $\kappa_{r,mx}$, $\kappa_{a,mx}$, and $\kappa_{rr,mx}$ are the corresponding viscous friction coefficients

for the mixture. Hence, for the friction viscous coefficients the following mixing rules have been suggested by Quiñones-Cisneros et al. (2000)

$$\kappa_{r,mx} = \sum_{i=1}^n z_i \kappa_{r,i} \quad (\text{I.7.27})$$

$$\kappa_{a,mx} = \sum_{i=1}^n z_i \kappa_{a,i} \quad (\text{I.7.28})$$

and

$$\kappa_{rr,mx} = \sum_{i=1}^n z_i \kappa_{rr,i} \quad (\text{I.7.29})$$

where a weighted fraction exponential rule for z_i has been proposed,

$$z_i = \frac{x_i}{M_{w,i}^{\varepsilon} MM} \quad (\text{I.7.30})$$

where

$$MM = \sum_{i=1}^n \frac{x_i}{M_{w,i}^{\varepsilon}} \quad (\text{I.7.31})$$

The reason for introducing this mixing rule for z_i was due to the fact that Quiñones-Cisneros et al. (2000) observed that for asymmetric mixtures, such as the methane + n-decane system, the small or lightest compound tends to enhance the mobility of the heavier compound further than linearly.

For the 5 constants f -theory model in connection with the SRK EOS Quiñones-Cisneros et al. (2000) found the best performance using $\varepsilon = 0.15$, whereas for the PRSV EOS $\varepsilon = 0.075$ has been obtained. However, it should be stressed that when $\varepsilon = 0$, $z_i = x_i$, which gives satisfactory results for mixtures composed of light and similar hydrocarbons.

I.7.2 Viscosity Prediction of Hydrocarbon Mixtures

The f -theory has been applied to viscosity predictions of n-alkane mixtures composed of n-alkanes ranging from methane to n-decane. Although these mixtures may be seen as very simple representations of refinery cuts or petroleum reservoir fluids, they can show the potential of extending this viscosity approach to real petroleum and reservoir fluids. Particularly, when it is taken into account that accurate viscosity modeling has been achieved using simple cubic EOSs commonly used by the oil industry.

The viscosity of binary and ternary n-alkane mixtures have been predicted according to the calculation procedure described for the *f-theory* in Section I.7.1.3 using the SRK and the PRSV EOS, below called *f-SRK* and *f-PRSV*, respectively. The required pure compound friction coefficients have been estimated using Eqs.(I.7.21) – (I.7.23). In the EOS models the original van der Waals mixing rules, Eqs.(I.3.15) and (I.3.16), have been used along with the binary interaction parameters reported by (Knapp et al. 1982). For the different binary and ternary systems studied in this work, the temperature and pressure ranges together with the total number of points and the number of different compositions are given for each system in Table I.16.

The predicted viscosities have been compared with the experimental values. The obtained AAD and the MxD are given in Table I.17. For comparison purposes the results obtained by the LBC-SRK, the LBC-SBWR, the CS2, and the PRVIS models are also reported in Table I.17. The calculation procedures for these viscosity models are similar to the procedures used in order to evaluate these models, see Section I.5.1.

From Table I.17, it can clearly be seen that the performance of the *f-theory* models is very satisfactorily compared with the other evaluated models. In most cases, the *f-theory* AAD obtained for the studied mixtures are within or close to the experimental uncertainty, which for most engineering and industrial applications is satisfactory. In the case of the methane + n-decane system, rather than the model performance, the obtained *f-theory* AAD largely reflects the experimental uncertainty of the binary data and the experimental uncertainty of the data used to obtain the pure n-decane parameters. In other cases, such as methane + propane, the MxD of 12.99% is found for a mole fraction of methane of 0.2207 at $T = 377.59$ K and $P = 55.161$ bar, which corresponds to conditions near the mixture critical point for which the experimental uncertainty is also large. For a better illustration of this system and composition, the *f-SRK* model predictions along with the experimental data are shown in Figure I.41. In addition, the performance of the *f-SRK* viscosity predictions for the binary n-pentane + n-decane mixture containing 40.80 mole% n-pentane and the ternary mixture containing 15.01 mole% n-pentane + 9.94 mole% n-octane + 75.05 mole% n-decane are shown together with the experimental data in Figures I.42 and I.43, respectively.

System	Reference	Mixtures		T -range [K]	P -range [bar]
		NM	NP		
C ₁ +C ₂	Diller (1984)	3	250	120 – 300	15 – 349
C ₁ +C ₃	Giddings et al. (1966)	4	282	311 – 411	1.0 – 552
C ₁ +n-C ₄	Carmichael et al. (1967)	1	104	278 – 478	1.4 – 358
C ₁ +n-C ₆	Berstad (1989)	3	53	293 – 451	150 – 428
C ₁ +n-C ₁₀	Knapstad et al. (1990)	4	96	292 – 431	98 – 420
n-C ₅ + n-C ₈	Barrufet et al. (1999)	9	295	298 – 373	1.0 – 246
n-C ₅ + n-C ₁₀	Estrada-Baltazar et al. (1998b)	9	312	298 – 373	1.0 – 246
n-C ₆ + n-C ₇	Assael et al. (1992)	2	53	303 – 323	1.0 – 717
n-C ₇ + n-C ₈	Aleskerov et al. (1979)	4	172	292 – 480	1.0 – 491
n-C ₇ + n-C ₉	Assael et al. (1992)	2	57	303 – 323	1.0 – 718
n-C ₈ + n-C ₁₀	Estrada-Baltazar et al. (1998a)	9	324	298 – 373	1.0 – 246
n-C ₅ +n-C ₈ +n-C ₁₀	Iglesias-Silva et al. (1999)	15	530	298 – 373	1.0 – 246

Table I.16. References for n-alkane mixtures. NM is the number of different mixtures, and NP is the number of points.

	AAD% / MxD%					
	LBC-SRK	LBC-SBWR	CS2	PRVIS	f -SRK	f -PRSV
C ₁ +C ₂	11.8 / 37.2	2.87 / 12.0	4.36 / 17.8	20.9 / 57.0	3.08 / 14.0	3.00 / 14.7
C ₁ +C ₃	3.52 / 20.2	3.52 / 16.7	6.52 / 32.9	19.8 / 67.3	3.33 / 13.4	2.23 / 8.82
C ₁ +n-C ₄	8.50 / 20.6	9.54 / 15.9	8.22 / 38.9	16.2 / 45.0	3.27 / 10.9	2.53 / 6.72
C ₁ +n-C ₆	7.94 / 30.1	11.0 / 18.8	9.22 / 24.8	35.6 / 80.2	2.84 / 7.40	2.07 / 9.86
C ₁ +n-C ₁₀	10.2 / 42.4	17.9 / 25.9	9.54 / 23.4	13.9 / 41.0	7.25 / 16.4	7.40 / 17.0
n-C ₅ + n-C ₈	16.0 / 53.9	8.93 / 23.2	7.73 / 18.2	9.80 / 66.7	3.53 / 11.3	3.42 / 11.2
n-C ₅ + n-C ₁₀	11.8 / 62.1	9.98 / 23.9	9.51 / 18.3	12.7 / 59.5	3.32 / 14.0	3.57 / 14.1
n-C ₆ + n-C ₇	40.5 / 63.4	5.98 / 16.6	3.77 / 11.4	3.16 / 12.8	0.51 / 1.03	1.03 / 1.74
n-C ₇ + n-C ₈	41.0 / 86.1	9.34 / 26.8	5.91 / 16.0	11.0 / 49.6	2.82 / 8.66	2.33 / 8.33
n-C ₇ + n-C ₉	46.6 / 79.0	5.46 / 15.1	3.98 / 11.2	7.03 / 16.8	0.97 / 2.37	0.67 / 1.70
n-C ₈ + n-C ₁₀	23.4 / 47.1	6.56 / 15.4	6.47 / 12.8	5.69 / 8.06	2.75 / 7.05	4.31 / 9.57
n-C ₅ +n-C ₈ +C ₁₀	19.3 / 47.3	5.14 / 14.2	5.20 / 12.4	7.41 / 40.6	4.11 / 18.1	3.77 / 17.5

Table I.17. Comparison of viscosity models for n-alkane mixtures. References for the different mixtures are given in Table I.16.

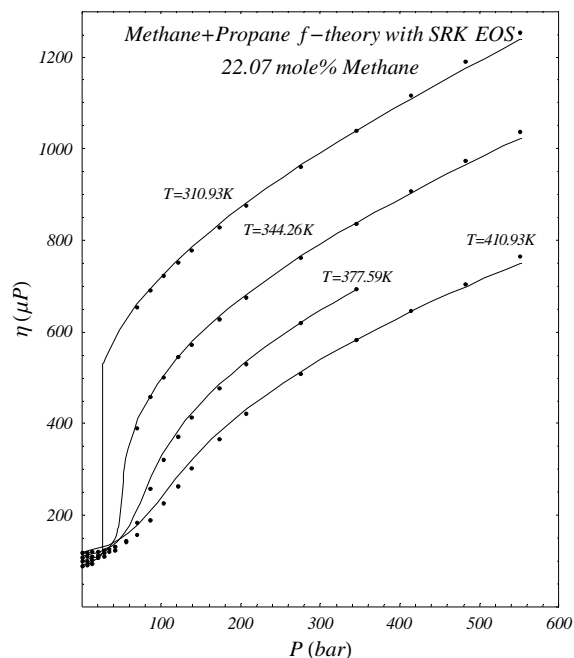


Figure I.41 Viscosity predictions of the binary mixture containing 22.07 mole% methane + 77.93 mole% propane using the SRK f -theory (—) compared with the experimental values (●) Giddings et al. (1966).

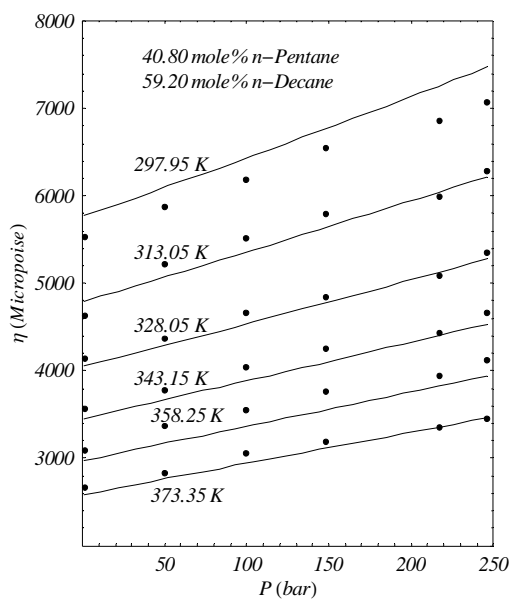


Figure I.42 Viscosity of the binary mixture containing 40.80 mole% n-pentane + 59.20 mole% n-decane, (—) predicted by the f -SRK, (●) experimental data (Estrada-Baltazar et al. 1998b).

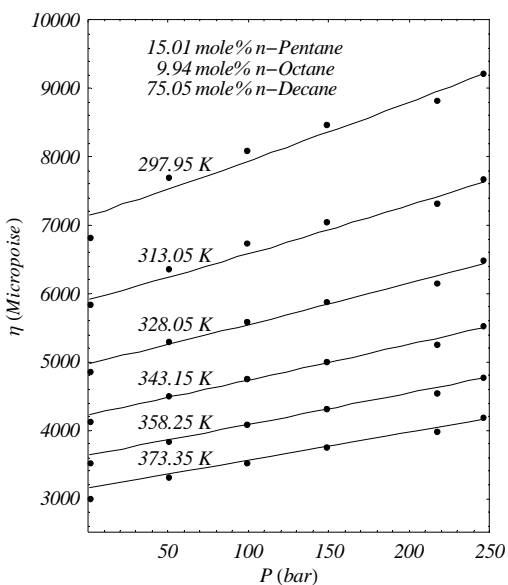


Figure I.43 Viscosity of the ternary mixture containing 15.01 mole% n-pentane + 9.94 mole% n-octane + 75.05 mole% n-decane, (—) predicted by the f -SRK, (●) experimental data (Iglesias-Silva et al. 1999).

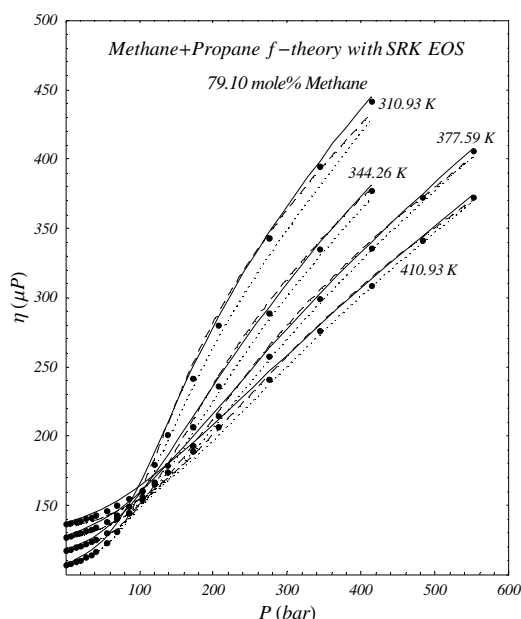


Figure I.44 Viscosity predictions of the binary mixture containing 79.10 mole% methane + 20.90 mole% propane, (—) predicted by the *f*-SRK model, (- - -) with the LBC-SBWR model, and (·····) with the LBC-SRK model, (●) experimental data (Giddings et al. 1966).

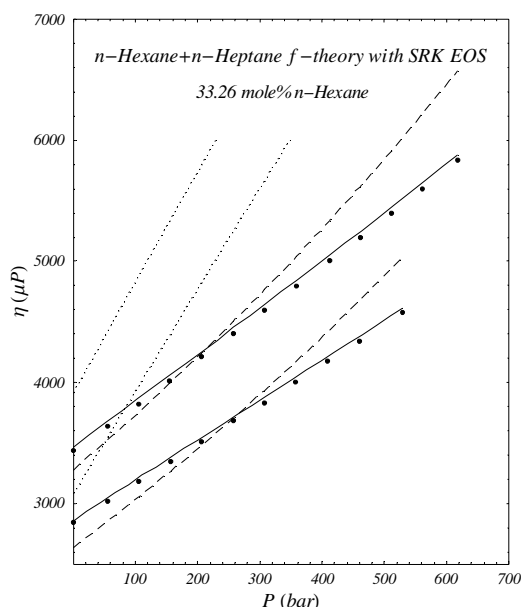


Figure I.45 Viscosity predictions of the binary mixture containing 33.26 mole% n-hexane + 66.74 mole% n-heptane, (—) predicted by the *f*-SRK model, (- - -) with the LBC-SBWR model, and (·····) with the LBC-SRK model, (●) experimental data (Assael et al. 1992).

Finally, a clearer comparison between the *f-theory* capabilities and the widely used LBC model is shown in Figures I.44 and I.45. Although, the LBC model is widely used by the oil industry for viscosity predictions, this model was developed for light hydrocarbons and tuned against experimental viscosities and densities. Therefore, when the LBC model is used to predict the viscosity of light, rich in methane, mixtures, both the LBC-SRK and the LBC-SBWR models, as well as an *f-theory* based model, predict the viscosity very accurately, see Figure I.44. However, if the components of a given mixture are slightly heavier than the main components of natural gases, the LBC-SRK model is not capable of providing acceptable results – even though a Péneloux volume shift has been used, see Figure I.45. Furthermore, even with accurate density values, as it is the case with the SBWR model, the LBC-SBWR model also fails to provide accurate viscosity predictions for mixtures composed of intermediate hydrocarbons,

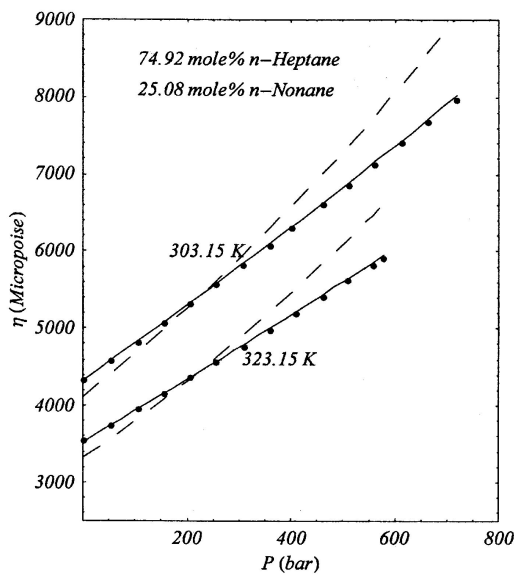


Figure I.46 Viscosity of the binary mixture containing 74.92 mole% n-heptane + 25.08 mole% n-nonane, (—) predicted by the *f*-SRK, (- - -) predicted by the LBC-SBWR, (•) experimental data (Assael et al., 1992).

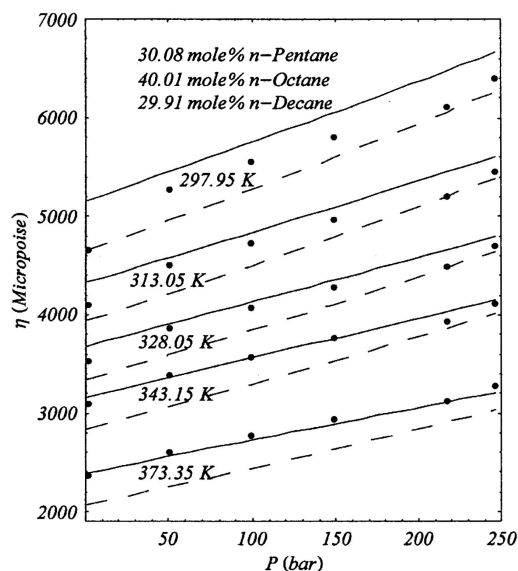


Figure I.47 Viscosity of the ternary mixture containing 30.08 mole% n-pentane + 40.01 mole% n-octane + 29.91 mole% n-decane, (—) predicted by the *f*-SRK, (- - -) predicted the by LBC-SBWR, (•) experimental data (Iglesias-Silva et al., 1999).

such as the binary mixtures composed of n-hexane + n-heptane or n-heptane + n-nonane, see Figures I.45 and I.46. In Figure I.47, the performance of the *f*-SRK and the LBC-SBWR models are shown for the ternary mixture containing 30.08 mole% n-pentane + 40.01 mole% n-octane + 29.91 mole% n-decane, respectively.

Further, the very accurate viscosity predictions obtained over wide ranges of temperature and pressure for n-alkane mixtures by the *f*-theory models can also clearly be seen in Figures I.41 through I.47 and in Table I.17.

I.7.3 Recommended Viscosities

In order to establish the functional dependency for the variables in a totally predictive viscosity model, tabulations of smoothed viscosity data versus temperature and pressure are required. The reason is that a more equally distribution of the viscosity versus temperature and pressure is obtained, than if raw viscosity data are directly taken from

different reference sources.

Although tabulations of recommended viscosities are given in the literature for many pure fluids, see e.g. Stephan and Lucas (1979), the *f-theory* has been used to estimate recommended viscosity data for n-alkanes ranging from methane to n-octadecane due to new viscosity measurements. The estimation of recommended viscosities have been performed within the experimental temperature and pressure ranges. Because the viscosity modeling with the *f-theory* does not depend on the accuracy of the density, since the viscosity is linked to the pressure in the *f-theory*, the *f-theory* approach is a faster method in order to obtain recommended viscosities.

In this estimation of recommended viscosities the PRSV EOS has been used in the *f-theory*, and the dilute gas viscosity has been calculated by Eq.(I.2.3). The required critical properties and parameters have been taken from the recommended values of Stryjek and Vera (1986). The critical volumes have been taken from Reid et al. (1987), except for n-pentane, which seems too low compared to the critical volumes of other n-alkanes. In case of n-pentane a more appropriate value for the critical volume is given by Anselme et al. (1990). The critical volumes for n-hexadecane (955 cm³/mole) and n-octadecane (1101 cm³/mole) have been extrapolated from the critical volumes reported by Reid et al. (1987).

In general, the uncertainty in the dilute gas viscosity predicted by Eq.(I.2.3) will not have any effect on the total predicted viscosity of subcritical liquids, since the total viscosity of a subcritical liquid is very high compared to the dilute gas viscosity contribution. However, when predicting the viscosity of light gases or dense fluids at high temperatures the estimated dilute gas viscosity term becomes important. This is due to the fact that the dilute gas viscosity increases with increasing temperature, as mentioned in Section I.1.1, while the viscosity of dense fluids decreases with increasing temperatures, see e.g. Figure I.3.

I.7.3.1 Estimating Recommended Viscosities

Recommended viscosities have been estimated versus the reduced pressure for different reduced temperatures by fitting the PRSV *f-theory* model to the experimental values. The isotherms have been selected, so that they are equally distributed over the entire

experimental temperature range. For a particular isotherm, experimental data lying within the temperature intervals adjacent to this isotherm have been used in the estimation of the recommended viscosities. These temperature intervals correspond to the intervals obtained by dividing the entire temperature range into selected isotherms. For isotherms around the critical region the experimental data have been further divided into two pressure intervals, one for pressures up to a reduced pressure slightly above 2 and the other from a reduced pressure slightly below 2 to the maximum reduced pressure, in order to improve the accuracy of the model used to estimate the recommended viscosities. In this work, the experimental data have been modeled using the basic parametric laws for the friction parameters given in Section I.7.1.

The data sets, which have been used in the estimation of the recommended viscosities, are all based on experimental measurements; no extrapolated values have been included. Due to the fact that most engineering processes are carried out at pressures below 1000 bars, only data up to 1000 bar has been used, regardless that some references contain measurements up to higher pressures. The selected data sets, which have been used in this work, are given in Appendix A3, Table A3.1 – A3.15. These tables contain the references, the number of points, and the temperature and the pressure ranges of the selected references. The experimental data reported in the literature have been measured with different techniques and uncertainties. Because of this, an error analysis of the experimental data has been necessary to ensure that only consistent experimental data have been used to estimate the recommended viscosity values.

The general procedure for analyzing the experimental data and estimating the recommended viscosities for a given isotherm can be described in the following way. For each of the experimental points the dilute gas viscosity η_0 has been calculated by Eq.(I.2.3) and the residual friction viscosity $\eta_f = \eta - \eta_0$ has been obtained. The PRSV EOS has been solved in order to obtain the repulsive and attractive pressure terms (p_r and p_a) that correspond to the given phase of the experimental point. Then, the constants in the equations for the friction coefficients have been estimated by fitting Eq.(I.7.13) to all of the T - p_r - p_a - η_f data using a least squares method. For each of the experimental points, the percentage deviation between the total viscosity predicted by the PRSV *f-theory* model using the fitted friction constants and the experimental value has been

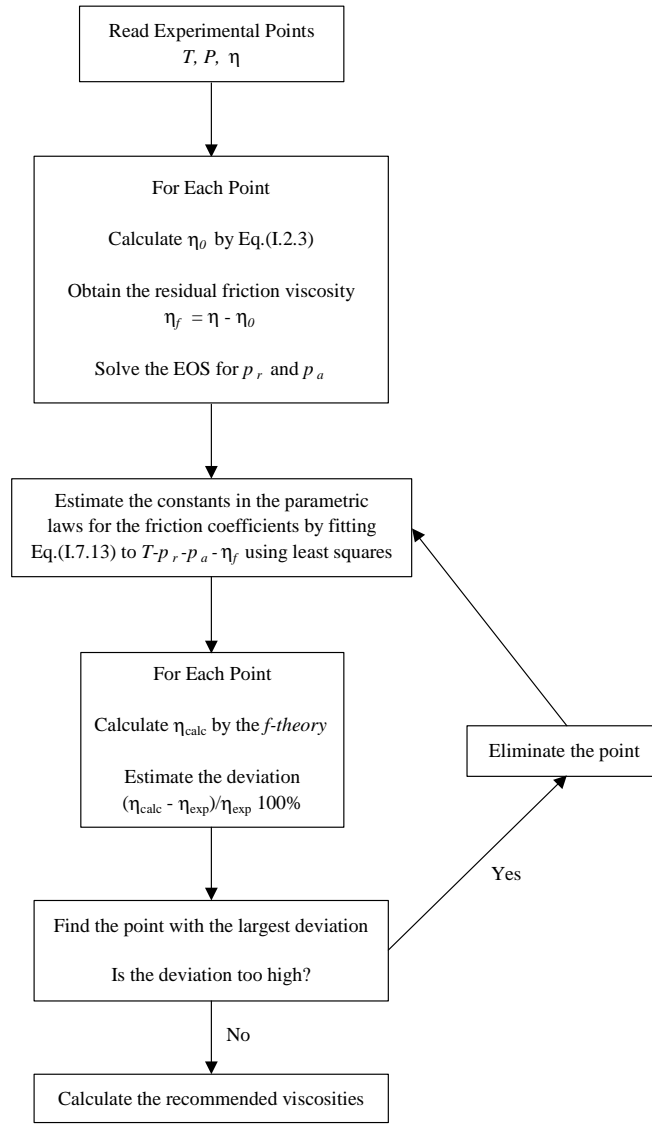


Figure I.48 Schematic representation of the calculation procedure of recommended viscosities.

calculated. Any point lying outside the experimental uncertainty or seems to be wrong has been eliminated. Based on this procedure recommended viscosities have been estimated at different reduced pressures using the PRSV *f-theory* model. A schematic representation of the estimation procedure for the recommended viscosities is illustrated in Figure I.48. The viscosity values recommended in this work are not extrapolated to reduced pressures above the corresponding maximum pressure of the experimental data that has been modeled.

I.7.3.2 Tabulations and Discussion

Tabulations of recommended viscosities for n-alkanes ranging from methane to n-octadecane are presented in Appendix A4, Table A4.1 to A4.15. For each fluid the reported viscosities are given at different reduced temperatures and reduced pressures, which are within the corresponding experimental temperature and pressure ranges. Below each table the used critical temperature and critical pressure are given in order to transform the reduced conditions to their corresponding real values. Further, the accuracy of the recommended viscosities for each isotherm is also reported in the tables as the average absolute deviation in percent (AAD%). The reported AAD values correspond to the accuracy with which the *f-theory* model reproduces the experimental data used for obtaining the recommended viscosities. For each isotherm the reported AAD has been found to be within the experimental uncertainty. The largest deviations are obtained for isotherms between reduced temperatures of 0.9 – 1.1 and in the vicinity of the critical region due to the fact that the derivative of the viscosity with respect to the pressure diverges at the critical point. Therefore, the accuracy of the recommended viscosities for these isotherms in the dense region will be better than the reported AADs in the tables, while the uncertainty of the recommended viscosities in the critical region will be higher.

Figure I.49, I.50, and I.51 show the behavior of the recommended viscosities for ethane at three different isotherms compared to the experimental data used for obtaining the recommended values. The three isotherms are the critical isotherm and the isotherms corresponding to a reduced temperature of 1.50 and 0.40, respectively. The recommended viscosities at a reduced temperature of 1.50 have been estimated by modeling the experimental data lying within the reduced temperature interval from 1.4 to 1.6. These experimental data are modeled with an AAD of 0.71% and an MxD of 3.00%, which are within the experimental uncertainty. This is also the case, when the experimental data within the reduced temperature interval from 0.3 to 0.5 are modeled in order to obtain the recommended viscosities at a reduced temperature of 0.40. The AAD is 0.55% and the MxD is 1.74%.

For the critical isotherm of ethane the AAD obtained for reduced pressures above 2 is 0.88% and the MxD is 3.07%, which is within the experimental uncertainty.

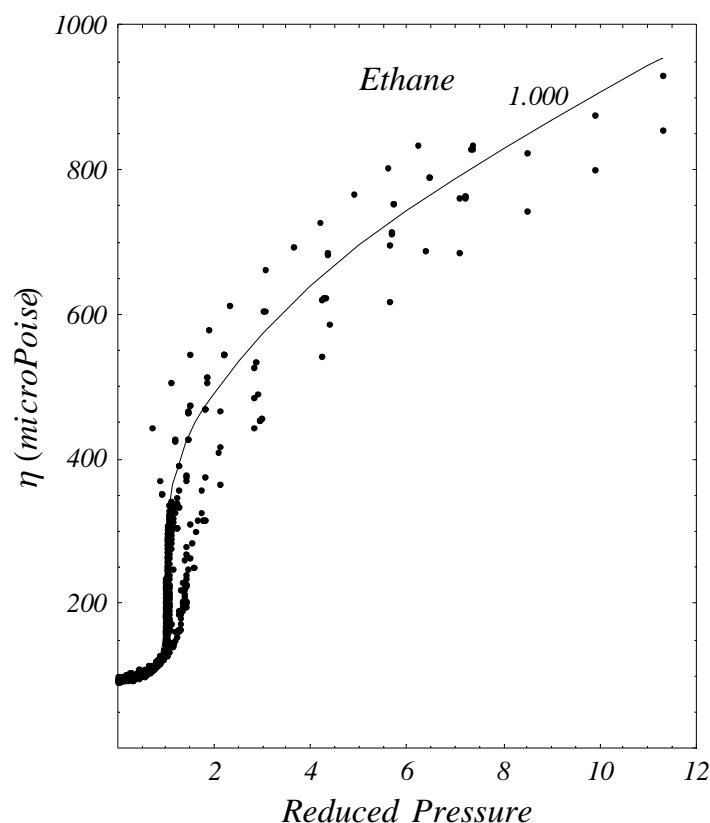


Figure I.49 Experimental data (●) for reduced temperatures between 0.9 and 1.1 used to obtain the critical isotherm correlation (—) from which the $T_r = 1.000$ recommended viscosity data have been taken.

This is also in agreement with the uncertainties obtained for viscosities in the liquid and supercritical region. But for reduced pressures below 2 an AAD of 4.38% and an MxD of 19.0% are obtained. The point with the MxD corresponds approximately to the critical point and therefore, since the derivative of the viscosity with respect to the pressure becomes infinite at the critical point, any small pressure deviation induces a large viscosity jump. Further, the uncertainty in the experimentally measured viscosity values also increases due to difficulties in carrying out measurements in the critical region.

Based on all of the tabulations the expected overall uncertainty for the recommended viscosities will be less than 1% outside the critical region. In the critical region the overall uncertainty will approximately be 5% with an MxD of around 10%.

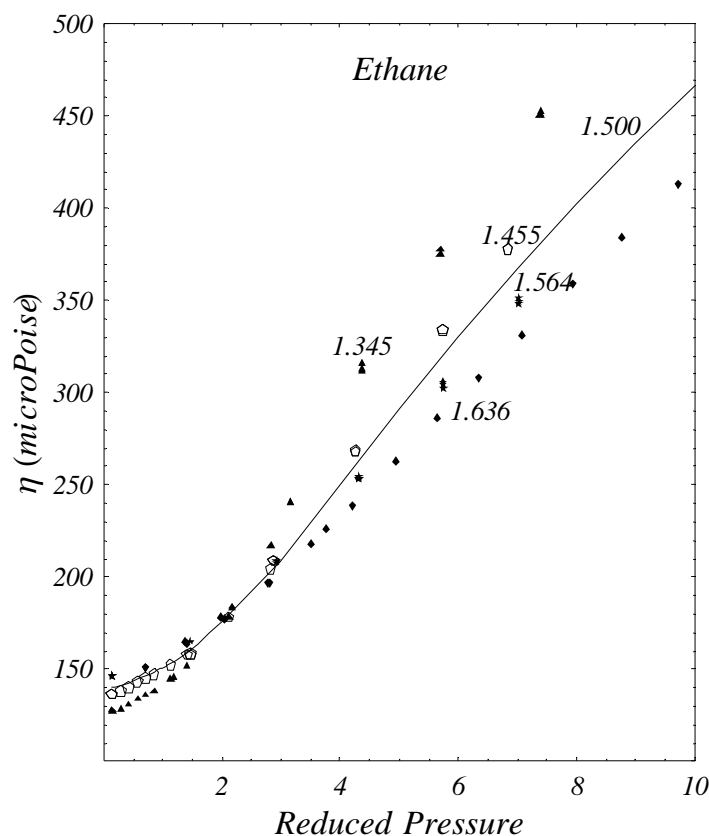


Figure I.50. Experimental data (points) corresponding to reduced temperatures between 1.4 and 1.6 used to obtain the 1.50 reduced temperature correlation (—) and the $T_r = 1.50$ recommended viscosity data.

As mentioned above a small change in the pressure will have a large effect on the predicted viscosity. Further, no special treatment has been made to improve the modeling of the viscosities in the critical region due to the fact that the critical region is not a main concern of this work. Nevertheless, the good performance of the *f-theory* in the critical region is clearly illustrated in Figure I.49.

I.7.3.3 Overall Representation

In order to derive *f-theory* models for the fluids, for which recommended viscosities have been estimated, a least square fitting of the recommended viscosities reported in Appendix A4, Tables A4.1 – A4.15 has been performed for the PRSV *f-theory* model. Since the recommended viscosity values reported in Appendix A4, Tables A4.1 – A4.15

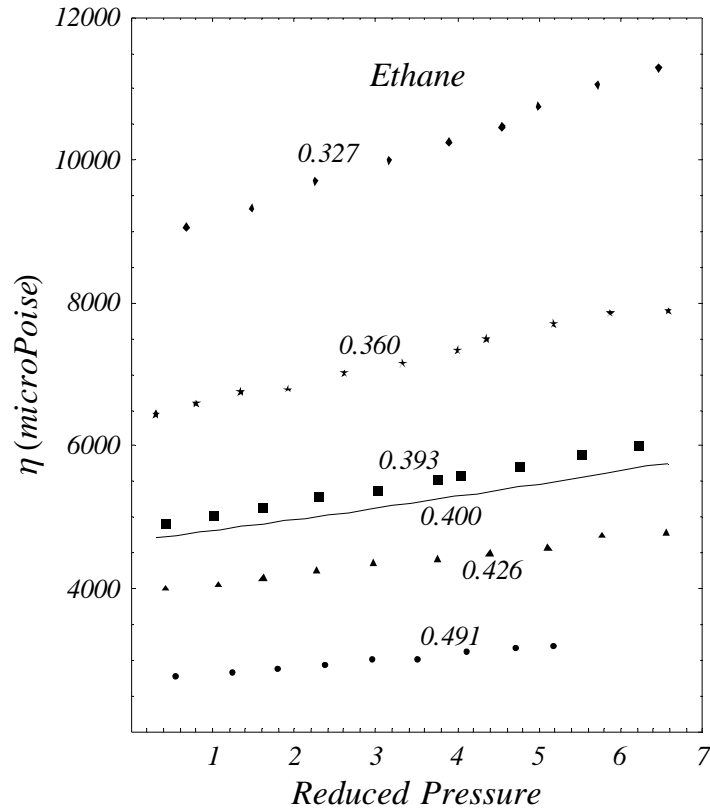


Figure I.51 Experimental data (points) corresponding to reduced temperatures between 0.3 and 0.5 used to obtain the correlation for a reduced temperature of 0.40 (—) and the recommended viscosity data.

are presented for wide ranges of temperature and pressure and in order to preserve a good accuracy, the 7 constants parametric law defined in Section I.7.1.1 has been used for the κ_r , κ_a , and κ_{rr} friction coefficients. In this case, the expressions for the friction coefficients are

$$\begin{aligned}\kappa_r &= a_0 + a_1(\exp(\Gamma - 1) - 1) + a_2(\exp(2(\Gamma - 1)) - 1) \\ \kappa_a &= b_0 + b_1(\exp(\Gamma - 1) - 1) + b_2(\exp(2(\Gamma - 1)) - 1) \\ \kappa_{rr} &= c_2(\exp(2\Gamma) - 1)\end{aligned}\tag{I.7.32}$$

where Γ is defined in Eq.(I.7.20).

The obtained friction constants for the 7 constants PRSV *f-theory* model are given in Table I.18. Figures I.52 through I.54 show the resulting modeling with the PRSV *f-theory* models for ethane, n-heptane and n-pentadecane. Clearly, the

	a_0 [$\mu\text{P}/\text{bar}$]	a_1 [$\mu\text{P}/\text{bar}$]	a_2 [$\mu\text{P}/\text{bar}$]	b_0 [$\mu\text{P}/\text{bar}$]	b_1 [$\mu\text{P}/\text{bar}$]	b_2 [$\mu\text{P}/\text{bar}$]	c_2 [$\mu\text{P}/\text{bar}^2$]	AAD%
Methane	0.053816	-0.124174	0.028406	-0.430873	-0.369093	0.116296	$9.71321 \cdot 10^{-6}$	1.02
Ethane	0.210510	0.524279	-0.226923	-0.460617	-0.010559	-0.098116	$6.97853 \cdot 10^{-6}$	1.21
Propane	0.275468	0.773038	-0.191915	-0.612507	0.020985	-0.059749	$8.98138 \cdot 10^{-6}$	1.80
n-Butane	0.024164	0.859899	-0.828038	-0.952995	-0.327070	-0.382722	$3.02572 \cdot 10^{-5}$	1.28
n-Pentane	0.423099	0.519851	-0.059803	-0.765609	-0.343983	0.095436	$1.50614 \cdot 10^{-5}$	1.18
n-Hexane	0.375053	0.676194	-0.153389	-1.02588	-0.121181	-0.043562	$2.04217 \cdot 10^{-5}$	1.47
n-Heptane	0.486876	0.357007	-0.047235	-0.962702	-0.636737	0.035438	$2.39899 \cdot 10^{-5}$	0.75
n-Octane	0.528242	-0.272297	0.126597	-1.08722	-1.34905	0.209537	$3.25271 \cdot 10^{-5}$	1.14
n-Decane	1.36796	-4.83660	1.35246	-0.899394	-4.82959	1.04980	$4.49837 \cdot 10^{-5}$	0.91
n-Dodecane	7.14537	-18.9732	3.66800	4.49233	-18.8211	3.36729	$7.81348 \cdot 10^{-5}$	0.50
n-Tridecane	7.16560	-15.4258	3.37122	6.20650	-18.3811	3.35921	$6.13474 \cdot 10^{-5}$	0.33
n-Tetradecane	19.1819	-39.4083	7.32513	13.2010	-33.8698	5.86977	$8.23832 \cdot 10^{-5}$	0.53
n-Pentadecane	12.6811	-31.3240	5.94936	8.42368	-28.9591	5.08195	$1.08073 \cdot 10^{-4}$	0.70
n-Hexadecane	20.0877	-43.4274	7.11506	11.2682	-35.3317	5.55183	$1.55344 \cdot 10^{-4}$	1.37
n-Octadecane	27.9413	-61.8540	12.9142	17.5532	-48.2830	9.13626	$8.38258 \cdot 10^{-5}$	1.91

Table I.18 Friction constants for Eq.(I.7.32) used in the PRSV *f-theory* model.

performance of the *f-theory* models, over the entire temperature and pressure ranges, is good. In order to show the stability of the *f-theory* models the isotherms in Figure I.52 and I.53 have been extrapolated outside the experimental reduced pressure range. However, regardless of the good stability revealed in these figures, any application of the *f-theory* models outside the fitted temperature and pressure range has to be done carefully. Table I.18 also contains the AAD performance for the overall PRSV *f-theory* models. The uncertainty of the viscosity modeling is close to the uncertainty of the experimental data. For the subcritical region, outside the critical region, the expected uncertainty of the estimated viscosities is less than 1.5% for liquids and around 2.5% for the vapor phase. In the supercritical region the uncertainty is between 1.0–2.5 with the highest deviations obtained at low pressures.

Further, the applications of the friction constants in Table I.18 are not limited to predictions of pure component viscosities. They can also be used in viscosity predictions of mixtures based on the *f-theory* mixing rules proposed by Quiñones-Cisneros et al (2000), described in Section I.7.1.3. As an example, the viscosity of the quaternary mixture containing n-decane, n-dodecane, n-tetradecane and n-hexadecane measured by Ducoulombier et al. (1986) has been predicted in the temperatures 313 – 353 K and for pressures from 1 to 1000 bars. By comparing the predicted viscosities with the experimental values an AAD of 2.57% and an MxD of 7.25% are obtained. This viscosity prediction is shown together with the experimental data in Figure I.55.

I.7.4 General One-Parameter Friction Theory Models

The recommended viscosities given in Appendix A4 for the n-alkane family provide accurate η -*P-T* values for n-alkanes ranging from methane to n-octadecane within uniform reduced pressure and reduced temperature intervals, as shown in Section I.7.3.2. These data have been used in the further development of the *f-theory* into general models with only one adjustable parameter – a characteristic critical viscosity η_c (Quiñones-Cisneros et al. 2001a). The general *f-theory* models are based on a corresponding states behavior. In deriving the universal parameters for the general models, the use of recommended viscosity data provides a more uniform weight distribution for the least squares fitting procedure. In addition, the wide reduced

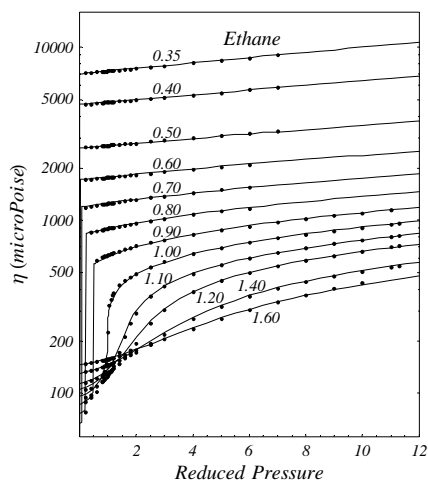


Figure I.52 Viscosity of ethane, (—) predicted by the PRSV *f*-theory model along with the recommended viscosity data (●) from Table A4.2 in Appendix A4.

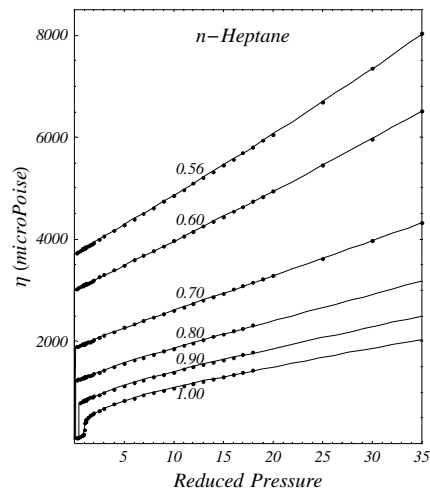


Figure I.53. Viscosity of n-heptane, (—) predicted by the PRSV *f*-theory model along with the recommended viscosity data (●) from Table A4.7 in Appendix A4.

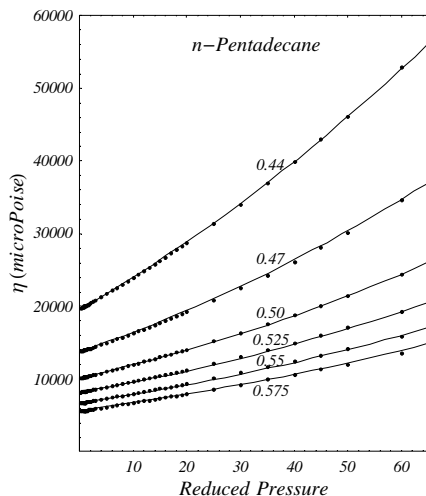


Figure I.54. Viscosity of n-pentadecane, (—) predicted by the PRSV *f*-theory model along with the recommended viscosity data (●) from Table A4.13 in Appendix A4.

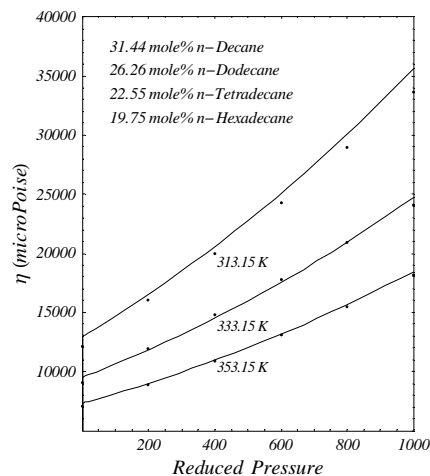


Figure I.55 Viscosity of the quaternary mixture n-decane + n-dodecane + n-tetradecane + n-hexadecane, (—) predicted by the PRSV *f*-theory model along with the experimental values (●) from Ducoulombier et al (1986).

pressure and reduced temperature ranges covered by the recommended viscosity data in Appendix A4 also provide a good overall model performance. In the development of the general one-parameter *f-theory* models (Quiñones-Cisneros et al. 2001a) have only used the critical pressure P_c and the critical temperature T_c in the estimation of the universal laws for the friction coefficients. This has the advantage that much of the uncertainty found in the estimation of parameters, such as the acentric factor ω or the critical molar volume v_c , is avoided. In the following sections the general one-parameter *f-theory* models are presented.

I.7.4.1 General Concepts

The friction term η_f in the *f-theory* can be expressed in a reduced form defined as

$$\hat{\eta}_f = \frac{\eta_f}{\eta_c} = \hat{\eta}_{f,r} + \hat{\eta}_{f,a} \quad (\text{I.7.33})$$

where η_c is a characteristic critical viscosity – the reducing parameter. It follows from the basic definition of the *f-theory* that the reduced friction viscosity term can be written in terms of a reduced attractive contribution $\hat{\eta}_{f,a}$ and a reduced repulsive contribution $\hat{\eta}_{f,r}$ as shown in Eq.(I.7.33). The reduced attractive friction contribution is given by

$$\hat{\eta}_{f,a} = \hat{\kappa}_a \left(\frac{p_a}{P_c} \right) \quad (\text{I.7.34})$$

and the reduced repulsive friction contribution by

$$\hat{\eta}_{f,r} = \hat{\kappa}_r \left(\frac{p_r}{P_c} \right) + \hat{\kappa}_{rr} \left(\frac{p_r}{P_c} \right)^2 \quad (\text{I.7.35})$$

The temperature dependent reduced friction coefficients have been separated into a critical temperature contribution, describing the reduced critical isotherm, and a residual temperature dependent contribution, leading to the following expressions for the reduced friction coefficients in Eqs.(I.7.34) and (I.7.35)

$$\hat{\kappa}_a = \hat{\kappa}_a^c + \Delta \hat{\kappa}_a \quad (\text{I.7.36})$$

$$\hat{\kappa}_r = \hat{\kappa}_r^c + \Delta \hat{\kappa}_r \quad (\text{I.7.37})$$

$$\hat{\kappa}_{rr} = \hat{\kappa}_{rr}^c + \Delta \hat{\kappa}_{rr} \quad (\text{I.7.38})$$

where, the critical friction coefficients $\hat{\kappa}_a^c$, $\hat{\kappa}_r^c$ and $\hat{\kappa}_{rr}^c$ are temperature independent constants and the contributions of the residual friction coefficients $\Delta\hat{\kappa}_a$, $\Delta\hat{\kappa}_r$ and $\Delta\hat{\kappa}_{rr}$ must vanish as the critical isotherm is approached.

I.7.4.2 The Critical Isotherm

In order to study a corresponding states type of viscosity behavior at the critical isotherm, the recommended viscosity data at the critical isotherm for n-alkanes reported in Appendix A4, from methane to n-octane, have been used. In addition, in order to achieve a more general performance, recommended data for carbon dioxide and nitrogen at the critical isotherm have also been generated for reduced pressure intervals between 0 and 20 and with the same procedure and reduced pressure distribution as described in Section I.7.3.1. The input data used in the estimation of the additional recommended data at the critical isotherm have been taken from Iwasaki and Takahashi (1981) for carbon dioxide and from Stephan et al. (1987) for nitrogen.

The analysis of the viscosity data at the critical isotherm has been performed using the reduced friction viscosity term $\hat{\eta}_f$ defined in Eq.(I.7.33). Since the characteristic critical viscosity η_c is not a tabulated value, Quiñones-Cisneros et al (2001a) have estimated the critical viscosity for several compounds by using an optimization procedure that minimizes the $\hat{\eta}_f$ differences, at each reduced pressure, found between all of the different systems considered. In Figure I.56 the estimated values of the considered $\hat{\eta}_f$ are shown. The points shown in this figure include the critical isotherm $\hat{\eta}_f$ of the lightest eight n-alkanes (methane through n-octane), nitrogen and carbon dioxide.

The overlap in all of the points presented in Figure I.56 supports the claim of a corresponding states type of behavior for the $\hat{\eta}_f$ critical isotherm. Due to this a least square fit to all of these points has been carried out using different *f-theory* models in connection with the SRK, the PR, and the PRSV EOS. The solid line in Figure I.56 shows the results for the critical isotherm modeling with the *f-theory* SRK model. The actual estimated friction parameters, along with the estimated overall AAD, are reported

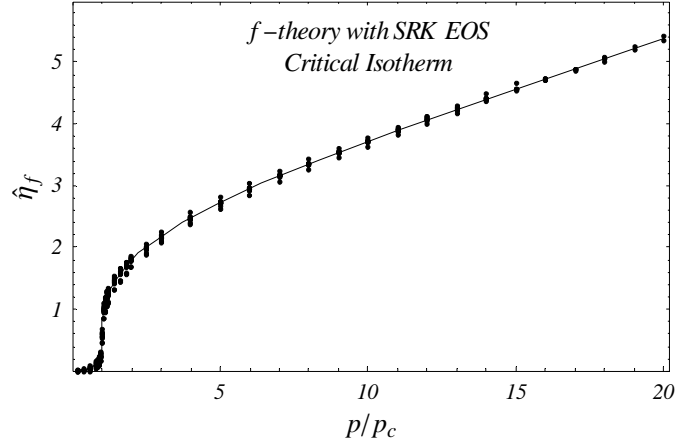


Figure I.56 Critical isotherm reduced friction viscosity data (•) for methane through n-octane, carbon dioxide, and nitrogen along with the critical isotherm modeling with the SRK *f-theory* (—).

	SRK	PR & PRSV
$\hat{\kappa}_a^c$	-0.165302	-0.140464
$\hat{\kappa}_r^c$	0.00699574	0.0119902
$\hat{\kappa}_{rr}^c$	0.00126358	0.000855115
Overall AAD%	2.63	2.85

Table I.19 Reduced critical isotherm friction parameters for the different *f-theory* models.

in Table I.19 for all of the studied *f-theory* models.

I.7.4.3 The Residual Friction Functions

For the temperature dependent residual friction contribution terms Quiñones-Cisneros et al. (2001a) proposed the following empirical functions with a simple empirical dependency on T_c and P_c

$$\begin{aligned} \Delta \hat{\kappa}_a = & \kappa_{a,0,0} (\Gamma - 1) + (\kappa_{a,1,0} + \kappa_{a,1,1} \psi) (\exp(\Gamma - 1) - 1) \\ & + (\kappa_{a,2,0} + \kappa_{a,2,1} \psi + \kappa_{a,2,2} \psi^2) (\exp(2\Gamma - 2) - 1) \end{aligned} \quad (\text{I.7.39})$$

$$\begin{aligned} \Delta \hat{\kappa}_r = & \kappa_{r,0,0} (\Gamma - 1) + (\kappa_{r,1,0} + \kappa_{r,1,1} \psi) (\exp(\Gamma - 1) - 1) \\ & + (\kappa_{r,2,0} + \kappa_{r,2,1} \psi + \kappa_{r,2,2} \psi^2) (\exp(2\Gamma - 2) - 1) \end{aligned} \quad (\text{I.7.40})$$

and

$$\Delta \hat{\kappa}_{rr} = \kappa_{rr,2,1} \psi (\exp(2\Gamma) - 1)(\Gamma - 1)^2 \quad (\text{I.7.41})$$

where

$$\psi = \frac{RT_c}{P_c} \quad [\text{cm}^3/\text{mole}] \quad (\text{I.7.42})$$

and with Γ defined in Eq.(I.7.20).

The constants contained in the parametric models for the residual friction contributions, Eqs.(I.7.39) through (I.7.41), have been fitted to the recommended viscosity data reported in Appendix A4. This fitting procedure was carried out using the critical isotherm *f-theory* models described in the previous section and an iterative optimization procedure for the constants. Table I.20 contains the estimated universal

	SRK	PR	PRSV
$\kappa_{a,0,0}$	- 0.114804	-0.0489197	0.0261033
$\kappa_{a,1,0}$	0.246622	0.270572	0.194487
$\kappa_{a,1,1}$	- 1.15648 10^{-4}	-1.10473 10^{-4}	-1.00432 10^{-4}
$\kappa_{a,2,0}$	-0.0394638	-0.0448111	-0.0401761
$\kappa_{a,2,1}$	4.18863 10^{-5}	4.08972 10^{-5}	3.94113 10^{-5}
$\kappa_{a,2,2}$	-5.91999 10^{-9}	-5.79765 10^{-9}	-5.91258 10^{-9}
$\kappa_{r,0,0}$	-0.315903	-0.357875	-0.325026
$\kappa_{r,1,0}$	0.566713	0.637572	0.586974
$\kappa_{r,1,1}$	-1.00860 10^{-4}	-6.02128 10^{-5}	-3.70512 10^{-5}
$\kappa_{r,2,0}$	-0.0729995	-0.079024	-0.0764774
$\kappa_{r,2,1}$	5.17459 10^{-5}	3.72408 10^{-5}	3.38714 10^{-5}
$\kappa_{r,2,2}$	-5.68708 10^{-9}	-5.65610 10^{-9}	-6.32233 10^{-9}
$\kappa_{rr,2,1}$	1.35994 10^{-8}	1.37290 10^{-8}	1.43698 10^{-8}

Table I.20 Residual friction parameters for the general one-parameter *f-theory* models.

	η_c [μP]	T/T_c Range	Max. P/P_c	SRK AAD%	PR AAD%	PRSV AAD%
Methane	152.930	0.55-2.50	20.0	3.98	3.53	4.17
Ethane	217.562	0.35-1.60	11.3	3.97	3.12	3.09
Propane	249.734	0.30-1.29	13.0	1.41	1.40	2.02
n-Butane	257.682	0.35-1.04	18.0	1.47	1.44	1.97
n-Pentane	258.651	0.64-1.16	30.0	3.18	2.81	2.66
n-Hexane	257.841	0.54-1.08	35.0	4.32	4.30	4.44
n-Heptane	254.303	0.56-1.00	35.0	1.91	1.91	2.08
n-Octane	256.174	0.50-1.00	40.0	1.54	1.56	1.77
n-Decane	257.928	0.45-0.76	48.0	1.40	1.36	1.58
n-Dodecane	245.148	0.45-0.60	55.0	1.14	1.33	1.52
n-Tridecane	240.550	0.44-0.53	60.0	1.34	1.21	1.08
n-Tetradecane	232.314	0.42-0.54	60.0	2.00	1.93	1.92
n-Pentadecane	229.852	0.44-0.58	65.0	1.44	1.06	0.86
n-Hexadecane	217.100	0.41-0.52	70.0	1.50	1.43	1.41
n-Octadecane	206.187	0.42-0.55	80.0	2.32	1.91	1.92
Overall				2.19	2.02	2.17

Table I.21. Overall performance for pure n-alkanes for the general one-parameter *f-theory* models based on the optimized characteristic critical viscosities η_c .

constants, whereas the characteristic critical viscosities along with the obtained AAD are given in Table I.21 for the general one-parameter *f-theory* models considered in this work. In Table I.22 the points, where the MxD has been obtained for the modeling of the recommended data, are given. The MxD reported in Table I.22 are reasonably low values. They are found in regions that correspond to extreme conditions, where there is also a higher uncertainty in the experimental measurements. Thus, the MxD obtained with the general one-parameter *f-theory* models are found around the critical point, at a light gas phase, or for a phase at low temperature and high pressure. Therefore, the combined information presented in Tables I.21 and I.22 show that the results of the general one-parameter *f-theory* models are close to the experimental uncertainty and

(SRK / PR / PRSV)			
	T/T_c	P/P_c	MxD (%)
Methane	2.10 / 0.55 / 0.55	5.00 / 6.80 / 6.80	10.9 / 9.92 / 13.0
Ethane	1.60 / 0.50 / 0.35	4.00 / 6.50 / 6.50	10.6 / 7.99 / 8.44
Propane	1.29 / 0.60 / 0.60	13.00 / 0.20 / 0.20	3.91 / 5.61 / 7.23
n-Butane	1.04	1.20	13.2 / 11.5 / 11.7
n-Pentane	1.16	1.60 / 1.80 / 1.60	7.75 / 7.78 / 7.51
n-Hexane	1.08	1.15	16.2 / 16.4 / 16.4
n-Heptane	1.00	1.00	9.73 / 10.8 / 10.8
n-Octane	0.90	0.40	10.8 / 10.5 / 10.4
n-Decane	0.76 / 0.45 / 0.60	5.0 / 48.0 / 17.0	3.53 / 3.25 / 3.41
n-Dodecane	0.60	54.8	5.30 / 5.14 / 4.12
n-Tridecane	0.44	50.0 / 40.0 / 60.0	3.04 / 2.94 / 3.15
n-Tetradecane	0.48 / 0.48 / 0.51	35.0 / 35.0 / 40.0	4.31 / 4.25 / 4.33
n-Pentadecane	0.575	65.0	7.86 / 7.85 / 6.92
n-Hexadecane	0.435	70.0	4.41 / 4.44 / 4.51
n-Octadecane	0.550	50.0 / 60.0 / 60.0	8.31 / 7.79 / 7.72

Table I.22 Maximum deviation point for the SRK, PR and PRSV *f-theory* models.

satisfactory for most engineering applications. In addition, Figure I.57 also shows good agreement between predicted viscosities and the recommended data for propane by Vogel et al. (1998). In the case of the 600 K isotherm a higher deviation is noticed in Figure I.57. This may be due to the fact that such isotherm is outside the tuning range for all models, since no experimental information is available up to this temperature. Actually, any application of the general one-parameter *f-theory* models outside the ranges reported in Table I.21 ought to be considered as extrapolations.

The critical properties and constants used in the fitting procedure of the constants required in the general one-parameter *f-theory* models have been taken from the recommended values by Stryjek and Vera (1986) whereas the remaining required constants have been taken from Reid et al. (1987). However, in the case of the critical volume for n-alkanes larger than n-octane, i.e. those alkanes that cannot experimentally

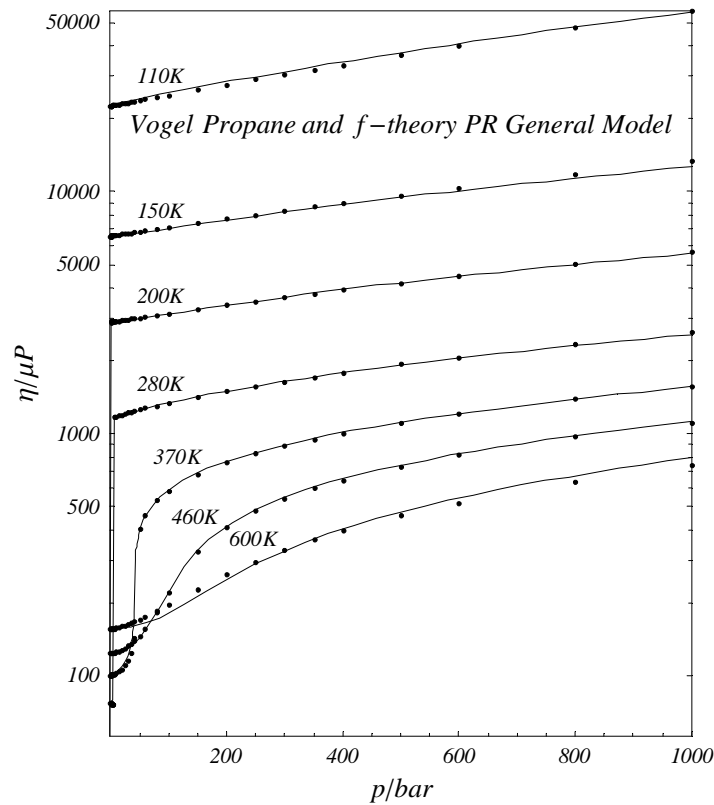


Figure I.57 Propane viscosity results for the general one-parameter PR *f-theory* model (—) along with the recommended data by Vogel et al. (1998) (•).

reach a critical temperature, the following derived empirical equation for the critical density (in mol/cm³) has been used

$$\rho_c = 0.000235751 \left(\frac{\text{mol}}{\text{cm}^3} \right) + 3.42770 \left(\frac{P_c}{RT_c} \right) \quad (\text{I.7.43})$$

where the units of $P_c R^{-1} T_c^{-1}$ must be in [mole/cm³]. This equation can reproduce the critical density for light n-alkanes and other compounds within 1% of accuracy and therefore it is a good estimation for the critical volume required in Eq.(I.2.3) (calculation of the dilute gas viscosity). Since Eq.(I.7.43) is only used in the dilute gas viscosity estimation, in case of heavy compounds in the liquid or dense region, the uncertainty in the estimation of the dilute gas viscosity will be negligible compared with the viscosity value in excess of the dilute gas viscosity.

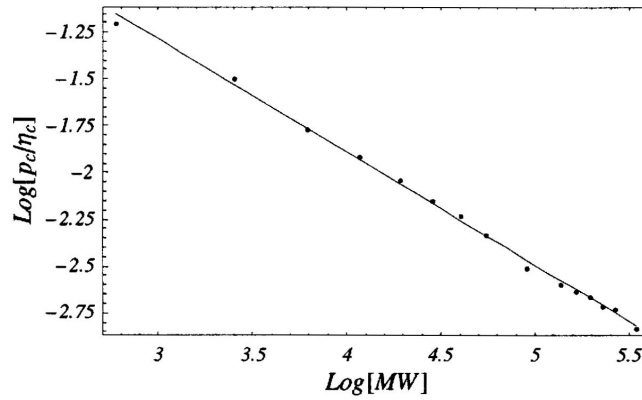


Figure I.58 Correlation of the critical pressure critical viscosity ratio against the molecular weight for n-alkanes.

For pure n-alkanes a simple correlation between the near dimensionless P_c/η_c ratio and the molecular weight can be obtained, as shown in Figure I.58 based on the characteristic critical viscosity values η_c given in Table I.21. The resulting empirical equation is given by

$$\eta_c = 0.597556 P_c M_w^{0.601652} \quad (\text{I.7.44})$$

where P_c must have the unit [bar] and η_c [μP].

I.7.4.4 Application of the General One-Parameter Models to n-Alkane Mixtures

In order to apply the general one-parameter *f-theory* models to an n component mixture, the mixture friction coefficients required in the *f-theory* can be obtained from the pure compound reduced friction coefficients defined in Eqs.(I.7.36) through (I.7.42). This leads to the following expressions for the mixture friction coefficients based on the general one-parameter *f-theory* models

$$\kappa_r = \sum_{i=1}^n z_i \frac{\eta_{c,i} \hat{\kappa}_{r,i}}{P_{c,i}} \quad (\text{I.7.45})$$

$$\kappa_a = \sum_{i=1}^n z_i \frac{\eta_{c,i} \hat{\kappa}_{a,i}}{P_{c,i}} \quad (\text{I.7.46})$$

$$\kappa_{rr} = \sum_{i=1}^n z_i \frac{\eta_{c,i} \hat{\kappa}_{rr,i}}{P_{c,i}^2} \quad (\text{I.7.47})$$

	Reference:	SRK	AAD/%	
			PR	PRSV
$C_1 + C_2$	a	6.19	6.27	5.55
$C_1 + C_3$	b	2.28	2.06	2.37
$C_1 + n-C_4$	c	3.38	2.88	2.55
$C_1 + n-C_6$	d	4.43	4.07	4.27
$C_1 + n-C_{10}$	e	7.60	6.94	6.37
$n-C_5+n-C_8$	f	4.00	4.02	4.19
$n-C_5+n-C_{10}$	g	3.80	3.70	3.69
$n-C_6 + n-C_7$	h	1.91	2.11	1.78
$n-C_7+n-C_8$	i	3.41	3.50	3.62
$n-C_7+n-C_9$	h	1.66	2.09	2.14
$n-C_8+n-C_{10}$	j	2.14	1.91	1.75
$n-C_{10}+n-C_{16}$	k	4.84	5.26	3.94
$n-C_5+n-C_8+n-C_{10}$	l	3.85	3.74	3.76
$n-C_{10}+n-C_{12}+n-C_{14}+n-C_{16}$	k	1.39	1.56	1.63

Table I.23 Overall performance of viscosity predictions for hydrocarbon mixtures with the general one-parameter *f-theory* in conjunction with different cubic EOSs.

a) Diller (1984), b) Giddings et al. (1966), c) Carmichael et al. (1967), d) Berstad (1989), e) Canet (2001), f) Barrufet et al. (1999), g) Estrada-Baltazar et al. (1998b), h) Assael et al. (1992), i) Aleskerov et al. (1979), j) Estrada-Baltazar et al. (1998a), k) Ducoulombier et al. (1986), l) Iglesias-Silva et al. (1999)

where z_i is defined by Eqs.(I.7.30) and (I.7.31). Thus, Quiñones-Cisneros et al. (2001a) found that

$$\varepsilon = 0.30 \quad (I.7.48)$$

when the SRK, the PR, or the PRSV EOS is used in the general one-parameter *f-theory* model. The mixture residual friction term η_f is given by

$$\eta_f = \kappa_r p_r + \kappa_a p_a + \kappa_{rr} p_{rr}^2 \quad (I.7.49)$$

where the mixture friction coefficients are obtained by Eqs.(I.7.45) through (I.7.47), and p_a and p_r are the attractive and repulsive pressure term of the mixture.

Table I.23 shows the AAD results obtained from viscosity predictions with the general one-parameter *f-theory* models for different kind of n-alkane mixtures, when the characteristic viscosities given in Table I.21 have been used. However, for n-nonane Eq.(I.7.44) has been used to estimate the characteristic critical viscosity η_c , since no direct estimation is available for η_c . In general, it can be appreciated that the accuracy of the mixture predictions is close to the experimental uncertainty. The slightly larger

deviation found for the methane + n-decane system may be due to factors such as that the uncertainty in the general *f-theory* models methane predictions, the experimental uncertainty itself or the large acentric difference between methane and n-decane.

I.7.4.5 Modeling of Other Pure Fluids

In addition to the viscosity modeling of pure n-alkanes using the general one-parameter *f-theory* models, the one-parameter *f-theory* models have also been applied to the modeling of other pure fluids than n-alkanes. The deriving of the general one-parameter models has been performed only taking into account viscosity data of n-alkanes. The molecular structure of these n-alkane data range from the rather small spherical molecule of methane to the quite large and acentric molecule of n-octadecane. Because of this the general one-parameter *f-theory* models may capture an essential corresponding states feature making the application of the *f-theory* possible to fluids other than n-alkanes. A few pure fluids given in Table I.24 have been selected in order to test the application of the general one-parameter *f-theory* models, when these models are used in order to estimate the characteristic critical viscosity of other fluids than n-alkanes. The recommended viscosity values used in the adjustment of the characteristic critical viscosities have been taken from Stephan and Lucas (1979), except the data for nitrogen (Stephan et al (1987)). The estimated characteristic critical viscosities along with the obtained AAD for the viscosity modeling of the non n-alkane compounds are reported in Table I.24. The obtained results for the pure non n-alkane fluids with the general one-parameter *f-theory* models are in agreement with the reported uncertainty of the modeled data and suitable for engineering applications.

I.7.5 Viscosity Modeling of Light Gases at Supercritical Conditions

In addition to the industrial importance hydrocarbon fluids have, the industrial use of hydrogen, nitrogen and oxygen at supercritical conditions is widespread. For instance, ammonia is manufactured by letting nitrogen and hydrogen react over a catalyst at temperatures between 700 and 900 K and at pressures between 200 – 600 bar. Nitrogen is now being used at a large scale in the Gulf of Mexico as an injection gas for oil recovery. Hydrogen is also used in petroleum refinery processes such as hydrocracking

	η_c [μP]	T/T_c	Max.	AAD/%		
		Range	P/P_c	SRK	PR	PRSV
Nitrogen	174.179	0.63-4.75	29.4	6.23	5.20	5.09
Carbon Dioxide	376.872	0.66-1.97	13.5	5.48	4.77	4.85
Toluene	304.978	0.50-0.93	9.74	2.53	2.00	1.45
Neopentane	360.820	0.72-1.02	17.3	7.45	7.58	7.80
Ethylbenzene	310.241	0.49-0.91	11.1	2.08	1.96	2.13
Propylene	272.446	0.79-1.78	19.3	5.82	4.83	4.30
Ethylene	220.874	1.06-2.48	15.9	5.35	4.67	4.68*
i-Butane	271.155	0.76-2.08	13.7	3.99	4.12	4.40*
i-Pentane	275.073	0.61-1.63	17.7	5.70	5.36	4.95*
Methylcyclohexane	426.985	0.51-0.93	28.8	4.31	4.09	4.07*
Ethylcyclohexane	359.924	0.48-0.87	16.7	3.72	3.75	3.65*

Table I.24 Performance of the general one-parameter *f-theory* models for different systems. The systems marked with (*) are not tabulated by Stryjek and Vera (1986) and therefore, all of the critical constants have been taken from Reid et al. (1987) and the corresponding “ κ_1 ” constants in the PRSV EOS alpha function have been set to zero.

or hydrotreating. Oxygen is used in a large number of applications, particularly in combustion processes. These gases are not only supplied in compressed gas cylinders or storage tanks, but also through pipelines in the case of industries that require large amounts of nitrogen, hydrogen or oxygen. In fact, at the homepage of the gas company Air Liquide it is mentioned that they have a network of approximately 7000 km of pipelines in Europe and USA, primarily for hydrogen, nitrogen, and oxygen. Also the noble gases, such as argon and helium, have found significant applications in industries such as the semiconductor and metallurgical industry in order to avoid oxidation. Therefore, due to the importance that light gases have in diverse industrial processes, modeling of their physical properties over wide ranges of temperature and pressure is important. Due to the industrial importance of light gases at supercritical conditions and because of the highly accurate viscosity modeling achieved by the *f-theory*, the concepts of the *f-theory*, given in Eqs.(I.7.1) and (I.7.2), have been applied to the accurate

viscosity modeling of light gases at supercritical conditions. The studied gases are argon, helium, hydrogen, krypton, methane, neon, nitrogen, and oxygen.

I.7.5.1 Data Sources

Since tabulations of recommended viscosities provide a more uniform weight distribution for a fitting procedure, they can be used in the development of accurate viscosity models. Thus, recommended viscosities for argon (Younglove and Hanley 1986), helium (Stephan and Lucas 1979), hydrogen (Stephan and Lucas 1979), krypton (Stephan and Lucas 1979), methane (Appendix A4, Table A4.1), neon (Stephan and Lucas 1979), nitrogen (Stephan et al 1987), and oxygen (Laesecke et al. 1990) have been used in order to derive *f-theory* models for each fluid at supercritical conditions. The main aim of this study has been to model the viscosity for temperature and pressure conditions commonly found in industrial processes. Therefore, in spite recommended viscosities are reported for some gases at higher pressures, only data up to 1000 bar have been included.

In the case of hydrogen, it should be mentioned that for temperatures above 200 K hydrogen (normal hydrogen) composes of 25% para (p-hydrogen) and 75% ortho (o-hydrogen) in equilibrium (see figure 1 in Vargaftik 1975). By decreasing the temperature the equilibrium is shifted towards p-hydrogen and below 20 K hydrogen is totally in its para form. Further, according to Vargaftik (1975, p.38) there should be no difference between the viscosity of p-hydrogen and hydrogen at supercritical conditions. But Stephan and Lucas (1979) have reported differences of 5 – 10% between their recommended viscosities for p-hydrogen and hydrogen. Due to this, only viscosity data above 200 K have been used in the *f-theory* viscosity modeling of hydrogen carried out in this work.

I.7.5.2 The Dilute Gas Limit

Since the total viscosity in the *f-theory* is separated into a dilute gas viscosity term and a residual friction term, any dilute gas viscosity model can be used. However, for the studied gases in this work, the dilute gas viscosities have been obtained by extrapolating the recommended viscosities of each fluid to zero pressure. Based on these values it has

been found that the following simple empirical expression can accurately model the dilute gas viscosity limit

$$\eta_0 = d_1\sqrt{T} + d_2T^{d_3} \quad (\text{I.7.50})$$

The estimated d_i -parameters are given in Table I.25. With these parameters the unit of η_0 is [μP] when the temperature is given in [K].

The accuracy of the empirical dilute gas viscosity model, Eq.(I.7.50), has been tested by comparing the calculated values against recommended dilute gas viscosity values found in the literature. In order to also test the performance of the model under extrapolation, the comparison has been performed for temperatures up to 2000 K. The AAD and the MxD obtained by the comparisons are presented in Table I.26. The found deviations are in agreement with the reported uncertainties for the tabulated dilute gas viscosity values, except for neon, where the largest deviations are obtained for temperatures below 100 K and above 1000 K. However, the obtained AAD for neon in the temperature range 100 – 1000 K is only 1.03% with an MxD% of 3.03% at 1000 K. It should also be mentioned that the only way to obtain “experimental” dilute gas viscosities is by extrapolating viscosity measurements performed at low densities to the

	d_1	d_2	d_3
Argon	28.2638	-80.5002	0.206762
Helium	3.65477	1.80913	0.758601
Hydrogen	-1.55199	2.92788	0.645731
Krypton	37.0292	-101.369	0.232700
Methane	13.3919	-47.9429	0.160913
Neon	36.6876	-49.5702	0.325255
Nitrogen	19.1275	-53.0591	0.184743
Oxygen	23.7298	-67.7604	0.192271

Table I.25 Dilute gas viscosity constants for Eq.(I.7.50).

	Reference	Number of points	T-range [K]	AAD%	MxD%
Argon	a	57	160 – 2000	0.43	1.01 at 2000 K
Helium	a	65	80 – 2000	1.49	3.56 at 2000 K
Hydrogen	b	181	200 – 2000	1.19	2.30 at 2000 K
Krypton	a	51	220 – 2000	0.96	1.68 at 250 K
Methane	c	117	195 – 1050	0.33	0.57 at 910 K
Methane	d	21	200 – 400	0.15	0.47 at 200 K
Neon	a	73	50 – 2000	3.30	7.52 at 2000 K
Nitrogen	e	225	130 – 2000	1.62	2.42 at 2000 K
Oxygen	e	219	160 – 2000	0.48	1.33 at 180 K

Table I.26 Comparison of deviations between estimated dilute gas viscosities with Eq.(I.7.50) and recommended values.

a) Bich et al. (1990), b) Assael et al. (1986), c) Trengove and Wakeham (1987), d) Friend et al. (1989), e) Cole and Wakeham (1985).

zero density limit. Further, due to the low value of the dilute gas viscosity, a difference of 1 – 1.5 μP can easily correspond to a deviation of 1 – 2%.

I.7.5.3 Use of Cubic EOS in the Supercritical Region

Since the viscosity modeling of light gases, such as hydrogen and helium, is performed at high reduced temperatures using cubic EOSs, further remarks concerning the alpha function of the attractive part of cubic EOSs, as mentioned in Section I.3.1.1, have to be addressed. The reason is that many modifications of the van der Waals cubic EOS have been carried out on the attractive part and, in many cases, based on the attractive function introduced by Soave (1972) in the SRK EOS for the accurate modeling of vapor/liquid equilibria. At high temperatures, cubic EOSs should approach the ideal gas limit, leading to the fact that the attractive part of the EOSs should either vanish or

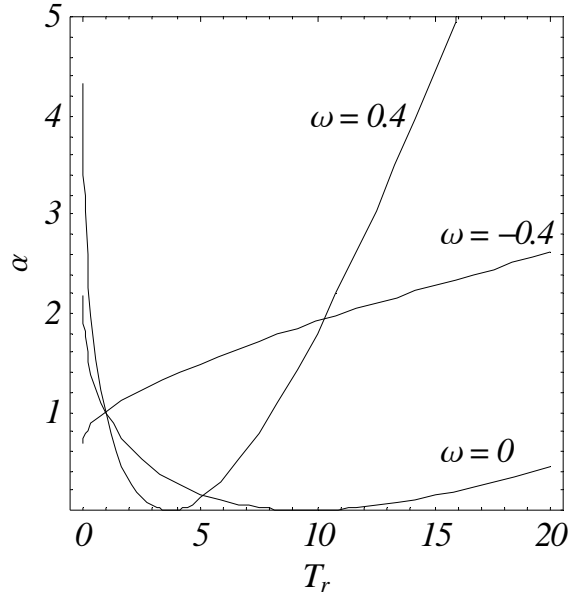


Figure I.59. Behavior of the Soave alpha function (Eq.(I.3.6) as a function of the reduced temperature T_r and the acentric factor ω .

become a constant. Thus, this is not the case with the Soave alpha function Eq.(I.3.6) that passes through a minimum as the temperature increases. The location of the minimum is given by Eq.(I.3.14). This alpha function is e.g. used in the SRK and the PR EOS, see Section I.3.1.1. In Figure I.59 the behavior of the original Soave alpha function (Eq.(I.3.6) with (I.3.7)) is shown for different acentric factors as a function of reduced temperatures. In Section I.3.1.1, it is mentioned that for methane, which has an acentric factor close to zero and a critical temperature close to 190.6 K, the performance of the Soave alpha function is adequate to temperature ranges of industrial applications, because the minimum in the alpha function is located around 1800 K. This adequate performance of the alpha function will also be the case for hydrocarbon fluids, because they both have a positive acentric factors and high critical temperatures. In case of nitrogen, which has an acentric factor close to zero and a critical temperature of 126.1 K, the minimum in the alpha function is located around 1200 K. However, in some cases, such as hydrogen, helium, and neon, the Soave alpha function at high reduced temperatures may not be adequate. These fluids have a negative acentric factor and a very low critical temperature T_c . For hydrogen $\omega = -0.215$ and $T_c = 33.18$ K; for helium $\omega = -0.390$ and $T_c = 5.20$ K; whereas for neon $\omega = -0.0414$ and $T_c = 44.40$ K (all

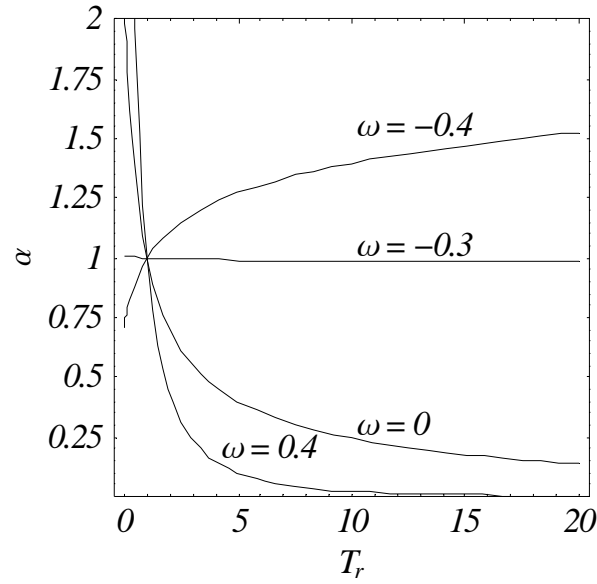


Figure I.60. Behavior of the Boston-Mathias alpha function correction (Eq.(I.3.10)) as a function of the reduced temperature T_r and the acentric factor ω

data taken from the DIPPR Data Compilation (Daubert and Danner 1989)). The performance of the Soave alpha function for a fluid with an acentric factor $\omega = -0.4$, corresponding to the acentric factor of helium, is shown in Figure I.59. As it can be seen, the alpha function increases with increasing temperature. One way to correct this problem is to use a different alpha function for the supercritical region, such as the Boston and Mathias (1980) (BM) expression, which is used in the Mathias modification of the SRK EOS (SRKM) (Mathias 1983), presented in Section I.3.1.1. The transition between the classical subcritical Soave alpha function and a BM type of supercritical modification is first order smooth, i.e. a continuous function up to the first derivative. As illustrated in Figure I.60, for reasonable values of the acentric factor, the BM correction ensures that the supercritical term of the alpha function will either vanish or remain bounded. However, although probably outside of realistic application ranges, it should be stressed that the mathematical structure of the BM correction for the supercritical alpha function also allows for the divergence of the alpha function for large positive or negative values of the acentric factor.

In this work, four different viscosity models for light gases are presented. Two of the models are based on the unmodified SRK EOS and PR EOS, i.e. the unmodified

original alpha function is extrapolated to the supercritical region. Whereas the other two viscosity models are based on the SRKM EOS and the PRSV EOS, in which the BM correction of the alpha function has been used for the supercritical region. In case of the SRKM EOS and the PRSV EOS the additional empirical parameter used in the alpha function has been neglected, because it is generally not tabulated in standard compilations, and the main purpose of this parameter is to improve the vapor/liquid equilibrium performance of the EOS. All of the EOS required compound properties have been taken from the DIPPR Data Compilation (Daubert and Danner 1989).

I.7.5.4 Friction Theory Modeling of Light Gases

The empirical observation of the viscosity behavior of supercritical fluids indicates that, as high reduced temperatures are approached, the viscosity turns into an almost linear function in pressure and also appears to increase linearly with temperature. On the other hand, at low reduced supercritical temperatures, close to the critical temperature, the viscosity is clearly not a linear function of pressure and for an accurate viscosity modeling a quadratic repulsive friction term is necessary. Thus, the following simple empirical expressions for the friction coefficients have been found to deliver a good performance

$$\kappa_a = k_a \quad (I.7.51)$$

$$\kappa_r = k_r \quad (I.7.52)$$

$$\kappa_{rr} = \frac{k_{rr}}{T_r^2} \quad (I.7.53)$$

For all of the considered EOSs, even for the SRK EOS and the PR EOS, Eqs.(I.7.51) and (I.7.52) are enough to model the viscosity in the linear regions, i.e. in the high-temperature region and at low pressures close to the critical temperature region. On the other hand, since the relative contribution of the second order repulsive term should decrease as the temperature increases away from the critical temperature, the mathematical structure of Eq.(I.7.53) should be such that the quadratic temperature dependency implicit in the p_r^2 term of Eq.(I.7.2) is cancelled out. Thus, Eq.(I.7.53) represents the simplest mathematical expression that would achieve this purpose. A more detailed discussion on the behavior and contribution of the different friction

viscosity terms has already been given by Quiñones-Cisneros et al. (2000) and presented in Section I.7.1.

Finally, based on a least squares fit, the friction constants in Eqs.(I.7.51) - (I.7.53) have been estimated for each fluid and the values are given in Table I.27 for the PR and SRK *f-theory* models and in Table I.28 for the PRSV and SRKM *f-theory* models. Table I.29 contains the AAD and the MxD obtained by the *f-theory* viscosity modeling together with the temperature and pressure ranges. Figures I.61 and I.62 show the performance of the PR *f-theory* models for argon and oxygen, respectively. The reported uncertainty of the recommended data for argon (Younglove and Hanley 1986) is within $\pm 2.0\%$. For oxygen (Laesecke et al. 1990) the reported uncertainty depends on the temperature and pressure conditions but primarily it is within $\pm 5\%$, except in the critical region and at high pressures, where the uncertainty of the recommended data can go up to $\pm 12\%$ and $\pm 8\%$, respectively. Thus, the obtained AAD and MxD for argon and oxygen are in good agreement with the reported uncertainties. This is also the case for helium, hydrogen and krypton where the uncertainty of the recommended data ranges from $\pm 1\%$ to $\pm 2\%$ (Stephan and Lucas 1979). For neon the largest deviations are obtained below 100 K, primarily in the critical region, as shown in Figure I.63 for the PR *f-theory* model. This is in excellent agreement with the reported uncertainty of $\pm 2\%$ for neon (Stephan and Lucas 1979) above 200 K and which increases with decreasing temperatures. If the viscosity of neon is calculated above 100 K, using the PR *f-theory* model, an AAD of 0.64% with an MxD of 2.40 at 100 K and 180 bar is obtained. For nitrogen the largest deviations are found at high temperatures and high pressures and close to the critical region, primarily due to the fact that the recommended viscosity data (Stephan et al. 1987) at high temperatures and high pressures are extrapolated values. In order to evaluate the PR *f-theory* model for methane a comparison with recommended viscosities (Friend et al 1989), which were not used in the parameter estimation for the *f-theory* models, in the temperature range 200 – 400 K and from 1 – 500 bar has been performed. The results of this comparison are shown in Figure I.64 indicating an AAD of 1.01% with an MxD of 4.56% at 200 K and 100 bar, which are in agreement with the deviations obtained for the modeled methane viscosity data.

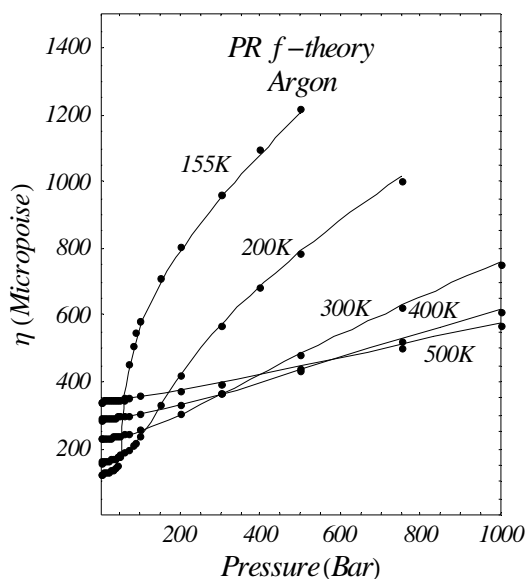


Figure I.61 Viscosity of argon with the PR *f*-theory model (—) along with the recommended values (•) (Younglove and Hanley 1986).

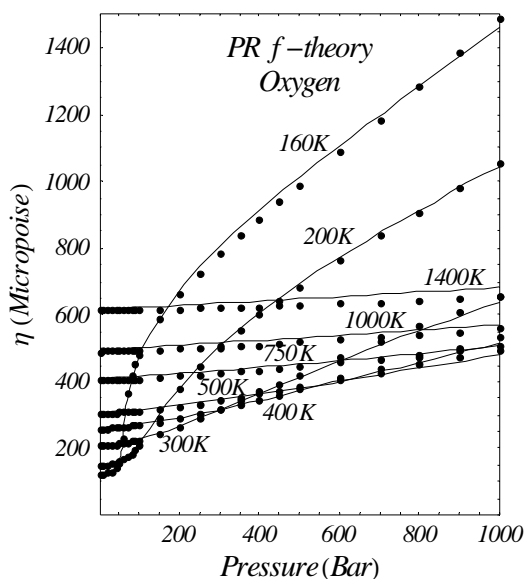


Figure I.62 Viscosity of oxygen with the PR *f*-theory model (—) along with the recommended values (•) (Laesecke et al. 1990).

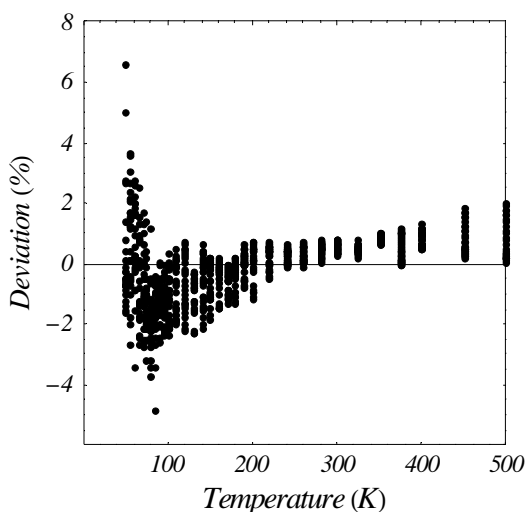


Figure I.63 Deviations of modeled viscosities for neon by the PR *f*-theory model from the recommended viscosities (Stephan and Lucas 1979).

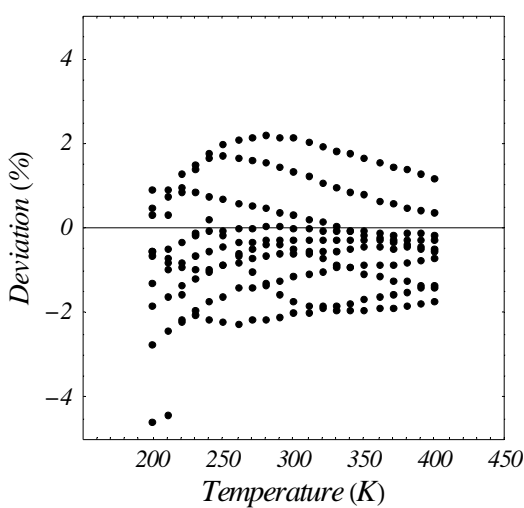


Figure I.64 Deviations of predicted viscosities for methane by the PR *f*-theory model from the recommended viscosities (Friend et al. 1989).

	k_r [$\mu\text{P}/\text{bar}$]	k_a [$\mu\text{P}/\text{bar}$]	k_{rr} [$\mu\text{P}/\text{bar}^2$]
PR EOS			
Argon	0.102756	-0.727451	$1.50831 \cdot 10^{-4}$
Helium	-0.0427035	-0.507319	$2.72888 \cdot 10^{-2}$
Hydrogen	-0.00185308	-0.332575	$1.35146 \cdot 10^{-4}$
Krypton	0.152164	-0.941704	$1.43747 \cdot 10^{-4}$
Methane	0.0731796	-0.382909	$6.63615 \cdot 10^{-5}$
Neon	0.0517444	-0.794717	$7.44634 \cdot 10^{-4}$
Nitrogen	0.0806720	-0.675406	$2.81086 \cdot 10^{-4}$
Oxygen	0.0633893	-0.643424	$1.17249 \cdot 10^{-4}$
SRK EOS			
Argon	0.115788	-0.835290	$1.78345 \cdot 10^{-4}$
Helium	-0.0367788	-0.831727	$2.64680 \cdot 10^{-2}$
Hydrogen	0.00256407	-0.436199	$2.29206 \cdot 10^{-4}$
Krypton	0.173573	-0.992514	$2.36628 \cdot 10^{-4}$
Methane	0.0803060	-0.422054	$9.48629 \cdot 10^{-5}$
Neon	0.0606315	-0.846085	$1.00209 \cdot 10^{-3}$
Nitrogen	0.0901145	-0.760370	$3.50877 \cdot 10^{-4}$
Oxygen	0.0724354	-0.714059	$1.57748 \cdot 10^{-4}$

Table I.27 Friction constants used in Eqs.(I.7.51) – (I.7.53) for the *f-theory* with the PR or the SRK EOS.

	k_r [$\mu\text{P}/\text{bar}$]	k_a [$\mu\text{P}/\text{bar}$]	k_{rr} [$\mu\text{P}/\text{bar}^2$]
PRSV EOS			
Argon	0.0652867	-0.761658	$1.67369 \cdot 10^{-4}$
Helium	-0.0213745	-1.14514	$1.48013 \cdot 10^{-2}$
Hydrogen	-0.00260014	-0.33798	$1.38423 \cdot 10^{-4}$
Krypton	0.122511	-0.957231	$1.58880 \cdot 10^{-4}$
Methane	0.0542854	-0.39996	$7.52500 \cdot 10^{-5}$
Neon	0.0378022	-0.784327	$7.95184 \cdot 10^{-4}$
Nitrogen	0.0498357	-0.684294	$3.03099 \cdot 10^{-4}$
Oxygen	0.0378931	-0.662772	$1.26928 \cdot 10^{-4}$
SRKM EOS			
Argon	0.0683988	-0.877401	$2.03442 \cdot 10^{-4}$
Helium	-0.0202833	-1.34900	$1.83984 \cdot 10^{-2}$
Hydrogen	-0.00136468	-0.400596	$2.22197 \cdot 10^{-4}$
Krypton	0.136152	-1.01227	$2.56269 \cdot 10^{-4}$
Methane	0.056294	-0.444138	$1.07892 \cdot 10^{-4}$
Neon	0.0431686	-0.825002	$1.08049 \cdot 10^{-3}$
Nitrogen	0.0540651	-0.765597	$3.80282 \cdot 10^{-4}$
Oxygen	0.0422321	-0.735723	$1.71242 \cdot 10^{-4}$

Table i.28. Friction constants used in Eqs.(I.7.51) – (I.7.53) for the *f-theory* with the PRSV or the SRKM EOS.

	Number of Points	T-range [K]	P-range [bar]	PR		SRK		PRSV		SRKM	
				AAD%	MxD%	AAD%	MxD%	AAD%	MxD%	AAD%	MxD%
				(MxD Point)	(MxD Point)	(MxD Point)	(MxD Point)	(MxD Point)	(MxD Point)	(MxD Point)	(MxD Point)
Argon	921	155 – 500	1 – 1000	0.95	5.14	0.89	7.80	1.33	5.14	1.28	6.53
				(160K, 60 bar)		(160K, 60 bar)		(155K, 70 bar)		(160K, 60 bar)	
Helium	69	80 – 1300	1 – 800	1.09	3.25	1.06	3.76	1.20	5.52	1.22	5.66
				(150K, 150 bar)		(80K, 300 bar)		(80K, 300 bar)		(80K, 300 bar)	
Hydrogen	60	200 – 1000	1 – 1000	0.72	2.15	0.87	2.47	0.70	2.10	0.75	2.28
				(200K, 600 bar)		(200K, 600 bar)		(200K, 600 bar)		(200K, 600 bar)	
Krypton	284	250 – 600	1 – 500	0.44	1.57	0.40	1.57	0.66	1.99	0.62	1.88
				(270K, 1 bar)		(270K, 1 bar)		(270K, 54 bar)		(270K, 54.3 bar)	
Methane	459	210 – 476	1 – 919	0.97	4.22	0.90	5.04	1.28	4.50	1.27	4.39
				(324K, 597 bar)		(229K, 92 bar)		(324K, 597 bar)		(324K, 597 bar)	
Neon	832	50 – 500	1 – 200	0.87	6.64	1.00	7.44	0.82	5.50	0.89	5.93
				(50K, 50 bar)		(50K, 50 bar)		(50K, 50 bar)		(50K, 50 bar)	
Nitrogen	1452	140 - 1100	1 – 1000	1.06	4.90	1.29	6.75	0.84	2.64	0.86	2.74
				(1100K, 1000 bar)		(1100K, 1000 bar)		(220K 70 bar)		(140K, 50 bar)	
Oxygen	816	160 - 1400	1 – 1000	1.15	5.26	1.36	7.38	0.80	4.90	0.85	6.29
				(170K, 70 bar)		(160K, 60 bar)		(160K, 70 bar)		(160K, 60 bar)	

Table I.29. *f-theory* viscosity modeling results.

It should be remarked that, in spite of the anomalous behavior that may be present at high-reduced temperatures in the attractive Soave alpha function of the PR and SRK EOS, in the case of the light gases studied in this work, all models deliver an equivalent good viscosity performance. Overall, the obtained AAD (0.4 – 1.4%) is in good agreement with the reported uncertainty of the recommended viscosities and is satisfactory for most industrial applications. The obtained MxDs are primarily found close to the critical region, where the viscosity-pressure slope tends to diverge, or at high pressures and at low temperatures. However, due to the fact that cubic EOSs are optimized to match the critical pressure and temperature of pure components and the fact that the *f-theory* is based on a correlation of stresses rather than the density, the *f-theory* models can also deliver a good viscosity-pressure performance close to the critical point – as illustrated in Figures I.61 and I.62.

Recently, Nabizadeh and Mayinger (1999) measured the viscosity of hydrogen using an oscillating disk viscometer in the temperature range 296 – 399 K and from 1 bar to 58 bar with an uncertainty of $\pm 1.0\%$. A comparison of the Nabizadeh and Mayinger hydrogen data with the *f-theory* models derived in this work for hydrogen gives an AAD of 0.86% for the PR, PRSV and SRKM *f-theory* models and 0.82% for the SRK *f-theory* model with an MxD of 2.06% at 399 K and 1 bar for all models. The obtained deviations are within the uncertainty of the *f-theory* models and the experimental data.

Using a vibrating-wire viscometer Wilhelm and Vogel (2000) recently measured the viscosity of argon up to 200 bar at temperatures between 298 – 423 K and krypton up to 160 bar at temperatures between 298 – 348 K. The claimed uncertainty for these measurements is $\pm 0.2\%$. Based on an EOS, the reported viscosity measurements are tabulated against density instead of pressure. In spite of this, the direct substitution of the reported densities in the derived *f-theory* models also gives good results. For argon, the obtained AADs are 0.63%, 0.37%, 1.20% and 0.98% for the PR, the SRK, the PRSV, and the SRKM *f-theory* models, respectively. For krypton, the AADs obtained with the PR, the SRK, the PRSV, and the SRKM *f-theory* models are 0.66%, 0.91%, 0.90% and 0.69%, respectively. Thus in spite of using simple cubic EOSs, the obtained AAD for argon and krypton are in good agreement with the reported uncertainty.

I.7.5.5 Concluding Remarks

Based on the concepts of the *f-theory*, the viscosity of argon, helium, krypton, methane, neon, nitrogen, normal hydrogen, and oxygen has been modeled at supercritical conditions from 1 bar to 1000 bar in conjunction with the PR, the SRK, the PRSV and the SRKM EOS. This modeling work also illustrates how accurate *f-theory* models for light gases can be obtained using a simple three-friction constants model. In addition, the viscosity modeling performed in this section further illustrates the *f-theory* potential for accurate viscosity modeling using simple cubic EOSs. Further, with the use of simple mixing rules for the *f-theory* friction coefficients it may be possible to achieve good viscosity predictions for light and dense fluid mixtures that may include the light gases studied in this section.

Finally, in sake of completeness and accuracy, simple three constants equations have been derived for the dilute gas viscosity term of the studied light gases. The performance of these equations is compared with recommended dilute gas viscosities up to 2000 K and an uncertainty within or close to the uncertainty of the recommended values is obtained. However, it is important to remark that the friction models presented here are not contingent to the dilute gas models also derived in this section. In fact any other accurate model for the dilute gas limit can also be used with good results.

I.7.6 Conclusion

Starting from basic principles of classical mechanics and thermodynamics Quiñones-Cisneros et al. (2000) introduced the *f-theory* for viscosity modeling. In the *f-theory* the viscosity in excess of the dilute gas limit is approached as a mechanical rather than a transport property. By linking the Amontons-Coulomb friction law with the van der Waals repulsive and attractive pressure terms of a simple cubic EOS, such as the SRK or the PR EOS, highly accurate viscosity modeling can be achieved. Quiñones-Cisneros et al. (2000) introduced the *f-theory* by modeling the viscosity of n-alkanes ranging from methane to n-decane accurately over wide ranges of temperature and pressure. In this work, the *f-theory* has been applied to viscosity predictions of well-defined hydrocarbon mixtures containing methane through n-decane over wide ranges of temperature, pressure, and composition. The obtained results with the *f-theory* for these

mixtures are within or close to the experimental uncertainty. Compared with the five existing viscosity models, commonly used within the oil industry, better results are obtained using the *f-theory*.

Based on the accurate viscosity modeling achieved by the *f-theory*, the *f-theory* has been used to estimate recommended viscosities for n-alkanes ranging from methane to n-octadecane, by smoothing experimental viscosity data. These tabulations contain only viscosity data within the experimental temperature and pressure ranges, and only up to 1000 bar, since most industry processes are carried out below 1000 bar. The reason for estimating these tabulations of recommended viscosities is due to the development of a general *f-theory* model. By using tabulations of recommended viscosities it is easier to establish the functional dependency of the parameters in the model, since the data are equally distributed compared with data taken from different sources. By using these data a corresponding states behavior has been observed for the critical viscosity isotherm. Based on this corresponding states behavior Quiñones-Cisneros et al. (2001a) developed general *f-theory* models in conjunction with the SRK, the PR, and the PRSV EOS. The general *f-theory* models depend only on one adjustable property – a characteristic critical viscosity. These general one-parameter *f-theory* models have been used to predict the viscosity of pure n-alkanes and their mixtures. The overall AAD for pure n-alkanes ranging from methane to n-octadecane is around 2%. Very satisfactory results are also obtained for n-alkane mixtures, see e.g. Table I.23. Although that these n-alkane systems may be seen as very simple representations of petroleum and reservoir fluids, the obtained results with the *f-theory* clearly shows its possible extension to real fluids of interest for the oil industry. Particularly, since the accurate *f-theory* viscosity modeling and prediction is achieved using simple cubic EOSs commonly used within the oil industry.

In addition and due to their industrial importance the viscosity of light gases, such as argon, hydrogen, nitrogen, and oxygen, at supercritical conditions up to 1000 bar have also been accurately modeled using *f-theory* models with three adjustable friction constants per compound. This accurate viscosity modeling of light gases is achieved using simple cubic EOSs.

I.8 Application of the Friction Theory to Industrial Processes

Because of the accurate viscosity modeling and prediction of pure n-alkanes and their mixtures over wide ranges of temperature and pressure achieved with the *f-theory* (Quiñones-Cisneros et al. 2000, 2001a), see also Chapter I.7, in conjunction with simple cubic EOSs commonly used within the oil and gas industry, the application and extension of the concepts of the *f-theory* to more complex systems of great importance and interest for the oil and gas industry have to be addressed. In this chapter the general one-parameter *f-theory* models have been tested by applying them to complex fluids, such as carbon dioxide + hydrocarbon mixtures, crude oils, and natural gases, over wide ranges of temperature and pressure.

I.8.1 Viscosity Prediction of Carbon Dioxide + Hydrocarbon Mixtures

Since carbon dioxide is widely used in enhance oil recovery processes, reliable modeling of the viscosity along with other properties of mixtures composed of carbon dioxide and hydrocarbons is required for an accurate simulation and modeling of the carbon dioxide displacement process. It is therefore important to have reliable and accurate viscosity models, which can be applied to carbon dioxide + hydrocarbon fluids over wide ranges of composition, temperature and pressure. In this section, the general one-parameter *f-theory* model, Quiñones-Cisneros et al. (2001a), described in Section I.7.4, is applied to viscosity predictions of well-defined mixtures composed of carbon dioxide and hydrocarbons. Although, these mixtures may be seen as very simple representations of petroleum fluids, they can be used to show the potential of extending the *f-theory* to the simulation of carbon dioxide enhance oil recovery processes based on a proposed *f-theory* procedure for accurate viscosity modeling of real reservoir fluids (Quiñones-Cisneros et al. 2001b) and described in Section I.8.2. However, it should be stressed that a successful viscosity modeling scheme requires that the used EOS is capable of describing the right phase behavior for the studied mixtures.

In addition, the required dilute gas viscosity of the carbon dioxide + hydrocarbon mixtures has been estimated using the mixing rule by Wilke (1950), Eq.(I.2.8) along with the dilute gas viscosity model of Chung et al. (1988) Eq.(I.2.3) for the pure compounds. This mixing rule is of a predictive nature since no information

about the properties of the mixture is required, only the dilute gas viscosity and the molecular weight along with the composition of the pure compounds.

I.8.1.1 Data Sources for Carbon Dioxide + Hydrocarbon Mixtures

In spite of the importance that carbon dioxide + hydrocarbon mixtures have for the oil industry, only a few viscosity measurements that have been carried out are reported in the open literature. Although a plethora of viscosity measurements must have been carried out within the oil industry, such data are generally not available in the open literature nor suitable for evaluation of models due to the lack of basic information, such as the compositional characterization of the reservoir fluids. Nevertheless, the viscosity of three binary mixtures composed of carbon dioxide and methane has been measured by de Witt and Thodos (1977) in the temperature range 323 to 474 K and in the pressure range 34 to 692 bar using a capillary viscometer. Diller et al. (1988) measured the viscosity of three carbon dioxide + ethane mixtures in the temperature range 210 to 320 K and for pressures between 21 and 363 bar using a torsional crystal viscometer with an experimental uncertainty of $\pm 3\%$. The viscosity of the same three carbon dioxide + ethane mixtures has been further measured by Diller and Ely (1989) in the temperature range 319 to 500 K and for pressures between 17 and 614 bar using a torsional crystal viscometer with an experimental uncertainty of $\pm 3\%$. As pointed out by Diller and Ely (1989), a discrepancy outside the experimental uncertainty is found for the viscosity data previously reported by Diller et al. (1988) for the binary mixture containing a mole fraction of 0.73978 carbon dioxide at 320 K. Consequently, the data by Diller et al. (1988) at 320 K and a mole fraction of 0.73978 carbon dioxide are not included in this study. Additionally, the viscosity of mixtures composed of carbon dioxide and n-decane has been measured by Cullick and Mathis (1984) using a capillary viscometer from 311 K to 403 K and pressures ranging from 70 to 300 bar with an experimental uncertainty $\pm 2\%$. However, Table IV and Table V in Cullick and Mathis (1984) contain the same viscosity values, but for two different compositions. Consequently, the data contained in these tables have not been used in this work. Finally, using a rolling ball viscometer Barrufet et al. (1996) measured the viscosity of

different binary through quinary mixtures composed of carbon dioxide and n-alkanes ranging from n-butane through n-decane.

I.8.1.2 Results and Discussion

The viscosity prediction of the above-mentioned mixtures composed of carbon dioxide and hydrocarbons has been performed with the general one-parameter *f-theory* model in conjunction with the SRK and the PR EOS, below called *f-SRK* and *f-PR*. The regular van der Waals mixing rules have been used in the SRK and the PR EOS and all required pure component properties have been taken from the DIPPR Data Compilation (Daubert and Danner 1989).

The viscosity predictions have been performed without using any binary interaction parameters in the van der Waals mixing rules and with the reported binary carbon dioxide + hydrocarbon interaction parameters by Knapp et al. (1982). It should be stressed that within the oil industry, in case of carbon dioxide and hydrocarbon mixtures, binary interaction parameters are used in the EOS. The predicted viscosities have been compared with the experimental values. The obtained AAD and the MxD are given in Table I.30 along with the number of points (NP), and the temperature and pressure ranges.

For binary mixtures composed of carbon dioxide and ethane the use of binary interaction parameters significantly improves the viscosity predictions. This follows from the fact that the correct phase behavior is predicted, when binary interaction parameters are used. Figures I.65 and I.66 show the change in the phase behavior that develops with the use of a recommended binary interaction parameter. When no binary interaction parameter is used in the PR EOS, an MxD of 136% is obtained with the *f-PR* model at 300 K and 60.5 bar for a mole fraction of 0.49245 carbon dioxide. This is due to the fact that the EOS describes the phase of the mixture as a liquid, see Figure I.65, resulting in too high viscosity and density predictions. In contrast, when a binary interaction parameter is used, a single phase is found in the entire pressure range for a mole fraction of 0.49245 carbon dioxide at 300 K, see Figure I.66, resulting in more accurate viscosity and density predictions. In this case, an MxD of 18.1% is obtained with the *f-PR* model at 220 K, 139.5 bar and 73.978 mole% carbon dioxide. According

	Ref.	T [K]	P [bar]	NP	No k_{ij}				With k_{ij}			
					f -PR		f -SRK		f -PR		f -SRK	
					AAD	MxD	AAD	MxD	AAD	MxD	AAD	MxD
Methane + CO ₂	a	323 - 474	34 - 695	132	4.49	17.6	5.30	14.6	3.94	13.0	5.83	10.5
Ethane + CO ₂	b	210 - 320	21 - 368	188	16.6	136	18.0	140	6.15	18.1	6.96	15.4
	c	319 - 500	7 - 614	174	8.55	42.0	9.00	35.4	5.62	14.2	7.03	15.7
n-Decane + CO ₂	d	311 - 403	67 - 347	57	5.07	10.9	5.60	12.1	7.35	15.0	7.92	16.2
	e	311 - 403	70 - 118	12	5.26	13.3	5.45	13.0	8.08	17.9	8.34	17.8
n-Pentane + n-Decane + CO ₂	e	354 - 401	25 - 49	10	4.84	8.51	5.01	8.45	6.29	10.5	6.48	10.5
n-Butane + n-Hexane + n-Decane + CO ₂	e	324 - 395	25 - 49	10	6.24	14.4	6.40	14.5	6.74	15.1	6.90	15.3
n-Pentane + n-Hexane + n-Heptane + n-Decane + CO ₂	e	360 - 395	25 - 49	8	4.69	8.74	4.70	8.72	6.23	10.7	6.27	10.8

Table I.30 Results of viscosity predictions with the general one-parameter f -theory.

k_{ij} refers to the EOS binary carbon dioxide + hydrocarbon interaction parameters reported by Knapp et al. (1982).

a) de Witt and Thodos (1977), b) Diller et al. (1988), c) Diller and Ely (1989), d) Cullick and Mathis (1984), e) Barrufet et al. (1996).

to Rowlinson and Swinton (1982), a Type II phase diagram with an azeotropic behavior is found for the binary system carbon dioxide + ethane. Therefore, reliable viscosity predictions are only obtained for the binary system carbon dioxide + ethane, when the EOS can describe the correct phase behavior. Figure I.67 shows the f -PR viscosity prediction at different temperatures versus pressure for the binary mixture composed of 49.245 mole% carbon dioxide and 50.755 mole% ethane using binary interaction parameters in the PR EOS. In contrast, binary mixtures composed of carbon dioxide and methane make Type I phase diagrams (Rowlinson and Swinton 1982) and the EOS does not have any problems describing the right phase behavior.

For mixtures composed of carbon dioxide and heavy hydrocarbons better results are obtained when no binary carbon dioxide + hydrocarbon interaction parameters are used. This is of course no guaranty that the correct phase behavior is described at all T, P, x conditions. In fact, in spite that the phase behavior of the binary carbon dioxide + n-decane system is of the Type II, cubic EOSs, such as the PR EOS, already start predicting Type III phase diagrams for the carbon dioxide + n-decane system

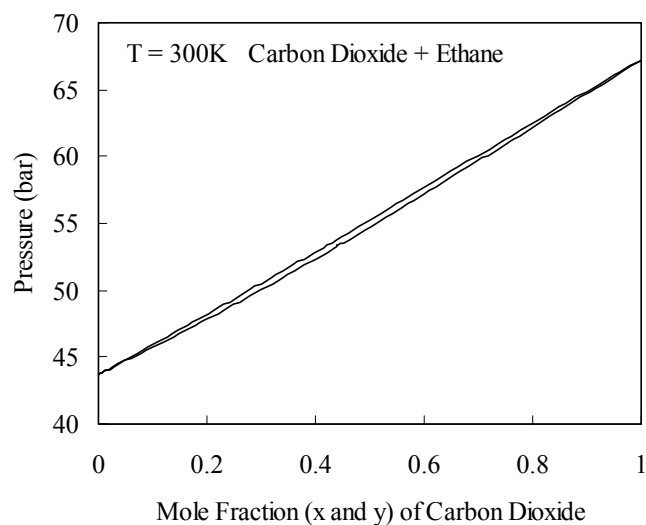


Figure I.65. P, x, y diagram at 300 K for carbon dioxide + ethane estimated by the PR EOS using no binary interaction parameter.

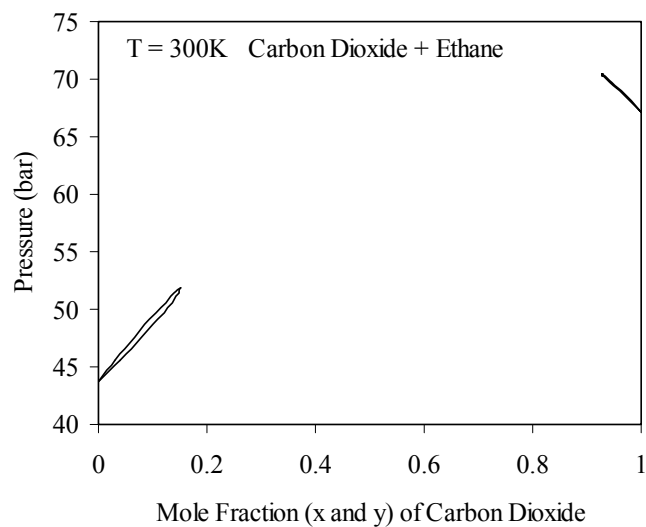


Figure I.66. P, x, y diagram at 300 K for carbon dioxide + ethane estimated by the PR EOS using the recommended binary interaction parameter by Knapp et al. (1982).

(Quiñones-Cisneros 1997). However Type III phase diagrams are first experimentally observed for the carbon dioxide + n-tridecane system (Rowlinson and Swinton 1982). This could be one of the reasons for the increase in the AAD for binary mixtures composed of carbon dioxide and n-decane, when binary interaction parameters are used

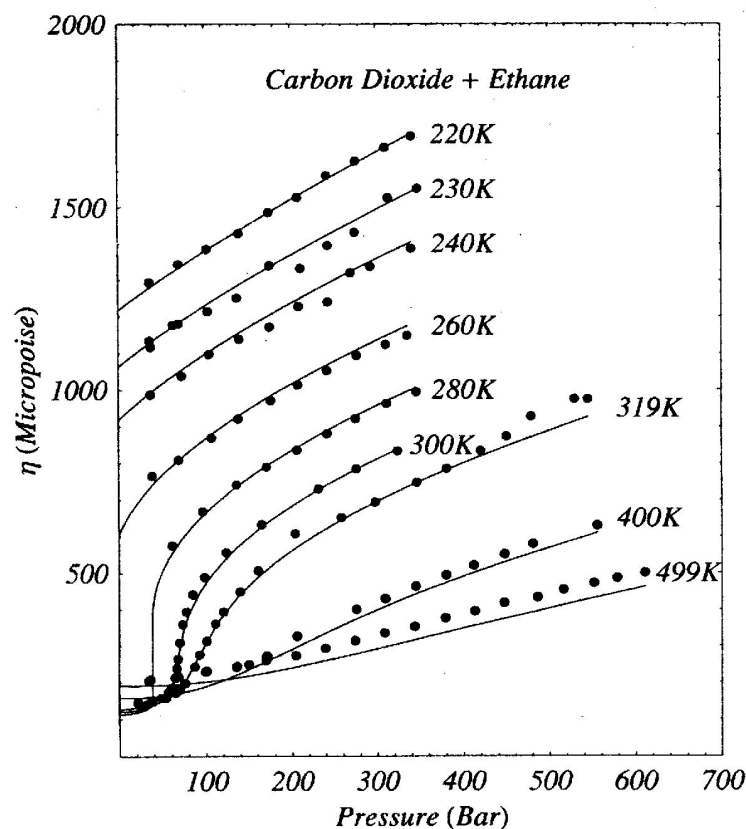


Figure I.67. Viscosity of the binary mixture containing 49.245 mole% carbon dioxide and 50.755 mole% ethane, (•) experimental points (Diller et al. 1988, Diller and Ely 1989) and (—) predicted by the *f*-PR model.

in the cubic EOS.

For comparison purposes, the viscosity of the studied mixtures has also been predicted with the well-known LBC model (Lohrenz et al. 1964), described in Section I.2.2.1. It has already been mentioned that this model is a sixteenth degree polynomial in the reduced density. Consequently the accuracy of the predicted viscosity will depend on the accuracy of the reduced density. Therefore, in order to obtain an optimal performance for the LBC model the experimental density values have been used in conjunction with the calculation procedure originally derived for the LBC model. The obtained AAD and MxD for the LBC model are given in Table I.31. A comparison of the LBC model with the two general one-parameter *f*-theory models shows that the LBC

	Ref.	T [K]	P [bar]	NP	LBC*		LBC-PR**	
					AAD	MxD	AAD	MxD
Methane + CO ₂	a	323 - 474	34 - 695	132	2.29	5.20	5.60	24.0
Ethane + CO ₂	b	210 - 320	21 - 368	188	7.46	23.5	28.7	114
	c	319 - 500	7 - 614	174	3.23	9.52	5.07	31.8
n-Decane + CO ₂	d	311 - 403	67 - 347	57	4.84	16.1	28.3	50.0
	e	311 - 403	70 - 118	12	5.17	11.5	29.7	48.2
n-Pentane + n-Decane + CO ₂	e	354 - 401	25 - 49	10	35.9	41.7	26.4	29.7
n-Butane + n-Hexane + n-Decane + CO ₂	e	324 - 395	25 - 49	10	14.4	29.7	22.4	37.8
n-Pentane + n-Hexane + n-Heptane + n-Decane + CO ₂	e	360 - 395	25 - 49	8	54.0	66.4	21.0	28.0

Table I.31 Results of viscosity predictions with the LBC model.

* with experimental densities.

** with densities obtained by the PR EOS using binary carbon dioxide + hydrocarbon interaction parameters.

a) de Witt and Thodos (1977), b) Diller et al. (1988), c) Diller and Ely (1989), d) Cullick and Mathis (1984), e) Barrufet et al. (1996).

model gives better results for the binary mixtures composed of carbon dioxide and methane or ethane at supercritical conditions, while similar results are obtained for carbon dioxide + n-decane mixtures, when no binary parameters are used in the EOS used in the *f-theory* models.

However, in spite that experimental densities have been used in the LBC model, for mixtures composed of carbon dioxide and heavy hydrocarbons the two *f-theory* models clearly predict the viscosity significantly better than the LBC model. The reason is that the LBC model has been derived based on experimental density and viscosity values of compounds primarily found in natural gas mixtures. The viscosity predictions using the LBC model and the *f*-PR model with binary interaction parameters are shown in Figure I.68 for the binary mixture composed of 15 mole% carbon dioxide and

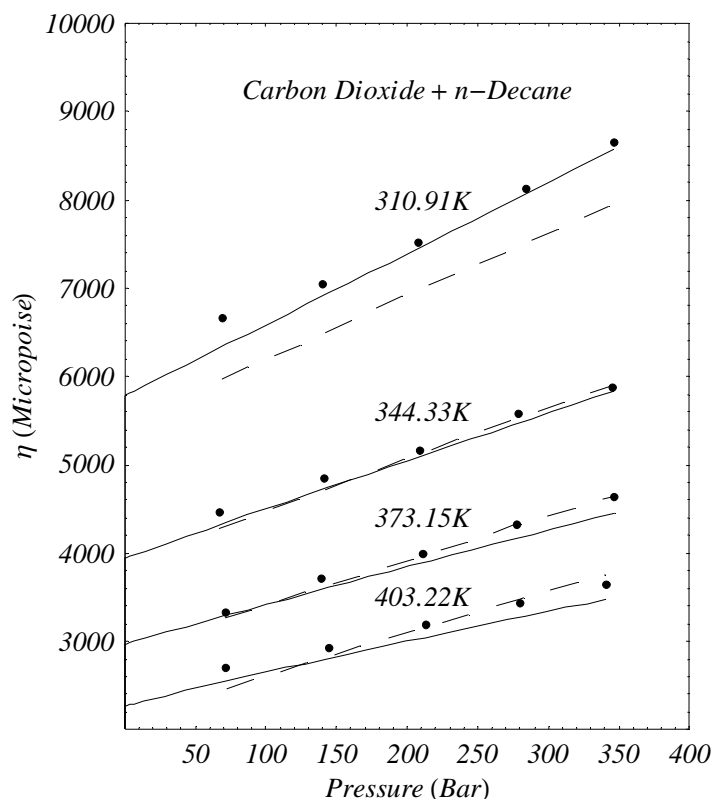


Figure I.68 Viscosity of the binary mixture containing 15 mole% carbon dioxide and 85 mole% n-decane, (•) experimental points (Cullick and Mathis 1984), (—) predicted by the *f*-PR, and (---) predicted by the LBC model using experimental densities.

85 mole% n-decane. In spite that both models have a relative close AAD, it can be appreciated from this figure that the *f*-theory model better describes the correct viscosity versus pressure trend than the LBC model.

The LBC model has also been evaluated, when the densities are predicted by the original PR EOS in conjunction with the binary carbon dioxide + hydrocarbon interaction parameters reported by Knapp et al. (1982). The obtained AAD and MxD with the LBC-PR model are given in Table I.31. As it can be seen from Table I.31 the performance of the LBC model strongly depends on how well the density is estimated. The optimal performance with the LBC model is obtained when experimental densities are available. Further, in spite that the right phase behavior is obtained by the PR EOS

for carbon dioxide + ethane, very large deviations are obtained with the LBC-PR model at low temperatures ($MxD = 114\%$, at 210 K, 362.7 bar, and 74.834 mole% carbon dioxide). In this case, in spite of being light compounds, these conditions are far from the natural gas conditions used in the original tuning of the LBC model. The performance of the *f-theory* models is significantly better than the LBC-PR.

I.8.1.3 Concluding Remarks

The viscosity of well-defined mixtures composed of carbon dioxide and hydrocarbons has been predicted by the general one-parameter *f-theory* model and the widely used LBC model. The *f-theory* models can predict the viscosity of carbon dioxide + hydrocarbons with an uncertainty acceptable for many engineering applications. However, the LBC model can only deliver good viscosity predictions in conjunction with experimental densities for mixtures mainly containing light hydrocarbons such as methane and ethane at relative high reduced temperatures. The reason is that these are the compounds and conditions used to derive the LBC model.

Although the studied mixtures are very simple representations of petroleum fluids with carbon dioxide, the obtained results support the potential application of the *f-theory* models for viscosity calculations of carbon dioxide displacement of real oils i.e. the simulation of carbon dioxide enhance oil recovery processes. However, it should be stressed that in order to achieve more accurate viscosity predictions the EOS must be able to describe the correct phase behavior. This is also the case for all other viscosity models that require density estimations from any type of EOS.

For all of the presented examples, the highest deviations are obtained for carbon dioxide rich mixtures. However, it should be pointed out that for hydrocarbon mixtures rich in carbon dioxide a more accurate *f-theory* prediction can be obtained by combining a 7 constants *f-theory* model for carbon dioxide with the general one-parameter *f-theory* model for the remaining components. This can easily be done, since the mixture friction coefficients are based on mixing rules related to the pure friction coefficients of the compounds in the mixture.

I.8.2 Viscosity Prediction of Reservoir Oils

So far the general one-parameter *f-theory* models have successfully been applied to the accurate modeling and prediction of the viscosity of pure hydrocarbons and well-defined hydrocarbon mixtures being very simple representations of reservoir fluids over wide ranges of temperature and pressure. Due to this accurate performance of the *f-theory*, a more challenging aspect has been to apply the general one-parameter *f-theory* models to the viscosity estimation of real reservoir fluids. The reason is that the oil industry needs accurate and reliable viscosity models applicable to wide ranges of temperature, pressure, and for compositional changes in order to predict the viscosity of reservoir fluids for the accurate simulation of the production profile of an oil reservoir. The reason is that the development of such fields, especially located offshore, depends on the production rate, which is related to the economy of the field. Further the viscosity is also required in order to design the necessary transport and process equipments from the reservoir field to within the refinery.

In spite of the great importance reservoir fluids has, only a few viscosity measurements have been reported in the open literature, for which enough information are given in order to perform a proper characterization of the plus fraction. The reason for performing a numerical characterization of reservoir fluids is due to the fact that the composition of these complex fluids can not be determined exactly. Thus, for reservoir fluids, a plethora of viscosity measurements along with compositional information for proper characterizations must have been carried out within the oil industry. But this information are generally not available.

Due to this and for illustration purposes, Quiñones-Cisneros et al. (2001b) have applied the general one-parameter *f-theory* model with the PR EOS to viscosity estimations of three North Sea oils (NSO) (Pedersen et al. 1989) for which all the required compositional information have been reported in the open literature. In addition and for comparison purposes the widely used LBC model (Lohrenz et al. 1964) within the oil industry has also been applied to the viscosity calculations of these three oils.

I.8.2.1 Calculation Procedure and Results

Before proceeding with the viscosity calculations of the three NSOs (Pedersen et al. 1989) some remarks have to be addressed concerning the characterization procedure used in this work. In the laboratory a chromatographic analysis of the composition of the reservoir fluid is carried out. Thus, it is only the composition of the light compounds ranging from methane to hexanes, carbon dioxide, nitrogen, and hydrogen sulfide, which is determined exactly, whereas the heavy hydrocarbon fraction is fractionated by TBP distillation into different cuts, which is then related to a carbon number. In addition to the determination of the mole or weight fractions of these cuts, their specific gravity and molecular weight are also determined. A more detailed description of the experimental procedures is given by Pedersen et al (1989). In Table I.32, the chromatographic characterization of the three NSOs obtained from the laboratory is shown. This information is used in order to perform the numerical characterization of the fluid. In this work, these three NSOs have been characterized using the in-house SPECS software package, which is an extension to the characterization procedure suggested by Aasberg-Petersen and Stenby (1991). The basic principles of this characterization procedure are described in Chapter I.4.

The applied characterization procedure gives the oil properties based on 10 well defined compounds: N_2 , CO_2 , CH_4 , C_2H_6 , C_3H_8 , i- C_4 , n- C_4 , i- C_5 , n- C_5 and C_6 , and a suggested number of additional pseudocomponents. For the characterization procedure applied to the NSOs in this work, all of the provided information for each oil has been used exactly as reported in Table I.32, except the density of the plus fraction. In this case, the density of the heaviest oil fraction has been iteratively modified until the saturation pressure reported in Table I.33 were matched in order to reproduce the break in the viscosity versus pressure curve correctly. Thus, it should be stressed that there are other ways, such as the tuning of the molecular weight, in order to model the right phase behavior of reservoir fluids using cubic EOSs. Furthermore, since in the case of the NSO 1 and NSO 2, detailed compositional information is given up to the C_{20+} fraction, in order to preserve as much information as possible, a total of 26 compound groups have been used (the 23 component groups reported in Table I.32, which go up to the C_{19} fraction, and 3 additional pseudocomponent groups for the C_{20+} fraction). For the

	NSO 1			NSO 2			NSO 3		
	Mole%	M_w	Density [g/cm ³]	Mole%	M_w	Density [g/cm ³]	Mole%	M_w	Density [g/cm ³]
N ₂	0.41			0.34			0.33		
CO ₂	0.44			0.84			0.19		
C1	40.48			49.23			35.42		
C2	7.74			6.32			3.36		
C3	8.20			4.46			0.9		
i-C4	1.23			0.86			0.69		
n-C4	4.22			2.18			0.26		
i-C5	1.43			0.93			0.26		
n-C5	2.21			1.33			0.14		
C6	2.83			2.06			0.72		
C7(+)	4.13	100	0.7294	3.33	99	0.7395	57.73	255	0.9165
C8	4.31	106	0.7492	4.06	106	0.7518			
C9	3.13	121	0.7697	2.76	120	0.7756			
C10	2.439	135	0.7861	1.33	139	0.7930			
C11	1.88	148	0.7919	1.79	146	0.7902			
C12	1.674	161	0.8037	1.7	160	0.8060			
C13	1.573	175	0.8191	1.81	174	0.8203			
C14	1.207	196	0.8331	1.46	194	0.8311			
C15	1.232	206	0.8359	1.49	205	0.8446			
C16	0.985	224	0.8429	1.08	218	0.8515			
C17	0.977	236	0.8400	1.13	234	0.8542			
C18	0.911	245	0.8458	0.99	248	0.8561			
C19	0.585	265	0.8575	0.88	265	0.8663			
C20+	6.382	453	0.9183	7.64	465	0.9350			

Table I.32. Chromatographic characterization of NSO 1, 2, and 3. Note: C7 is the plus fraction for NSO3 (Pedersen et al. 1989).

NSO 1 (97.8°C)		NSO 2 (93.3°C)		NSO 3 (71.1°C)	
Pressure	Viscosity	Pressure	Viscosity	Pressure	Viscosity
[bar]	[cP]	[bar]	[cP]	[bar]	[cP]
401.9	0.356	389.8	0.469	345.7	2.64
376.8	0.352	347.7	0.447	272.7	2.44
325.7	0.340	302.1	0.425	242.3	2.34
275.3	0.322	285.9	0.413	207.8	2.24
251.3	0.316	275.6	0.406	158.9*	2.10
223.8	0.306	274.5*	0.404	145.5	2.21
203.5*	0.299	260.9	0.424	125.1	2.41
180.8	0.316	225.1	0.484	104.4	2.65
151.6	0.360	143.2	0.651	83.7	2.93
126.8	0.404	107.9	0.761	63.0	3.29
101.1	0.448	64.7	0.911	42.4	3.70
77.1	0.512	35.8	1.051	21.7	4.23
58.2	0.570			7.9	4.82
26.6	0.715				

Table I.33. Measured viscosities for NSO 1, 2, and 3 (Pedersen et al. 1989). *Saturation pressure.

NSO 3 black oil, for which only compositional information is given up to the C₇₊ fraction, the characterization has been carried out using a total of 26 compound groups.

In order to apply the general one-parameter *f-theory* model, described in Section I.7.4, to viscosity calculations of the three NSOs, the characteristic critical viscosity of each compound group is required. For the 10 well-defined compounds, the characteristic critical viscosities have been determined by Quiñones-Cisneros et al. (2001a). These values are reported in Table I.34. However, in order to obtain the characteristic critical viscosity of the heavy pseudocomponents, the following modification of the Uyehara and Watson (1944) expression for the critical viscosity can be used

$$\eta_c = 7.9483 \frac{\sqrt{M_w} P_c^{2/3}}{T_c^{1/6}} \quad (\text{I.8.1})$$

	η_c [μP]
N ₂	174.179
CO ₂	376.872
Methane	152.930
Ethane	217.562
Propane	249.734
i-Butane	271.155
n-Butane	257.682
i-Pentane	275.073
n-Pentane	258.651
Hexane	257.841

Table I.34 Characteristic critical viscosities for the general *f-theory* models.

The critical viscosity is given in [μP], P_c in [bar] and T_c in [K].

In addition, in the case of components for which the critical molar volume required in the dilute gas viscosity model, Eq.(I.2.3), is not available, the derived empirical equation for the critical density, Eq.(I.7.43) can be used. This expression can reproduce the critical density of light n-alkanes and other light compounds within an uncertainty of 1%. However, in the case of dense fluids, the use of Eq.(I.7.43) in Eq.(I.2.3) will not introduce a significant error since the total viscosity of dense fluids is always much larger than the dilute gas viscosity contribution.

For the viscosity predictions of the three NSOs with the general *f-theory*, the calculation procedure described in Section I.7.4 for mixtures have been used. In the case of the basic 10 well-defined compounds the required characteristic critical viscosities reported in Table I.34 have been used, whereas for the pseudocomponents, the estimation of the characteristic critical viscosities has been performed using Eq.(I.8.1).

In the viscosity predictions carried out with the LBC model, the required density has been estimated using the PR EOS, whereas the critical density has been estimated by Eq.(I.7.43). The calculation procedure for the LBC model is described in Section I.2.2.1.

Figures I.69 – I.71 show the performance of the general one-parameter PR

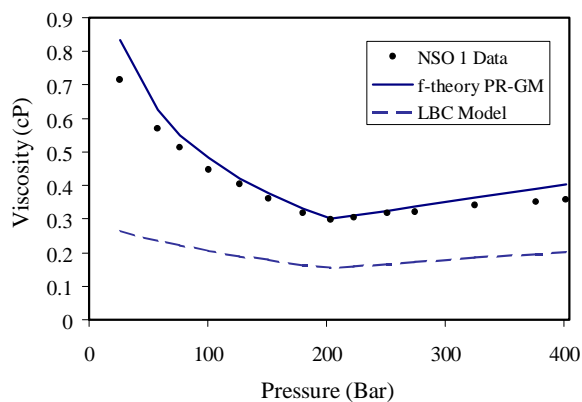


Figure I.69. Viscosity predictions with the LBC model and the general one-parameter PR *f-theory* model for NSO 1 at 97.8°C (Pedersen et al. (1989)).

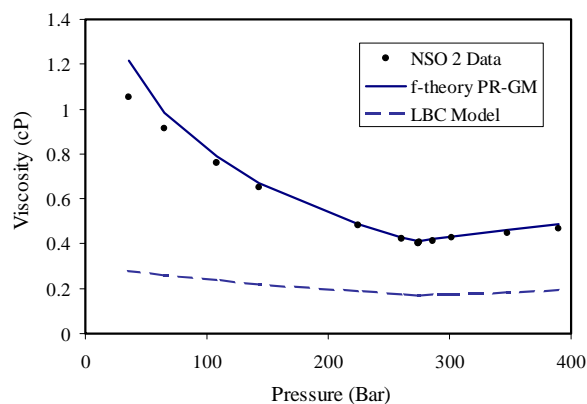


Figure I.70. Viscosity predictions with the LBC model and the general one-parameter PR *f-theory* model for NSO 2 at 93.3°C (Pedersen et al. (1989)).

f-theory model for NSO 1, 2, and 3, respectively, along with the results for the viscosity predictions obtained with the LBC model. Clearly, Figures I.69 and I.70 show that for the lighter NSO 1 and NSO 2 for which an extensive detailed chromatographic characterization (up to C_{20+}) is available, the general one-parameter *f-theory* model is capable of predicting the viscosity accurately based on the simple unmodified PR EOS. On the other hand, Figure I.71 shows that for the heavy NSO 3 black oil, which has a poorer chromatographic characterization (only up to C_{7+}), the general one-parameter *f-theory* model under predicts the viscosity by a factor close to 40%. In contrast, in all cases the LBC model shows deviations near to one order of magnitude off, i.e.

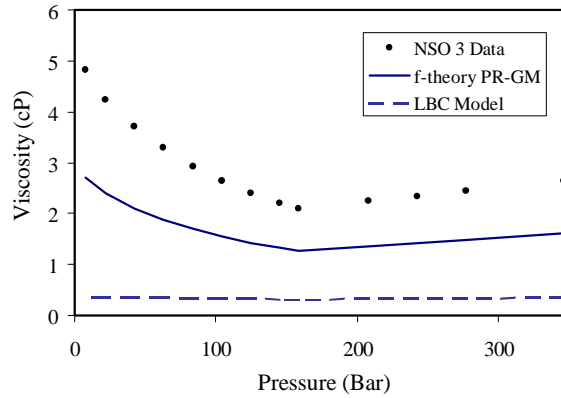


Figure I.71. Viscosity predictions with the LBC model and the general one-parameter PR *f-theory* model for NSO 3 at 71.1°C (Pedersen et al. (1989)).

deviations ranging from 50 to 90%. However, it should be stressed that using a more accurate density model, would result in better LBC results.

I.8.2.2 Tuning of the General *f-theory* Model

As it can be seen from Figure I.71, there may be cases when a model tuning may be necessary. This is a common practice in the oil industry every time the LBC model is used in applications such as reservoir simulations. One way to tune the LBC model is by iteratively changing the critical volume of the heaviest fraction until a reasonable viscosity match is obtained. This is a trial and error procedure, since the LBC model is a sixteenth order polynomial in the reduced density and therefore the parameter to be tuned cannot be factored out. In contrast, the general one-parameter *f-theory* model can be written in terms of a linear function on the tuning parameter, as described below.

In the *f-theory* tuning procedure introduced by Quiñones-Cisneros et al. (2001b) it is assumed that the oil can be described in terms of n component groups, out of which the first m components are well defined. In the test cases, $m = 10$ corresponding to the following well-defined components: N_2 , CO_2 , CH_4 , C_2H_6 , C_3H_8 , $i-C_4$, $n-C_4$, $i-C_5$, $n-C_5$ and C_6 , for which the characteristic critical viscosity is reported in Table I.34. For the remaining pseudocomponents for which an estimated characteristic critical viscosity is not available, it is possible to write

$$\eta_{c,i} = Kc \frac{\sqrt{M_{wi}} P_{ci}^{2/3}}{T_{ci}^{1/6}} \quad (\text{I.8.2})$$

where Kc can be taken as the adjustable parameter for all components with $i > m$. Therefore, upon substitution of Eq.(I.8.2) in the general one-parameter *f-theory* model it can be shown that the total viscosity can be written as follows:

$$\eta = \eta_I + Kc \eta_{II} \quad (\text{I.8.3})$$

where

$$\eta_I = \eta_{0, \text{mx}} + \kappa_{r,I} p_r + \kappa_{a,I} p_a + \kappa_{rr,I} p_r^2 \quad (\text{I.8.4})$$

and

$$\eta_{II} = \kappa_{r,II} p_r + \kappa_{a,II} p_a + \kappa_{rr,II} p_r^2 \quad (\text{I.8.5})$$

In Eq.(I.8.4) the friction parameters are defined as follows:

$$\kappa_{r,I} = \sum_{i=1}^m z_i \frac{\eta_{c,i} \hat{\kappa}_{r,i}}{P_{c,i}} \quad (\text{I.8.6})$$

$$\kappa_{a,I} = \sum_{i=1}^m z_i \frac{\eta_{c,i} \hat{\kappa}_{a,i}}{P_{c,i}} \quad (\text{I.8.7})$$

$$\kappa_{rr,I} = \sum_{i=1}^m z_i \frac{\eta_{c,i} \hat{\kappa}_{rr,i}}{P_{c,i}^2} \quad (\text{I.8.8})$$

For Eq.(I.8.5) the friction parameters are given by:

$$\kappa_{r,II} = \sum_{i=m+1}^n z_i \left(\frac{\sqrt{M_{w,i}} P_{c,i}^{2/3}}{T_{c,i}^{1/6}} \right) \frac{\hat{\kappa}_{r,i}}{P_{c,i}} \quad (\text{I.8.9})$$

$$\kappa_{a,II} = \sum_{i=m+1}^n z_i \left(\frac{\sqrt{M_{w,i}} P_{c,i}^{2/3}}{T_{c,i}^{1/6}} \right) \frac{\hat{\kappa}_{a,i}}{P_{c,i}} \quad (\text{I.8.10})$$

and

$$\kappa_{rr,II} = \sum_{i=m+1}^n z_i \left(\frac{\sqrt{M_{w,i}} P_{c,i}^{2/3}}{T_{c,i}^{1/6}} \right) \frac{\hat{\kappa}_{rr,i}}{P_{c,i}^2} \quad (\text{I.8.11})$$

Therefore, for a characterized oil Eq.(I.8.3) becomes a linear equation with one unknown: Kc . Kc is only related to the heavy fraction (liquid phase) of the reservoir

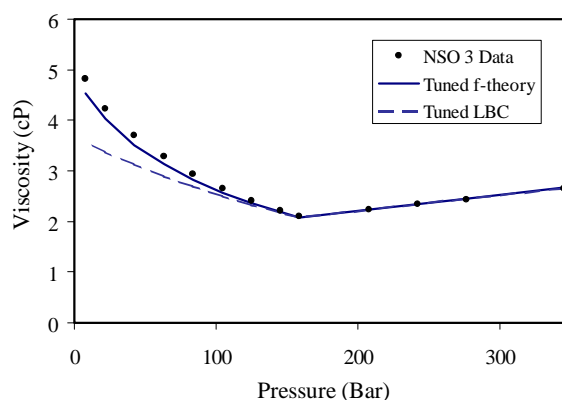


Figure I.72. Tuning of the LBC model and the general PR *f-theory* model for viscosity predictions of NSO 3 at 71.1°C (Pedersen et al. (1989)).

fluid. Thus, for every viscosity point that is known, the corresponding Kc that would exactly match such a point can be found. In the case when several viscosity points are available, a least squares fit or a simple average procedure can be used to estimate an optimal Kc .

For illustration purposes, the NSO 3 viscosity data above the saturation pressure have been used in order to tune the LBC model and the general *f-theory* model. The reason for not using data below the saturation pressure follows from the fact that in most cases such information is not available and therefore, it is important to analyze the models prediction capabilities on data, which may be more representative of available data and conditions. Figure I.72 shows the results of the tuned models for the NSO 3. Clearly, for pressures above the saturation pressure both models can precisely describe the fluid viscosity. However, as the composition of the fluid changes, as it happens below the saturation pressure, the tuned LBC model starts to fail. In contrast, the tuned general *f-theory* model is capable of prediction the viscosity satisfactory for pressures substantially below the saturation pressure.

Additionally, the accuracy of the general *f-theory* model for viscosity predictions is clearly dependent on the degree of how detailed the oil characterization information are. To illustrate this, the NSO 2 information in Table I.32 for all component groups above C_6 has been lumped into a C_{7+} fraction. Then, a new SPECS characterization has been carried out, as described before, but using a total of only 16

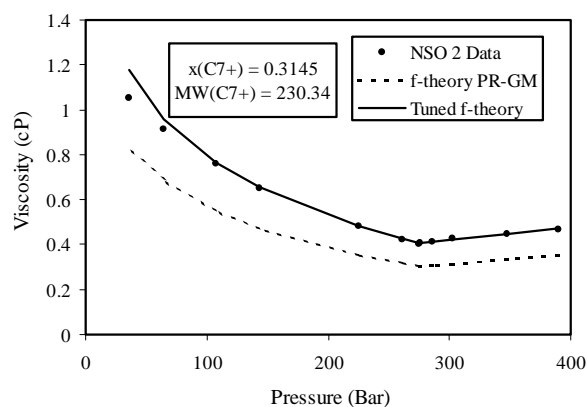


Figure I.73 Viscosity predictions of NSO 2 with the general *f-theory* model and with a tuned *f-theory* model using a lumped C_{7+} fraction.

compound groups This results in a deterioration of the accuracy of the direct viscosity predictions from an AAD of around 3%, which is within the experimental uncertainty, to an AAD of around 25%. However, in spite having less detailed information for the oil characterization, which may result in poorer viscosity predictions, an accurate tuning can still be achieved. Figure I.73 shows the results of the prediction with the general PR *f-theory* model for the NSO 2 as well as the tuned PR *f-theory* results, along with the C_{7+} fraction information. In addition to these viscosity estimations, the general *f-theory* models in conjunction with the SRK and the PR EOS have also been applied to 20 African reservoir fluids, showing an AAD of around 20% if a direct prediction is carried out. But if the *f-theory* models are tuned the AAD is around 5%, which is in agreement with the experimental uncertainty. Further, Marker (2000) obtained similar results for 26 reservoir fluids.

I.8.2.3 Concluding Remarks

The general one-parameter *f-theory* models have been extended to reservoir fluids. The results presented, as well as additional studies made on other oil samples coming from different sources show a good predictive viscosity performance for reservoir fluids. However, depending on direct factors such as the actual properties of the oil, or indirect factors such as the detailed information of the oil characterization, the accuracy of the viscosity predictions with the general *f-theory* models may fluctuate within a 25%

accuracy range. In contrast, the LBC model clearly fails to provide any reasonable viscosity predictions of oil fluids other than natural gas (the kind of fluids for which the LBC model was developed). Another point to be emphasized is that the *f-theory* models can be used in conjunction with simple cubic EOSs, such as the PR EOS and the SRK EOS and still deliver accurate viscosity modeling. These EOSs are commonly used within the oil industry

The main point shown in this section relates to the tuning flexibility of the general *f-theory* models. The tuning of the general *f-theory* models only requires solving a simple linear equation. This is a major advantage in comparison to the iterative procedure that is required in order to tune the LBC model, which is a sixteenth order polynomial in the reduced density. Furthermore, it has also been illustrated how even a tuned LBC model fails to accurately predict the viscosity of an oil with important compositional changes with respect to the composition of the original tuning. This represents a major shortcoming of the LBC model for applications such as computer simulations of oil reservoir depletion processes. In contrast, a tuned *f-theory* model performs with good predictive accuracy even in cases for which strong compositional changes take place, as it is the case for pressures substantially below the saturation pressure. Further, it should be noticed that the results shown in this section do not depend upon the particular computer characterization procedure that has been used.

Finally, it should be stressed that the tuning parameter in the general *f-theory* models only is related to the heavy fraction of the reservoir fluid, which will be kept in the liquid phase at all T,P conditions. Due to this, it should be possible to tune Kc using the measured viscosities at 1 atm of a dead oil, and predict the viscosity of a live oil at reservoir conditions. This is one more advantage of the tuning procedure of the general *f-theory* models.

I.8.3 Viscosity Prediction of Natural Gas

In case of natural gas, which has become an important energy resource, an accurate prediction of the viscosity is also required. Currently, the most commonly used models for predicting the viscosity of natural gases are either based on empirical equations, the corresponding states principle, or kinetic gas theory.

EOS	a_0 [$\mu\text{P bar}^{-1}$]	a_1 [$\mu\text{P bar}^{-1}$]	a_2 [$\mu\text{P bar}^{-1}$]	b_0 [$\mu\text{P bar}^{-1}$]	b_1 [$\mu\text{P bar}^{-1}$]	b_2 [$\mu\text{P bar}^{-1}$]	c_2 [$\mu\text{P bar}^{-2}$]
PR	0.0517769	-0.125387	0.0273166	-0.433077	-0.373055	0.115805	$9.77243 \cdot 10^{-6}$
PRSV	0.0538162	-0.124174	0.0284064	-0.430873	-0.369093	0.116296	$9.71321 \cdot 10^{-6}$
SRK	0.0111800	-0.0452636	-0.0927798	-0.538915	-0.422842	0.0493449	$1.55113 \cdot 10^{-5}$

Table I.35 Friction constants for methane.

Thus, the main aim of this work is to introduce a procedure based on the concepts of the *f-theory* for the accurate viscosity calculation of hydrocarbon mixtures rich in one component. This is the case for natural gases, which mainly contain methane (generally 75 – 90 mole% methane).

I.8.3.1 Calculation Procedure

Since natural gas mainly contain methane, an efficient and accurate viscosity prediction can be achieved with the *f-theory* by estimating the methane friction coefficients by a 7 constants *f-theory* model (Eqs.(I.7.17) – (I.7.19)), whereas the other pure friction coefficients of the remaining compounds are estimated using the general one-parameter *f-theory* model. This combination of different *f-theory* models can be achieved, because the mixture friction coefficients are estimated from pure compound friction coefficients. The only requirement is that the different *f-theory* models are related to the same EOS model. The 7 friction constants required in Eqs.(I.7.17) – (I.7.19) for methane have been estimated by a least squares fit to recommended methane viscosity values reported in Appendix A4, Table A4.1, and the constants are reported in Table I.35 for the SRK, the PR and the PRSV EOS, respectively. These cubic EOSs have been used in the viscosity predictions of natural gases. All of the required compound constants are taken from the DIPPR data compilation (Daubert and Danner 1989) and the regular van der Waals mixing rules, Eq.(I.3.15) and (I.3.16) have been used in the cubic EOSs without any binary interaction parameters.

Since the total viscosity in the *f-theory* is separated into a dilute gas viscosity term and a friction term, any accurate dilute gas viscosity model can be used. However, it should be stressed that the contribution coming from the dilute gas viscosity term to the total viscosity will be important. In this work, the mixing rule by Herning and Zipperer (1936), Eq.(I.2.10) have been used in conjunction with the dilute gas viscosity model by Chung et al. (1988), Eq.(I.2.3) for the pure components, since they combine simplicity with a sufficient accuracy for hydrocarbon multicomponent mixtures, such as natural gases. Further, the Herning and Zipperer mixing rule is also used in the LBC viscosity model for hydrocarbon mixtures (Lohrenz et al. 1964). Nevertheless, if required other models, such as those described by Hirschfelder et al. (1964), can be incorporated for the dilute gas limit.

I.8.3.2 Results and Discussion

In spite of the importance of natural gases, only a few accurate measurements covering wide ranges of temperature and pressure have recently been carried out (Assael et al. 2001, Nabizadeh and Mayinger 1999). Other older measurements from the 1960's are reported by Lee et al. (1966). Thus, 6 mixtures have been studied in this work, and the corresponding compositions along with the literature sources, are given in Table I.36. The components referred to as pentanes, hexanes and heptanes in Lee et al. (1966) have been taken as equivalent to n-pentane, n-hexane, and n-heptane, respectively. Although that some natural gas mixtures contain very small amounts of helium, the contribution from helium to the total viscosity of the natural gas mixtures is negligible.

Using the suggested procedure of combining the 7 constants *f-theory* model with the one-parameter *f-theory* general model (Quiñones-Cisneros et al. 2001a), the viscosity of the 6 natural gas mixtures has been predicted with the SRK, the PR, and the PRSV EOS, respectively, and compared with the experimental values. The obtained AAD and MxD are reported in Table I.37, and similar results are obtained using the three different EOS.

For mixture 1 (Assael et al. 2001) and mixture 2 (Nabizadeh and Mayinger 1999), the obtained AADs are in excellent agreement with the experimental values, which have an uncertainty of 1.0%. Figure I.74 and I.75 shows the predicted viscosity

	Mixture 1	Mixture 2	Mixture 3	Mixture 4	Mixture 5	Mixture 6
	[a]	[b]	[c]	[c]	[c]	[c]
Nitrogen	5.60	1.83		1.40	4.80	0.55
Carbon Dioxide	0.66		3.20	1.40	0.90	1.70
Helium				0.03	0.03	
Methane	84.84	94.67	86.33	71.71	80.74	91.46
Ethane	8.40	3.50	6.80	14.00	8.70	3.10
Propane	0.50		2.40	8.30	2.90	1.40
i-Butane			0.43	0.77		0.67
n-Butane			0.48	1.90	1.70	0.50
n-Pentane			0.22	0.39	0.13	0.28
n-Hexane			0.10	0.09	0.06	0.26
n-Heptane			0.04	0.01	0.03	0.08

Table I.36. Composition of natural gases in mole%.

a) Assael et al. (2001), b) Nabizadeh and Mayinger (1999), c) Lee et al. (1966).

	Ref.	NP	T-range K	P-range bar	SRK		PR		PRSV	
					AAD%	MxD%	AAD%	MxD%	AAD%	MxD%
Mixture 1	a	40	241 – 455	2.4 – 140	0.91	3.18	0.83	3.12	0.83	3.12
Mixture 2	b	59	299 – 399	1.0 – 67	0.89	1.95	0.86	1.81	0.84	1.78
Mixture 3	c	30	311 – 444	1.4 – 276	3.92	5.84	3.85	5.60	3.81	5.52
Mixture 4	c	33	311 – 444	48 – 552	3.76	6.60	3.49	6.37	3.39	6.33
Mixture 5	c	26	344 – 444	14 – 172	4.00	6.84	3.89	6.64	3.85	6.58
Mixture 6	c	26	311 – 444	28 – 552	4.17	10.8	4.13	10.8	4.12	10.8

Table I.37 Performance of the *f-theory* viscosity models.

a) Assael et al. (2001), b) Nabizadeh and Mayinger (1999), c) Lee et al. (1966).

versus pressure for mixture 1 and mixture 2, whereas Figure I.76 shows the deviations obtained for mixture 1 with the PR *f-theory* model. Clearly, the largest deviations for mixture 1 are found at low temperatures close to the dilute gas viscosity limit. However, at these conditions a difference of 1 to 2 μP can easily correspond to a deviation of 1 – 2%. Nevertheless, the obtained deviations at low pressures are still within the accuracy of the model and of the experimental results, as shown in Figure I.77, where the

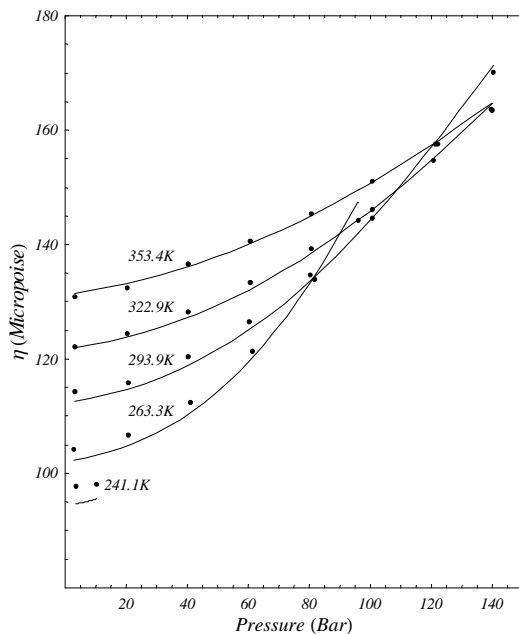


Figure I.74 Viscosity prediction with the PR *f*-theory (—) of natural gas mixture 1, experimental data (●) (Assael et al. 2001).

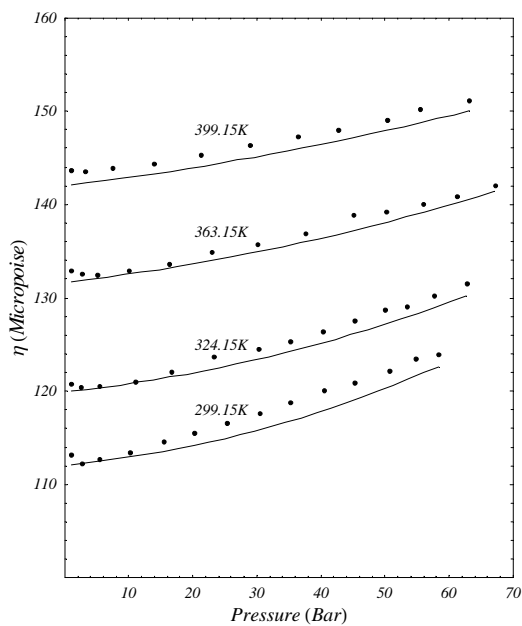


Figure I.75 Viscosity prediction with the PR *f*-theory (—) of natural gas mixture 2, experimental data (●) (Nabizadeh and Mayinger 1999).

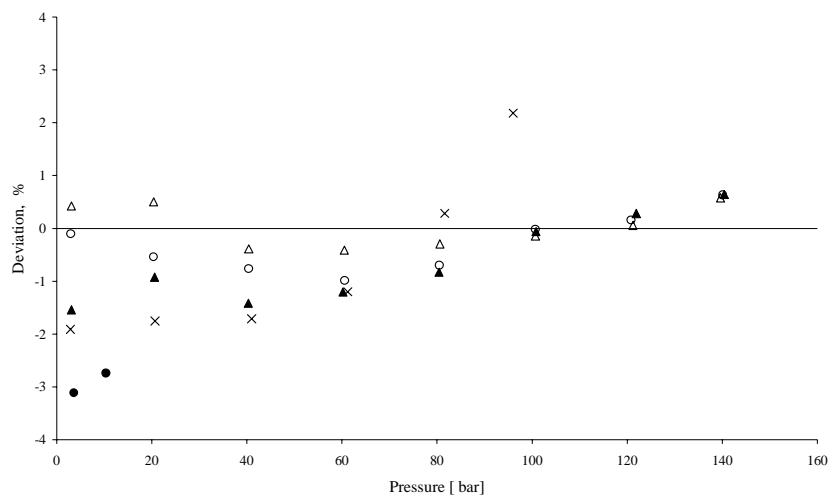


Figure I.76. Deviation of the predicted viscosities using the *f*-theory with the PR EOS for mixture 1 (Assael et al. 2001). (●) 241.1 K; (×) 263.3 K; (▲) 293.9 K; (○) 322.9 K; (△) 353.4 K.

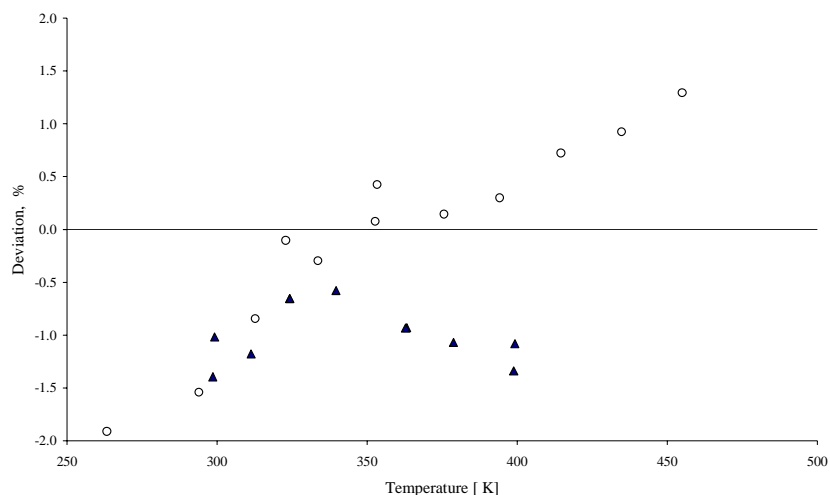


Figure I.77 Deviation of the predicted viscosities at low pressure using the *f-theory* with the PR EOS for mixture 1 (o) (2.4 – 3.1 bar) (Assael et al. 2001); and mixture 2 (▲) (1 bar) (Nabizadeh and Mayinger 1999).

deviations from the low pressure measurements are plotted as a function of temperature for mixture 1 (2.4 – 3.1 bar) and mixture 2 (1 bar). At these low pressure conditions, the main contribution to the total viscosity is coming from the dilute gas viscosity limit. Therefore, Figure I.77 shows that the dilute gas viscosity limit is satisfactorily predicted by the simple models used in this work. Further, Assael et al. (2001) observed the same trend, when they compared their measurements with the Vesovic and Wakeham model (Vesovic and Wakeham 1989a, 1989b, and Vesovic et al. 1998). Overall, for mixture 1, Assael et al. (2001) obtained an AAD of 1.5% and an MxD = 3.8%, compared to the AAD of 0.8% and MxD of 3.1% obtained in this work.

For the older measurements, mixtures 3 to 6, a larger deviation is obtained mainly due to the higher experimental uncertainty. These measurements, together with their density measurements, were carried out in the mid 1960's by Lee et al. (1966), who also modeled the measured data using a density-dependent empirical equation with an overall AAD of 2.7%. The overall AAD in this work is 3.8% with the PR EOS for mixtures 3 to 6. Mixture 6 contains more than 91 mole% methane, and it should therefore be expected that the predicted viscosities should be in good agreement with the experimental data and similar to the results for mixture 2 (94.7 mole% methane), but

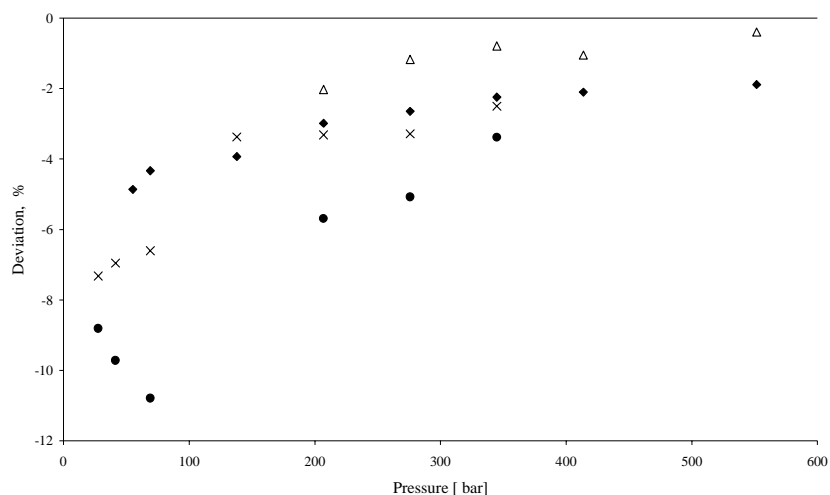


Figure I.78. Deviation of the predicted viscosities using the *f-theory* with the PR EOS for mixture 6 (Lee et al. 1966). (Δ) 310.93 K; (\blacklozenge) 344.26 K; (\bullet) 410.93 K; (\times) 444.26 K.

this is not the case. From the deviation plot for mixture 6, Figure I.78, it is seen that for pressures below 100 bar and temperatures above 410.9 K very large deviations are obtained. The other points have deviations around -3.5% , indicating problems with the high temperature, lower pressure measurements – this is the main reason for the high AAD in mixture 6. The lowest AAD for the old measurements is found for mixture 4, which contains 71.7 mol% methane, but again the largest deviations are found at the lowest pressures, as shown in Figure I.79.

Since the viscosity of the more accurate and recent measurements (Assael et al. 2001, Nabizadeh and Mayinger 1999) are predicted within the experimental uncertainty, it is believed that the results obtained for these mixtures better illustrate the application of the introduced *f-theory* scheme for predicting the viscosity of natural gases.

I.8.3.3 Concluding Remarks

A scheme has been introduced for viscosity prediction of natural gases by combining two different *f-theory* models. This can be done because the mixture friction coefficients are linked to mixing rules based on the friction coefficients of the pure components, provided that the same EOS is used. Since natural gases are multicomponent mixtures, mainly containing methane (75 – 90 mol%), an efficient and accurate scheme for

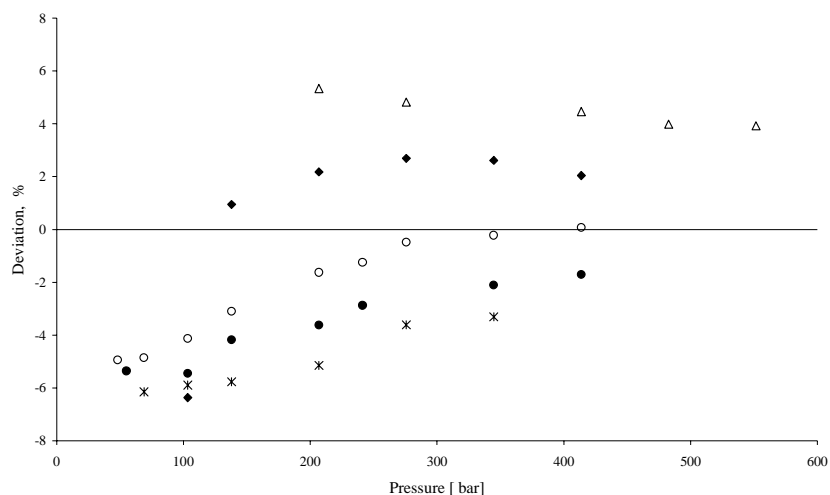


Figure I.79. Deviation of the predicted viscosities using the *f-theory* with the PR EOS for mixture 4 (Lee et al. 1966). (Δ) 310.93 K; (\blacklozenge) 344.26 K; (\circ) 377.59 K; (\bullet) 410.93 K; (\times) 444.26 K.

predicting the viscosity of natural gases is obtained by using an accurate 7 constant *f-theory* model for the pure methane friction coefficients, and the general one-parameter *f-theory* model for the friction coefficients of the remaining components. Based on this scheme, the viscosity of 6 natural gas mixtures has been predicted with the SRK, the PR, and the PRSV EOS. For all of the models, it has been found that for the most accurate, recent measured viscosities, mixture 1 and 2, the obtained AAD (0.9 – 1.1%) is in excellent agreement with the experimental uncertainty (± 1.0). The maximum deviations are obtained at low temperatures for low pressures, and this may be ascribed to the uncertainty in the prediction of the dilute gas viscosity. For the older measurements, mixtures 3 – 6, an overall AAD of around 4.0% is obtained due to a higher experimental uncertainty in the measurements, but also due to problems with the measurements themselves, as it was found for mixture 6 at high temperatures and pressures below 100 bar. Nevertheless, the obtained results in this work are satisfactory for most applications related to the gas industry.

Further, since the *f-theory* can be linked to cubic EOSs, and such EOSs are widely used within the petroleum industry, the introduced *f-theory* scheme for the viscosity prediction of natural gases can be easily implemented. The only external input

required for the *f-theory* approach presented here is the actual temperature, pressure, and composition of the mixture.

I.8.4 Viscosity Prediction of Hydrogen + Natural Gas Mixtures (Hythane)

In the 19th century coal gas, a mixture composed mainly of hydrogen (50%) and methane (26%), was used in Great Britain for lighting. Today, mixtures of hydrogen and natural gas, called hythane, are being investigated as alternative fuels in combustion engines. The aim is to reduce the emission of greenhouse gases, such as CO_x. Since hythane may in the future become an alternative fuel, knowledge of its physical properties, such as the viscosity is important. It is therefore important to have reliable and accurate models for predicting the viscosity of hythane over wide ranges of temperature, pressure and composition. The scheme introduced for predicting the viscosity of natural gases (Section I.8.3) based on the concepts of the *f-theory* has been extended to viscosity predictions of hythane mixtures by including an *f-theory* model for hydrogen (Section I.7.5), since the main components of hythane are hydrogen and methane.

I.8.4.1 Viscosity Prediction Procedure for Hythane

Since, the mixture friction coefficients are estimated based on the temperature dependent friction coefficients of the pure components ($\kappa_{r,i}$, $\kappa_{a,i}$ and $\kappa_{rr,i}$), the mixture friction coefficients can be directly obtained by combining different kind of *f-theory* models, as shown in the *f-theory* scheme for viscosity predictions of natural gases, see Section I.8.3. Thus, since hythane is a mixture composed of hydrogen and natural gas, the *f-theory* natural gas scheme can be further combined with the 3 constants *f-theory* model derived for hydrogen, see Section I.7.5. In this way, an accurate and efficient procedure for predicting the viscosity of hythane can be achieved. The hydrogen *f-theory* model has been derived for supercritical conditions above 200 K, since hydrogen (normal hydrogen) at these conditions consists of 25% para-hydrogen and 75% ortho-hydrogen in equilibrium (Vargaftik 1975). Further, since the application of the introduced *f-theory* scheme for viscosity predictions of hythane is for temperatures above 200 K, which correspond to temperatures above the critical temperature of

methane, the derived 3 constants *f-theory* model for methane, see Section I.7.5, is also used in this work. Therefore, both the hydrogen and the methane friction coefficients are obtained with the following expressions

$$\begin{aligned}\kappa_r &= k_r \\ \kappa_a &= k_a \\ \kappa_{rr} &= k_{rr} \Gamma^2\end{aligned}\tag{I.8.12}$$

while the friction coefficients of the other components in the natural gas are estimated with the general one-parameter *f-theory* model (Quiñones-Cisneros et al. (2001a) described in Section I.7.4.

For light gas mixtures, the friction coefficients κ_r , κ_a and κ_{rr} can be estimated using the following linear mixing rules

$$\begin{aligned}\kappa_r &= \sum_{i=1}^n x_i \kappa_{r,i} \\ \kappa_a &= \sum_{i=1}^n x_i \kappa_{a,i} \\ \kappa_{rr} &= \sum_{i=1}^n x_i \kappa_{rr,i}\end{aligned}\tag{I.8.13}$$

where x_i is the mole fraction of component i , while $\kappa_{r,i}$, $\kappa_{a,i}$ and $\kappa_{rr,i}$ are the friction coefficients of the pure components. In the case of light gases, such as hythane, these simple mixing rules can deliver satisfactory results for industrial applications. However, if further accuracy enhancement is required, this can be achieved using the mass weighted mixing rules originally derived for the *f-theory* (Quiñones-Cisneros et al. 2000).

The PR and the SRK EOS have been used in this work for viscosity predictions of hythane mixtures, along with the original van der Waals mixing rules, Eqs.(I.3.15) and (I.3.16), and without any binary interaction parameters. Thus, the 3 constants required in Eq.(I.8.12) for hydrogen and for methane are taken from Table I.27 for the PR and the SRK EOS, respectively. All of the other required compound constants in the EOS are taken from the DIPPR Data Compilation (Daubert and Danner 1989).

In addition and due to the fact that the dilute gas viscosity of hythane mixtures will be the main contribution to the total viscosity, some remarks have to be addressed.

For pure fluids, such as hydrocarbons, the dilute gas viscosity model. Eq.(I.2.3) (Chung et al. 1988) can be applied for the prediction of the dilute gas viscosity over wide ranges of temperature within an uncertainty of $\pm 1.5\%$. For hydrogen, however, Eq.(I.2.3) is not suitable, and due to this the following empirical expression has been found to model better the dilute gas viscosity limit (Section (I.7.5) with an uncertainty of 1.2%

$$\eta_0 = -1.55199\sqrt{T} + 2.92788 T^{0.645731} \quad (\text{I.8.14})$$

where η_0 is in $[\mu\text{P}]$ and the temperature in $[\text{K}]$.

At low pressure and constant temperature, gas mixtures composed of hydrogen and hydrocarbons show a viscosity maximum as a function of the composition. This kind of behavior is normal in the case of gas mixtures composed of compounds with large differences in size and shape. For the dilute gas viscosity limit, the mixing rule based on a simplification of the kinetic gas theory proposed by Wilke (1950) is capable of describing this kind of behavior and is used in this work. This mixing rule is totally predictive since no information about the mixture properties is required, only the dilute gas viscosity, the molecular weight and the mole fraction of the pure components are needed.

I.8.4.2 Results and Discussion

Recently, Nabizadeh and Mayinger (1999) measured the viscosity of four hythane mixtures in the temperature range 298 – 400 K and from 1 to 71 bar using an oscillating-disk viscometer with an experimental uncertainty of $\pm 1.0\%$. The viscosities of hydrogen and the natural gas, used to prepare the hythane mixtures, were also measured within the same temperature and pressure conditions. The compositions of these four hythane mixtures and the natural gas are given in Table I.38.

Thus, the viscosity of the four hythane mixtures, as well as the related hydrogen and natural gas, has been predicted using the procedure outlined above in conjunction with the PR and the SRK EOS, respectively. The obtained AAD and MxD for the viscosity predictions of the four hythane mixtures, hydrogen and the natural gas are given in Table I.39. The performance of the PR *f-theory* procedure is shown in Figure I.80 through I.83 for the four hythane mixtures. It should be remarked that, in the cases studied in this work, the dilute gas viscosity is the main contribution to the total

	Hydrogen	Methane	Ethane	Nitrogen
Natural Gas ¹		94.67	3.50	1.83
Mixture 1 ¹	4.95	89.98	3.33	1.74
Mixture 2 ¹	15.4	80.09	2.96	1.55
Mixture 3 ¹	29.9	66.364	2.454	1.283
Mixture 4 ¹	74.9	23.762	0.879	0.459

Table I.38. Composition of the natural gas and the hythane mixtures given in mole%.

¹ Nabizadeh and Mayinger (1999).

		<i>T</i> -range	<i>P</i> -range	PR- <i>f</i> -theory		SRK- <i>f</i> -theory	
	NP	[K]	[bar]	AAD%	MxD%	AAD%	MxD%
Mixture 1 ¹	56	299 – 399	1 – 67	0.90	1.84	0.82	1.68
Mixture 2 ¹	53	299 – 399	1 – 63	0.75	1.55	0.67	1.40
Mixture 3 ¹	56	299 – 399	1 – 68	0.41	1.46	0.35	1.29
Mixture 4 ¹	33	300 – 400	1 – 71	1.42	1.97	1.51	2.12
Hydrogen ¹	76	296 – 399	1 – 58	0.86	2.06	0.82	2.06
Natural Gas ¹	59	299 – 399	1 – 67	1.14	2.07	1.06	1.93

Table I.39. Performance of the *f*-theory model for viscosity predictions of the hythane mixtures, hydrogen, and the natural gas. NP is the number of points.

¹ Nabizadeh and Mayinger (1999).

viscosity. The maximum contribution of the viscosity in excess of the dilute gas limit is of the order of 10% compared to the total viscosity. Overall, as indicated by the results reported in Table I.39, the obtained AAD with the PR and SRK *f*-theory models are within or close to the uncertainty reported for the experimental values. The slightly higher deviation that mixture 4 shows is related to a small over prediction of the dilute gas limit. However, if the dilute gas viscosity of mixture 4 is reduced by 1%, an AAD of 0.53% and an MxD of 0.96% are obtained with the PR *f*-theory, while the SRK *f*-theory gives an AAD of 0.61% and an MxD of 1.12%.

In Figure I.84, the deviations between the predicted viscosities using the PR *f*-theory model and the reported values at 1 bar are shown. At this pressure the friction viscosity contribution in excess of the dilute gas viscosity is less than 0.5%. Therefore, Figure I.84 mainly shows the performance of the mixing rule by Wilke (1950) used to predict the dilute gas viscosity of the studied hythane mixtures. The overall AAD for all

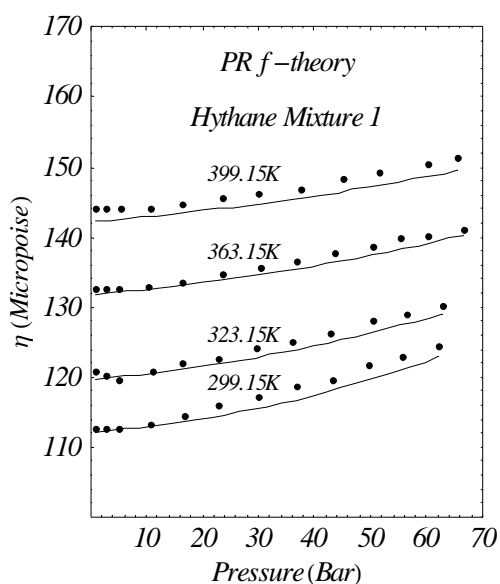


Figure I.80 Performance of the PR *f*-theory model for viscosity prediction of hythane mixture 1 (—) along with the experimental points (•) Nabizadeh and Mayinger (1999).

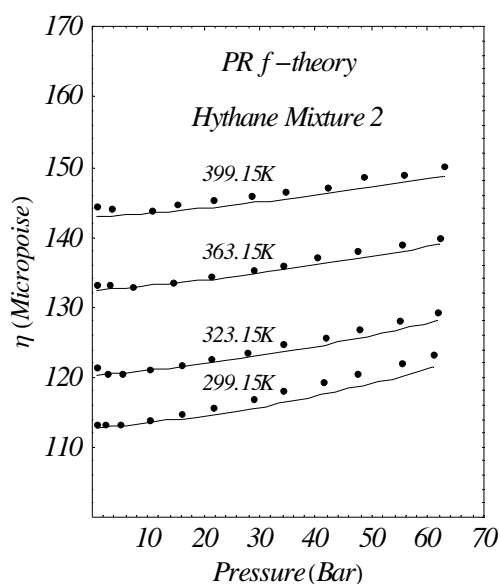


Figure I.81 Performance of the PR *f*-theory model for viscosity prediction of hythane mixture 2 (—) along with the experimental points (•) Nabizadeh and Mayinger (1999).

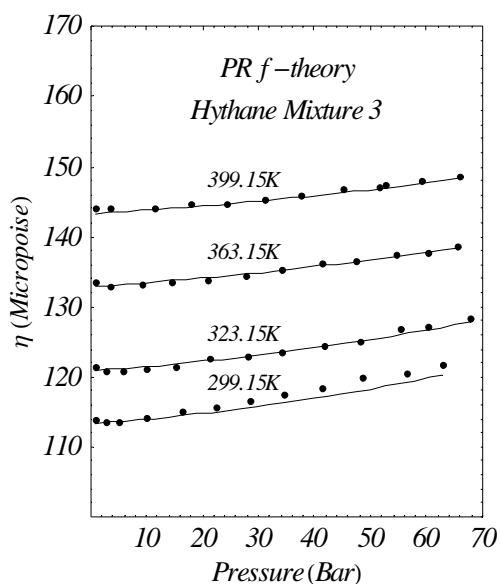


Figure I.82 Performance of the PR *f*-theory model for viscosity prediction of hythane mixture 3 (—) along with the experimental points (•) Nabizadeh and Mayinger (1999).

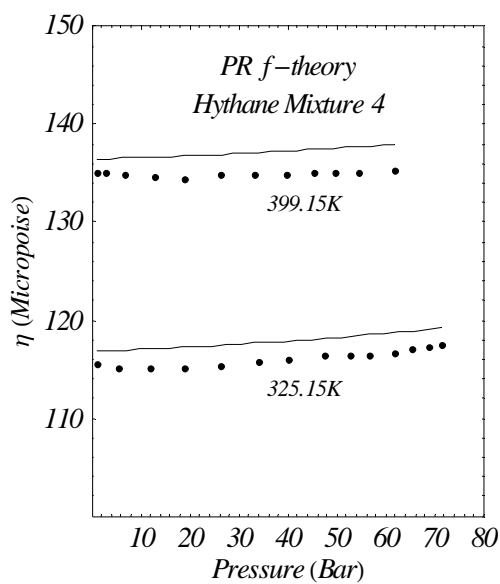


Figure I.83 Performance of the PR *f*-theory model for viscosity prediction of hythane mixture 4 (—) along with the experimental points (•) Nabizadeh and Mayinger (1999).

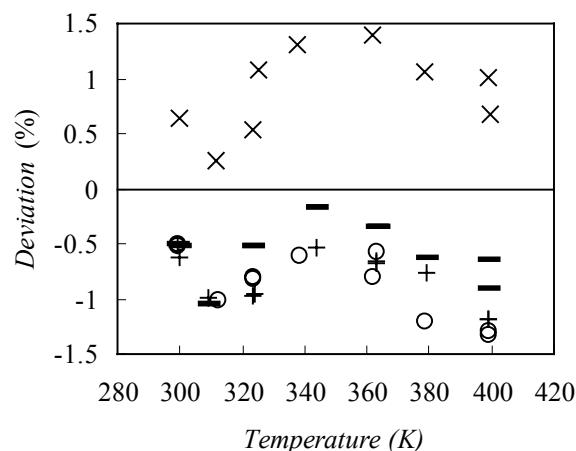


Figure I.84 Deviation between PR *f-theory* predicted viscosities of hythane and reported values at 1 bar. (o) mixture 1, (+) mixture 2, (-) mixture 3, (x) mixture 4.

mixtures is 0.78% with an MxD of 1.39% and the highest deviations are found for mixture 4, or at the highest temperatures. These results demonstrate that the simple mixing rule proposed by Wilke (1950) can be used to estimate the dilute gas viscosity limit of hythane, since the obtained deviations are within the uncertainty of the pure compound dilute gas viscosity estimations. It should also be stressed that due to the low viscosity values of hythane, a difference of only 1 μP can easily correspond to a deviation of 1 – 1.5%.

As a comparison, based on the assumption that the hythane mixtures correspond to binary mixtures composed of hydrogen and natural gas Nabizadeh and Mayinger (1999) modeled their measured hythane viscosities at 1 bar using the procedure proposed by Hirschfelder et al. (1964, p. 530). After fitting the characteristic binary parameters in the Chapman-Enskog theory, σ_{12} and ϵ_{12} , to the experimental data, Nabizadeh and Mayinger obtained a mean deviation of $\pm 0.3\%$ with an MxD of 0.5%. However, such approach can not be considered predictive since the fitted binary parameters correspond to hythane mixtures prepared from the specific used natural gas and can only be applied to these specific mixtures. On the other hand, although better results for the mixture dilute gas viscosity can be obtained by directly modeling the experimental data at low pressure, the results obtained in this work are satisfactory given their predictive nature.

I.8.4.3 Concluding Remarks

A scheme based on the concepts of the *f*-theory has been introduced for viscosity predictions of hythane mixtures by combining the simple mixing rule of Wilke (1950) for the dilute gas viscosity with three different *f*-theory models for the friction viscosity term. This can be done, because the mixture friction coefficients are linked to mixing rules based on the friction coefficients of the pure components, provided that the same EOS is used. Since the main components in hythane are hydrogen and methane, an efficient and accurate scheme for predicting the viscosity of hythane is achieved using a 3 constants *f*-theory model for both hydrogen and methane together with the general one-parameter *f*-theory model for the remaining components. Based on this scheme the viscosity of four hythane mixtures has been predicted with the SRK and the PR EOS. The obtained AAD ranges from 0.4% to 1.5% and is within or close to the experimental uncertainty. Although, the use of more complex models may deliver better results, the mixing rule proposed by Wilke (1950), in conjunction with simple models for the pure dilute gas viscosities, and the linear mixing rules for the friction coefficients used in this work give satisfactory results for hythane. The scheme introduced in this work for the viscosity prediction of hythane is totally predictive, since only properties and parameters of the pure compounds are required. Furthermore, the use of the PR and the SRK EOS for non-polar light gases are well-known to deliver satisfactory density estimations for most industrial applications. In fact, for the studied mixtures in this work the density predictions are within an AAD of 1.2%. Therefore, the approach described in this work can deliver viscosity and density estimations within a satisfactory accuracy.

I.9 Conclusion

The work described in Part I of this thesis can be summarized in three major groups: *Existing Viscosity Models*, *The Friction Theory*, and *Applications of the Friction Theory to Reservoir Fluids*.

Existing Viscosity Models

An extensive evaluation of five existing viscosity models, derived for hydrocarbon fluids, has been performed over wide ranges of temperature, pressure and composition. In order to carry out this evaluation a database containing 35 pure hydrocarbons, carbon dioxide, nitrogen, and 39 well-defined hydrocarbon mixtures have been used. The evaluated models were the well-known LBC model, a modified LBC model called LABO, and two corresponding states models with one and two reference fluids, respectively. In addition also a viscosity model based on the PR EOS has been evaluated. From this evaluation it has been observed that a more reliable and accurate viscosity model is required in order to obtain more accurate viscosity predictions.

An investigation of the possibility of improving the corresponding states model with two references fluids, methane and n-decane, (CS2) (Aasberg-Petersen et al 1991), has been performed by exchanging the second reference fluid n-decane with n-hexane. This results in significantly better viscosity predictions of light and intermediate pure hydrocarbons. In addition the viscosity prediction of the heavy hydrocarbons with the CS2 model can be improved by using the interpolation parameter defined in Eq.(I.6.3). However the modified CS2 model did not improve the viscosity prediction of hydrocarbon mixtures, compared with the original CS2 model. The CS2 model is the model giving the best results for hydrocarbon mixtures, when the five evaluated models are compared.

The Friction Theory

In the friction theory (Quiñones-Cisneros et al. 2000) the total viscosity η is separated into a dilute gas viscosity term η_0 and a residual friction term η_f . The dilute gas viscosity η_0 is defined as the viscosity at the zero density limit, while the residual term

η_f is related to friction concepts of classical mechanics. According to the *f-theory*, the residual friction term is linked to the van der Waals attractive and repulsive pressure terms by means of two linear friction coefficients, κ_r , κ_a , and one quadratic friction coefficient κ_{rr} . These repulsive and attractive pressure terms can be obtained from simple cubic EOSs, such as the SRK EOS or the PR EOS. In the case of mixtures, simple, mass weighted, linear mixing rules for the friction coefficients are proposed. An important further development of the *f-theory* has been the introduction of the one-parameter general models. The one-parameter *f-theory* models depend on one *reducing* parameter: a characteristic critical viscosity η_c . Further, the general one-parameter *f-theory* models depend on 16 universal constants. These constants have been fitted against a database of smoothed viscosity data of n-alkanes, from methane to n-octadecane. The database was obtained, after an evaluation of all the available experimental information given in the literature for n-alkanes, by smoothing the experimental data using *f-theory* models in order to generate an unbiased uniform database that would give optimal fitting results. The database of recommended data incorporates more than four thousand recommended data. The general one-parameter *f-theory* model, as well as the other more specific *f-theory* models developed in association to this work, have shown excellent accuracy in the modeling of pure hydrocarbons and the viscosity prediction, based on pure component properties, of a large number of hydrocarbon mixtures. For example, in the case of pure n-alkanes, the one-parameter general models can reproduce the viscosity of the entire n-alkane family from methane up to n-octadecane with an overall absolute average deviation (AAD) of around 2%. In the case of mixtures, the prediction results are also highly accurate, as illustrated in Table I.23.

Application of the Friction Theory to Reservoir Fluids

One of the main advantages of the *f-theory* lies on the accuracy and simplicity that is obtained when it is applied to reservoir fluids. This has been broadly illustrated with the viscosity prediction of systems such as carbon dioxide + hydrocarbon mixtures (Section I.8.1), natural gas (Section I.8.3), hythane (Section I.8.4) and, most important, crude oils (Quiñones-Cisneros et al. 2001b and Section I.8.2). In the case of crude oils,

the *f-theory* was used in conjunction with regular characterization procedures for the PR EOS. The results show that if there is an extensive experimental oil characterization available, for instance up to the C₂₀₊ fraction, the general *f-theory* models may be able to deliver a good viscosity prediction for oils at reservoir conditions. This is in sharp contrast with the capabilities of the LBC model, which is widely used in the oil industry, as illustrated in Figure I.70. However, even in the case when poor compositional information is available, i.e. just up to the C₇₊ fraction, the *f-theory* models can be easily tuned to obtain a highly accurate viscosity model with excellent predictive properties under severe compositional changes – as it is the case during the producing life of an oil reservoir. Tuning an *f-theory* model only requires solving a simple linear equation against at least one experimental viscosity point, as illustrated in (Quiñones-Cisneros et al. 2001b). The tuning parameter is only related to the heavy fraction of the oil. In contrast, a more mathematically unstable sixteenth order polynomial has to be iteratively solved in order to tune an LBC model. However, as illustrated in Figure I.72, the main problem of a tuned LBC model is its failure to deliver an adequate performance under compositional changes. Consequently, in contrast to the LBC model, an *f-theory* model can be safely applied for an accurate forecast of the viscosity behavior in a reservoir simulator.

In addition, the *f-theory* models have also been extended to applications beyond reservoir fluids as it is the case of light gases, such as argon, hydrogen, nitrogen, and oxygen, or other additional systems mentioned in Appendix C under selected articles.

I.10 List of Symbols

Latin Letters

A	area
C	carbon number
F	force
F_k	kinetic friction force
h	distance
K_{CS}	interpolation parameter in the CS2 model
k_B	Boltzmann's constant
k_{ij}	binary interaction parameter
MM	weighted molecular weight
M_w	molecular weight
M_{wn}	number average molecular weight
M_{ww}	mass weight average molecular weight
N	normal force
N_A	Avogadro's constant
P	pressure
P_c	critical pressure
P_r	reduced pressure
P^{sat}	saturation pressure
p_a	attractive pressure term
p_r	repulsive pressure term
R	gas constant
SG	specific gravity
T	temperature
T_c	critical temperature
T_F	freezing point
T_r	reduced temperature
t	time
U	displacement velocity
u	velocity
v	molar volume
v_c	critical molar volume
v_L^{sat}	saturated liquid molar volume
v_r	reduced molar volume
v_0	close packing molar volume
x	mole fraction
y	distance
Z	compressibility factor
Z_c	critical compressibility factor
Z_{RA}	Rackett's compressibility factor
z	mass weighted fraction

Greek Letters

Γ	defined in Eq.(I.7.33)
γ	shear rate
η	viscosity
η_c	characteristic critical viscosity
η_f	residual friction viscosity term
η_r	reduced viscosity
η_{res}	residual viscosity
η_0	dilute gas viscosity
κ_a	linear attractive friction coefficient
κ_r	linear repulsive friction coefficient
κ_{rr}	quadratic repulsive friction coefficient
μ_k	kinetic friction coefficient
ν	kinematic viscosity
ρ	density of fluid
ρ_c	critical density
ρ_r	reduced density
τ	shear stress
Ω^*	reduced collision integral
ω	acentric factor
ξ	viscosity reducing parameter

I.11 References

Aasberg-Petersen K.: *Prediction of Phase Equilibria and Physical Properties for Mixtures with Oils, Gases, and Water*. Ph.D. Thesis. Technical University of Denmark, Lyngby, Denmark. (1991).

Aasberg-Petersen K. and Stenby E.: *Prediction of Thermodynamic Properties of Oil and Gas Condensate Mixtures*. Industrial & Engineering Chemical Research. **30** (1991) 248 – 254.

Aasberg-Petersen K., Knudsen K., and Stenby E.H.: *Prediction of Viscosities of Hydrocarbon Mixtures*. Fluid Phase Equilibria. **70** (1991) 293 – 308.

Adachi Y., Lu B.C.-Y.; Sugie H.: *A Four-Parameter Equation of State*. Fluid Phase Equilibria. **11** (1983) 29 – 48.

Agaev N.A. and Golubev I.F.: *The Viscosity of n-Hexane in the Liquid and Gaseous State at High Pressures and Different Temperatures*. Doklady Physical Chemistry Proceedings of the Academy of Sciences of the USSR. **151** (1963b) 635 – 640.

Aleskerov M.A., Mamedov A., and Khalilov A.K.: *Experimental Study of the Dependence of the Dynamic Viscosity of the Binary Liquid Mixture Heptane – Octane Versus Temperature and Pressure*. Neft' i Gaz Izvestija Vyssich Ucebnych Zavedenij. **22** (1979) 58 – 60.

Alliez J., Boned C., Lagourette B., and Et-Tahir A.: *Viscosity Under High Pressure of Pure Hydrocarbons and Their Mixtures: Critical Study of a Residual Viscosity Correlation (Jossi)*. Special Publication of the Royal Society of Chemistry. **222** (1998) 75 – 80.

Anselme M.J., Gude M, and Teja A.S.: *Critical Temperatures and Densities of the n-Alkanes from Pentane to Octadecane*. Fluid Phase Equilibria. **57** (1990) 317 – 326.

Assael M.J., Mixafendi S., and Wakeham W.A.: *The Viscosity and Thermal Conductivity of Normal Hydrogen in the Limit of Zero Density*. Journal of Physical and Chemical Reference Data. **15** (1986) 1315 – 1322.

Assael M.J., Karagiannidis L., and Papadaki M.: *Measurements of the Viscosity of n-Heptane + n-Undecane Mixtures at Pressures up to 75 MPa*. International Journal of Thermophysics. **12** (1991) 811 – 820.

Assael M.J., Charitidou E., Dymond J.H., and Papadaki M.: *Viscosity and Thermal Conductivity of Binary n-Heptane + n-Alkane Mixtures*. International Journal of Thermophysics. **13** (1992) 237 – 249.

Assael M.J. Dalaouti N.K., and Vesovic V.: *Viscosity of Natural Gas Mixtures: Measurements and Prediction*. International Journal of Thermophysics. **22** (2001) 61 – 71.

Barrufet M.A., El-Sayed Salam S.K., Tantawy M., and Iglesias-Silva G.A.: *Liquid Viscosities of Carbon Dioxide + Hydrocarbons from 310 K to 403 K*. Journal of Chemical and Engineering Data. **41** (1996) 436 – 439.

Barrufet M.A., Hall K.R., Estrada-Baltazar A., and Iglesias-Silva: G.A.: *Liquid Viscosity of Octane and Pentane + Octane Mixtures from 298.15 K to 373.15 K up to 25 MPa*. Journal of Chemical and Engineering Data. **44** (1999) 1310 – 1314.

Baylaucq A., Boned C., Daugé P., and Lagourette B.: *Measurements of the Viscosity and Density of Three Hydrocarbons and the Three Associated Binary Mixtures Versus Pressure and Temperature*. International Journal of Thermophysics. **18** (1997a) 3 – 23.

Baylaucq A., Daugé P., and Boned C.: *Viscosity and Density of the Ternary Mixture Heptane + Methylcyclohexane + 1-Methylnaphthalene*. International Journal of Thermophysics. **18** (1997b) 1089 – 1107.

Benedict M., Webb G.B., and Rubin L.C.: *An Empirical Equation for Thermodynamic Properties of Light Hydrocarbons and Their Mixtures I. Methane, Ethane, Propane, and n-Butane*. Journal of Chemical Physics. **8** (1940) 334 – 345.

Berstad D.A.: *Viscosity and Density of n-Hexane, Cyclohexane and Benzene, and Their Mixtures with Methane*. Ph.D. Thesis, (IUK-Thesis 55), Insititutt for Uorganisk Kjemi, Universitetet i Trondheim, Norges Tekniske Høgskole, Trondheim, Norway. (1989).

Bich E., Millat J., and Vogel E.: *The Viscosity and Thermal Conductivity of Pure Monatomic Gases from Their Normal Boiling Point up to 5000 K in the Limit of Zero Density and at 0.101325 MPa*. Journal of Physical and Chemical Reference Data. **19** (1990) 1289 – 1305.

Bird R.B., Stewart W.E., and Lightfoot E.N.: *Transport Phenomena*. John Wiley & Sons, New York, USA. (1960).

Boston J.F. and Mathias P.M.: *Phase Equilibria in a Third-Generation Process Simulator*. 2nd International Conference on Phase Equilibria and Fluid Properties in the Chemical Process Industries. Berlin (West). 17 – 21 March (1980).

Brebach W.J. and Thodos G.: *Viscosity-Reduced State Correlation for Diatomic Gases*. Industrial and Engineering Chemistry. **50** (1958) 1095 – 1100.

Canet X.: *Viscosité Dynamique et Masse Volumique sous Hautes Pressions de Mélanges Binaires et Ternaires d'Hydrocarbures Lourds et Legers*. Thèse de Doctorant, Université de Pau, Pau, France. (2001).

Canet X., Daugé P., Baylaucq A., Boned C., Zéberg-Mikkelsen C.K., Quiñones-Cisneros S.E., and Stenby E.H.: *Density and Viscosity of 1-Methylnaphthalene + 2,2,4,4,6,8,8-Heptamethylnonane System from 293.15 K to 353.15 K at Pressures up to 100 MPa*. International Journal of Thermophysics. **22** (2001) 1669 – 1689.

Carmichael L.T., Berry V., and Sage B.H.: *Viscosity of a Mixture of Methane and n-Butane*. Journal of Chemical and Engineering Data. **12** (1967) 44 – 47.

Chapman S., Cowling T.G., and Burnett D.: *The Mathematical Theory of Non-Uniform Gases*. Third Edition, Cambridge University Press, UK. (1970).

Chou G.F. and Prausnitz J.M.: *A Phenomenological Correction to an Equation of State for the Critical Region*. AIChE Journal. **35** (1989) 1487 – 1496.

Christensen P.L. and Fredenslund Aa.: *A Corresponding States Model for the Thermal Conductivity of Gases and Liquids*. Chemical Engineering Science **35** (1980) 871 – 875.

Chung T.-H., Lee L.L., and Starling K.E.: *Applications of Kinetic Gas Theories and Multiparameter Correlation for Prediction of Dilute Gas Viscosity and Thermal Conductivity*. Industrial & Engineering Chemistry Fundamental. **23** (1984) 8 – 13.

Chung T.-H., Ajlan M., Lee L.L., and Starling K.E.: *Generalized Multiparameter Correlations for Nonpolar and Polar Fluid Transport Properties*. Industrial & Engineering Chemistry Research. **27** (1988) 671 – 679.

Cole W.A. and Wakeham W.A.: *The Viscosity of Nitrogen, Oxygen, and Their Binary Mixtures in the Limit of Zero Density*. **14** (1985) 209 – 226.

Cullick A.S. and Mathis M.L.: *Densities and Viscosities of Mixtures of Carbon Dioxide and n-Decane from 310 K to 403 K and 7 MPa to 30 MPa*. Journal of Chemical and Engineering Data. **29** (1984) 393 – 396.

Curtiss C.F. and Hirschfelder J.O.: *Transport Properties of Multicomponent Gas Mixtures*. The Journal of Chemical Physics. **17** (1949) 550 – 555.

Daubert T.E. and Danner R.P.: *Physical and Thermodynamic Properties of Pure Chemicals Data Compilation*. DIPPR. Hemisphere Publishing Corporation, New York, USA. (1989).

de Witt K.J. and Thodos G.: *Viscosities of Binary Mixtures in the Dense Gaseous State: The Methane + Carbon Dioxide System*. SPE Paper Number 1335 (1977).

Diller D.E.: *Measurements of the Viscosity of Compressed Gaseous and Liquid Methane + Ethane Mixtures*. Journal of Chemical and Engineering Data. **29** (1984) 215 – 221.

Diller D.E., van Poolen L.J., and dos Santos F.V.: *Measurements of Viscosities of Compressed Fluid and Liquid Carbon Dioxide + Ethane Mixtures*. Journal of Chemical and Engineering Data. **33** (1988) 460 – 464.

Diller D.E. and Ely J.F.: *Measurements of the Viscosities of Compressed Gaseous Carbon Dioxide, Ethane, and Their Mixtures, at Temperatures up to 500 K*. High Temperatures-High Pressures. **21** (1989) 613 – 620.

Ducoulombier D., Zhou H., Boned C., Peyrelasse J., Saint-Guirons H., and Xans P.: *Condensed Phases and Macromolecules. Pressures (1 – 1000 bars) and Temperatures (20 – 100°C) Dependence of the Viscosity of Liquid Hydrocarbons*. Journal of Physical Chemistry. **90** (1986) 1692 – 1700.

Dymond J.H., Young K.J., and Isdale J.D.: *Transport Properties of Nonelectrolyte Liquid Mixtures – II. Viscosity Coefficients for the n-Hexane + n-Hexadecane System at Temperatures from 25 to 100°C at Pressures up to the Freezing Pressure or 500 MPa*. International Journal of Thermophysics. **1** (1980) 345 – 373.

Dymond J.H., Awan M.A., Glen N.F., and Isdale J.D.: *Transport Properties of Nonelectrolyte Liquid Mixtures VIII. Viscosity Coefficients for Toluene and for Three Mixtures of Toluene + Hexane from 25 to 100 C at Pressures up to 500 MPa*. International Journal of Thermophysics. **12** (1991) 275 – 287.

Ely J.F. and Hanley H.J.M.: *Prediction of Transport Properties. 1. Viscosity of Fluids and Mixtures*. Industrial & Engineering Chemistry Fundamentals. **20** (1981) 323 – 332.

Estrada-Baltazar A., Alvarado J.F.J., Iglesias-Silva G.A., and Barrufet M.A.: *Experimental Liquid Viscosities of Decane and Octane + Decane from 298.15 K to 373.15 K and up to 25 MPa*. Journal of Chemical and Engineering Data. **43** (1998a) 441 – 446.

Estrada-Baltazar A., Iglesias-Silva G.A., and Barrufet M.A.: *Liquid Viscosities of Pentane and Pentane + Decane from 298.15 K to 373.15 K and up to 25 MPa*. Journal of Chemical and Engineering Data. **43** (1998b) 601 – 604.

Et-Tahir A.: *Determination des Variations de la Viscosité de Divers Hydrocarbures en Fonction de la Pression et de la Temperature. Etude Critique de Models Representatifs*. Thèse de Doctorant, Université de Pau, Pau, France. (1993).

Et-Tahir A., Boned C., Lagourette B., and Xans P.: *Determination of the Viscosity of Various Hydrocarbons and Mixtures of Hydrocarbons Versus Temperature and Pressure*. International Journal of Thermophysics. **16** (1995) 1309 – 1334.

Fenghour A, Wakeham W.A., and Vesovic V.: *The Viscosity of Carbon Dioxide*. Journal of Physical and Chemical Reference Data. **27** (1998) 31 – 44.

Friend D.G., Ely J.F., and Ingham H.: *Thermophysical Properties of Methane*. Journal of Physical and Chemical Reference Data. **18** (1989) 583 – 638.

Friend D.G., Ingham H., and Ely J.F.: *Thermophysical Properties of Ethane*. Journal of Physical and Chemical Reference Data. **20** (1991) 275 – 347.

Gehrig M. and Lents H.: *Values of $P(V_m, T)$ for n-Decane up to 300 MPa and 673 K*. Journal of Chemical Thermodynamics. **15** (1983) 1159 – 1167.

Giddings J.G., Kao J.T.F., and Kobayashi R.: *Development of a High-Pressure Capillary-Tube Viscometer and Its Application to Methane, Propane, and Their Mixtures in the Gaseous and Liquid Regions*. The Journal of Chemical Physics. **45** (1966) 578 – 586.

Gonzales H. and Lee A.L.: *Viscosity of 2,2-Dimethylpropane*. Journal of Chemical and Engineering Data. **13** (1968) 66 – 69.

Guo -T.-M.: *Private Communication*. (1998).

Guo X.-Q., Wang L.-S., Rong S.-X. and Guo T.-M.: *Viscosity Model Based on Equations of State for Hydrocarbon Liquids and Gases*. **139** (1997) 405 – 421.

Hanley H.J.M., McCarty R.D., and Haynes W.M.: *Equations for the Viscosity and Thermal Conductivity Coefficients of Methane*. *Cryogenics*. **15** (1975) 413 – 417.

Händel G., Kleinrahm R., and Wagner W.: *Measurements of the (Pressure, Density, Temperature) Relation of Methane in the Homogeneous Gas and Liquid Regions in the Temperature Range from 100 K to 260 K and at Pressures up to 8 MPa*. *Journal of Chemical Thermodynamics*. **24** (1992) 685 – 695.

Hendl S. and Vogel E.: *The Viscosity of Gaseous Ethane and Its Initial Density Dependency*. *Fluid Phase Equilibria*. **76** (1992) 259 – 272.

Herning F. and Zipperer L.: *Beitrag zur Berechnung der Zähigkeit Technischer Gasgemische aus den Zähigkeitswerten der Einzelbestandteile*. *Das Gas- und Wasserfach*. **79** (1936) 49 – 54 and 69 – 73.

Hirschfelder J.O., Curtiss C.F., Bird R.B.: *Molecular Theory of Gases and Liquids*. Fourth Edition. John Wiley & Sons, New York, USA. (1964).

Holland P.M.; Eaton B.E., and Hanley H.J.M.: *A Correlation of the Viscosity and Thermal Conductivity Data of Gaseous and Liquid Ethylene*. *Journal of Physical and Chemical Reference Data*. **12** (1983) 917 – 932.

Iglesias-Silva G.A., Estrada-Baltazar A., Hall K.R., and Barrufet M.A. *Experimental Liquid Viscosity of Pentane + Octane + Decane Mixtures from 298.15 K to 373.15 K up to 25 MPa*. *Journal of Chemical and Engineering Data*. **44** (1999) 1304 – 1309.

Isdale J.D., Dymond J.H., and Brawn T.A.: *Viscosity and Density of n-Hexane - Cyclohexane Mixtures between 25 and 100°C up to 500 MPa*. *High Temperature - High Pressure*. **11** (1979) 571 – 580.

Iwasaki H. and Takahashi M.: *Viscosity of Carbon Dioxide and Ethane*. *Journal of Chemical Physics*. **74** (1981) 1930 – 1943.

Jensen B.H.: *Densities, Viscosities and Phase Equilibria in Enhance Oil Recovery*. Ph.D. Thesis. Technical University of Denmark, Lyngby, Denmark. (1987).

Jossi J.A., Stiel L.I., and Thodos G.: *The Viscosity of Pure Substances in the Dense Gaseous and Liquid Phases*. *AIChE Journal*. **8** (1962) 59 – 63.

Kleinrahm R., Duschek W., and Wagner W.: *(Pressure, Density, Temperature) Measurements in the Critical Region of Methane*. Journal of Chemical Thermodynamics. **18** (1986) 1103 – 1114.

Knapp H., Döring R., Oellrich L., Plöcker U., and Prausnitz J.M. *Vapor-Liquid Equilibria for Mixtures of Low Boiling Substances*. Volumen VI, DECHEMA, Frankfurt Germany (1982).

Knapstad B., Skjølsvik P.A., and Øye H.A.: *Viscosity of the n-Decane – Methane System in the Liquid Phase*. Berichte der Bunsengesellschaft für Physikalische Chemie. **94** (1990) 1156 – 1165.

Knudsen K.: *Phase Equilibria and Transport of Multiphase Systems*. Ph.D. Thesis. Technical University of Denmark, Lyngby, Denmark. (1992).

Krahn U.G. and Luft G.: *Viscosity of Mixtures of Liquid Hydrocarbons with Ethene in the Temperature Range 298 - 453 K and Pressures up to 200 MPa*. Journal of Chemical and Engineering Data. **39** (1994) 673 – 678.

Küchenmeister C. and Vogel E.: *The Viscosity of Gaseous n-Butane and Its Initial Density Dependence*. International Journal of Thermophysics. **19** (1998) 1085 – 1097.

Küchenmeister C. and Vogel E.: *The Viscosity of Gaseous Isobutane and Its Initial Density Dependence*. International Journal of Thermophysics. **21** (2000) 329 – 341.

Laesecke A., Krauss R., Stephan K., and Wagner W. *Transport Properties of Fluid Oxygen*. Journal of Physical and Chemical Reference Data. **19** 1990 1089 - 1122

Lee A.L. and Ellington R.T.: *Viscosity of n-Decane in the Liquid Phase*. Journal of Chemical and Engineering Data. **10** (1965b) 346 – 348.

Lee A.L., Gonzalez M.H., and Eakin B.E.: *The Viscosity of Natural Gases*. Journal of Petroleum Engineering. August (1966) 997 - 1000

Lee. B.I. and Kesler M.G.: *A Generalized Thermodynamic Correlation Based on Three-Parameter Corresponding States*. AIChE Journal. **21** (1975) 510 – 527.

Leland T.W., Rowlinson J.S., and Sather G.A.: *Statistical Thermodynamics of Mixtures of Molecules of Different Sizes*. Transactions Faraday Society. **64** (1968) 1447 – 1460.

Little J.E. and Kennedy H.T.: *A Correlation of the Viscosity of Hydrocarbon Systems with Pressure, Temperature and Composition*. Society of Petroleum Engineers Journal. (June, 1968) 157 – 162.

Lohrenz J., Bray B.G., and Clark C.R.: *Calculating Viscosities of Reservoir Fluids from Their Compositions*. Journal of Petroleum Technology. **16** (1964) 1171 – 1176.

Marker M.F.: *Viscosity Prediction*. Pre-M.Sc.Project. (IVCSEP), Department of Chemical Engineering, Technical University of Denmark. (2000).

Mathias P.M.: *A Versatile Phase Equilibrium Equation of State*. Industrial Engineering Chemistry Process Design and Development. **22** (1983) 385 – 391.

McCarty R.D.: *A Modified Benedict-Webb-Rubin Equation of State for Methane Using Recent Experimental Data*. Cryogenics. **14** (1974) 276 – 280.

Mehrotra A.K., Monnery W.D., and Svrcek W.Y.: *A Review of Practical Calculation Methods for the Viscosity of Liquid Hydrocarbons and Their Mixtures*. Fluid Phase Equilibria. **117** (1996) 344 – 355.

Moha-Ouchane M.; Boned C., Allal A.; and Benseddik M.: *Viscosity and Excess Volume at High Pressure in Associated Binaries*. International Journal of Thermophysics. **19** (1998) 161 – 189.

Monnery W.D., Svrcek W.Y., and Mehrotra A.K.: *Viscosity: A Critical Review of Practical Predictive and Correlative Methods*. The Canadian Journal of Chemical Engineering. **73** (1995) 3 – 40.

Monteil J.M., Lazzar F., Salvinien J., and Viallet P.: *Viscomètre a Measures Relative Pour Étude de H₂S Gazeux au Voisinage du Point Critique*. Journal de Chimie Physique. **66** (1969) 1673 – 1675.

Nabizadeh H. and Mayinger F.: *Viscosity of Binary Mixtures of Hydrogen and Natural Gas (Hythane) in the Gaseous Phase*. High Temperatures – High Pressures. **31** (1999) 601 – 612.

Neufeld P.D., Janzen A.R., and Aziz R.A.: *Empirical Equations to Calculate 16 of the Transport Collision Integrals $\Omega^{(l,s)*}$ for the Lennard-Jones (12-6) Potential*. The Journal of Chemical Physics. **57** (1972) 1100 – 1102.

Patel N.C. and Teja A.S.: *A New Cubic Equation of State for Fluids and Fluid Mixtures*. Chemical Engineering Science. **37** (1982) 463 – 473.

Pedersen K.S., Fredenslund Aa., Christensen P.L., and Thomassen P.: *Viscosity of Crude Oils*. Chemical Engineering Science. **39** (1984a) 1011 – 1016.

Pedersen K.S., Thomassen P., and Fredenslund Aa.: *Thermodynamic of Petroleum Mixtures Containing Heavy Hydrocarbons. I Phase Envelope Calculations by Use of the Soave-Redlich-Kwong Equation of State*. Industrial & Engineering Chemistry Process Design and Development. **23** (1984b) 163 – 170.

Pedersen K.S. and Fredenslund Aa.: *An Improved Corresponding States Model for the Prediction of Oil and Gas Viscosities and Thermal Conductivities*. Chemical Engineering Science. **42** (1987) 182 – 186.

Pedersen K.S., Fredenslund Aa., and Thomassen P.: *Properties of Oils and Natural Gases*. Gulf Publishing Company, Houston, Texas, USA. (1989).

Peneloux A., Rauzy E., Freze R.: *A Consistent Correction for Redlich-Kwong-Soave Volumes*. Fluid Phase Equilibria. **8** (1982) 7 – 23.

Peng D.-Y. and Robinson D.B.: *A New Two-Constant Equation of State*. Industrial & Engineering Chemistry Fundamentals. **15** (1976) 59 – 64.

Phillips P.: *The Viscosity of Carbon Dioxide*. Proceedings of the Royal Society of London. **87A** (1912) 48 – 61.

Quiñones-Cisneros S.E.: *Phase and Critical Behavior in Type III Phase Diagrams*. Fluid Phase Equilibria. **134** (1997) 103 – 112.

Quiñones-Cisneros S.E., Zéberg-Mikkelsen C.K., and Stenby E.H.: *The Friction Theory (f-theory) for Viscosity Modeling*. Fluid Phase Equilibria. **169** (2000) 249 – 276.

Quiñones-Cisneros S.E., Zéberg-Mikkelsen C.K., and Stenby E.H.: *One Parameter Friction Theory Models for Viscosity*. Fluid Phase Equilibria. **178** (2001a) 1 – 16.

Quiñones-Cisneros S.E., Zéberg-Mikkelsen C.K., and Stenby E.H.: *The Friction Theory for Viscosity Modeling: Extension to Crude Oil Systems*. Chemical Engineering Science, **56** (2001b) 7007 – 7015.

Rackett H.G.: *Equation of State for Saturated Liquids*. Journal of Chemical and Engineering Data. **15** (1970) 514 – 517.

Redlich O. and Kwong J.N.S.: *On the Thermodynamic of Solutions. V An Equation of State. Fugacities of Gaseous Solutions*. Chemical Review. **44** (1949) 233 – 244.

Reid R.C., Prausnitz J.H., and Poling B.E.: *The Properties of Gases & Liquids*. Fourth Edition, McGraw-Hill, New York, USA, (1987).

Roetling J.A., Gebhardt J.J., and Rouse F.G.: *Effect of Pressure on Viscosity of Naphthalene, Phenanthrene, and Impregnation Pitches*. Carbon. **25** (1987) 233 – 242.

Rowlinson J.S. and Swinton F.L.: *Liquids and Liquid Mixtures*. Third Edition. Butterworths, London, UK. (1982).

Soave G.: *Equilibrium Constants from a Modified Redlich-Kwong Equation of State*. Chemical Engineering Science. **27** (1972) 1197 – 1203.

Soave G.S.: *A Noncubic Equation of State fro the Treatment of Hydrocarbon Fluids at Reservoir Conditions*. Industrial & Engineering Chemistry Research. **34** (1995) 3981 – 3994.

Soave G.S.: *A Noncubic Equation of State fro the Treatment of Hydrocarbon Fluids at Reservoir Conditions*. Industrial & Engineering Chemistry Research. **35** (1996) 1794.

Stephan K. and Lucas K.: *Viscosity of Dense Fluids*. Plenum Press, New York, USA. (1979).

Stephan K, Knauss R., and Laesecke A.: *Viscosity and Thermal Conductivity of Nitrogen for a Wide Range of Fluid States*. Journal of Physical and Chemical Reference Data. **16** (1987) 993 – 1023.

Stiel L.I. and Thodos G.: *The Viscosity of Nonpolar Gases at Normal Pressure*. AIChE Journal. **7** (1961) 611 – 615.

Strumpf H.J., Collings A.F., and Pings C.J.: *Viscosity of Xenon and Ethane in the Critical Region*. The Journal of Chemical Physics. **60** (1974) 3109 – 3123.

Stryjek R. and Vera J.H.: *PRSV: An Improved Peng-Robinson Equation of State for Pure Compounds and Mixtures*. The Canadian Journal of Chemical Engineering. **64** (1986) 323 – 333.

Tanaka Y., Hosokawa H., Kubota H., and Makita T.: *Viscosity and Density of Binary Mixtures of Cyclohexane with n-Octane, n-Dodecane and, n-Hexadecane under High Pressures*. International Journal of Thermophysics. **12** (1991) 245 – 264.

Teja A.S. and Rice P.: *Generalized Corresponding States Method for the Viscosities of Liquid Mixtures*. Industrial & Engineering Chemistry Fundamentals. **20** (1981) 77 – 81.

Tohidi B., Burgass R.W., Danesh A, and Todd A.C.: *Viscosity and Density of Methane + Methylcyclohexane from (323 to 423) K and Pressures to 140 MPa*. Journal of Chemical and Engineering Data. **46** (2001) 385 – 390.

Trengove R.D. and Wakeham W.A.: *The Viscosity of Carbon Dioxide, Methane, and Sulfur Hexafluoride in the Limit of Zero Density*. Journal of Physical and Chemical Reference Data. **16** (1987) 175 – 187.

Ungerer P., Faissat B., Leibovici C., Zhou H., Behar E., Moracchini G., and Courcy J.P.: *High Pressure-High Temperature Reservoir Fluids: Investigation of Synthetic Condensate Gases Containing a Solid Hydrocarbon*. Fluid Phase Equilibria. **111** (1995) 287 – 311.

Uyehara O.A. and Watson K.M.: *A Universal Viscosity Correlation*. National Petroleum News. (October 4, 1944) R-714 – R-722.

van der Gulik P.S., Mostert R., and van den Berg H.R.: *The Viscosity of Methane at 25°C up to 10 kbar*. Physica. **151A** (1988) 153 – 166.

van der Gulik P.S., Mostert R., and van den Berg H.R.: *The Viscosity of Methane at 273 K up to 1 GPa*. Fluid Phase Equilibria. **79** (1992) 301 – 311.

Vargaftik N.B. *Tables on the Thermophysical Properties of Liquids and Gases*. Hemisphere Publishing Corporation: Washington – London. (1975).

Vesovic V. and Wakeham W.A.: *The Prediction of the Viscosity of Dense Gas Mixtures*. International Journal of Thermophysics. **10** (1989) 125 – 132.

Vesovic V. and Wakeham W.A.: *The Prediction of the Viscosity of Fluid Mixtures Over Wide Ranges of Temperature and Pressure*. Chemical Engineering Science. **44** (1989) 2181 – 2189.

Vesovic V. Assael M.J., and Gallis Z.A.: *Prediction of the Viscosity of Supercritical Fluid Mixtures*. International Journal of Thermophysics. **19** (1998) 1297 – 1313.

Vogel E.: *The Viscosity of Gaseous Propane and Its Initial Density Dependence*. International Journal of Thermophysics. **16** (1995) 1335 – 1351.

Vogel E.; Bich E.; and Nimz R.: *The Initial Density Dependence of the Viscosity of Organic Vapours: Benzene and Methanol*. Physica. **139A** (1986) 188 – 207.

Vogel E. and Hendl S.: *Vapor Phase Viscosity of Toluene and p-Xylene*. Fluid Phase Equilibria. **79** (1992) 313 – 326.

Vogel E. and Holdt B.: *Temperature and Initial-Density Dependence of the Vapour Phase Viscosity of n-Alkanes (n = 5 – 7)*. High Temperatures – High Pressures. **23** (1991) 473 – 483.

Vogel E., Holdt B., and Strehlow T.: *The Initial Density Dependence of the Viscosity of Organic Vapours: Cyclohexane and Neopentane*. Physica. **148A** (1988) 46 – 60.

Vogel E., Küchenmeister C., Bich E., and Laesecke A.: *Reference Correlation of the Viscosity of Propane*. Journal of Physical and Chemical Reference Data. **27** (1998) 947 – 970.

Vogel E. and Strehlow T.: *Temperature Dependence and Initial Density Dependence of the Viscosity of n-Hexane Vapour*. Zeitschrift für Physikalische Chemie. **269** (1988) 897 – 907.

Wagner W. and Kruse A.: *Properties of Water and Steam*. IAPWS-97. Springer, Berlin (1998).

Wakeham W.A., Nagashima A., and Sengers J.V.: *Measurements of the Transport Properties of Fluids Experimental Thermodynamic Vol. III*, IUPAC, Blackwell Scientific Publications, Oxford, England. (1991).

Wilhelm J. and Vogel E.: *Viscosity Measurements on Gaseous Argon, Krypton, and Propane*. International Journal of Thermophysics. **21** (2000) 301 – 318.

Wilke C.R.: *A Viscosity Equation for Gas Mixtures*. The Journal of Chemical Physics. **18** (1950) 517 – 519.

Yokoyama C., Takahashi M., and Takahashi S.: *Viscosity of Nitrous Oxide in the Critical Region*. International Journal of Thermophysics. **15** (1994) 603 – 626.

Younglove B.A. and Hanley H.J.M. *The Viscosity and Thermal Conductivity Coefficients of Gaseous and Liquid Argon*. Journal of Physical and Chemical Reference Data. **15** (1986) 1323 – 1337.

Younglove B.A. and Ely J.F.: *Thermophysical Properties of Fluid. II. Methane, Ethane, Propane, Isobutane, and Normal Butane*. Journal of Physical and Chemical Reference Data. **16** (1987) 577 – 798.

Zéberg-Mikkelsen C.K., Canet X., Baylaucq A., Quiñones-Cisneros S.E., Boned C., and Stenby E.H.: *High Pressure Viscosity and Density Behaviour of Ternary Mixtures: 1-Methylnaphthalene + n-Tridecane + 2,2,4,4,6,8,8-Heptamethylnonane*. International Journal of Thermophysics. **22** (2001) 1691 – 1726.

Zhang J., and Liu H.: *Determination of Viscosity under Pressure for Organic Substances and Its Correlation with Density under High Pressure*. Journal of Chemical Industry and Engineering (China). **3** (1991) 269 – 277.

Zozulya V.N. and Blagoi Y.P.: *Viscosity of Nitrogen Near the Liquid-Vapor Critical Point*. Soviet Physics JETP. **39** (1974) 99 – 105.

PART II

VISCOSITY MEASUREMENTS AND MODELLING

II.1 Introduction

In spite, the importance of studying the viscosity of fluids versus temperature, pressure and composition or deriving accurate viscosity models, the literature mainly contains viscosity measurements versus temperature and composition at atmospheric pressure, whereas studies of variations versus pressure are less frequent, particularly for mixtures and those likely to be used to model a real petroleum fluid: in other words, a complex fluid. It is important to stress that viscosity data are available for some binary systems for which the variation of the viscosity as a function of composition, pressure and temperature is well described, but only very few systematic studies concerning multicomponent mixtures have been performed. To the knowledge of the author only systematic viscosity studies of multicomponent mixtures have been performed by Baylaucq et al. (1997b) for 21 ternary mixtures composed of n-heptane + methylcyclohexane + 1-methylnaphthalene up to 1000 bar: 378 experimental data, by Iglesias-Silva et al. (1999) for 15 ternary mixtures composed of n-pentane + n-octane + n-decane up to 250 bar: 358 experimental data, and by Boned et al. (1998) for 36 ternary mixtures composed of water + 2-propanol + 4-hydroxy-4-methyl-2-pentanone up to 1000 bar: 648 experimental data. Due to this, existing compositional dependent viscosity models have been derived based on viscosity measurements of pure compounds and binary mixtures. In order to study the possible extension of these models to real petroleum fluids and their application within the oil industry experimental viscosity measurements versus temperature, pressure, and composition are required for synthetic mixtures representative of petroleum fluids.

However, since petroleum fluids are multicomponent mixtures, it is impossible to determine the exact composition (mole% or weight%) of all components. To simplify the problem, the petroleum fluid is fractionated by distillation into different fractions (cuts). Generally, these cuts are related to their true boiling point, but it is also possible to use the carbon number (Pedersen et al. 1989). Although, these cuts still contain a large number of compounds, their composition is simpler than the composition of the crude oil. It is then possible to represent each distillation fraction by a more or less complex mixture of model molecules, which may be representative of the considered cut. In this way, a synthetic representation of the considered crude oil can be obtained.

Based on this, there are many ways to model a real petroleum fluid. For some years ago Groupe Haute Pression at Université de Pau, France and TotalFinaElf, France decided to perform an extensive experimental study of the viscosity along with the density for the ternary system composed of 1-methylnaphthalene, n-tridecane, and 2,2,4,4,6,8,8-heptamethylnonane versus temperature, pressure, and composition, as a part of a simple representation of some distillation cuts at 510 K. At atmospheric pressure, the boiling temperature is 514.7 K for 1-methylnaphthalene, 507.1 K for n-tridecane, and 513.1 K for 2,2,4,4,6,8,8-heptamethylnonane. The chemical structure of the three compounds is shown in Figure II.1.

The viscosity and density of the three pure compounds and their binary systems have already been measured up to 1000 bar and in the temperature range 293.15 – 353.15 K by Daugé et al. (1999), Daugé et al. (2001), and Canet et al. (2001). The experimental uncertainty of these viscosity measurements is 2.0%, whereas the uncertainty of the density measurements is less than 1 kg/m³. For the three pure compounds, the behavior of the viscosity and the density at 293.15 K and 353.15 K are shown in Figures II.2 and II.3 versus pressure. As the pressure increases, a significantly sharper increase in the viscosity is found for 2,2,4,4,6,8,8-heptamethylnonane than for

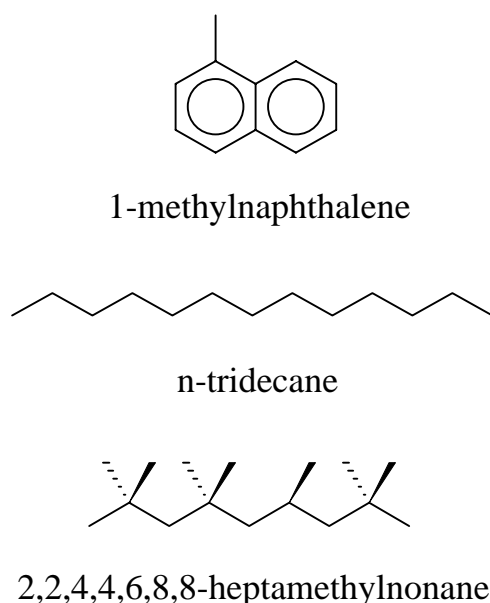


Figure II.1 Chemical structure of the compounds of the ternary system.

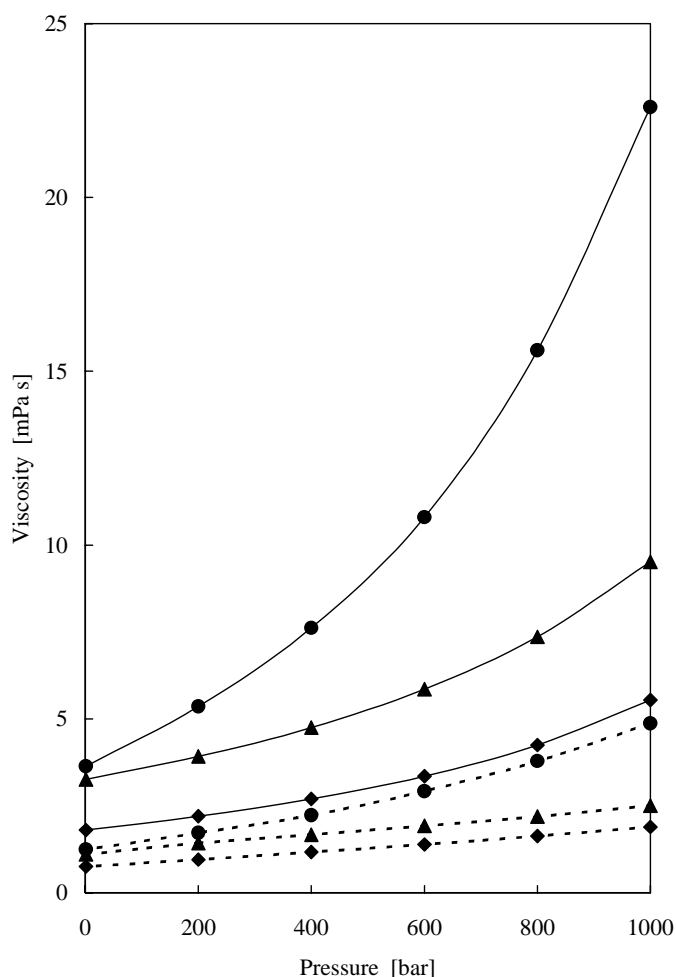


Figure II.2 Viscosity versus pressure for 1-methylnaphthalene (▲) (Daugé et al. 1999), n-tridecane (◆) (Daugé et al. 1999), and 2,2,4,4,6,8,8-heptamethylnonane (●) (Canet et al. 2001) at 293.15 K (—) and 353.15 K (---).

1-methylnaphthalene and n-tridecane, see Figure II.2. This may be related to the molecular structure of the compounds. Because when a fluid is brought under pressure (compressed), the flexibility and mobility of the molecules are reduced, since the distance between the molecules becomes shorter, resulting in an increase in the viscosity. For the three compounds illustrated in Figure II.1 n-tridecane is the most flexible molecule which can easily rearrange and twist, whereas as 1-methylnaphthalene is a stiff and inflexible molecule due to the aromatic rings. The molecular structure of 2,2,4,4,6,8,8-heptamethylnonane is very complex due to the great number of attached

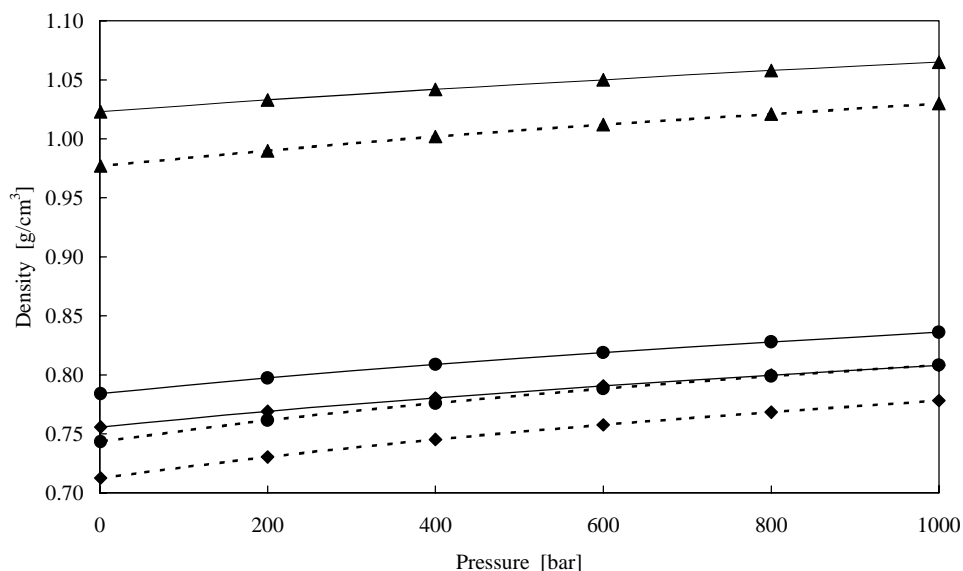


Figure II.3 Density versus pressure for 1-methylnaphthalene (▲) (Daugé et al. 1999), n-tridecane (◆) (Daugé et al. 1999), and 2,2,4,4,6,8,8-heptamethylnonane (●) (Canet et al. 2001) at 293.15 K (—) and 353.15 K (---).

methyl groups to the nonane chain, making the molecule very inflexible and stiff. However, the drastically increase in the viscosity of 2,2,4,4,6,8,8-heptamethylnonane with pressure may not only be related to the lower flexibility of the molecules, but also because of an interlinking effect between adjacent molecules due to the highly branched 2,2,4,4,6,8,8-heptamethylnonane molecule, resulting in an important reduction in the fluid mobility (higher viscosity) when brought under pressure.

In addition, Kioupis and Maginn (2000) studied the viscosity and the self-diffusion of n-octadecane, 7-butyltetradecane, and 4,5,6,7-tetraethyldecane up to 10000 bar by molecular dynamics (MD) simulations. MD simulations can be used to study the behavior of fluids at an atomized level, which is impossible to do from experimental studies. Kioupis and Maginn (2000) found that the highly branched molecule 4,5,6,7-tetraethyldecane exhibits a much larger increase in the viscosity with pressure than the linear alkane n-octadecane and explained it by a reduction in the liquid void volume coupled with the stiffness of the highly branched molecules. As the pressure is increases the voids in the fluid decrease. This results in a lower motion of the molecules, because the motion is related either to molecules jumping or forcing adjacent

molecules into these voids. Since, the number of voids decreases with increasing pressure, molecules with a low flexibility will have difficulties of making these jumps or forcing other molecules into these voids, resulting in the trapping of the molecules. Flexible molecules can easily rearrange to conformations able to move into these voids. The voids in the fluid can be related to the concepts of the free volume defined as the fluid volume per molecule minus the van der Waals volume. By modeling the viscosity of their studied fluids using the concepts of the free volume Kioupis and Maginn (2000) found that the right viscosity behavior versus pressure is captured. These observations made by Kioupis and Maginn (2000) may also be used to explain the viscosity behavior of 2,2,4,4,6,8,8-heptamethylnonane compared to n-tridecane or 1-methylnaphthalene.

Although, the strong pressure dependency on the viscosity of 2,2,4,4,6,8,8-heptamethylnonane, the shape of the density versus pressure curves is approximately the same for all three pure compounds, see Figure II.3. The shape of the density versus pressure curves is compatible with the logarithmic relation proposed by Tait (1888) to model the influence of the pressure on $1/\rho$.

For the binary system 1-methylnaphthalene + 2,2,4,4,6,8,8-heptamethylnonane, in spite that these compounds are non-polar, a non-monotonic behavior of the viscosity curves versus composition is obtained (Canet et al. 2001), see Figure II.4, with a minimum located in the vicinity of a mole fraction of 0.625 1-methylnaphthalene. This may be the effect of repulsive interactions or the effect related to the molecular structures. For the studied temperature and pressure conditions, this non-monotonic behavior is most pronounced at 1 bar and 293.15 K. When the temperature or the pressure is increased, the non-monotonic behavior disappears, see Figures II.4 and II.5. A similar behavior of the viscosity versus composition has been observed by Zhang and Liu (1991) for the binary system benzene + cyclohexane at 298.15 K and different pressures.

In order to complete this extensive study of the ternary system 1-methylnaphthalene, n-tridecane, and 2,2,4,4,6,8,8-heptamethylnonane, and to provide a complete coverage of the representative ternary diagram the viscosity and density of 21 ternary mixtures have been measured under the same temperature and pressure conditions as for the pure compounds and the binary systems.

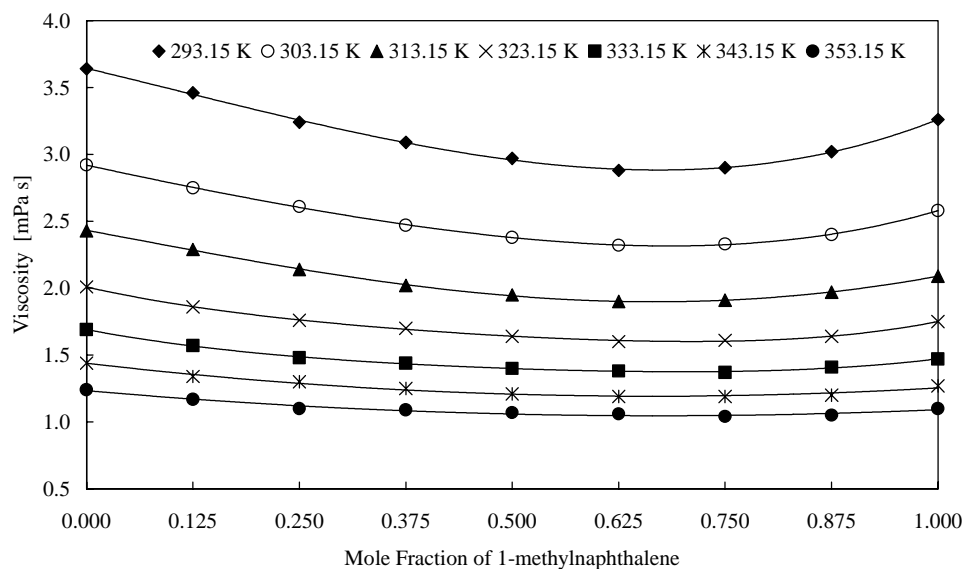


Figure II.4 Viscosity isotherms versus composition at 1 bar for the binary system 1-methylnaphthalene + 2,2,4,4,6,8,8-heptamethylnonane (Canet et al. 2001).

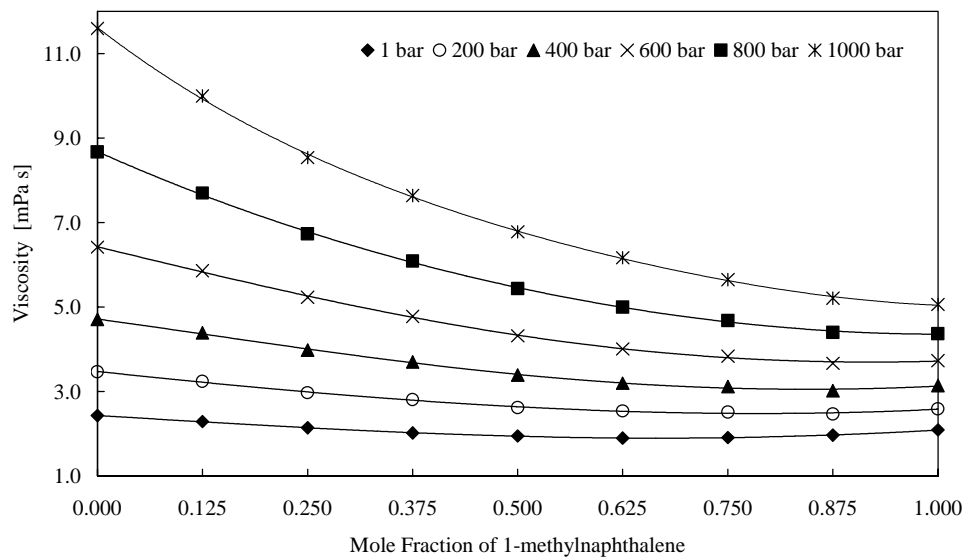


Figure II.5 Viscosity isobars versus composition at 313.15 K for the binary system 1-methylnaphthalene + 2,2,4,4,6,8,8-heptamethylnonane (Canet et al. 2001).

II.2 Experimental Techniques and Procedures

The experimental equipments used to measure the viscosity and density of the ternary mixtures are described below along with the operating procedures. The viscosity at high pressure has been determined with the aid of a falling body viscometer, whereas a classical capillary viscometer (Ubbelohde viscometer) has been used at atmospheric pressure. These viscometers belong to the well-characterized viscometers for which full-developed working equations exist.

II.2.1 Falling Body Viscometer

The principle of the falling body viscometer is that a solid body (sinker) with a geometric shape enabling it to revolve falls vertically under gravitational influence through a fluid. The fluid is forced to flow through the annulus between the sinker and the measuring tube. During the free fall, the sinker will accelerate until the viscous force is equal to the gravitational force, where the maximal velocity of the sinker is reached. In this way, the viscosity of the fluid can be related to the velocity of the sinker. The velocity of the sinker can be obtained by measuring the time Δt it takes the sinker to fall the distance between two fixed reference points, see Kawata et al. (1991b). Based on this, the following working equation is obtained

$$\eta = K(\rho_s - \rho)\Delta t \quad (\text{II.2.1})$$

where ρ_s and ρ are the density of the sinker and the fluid, respectively. K is a quantity characteristic of the viscometer and of the falling body (Kawata et al. 1991b). Falling body viscometers are commonly used to measure the viscosity at high pressure, and they can be applied to very viscous fluids. The reason is that they are easy to operate.

The falling body viscometer used for the high-pressure viscosity measurements is described in details by Ducoulombier et al. (1985) and illustrated in Figure II.6. The viscometer consists of a measuring tube placed in an oil bath inside a high-pressure vessel. The oil is used as the compression medium and to control the temperature of the viscometer. In order to transmit pressure to the sample, the measuring tube is sealed with a teflon bellow at one end. The measuring tube is made of stainless steel, having a length of 23 cm, and an inner diameter of $6.7 \text{ mm} \pm 0.01 \text{ mm}$. Attached to the measuring

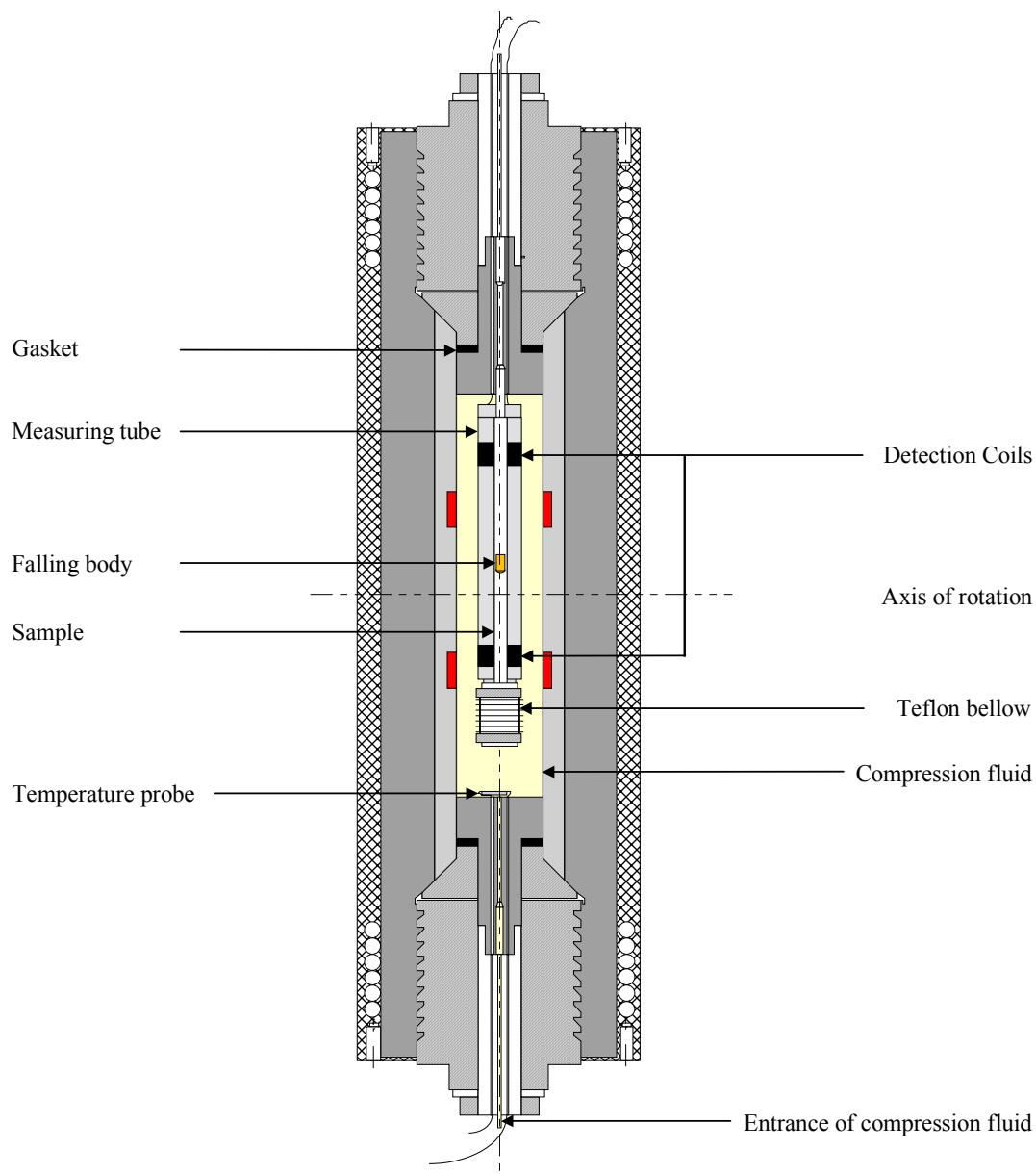


Figure II.6 High-pressure falling body viscometer.

tube is two pairs of electrical coils used to detect the passage of the sinker in order to measure the time it takes the sinker to fall the distance between the two coils. The distance between the two coils is $16.6 \text{ cm} \pm 0.1 \text{ cm}$. The falling time of the sinker is measured, when the viscometer is placed in the position shown in Figure II.6. Since, the viscometer is fully rotatable, a continuous series of measurements can be carried out

over wide ranges of temperature and pressure without disturbing the sample. After each measure the viscometer is turned in order to bring the sinker back to its starting position. The viscometer is rotated by an engine, which also ensures that the viscometer is vertically placed.

The sinker is a solid stainless steel cylinder with hemispherical ends. It has a diameter of $6.45 \text{ mm} \pm 0.01 \text{ mm}$ and a length of 18 mm, whereas its density, ρ_s , is 8.7 g/cm^3 . The sinker is designed, so that laminar conditions are obtained in the annulus during the fall of the sinker. Further, the ratio of the sinker to tube radii is 0.963, which is greater than the value of 0.93 suggested by Kiran et al. (1990) to minimize eccentricity effects (deviation from axial fall).

The detection of the sinker is based on an electromagnetic effect induced by the sinker when passing the two pairs of coils located on the measuring tube. Each pair of coils consists of a primary coil with a resistance of 60Ω and a secondary coil with a resistance of 150Ω . The two secondary coils are connected in series, whereas the primary coils are connected in parallel to a variable frequency generator, which provides an input signal of 1000 Hz, 5 V. The secondary coils have an opposite phase in order to have a residual signal equal to zero. In the absence of the sinker, the corresponding induced signal is related to the metallic tube and the studied fluid. When the metallic sinker passes a detection coil, the signal induced on the secondary coil reaches a maximum. The variation in the signal is illustrated in Figure II.7 as the sinker passes through the measuring tube. Δt represents the time it takes the sinker to fall from the upper coil to the lower coil, and $\tilde{V}_s(t)$ represents the variation of the tension used in the detection as a function of the time.

In the electronic system used to detect the maximum of the sinker, the sinusoidal signal is respectively amplified, filtered, and converted into a continuous signal. This system contains a circuit, which detects any small changes in the variation of the tension. When the entering signal gives an increase, this circuit delivers a top and when the maximum is reached, the trigger then either starts or stops the electronic timer (Chronometer).

The regulation of the temperature in the viscometer is schematically illustrated in Figure II.8. The heating of the viscometer is performed with several heating coils

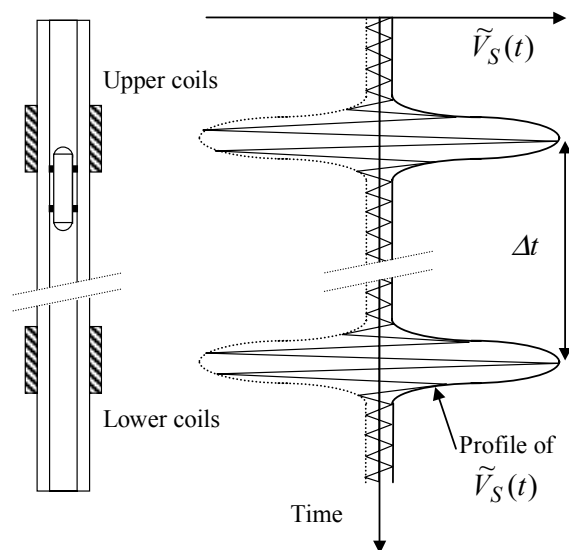


Figure II.7 Variation of the tension for detecting the falling body as a function of its fall.

placed at the same level as the rotating axis. A platinum probe ($100\ \Omega$) is placed on the bottom of the high-pressure vessel in the vicinity of the teflon bellow. The platinum probe is connected to a calibrated thermostat, which regulates the temperature within $\pm 0.1\ \text{K}$ by a control proportional to the current applied to the heating coils. In addition, a cooling circuit is also connected to the viscometer.

The filling of the measuring cell with the sample is performed by gravity. The measuring cell is first evacuated through a valve, which has been connected to the cell for the filling. After vacuum has been applied, the valve is closed and a funnel is

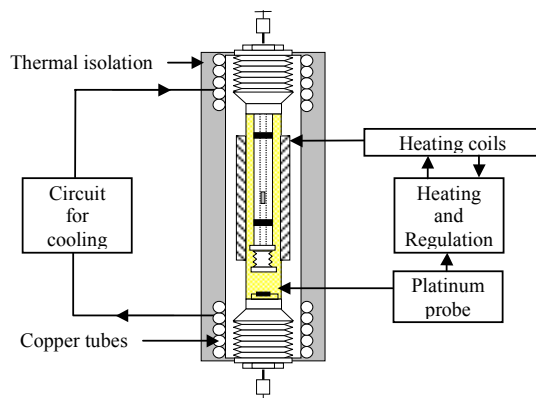


Figure II.8 Regulation of the temperature.

connected to the valve. The funnel is filled with the sample and the valve is opened. After the sample has been added free of any air, the cell is sealed off and placed in the high-pressure vessel. The vessel is pressurized by pumping oil into it using a pneumatic pump. The pressure within the vessel is measured at the entrance for the compression oil. The uncertainty in the measured pressure is ± 1 bar, except at atmospheric pressure. The viscometer is then heated and the conditions are adjusted to the desired experimental temperature and pressure.

The viscometer is calibrated in order to determine the quantity K used in Eq.(II.2.1). In order to perform the calibration of the viscometer, a reference fluid is needed for which reliable viscosity and density data are available within the studied temperature and pressure ranges. For this purpose, toluene has been chosen, since abundant viscosity and density data are given in the literature (Kashiwagi and Makita 1982, Assael et al. 1991, Dymond et al. 1991, Krall et al. 1992, Oliveira and Wakeham 1992, Vieira dos Santos and Nieto de Castro 1997, and Harris 2000). The quantity $K(P,T)$ has been determined for each temperature T and pressure P for which the viscosity of the studied mixtures has been measured.

The viscosity determined for a given temperature and pressure is based on an average of seven measurements of the falling time. For the described falling body viscometer the estimated experimental uncertainty on the viscosity is of the order of 2%. As it has previously been discussed by Kanti et al. (1991), Et-Tahir et al. (1995), Baylaucq et al. (1997a), Baylaucq et al. (1997b), Moha-Ouchane et al. (1998), and Daugé et al. (2001), this error is comparable with the error obtained by other authors for similar experimental system. Comparative curves have been reported for n-heptane and methylcyclohexane by Baylaucq et al. (1997a), for water and 2-propanol by Moha-Ouchane et al. (1998), and for 2,2,4,4,6,8,8-heptamethylnonane by Daugé et al. (2001).

II.2.2 Ubbelohde Viscometer

The Ubbelohde viscometer, shown in Figure II.9, belongs to the classical capillary glass viscometers, which are widely used to measure the kinematic viscosity $\nu = \eta/\rho$ of liquids at atmospheric pressure due to their high precision. For any capillary viscometer, the working equation is related to the Hagen-Poiseuille equation

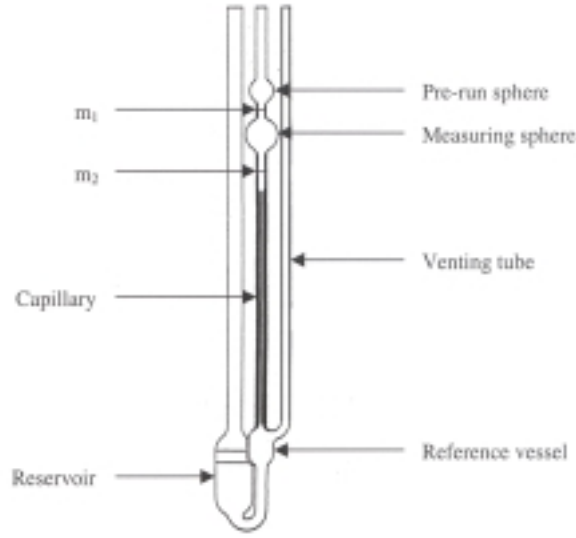


Figure II.9 Ubbelohde viscometer.

$$\eta = \frac{\pi r^4 \Delta P}{8 Q L} \quad (\text{II.2.2})$$

where r is the radius of the tube, L the length of the tube, Q the volumetric flow rate, and ΔP the pressure drop through the tube. In Eq.(II.2.2) it is assumed that the flow is steady state, laminar, and isothermal, and the fluid is incompressible. For the classical capillary viscometers, such as the Ubbelohde viscometer, Eq.(II.2.2) can be written as

$$\nu = \frac{\eta}{\rho} = \frac{\pi r^4 g \bar{h} t}{8 V L} \quad (\text{II.2.3})$$

where the pressure difference ΔP is replaced with the mean hydrostatic pressure $\Delta P = g h \rho$. Here, g is the gravitational acceleration, ρ the density of the liquid, and h the mean hydrostatic height when the flow rate becomes equal to the mean flow rate V/t . In Eq.(II.2.3) V is the volume of the measuring sphere and t is the time required for the volume V to flow through the capillary. However, in order to perform highly accurate measurements, corrections must be made for kinetic energy effects, end-effects etc. as described by Kawata et al. (1991a). When these correction factors are incorporated, the working equation can generally be expressed as

$$\nu = \frac{\eta}{\rho} = K_1 t - \frac{K_2}{t} \quad (\text{II.2.4})$$

where K_1 and K_2 are constants characteristic of the viscometer. However, in the design of classical viscometers the contribution from the second term in Eq.(II.2.4) is made almost negligible.

The working equation derived by the manufacturer for the Ubbelohde viscometers used in this work can be written in the following way

$$\nu = \frac{\eta}{\rho} = K(t - y) \quad (\text{II.2.5})$$

where K is the constant of the viscometer. This constant is normally written on the viscometer. The parameter y is the Hagenbach correction factor, which is determined by the manufacturer, for the specific viscometer at different flow times.

The basic principles of measuring the kinematic viscosity of a liquid with an Ubbelohde viscometer can be described in the following way: Liquid is added to the viscometer until the level of the liquid is between the two marks indicated on the reservoir. By closing the end of the venting tube and applying vacuum to the capillary tube will result in the successive filling of the reference vessel, the capillary, the measuring sphere, and the pre-run sphere. The filling is stopped, when the pre-run sphere is filled, by opening the venting tube. This results in the separation between the liquid level in the reference vessel and the liquid level at the capillary exit. In this way, the liquid level at the capillary exit is kept constant, and the liquid emerging from the capillary flows down as a thin film on the walls of the reference vessel. Therefore, the Ubbelohde viscometer is also called a suspended-level viscometer. Because of this, it is not necessary to know exactly the volume initially added to the viscometer. Further, this also eliminates the temperature correction for glass expansion, and the apparatus constant K becomes temperature independent. The time t required for the liquid surface to pass from the upper mark (m_1) to the lower mark (m_2) is measured. In order to obtain accurate measurements the viscometer is placed vertically in a thermostatic bath. The type of the used Ubbelohde viscometer is chosen, so that the Hagenbach correction does not exceed the error allowed for the time measurements. Generally, the application range for the different types of Ubbelohde viscometers is given by the manufacturer.

In this work, the kinematic viscosities have been measured using several Ubbelohde viscometers, connected to an automatic AVS 350 Schott-Geräte analyzer. In this way the filling and the time measuring have been performed automatically, along with the calculation of the kinematic viscosity including the Hagenbach correction. The measured kinematic viscosity is based on an average of 6 runs. The temperature of the thermostatic bath has been controlled within ± 0.05 K. After multiplying the kinematic viscosity with the density, the uncertainty of the obtained dynamic viscosity values is less than $\pm 1.0\%$.

II.2.3 Densimeter

The density as a function of temperature and pressure has been determined with an Anton Paar DMA 60 resonance densimeter combined with an additional DMA 512P cell, which is designed to operate up to 700 bar and in the temperature range 263.15 K to 423.15 K. The density of a sample is determined by measuring the period of the oscillation excited on the measuring tube in the following way: For a given temperature and pressure (T, P) , the oscillation of the measuring tube can be modeled as a frictionless oscillation of a body with a mass M placed at the end of a spring with an elasticity constant C_e . The measuring tube has an unknown but fixed mass M_t and an unknown volume V_t containing the studied liquid with the density ρ . The frequency of the oscillation is then given by

$$f = \frac{1}{2\pi} \sqrt{\frac{C_e}{M}} = \frac{1}{2\pi} \sqrt{\frac{C_e}{M_t + \rho V_t}} \quad (\text{II.2.6})$$

and the period is defined as

$$A = \frac{1}{f} \quad (\text{II.2.7})$$

The measured period of the studied sample can then be converted to the density by the following equation

$$\rho = A(P, T)A^2 + B(P, T) \quad (\text{II.2.8})$$

where $A(P, T)$ and $B(P, T)$ are two characteristic constants of the apparatus defined as

$$A(P, T) = \frac{C_e(P, T)}{4\pi^2 V_t(P, T)} \quad \text{and} \quad B(P, T) = \frac{-M_t}{V_t(P, T)} \quad (\text{II.2.9})$$

These constants have to be evaluated by calibrating the densimeter with two fluids, for which the density is known within the desired temperature and pressure ranges.

The measuring cell is a U shaped tube, which can contain a few cm³ of the sample. It is placed in a double-wall cylinder, sealed in both ends. This cylinder contains a gas with a high thermal conductivity. A thermostatic bath is used to control the temperature of the measuring tube. The temperature of the sample is measured within the cell by a Pt100 probe connected to a calibrated digital thermometer. The uncertainty in the measured temperature is within ± 0.05 K. In order to carry out high-pressure measurements, the U-shaped measuring tube is connected to a sample reservoir vessel and a mercury ROP pump. The experimental arrangement is illustrated in Figure II.10.

The operation procedure in order to carry out density measurements is described below. A vacuum pump is connected to valve (b), where the tube between valve (b) and valve (a) has been disconnected, in order to evacuate the measuring tube and the reservoir vessel. After vacuum has been applied, valve (b) is closed and the studied sample is introduced through valve (d). The filling of the measuring tube and the reservoir vessel is performed free of any air and gas bubbles. Before the tube between valve (a) and (b) is connected with valve (b), it is ensured that no air is present by using mercury to force out any air. After this tube has been connected, valves (a) and (b) are opened. The liquid will then be in contact with the mercury at atmospheric pressure. When thermal equilibrium is reached in the measuring tube, the period of the sample at 1 atm is measured. Then, valve (d) is closed and the pressure is increased using the mercury ROP pump. Measurements are then carried out at the desired pressures, while the temperature is kept constant. When the maximum pressure is reached, the pressure is decreased to 1 atm and the temperature of the thermostatic bath is changed. When thermal equilibrium is reached, measurements can be carried out for a new isotherm. In this way, the measurements can be performed for different pressures and temperatures without disturbing the sample. The volume in the tube between valve (c) and (d) is

necessary to know the density and to measure the period as a function of pressure and temperature for one of the reference compounds. For the other reference compound, it is only necessary to measure the period and to know the density as a function of temperature. This is an advantage, since extensive studies of the density versus temperature and pressure have only been performed for a few compounds. One of these compounds is water. Therefore, Lagourette et al. (1992) chose water as one of the calibration fluids, since Kell and Whalley (1975) measured the density of water up to 1000 bar and from 273.15 K to 423.15 K. These measurements were carried out for every 10 K and 50 bar with an uncertainty of 0.01 kg/m³. As the other reference compound Lagourette et al. (1992) chose vacuum ($P < 0.001$ bar). At 1 bar the density of air is 1 kg/m³, whereas the density at a pressure below 0.001 bar is less than 0.01 kg/m³ (less than the uncertainty of the density of water). Further, Lagourette et al. (1992) assumed that $B(0, T) = B(1 \text{ bar}, T)$. By combining the relation

$$\rho(P, T) = A(T)A^2 + B(P, T) \quad (\text{II.2.10})$$

for water and vacuum, Lagourette et al. (1992) derived the following density equation

$$\rho(P, T) = \frac{\rho_w(1 \text{ bar}, T)}{A_w^2(1 \text{ bar}, T) - A_{vac}^2(T)} \left[A_{liq}^2(P, T) - A_{vac}^2(T) \right] + \Delta(T, P) \quad (\text{II.2.11})$$

with

$$\Delta(T, P) = \rho_w(P, T) - \frac{\rho_w(1 \text{ bar}, T)}{A_w^2(1 \text{ bar}, T) - A_{vac}^2(T)} \left[A_w^2(P, T) - A_{vac}^2(T) \right] \quad (\text{II.2.12})$$

where subscripts w and vac refer to water and vacuum.

The densimeter has been calibrated by measuring the period $A_w(P, T)$ of double distilled water, and the period $A_{vac}(T)$ by applying vacuum to the cell. Further, the values $\rho_w(1 \text{ bar}, T)$ and $\rho_w(P, T)$ used in Eqs.(II.2.11) and (II.2.12) have been taken from Kell and Whalley (1975).

Since, the density of the studied samples has only been determined up to 600 bar, and density values are needed up to 1000 bar, an extrapolation of the measured densities has been performed. The extrapolation has been performed using the modification of the Tait equation (Tait 1888) proposed by Hogenboom et al. (1967) and shown below

$$\frac{1}{\rho(P,T)} = \frac{1}{\rho(0.1 \text{ MPa}, T)} + A \ln \left[1 + \frac{P - 0.1}{B} \right] \quad (\text{II.2.13})$$

where A and B are two adjustable constants, and the pressure P has the unit of [MPa]. The Tait type equations are able to describe the density behavior of liquids versus pressure in an excellent way. Due to this, this type of equation is commonly used in the interpolation and extrapolation of measured liquid densities versus pressure.

The overall uncertainty in the reported densities is estimated to be less than 1 kg/m^3 . This uncertainty will not have any significant influence on the measured viscosities; see Eq.(II.2.1) due to the fact that the density of the sinker is 8700 kg/m^3 . Because of this, the uncertainty in the measured viscosities is related to the viscometer.

II.2.4 Characteristics of the Samples

The three substances used to prepare the ternary mixtures are commercially available chemicals with the following purity levels: 1-methylnaphthalene ($\text{C}_{11}\text{H}_{10}$: Fluka, purity > 97% and $M_w = 142.20 \text{ g/mol}$), n-tridecane ($\text{C}_{13}\text{H}_{28}$: Tokyo Kasei, purity > 99% and $M_w = 184.37 \text{ g/mol}$), and 2,2,4,4,6,8,8-heptamethylnonane ($\text{C}_{16}\text{H}_{34}$: Aldrich, purity > 98% and $M_w = 226.44 \text{ g/mol}$).

The ternary mixtures have been prepared by weighting at atmospheric pressure and ambient temperature to obtain the molar fractions:

$$x_i = 0.125, 0.250, 0.375, 0.500, 0.625, \text{ and } 0.750 \text{ (with } \sum_{i=1}^{i=3} x_i = 1)$$

corresponding to the 21 points shown in the ternary diagram, Figure II.11. The systems corresponding to the points at the three summits (pure compounds) and the three sides (binaries) have already been studied by Daugé et al. (1999), Daugé et al. (2001), and Canet et al. (2001). The samples have been studied immediately after their preparation in order to prevent absorption from the ambient air. The pure fluids, not degassed, have been stored in hermetically sealed bottles. Further, the studied mixtures are in their liquid state within the studied experimental temperature and pressure domain.

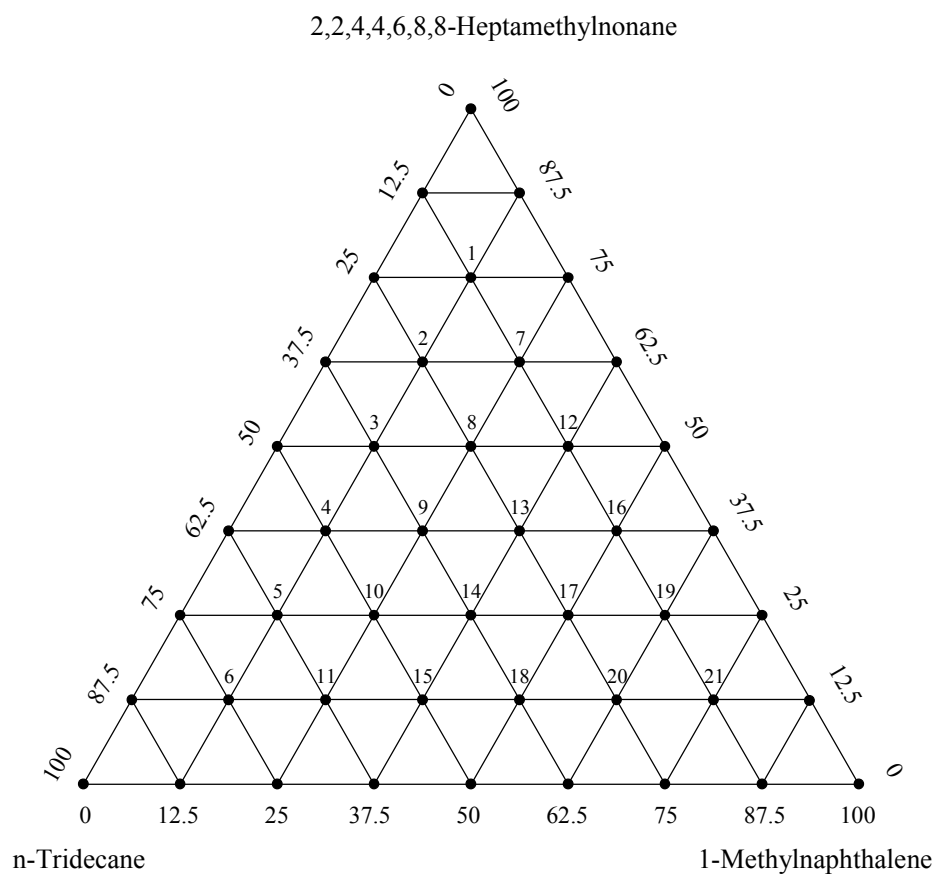


Figure II.11 Ternary diagram representing the composition in mole percent of the studied ternary mixtures (point 1 – 21).

II.3 Results of Viscosity and Density Measurements

Measurements of the dynamic viscosity η have been carried out at 7 temperatures (293.15, 303.15, 313.15, 323.15, 333.15, 343.15 and 353.15 K) and at 6 pressures (1, 200, 400, 600, 800 and 1000 bar) for the 21 compositions indicated in Figure II.11. A total of 882 values have been obtained for the viscosity. The density measurements have been carried out at the same temperatures and compositions at pressures from 1 bar to 600 bar in steps of 50 bar (13 different pressures), corresponding to 1911 experimental values for the density. These values have been extrapolated with the aid of the modified Tait equation given in Eq.(II.2.13) in order to obtain the densities at 800 and 1000 bar (294 values). The measured dynamic viscosity and density values are given in Appendix B1, Table B1.1 as a function of temperature T , pressure P , and composition expressed as the mole fraction (x_m for 1-methylnaphthalene, x_t for n-tridecane, and x_h for 2,2,4,4,6,8,8-heptamethylnonane; for $x_m, x_t, x_h \neq 0$ and 1). Additional density data are reported in Appendix B2, Table B2.1 through B2.21. The experimental uncertainty for the viscosity measurements is of the order of 2%, except at 1 bar where the uncertainty is less than 1%. The density measurements have an overall uncertainty of 1 kg/m³.

Figures II.12 and II.13 show respectively the variations of the density and the dynamic viscosity as a function of the pressure (for different temperatures) in the case corresponding to point 9, which is close to the middle of the ternary diagram in Figure II.11 ($x_m = 0.250$, $x_t = 0.375$, $x_h = 0.375$). Figures II.14 and II.15 show respectively the variations of the density and the dynamic viscosity as a function of the temperature (for different pressures) for point 9. Table B1.1 in Appendix B and Figures II.12 through II.15 present a general pattern consistent with previous observations made by other authors on either pure hydrocarbons, binary or ternary mixtures composed of hydrocarbons. For each composition, the pressure coefficient of the viscosity variation $(\partial\eta/\partial P)_T$ is positive and the shape of the $\eta(P)$ variations shows a sharp increase, while on contrary, the temperature coefficient of the viscosity variation $(\partial\eta/\partial T)_P$ is always negative. The group of isothermal and isobaric curves is regular. This is also true for the density, but in the case of isothermal curves a concavity is observed associated with a second negative derivative. This form is compatible with the

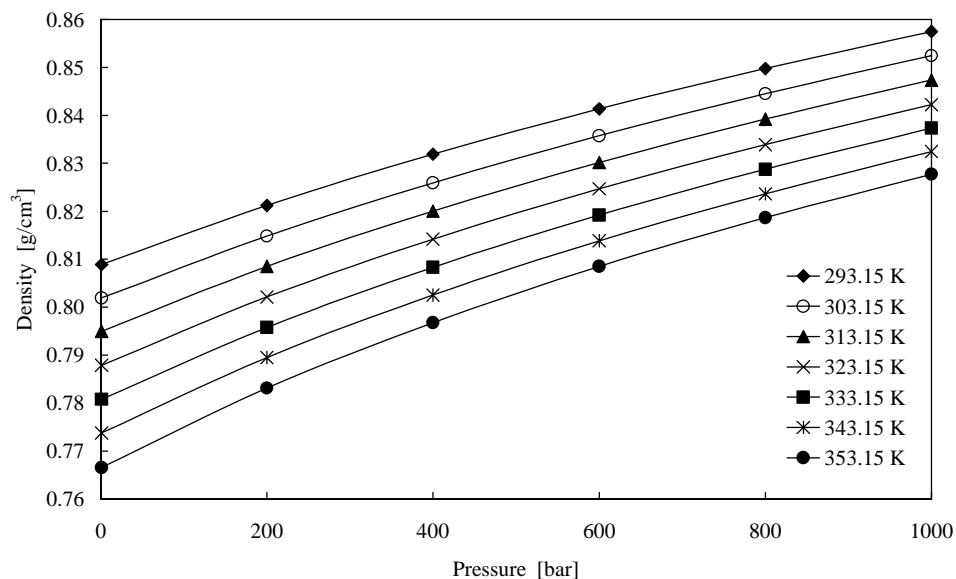


Figure II.12 Density versus pressure at various temperatures for the ternary mixture containing 25.0 mole% 1-methylnaphthalene + 37.5 mole% n-tridecane + 37.5 mole% 2,2,4,4,6,8,8-heptamethylnonane.

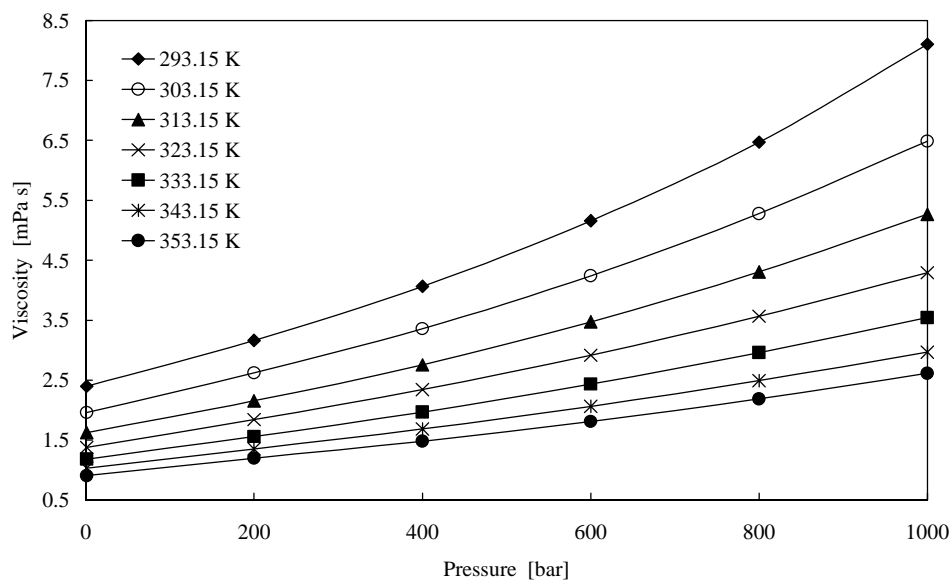


Figure II.13 Viscosity versus pressure at various temperatures for the ternary mixture containing 25.0 mole% 1-methylnaphthalene + 37.5 mole% n-tridecane + 37.5 mole% 2,2,4,4,6,8,8-heptamethylnonane.

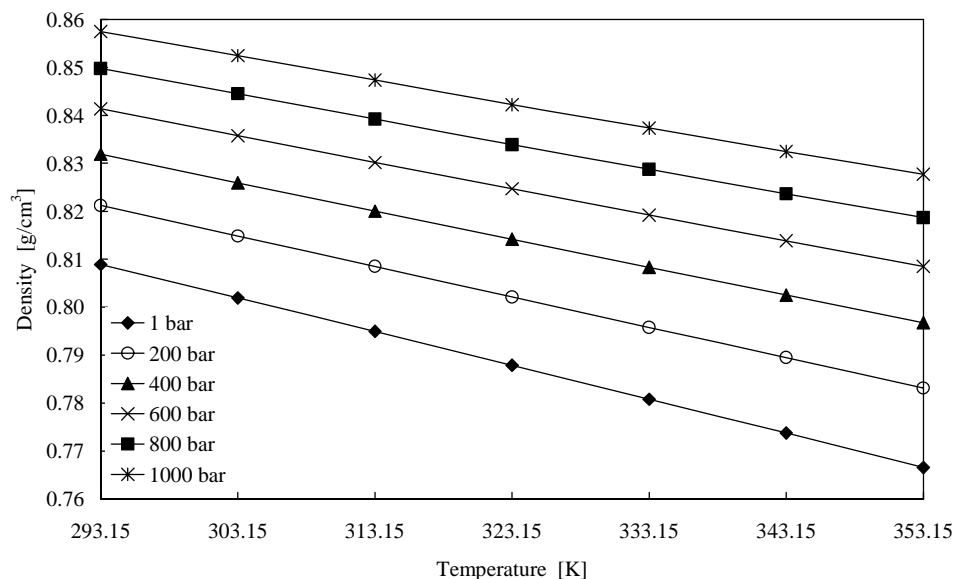


Figure II.14 Density versus temperature at various pressures for the ternary mixture containing 25.0 mole% 1-methylnaphthalene + 37.5 mole% n-tridecane + 37.5 mole% 2,2,4,4,6,8,8-heptamethylnonane.

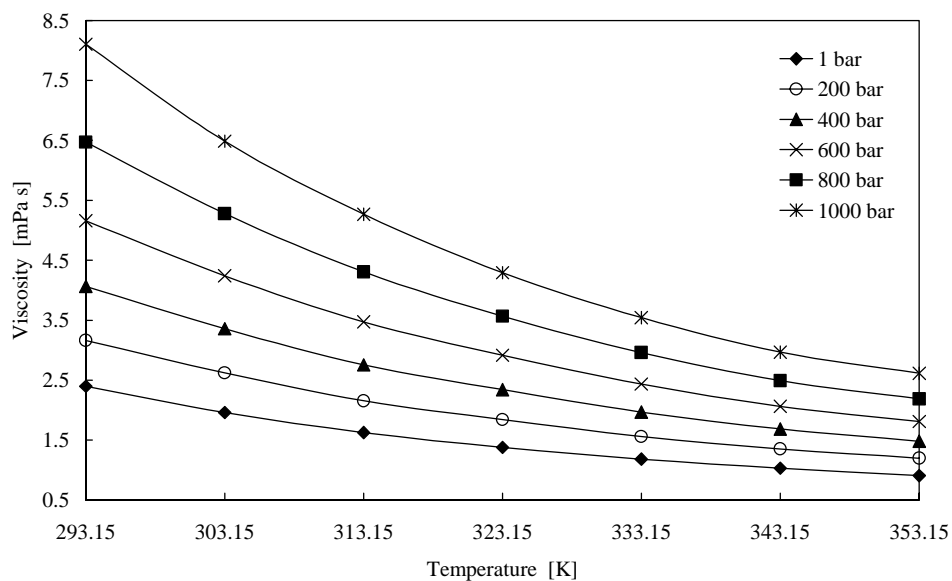


Figure II.15 Viscosity versus temperature at various pressures for the ternary mixture containing 25.0 mole% 1-methylnaphthalene + 37.5 mole% n-tridecane + 37.5 mole% 2,2,4,4,6,8,8-heptamethylnonane.

logarithmic form proposed by Tait (1888) to model the influence of pressure on $1/\rho$, which is the form used for the extrapolation, see Eq.(II.2.13). It should be mentioned that the variations of density versus temperature are practically linear due to the small temperature interval (60 K) in this investigation, because the main aim has been to observe the variations of density and viscosity as a function of pressure and composition for the studied ternary system.

Figure II.16 shows for $P = 400$ bar and $T = 323.15$ K the variations of density as a function of the mole fraction of n-tridecane for constant compositions of 1-methylnaphthalene. Points M, T and H correspond to 1-methylnaphthalene, n-tridecane and 2,2,4,4,6,8,8-heptamethylnonane, respectively, and the sides MT, MH and TH correspond to the associated binaries. In order to complete Figure II.16 and the following figures, the reported data for the pure compounds and the binaries given by Daugé et al. (1999), Daugé et al. (2001) and Canet et al. (2001) have been used. Within the experimental accuracy, the variations of the density are practically linear, which corresponds to very low excess volumes. Figure II.17 shows the variations of viscosity as a function of the mole fraction of 1-methylnaphthalene for constant compositions of

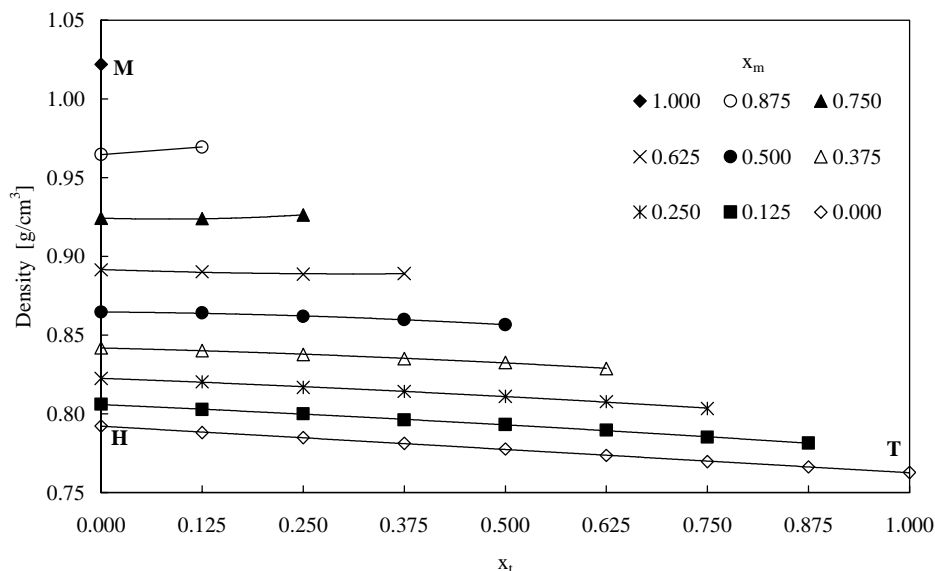


Figure II.16 Density versus mole fraction of n-tridecane (x_t) for various mole fractions of 1-methylnaphthalene (x_m) at 400 bar and 323.15 K. Points M, T, and H refer to pure 1-methylnaphthalene, n-tridecane, and 2,2,4,4,6,8,8-heptamethylnonane, respectively.

n-tridecane at $P = 400$ bar and $T = 323.15$ K, and Figure II.18 gives an other point of view as it corresponds to the viscosity as a function of the mole fraction of 1-methylnaphthalene for constant compositions of 2,2,4,4,6,8,8-heptamethylnonane at $P = 400$ bar and $T = 323.15$ K. Figures II.19 and II.20 present the viscosity surface and density surface in a ternary representation for $P = 400$ bar and $T = 323.15$ K. It should be mentioned that near the side 1-methylnaphthalene + 2,2,4,4,6,8,8-heptamethylnonane for a given P, T the viscosity curves reveal a non-monotonous behaviour with respect to the composition. This may be the effect of repulsive interactions or structural effects (as for the binary; see Canet et al. (2001) or Figures II.4 and II.5). The minimum disappears when the amount of n-tridecane increases. For a given composition, Table B1.1 shows that the minimum also disappears when the pressure increases. Further, by keeping the concentration of 2,2,4,4,6,8,8-heptamethylnonane constant for $x_h \leq 0.375$ and plotting the viscosity as a function of the concentration of 1-methylnaphthalene, a very slow increase in the viscosity is observed for $0 < x_m < 0.500$, see Figure II.18. Overall for the viscosity of this ternary system, there is a negative deviation from an ideal mixture, indicating that the viscosity is influenced by repulsive interactions.

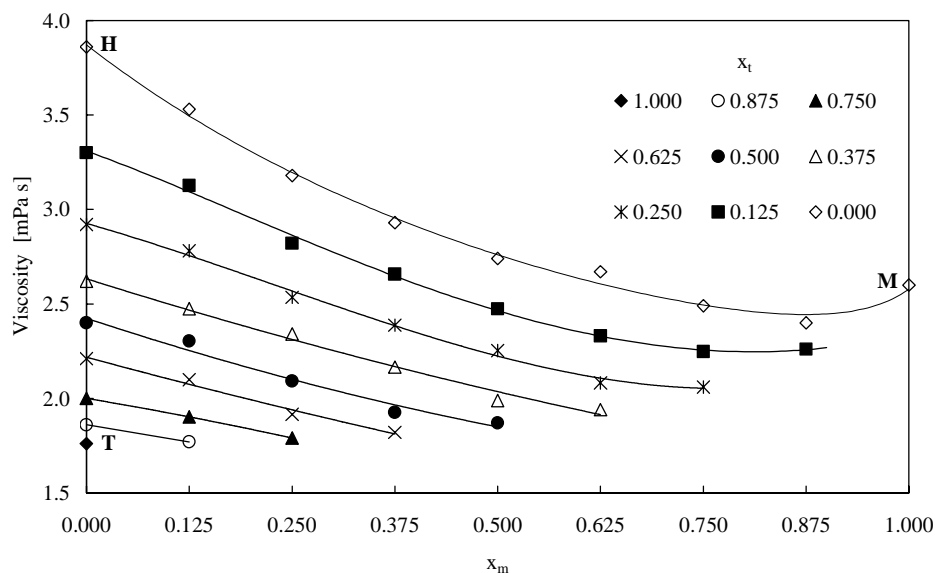


Figure II.17 Viscosity versus mole fraction of 1-methylnaphthalene (x_m) for various mole fractions of n-tridecane (x_t) at 400 bar and 323.15 K. Points M, T, and H refer to pure 1-methylnaphthalene, n-tridecane, and 2,2,4,4,6,8,8-heptamethylnonane, respectively.

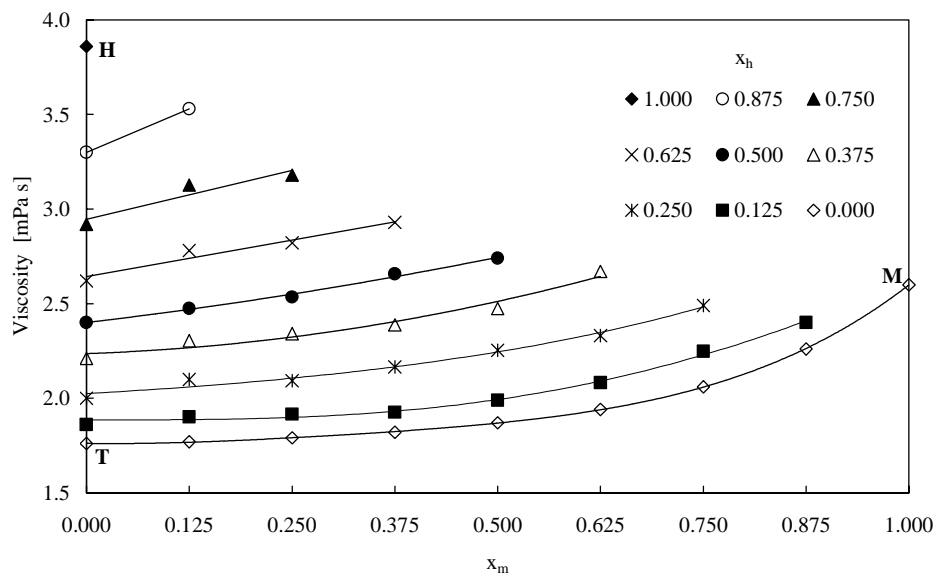


Figure II.18 Viscosity versus mole fraction of 1-methylnaphthalene (x_m) for various mole fractions of 2,2,4,4,6,8,8-heptamethylnonane (x_h) at 400 bar and 323.15 K. Points M, T, and H refer to pure 1-methylnaphthalene, n-tridecane, and 2,2,4,4,6,8,8-heptamethylnonane, respectively.

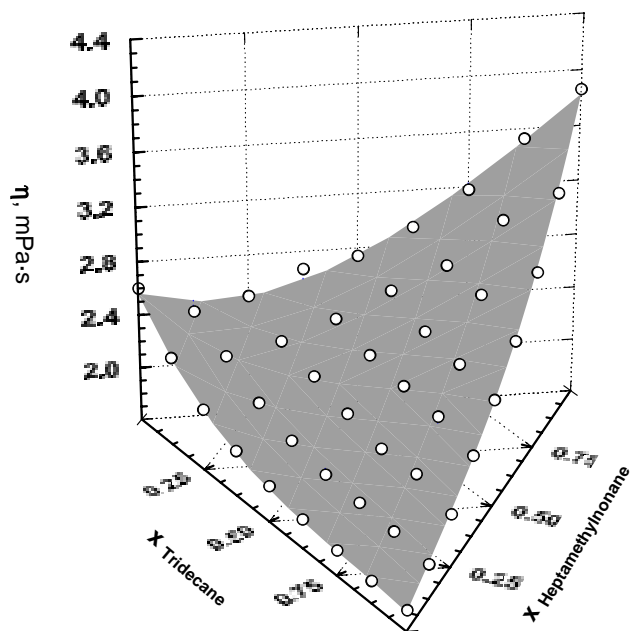


Figure II.19 Surface of the viscosity η versus the mole fraction of 1-methylnaphthalene, the mole fraction of n-tridecane, and the mole fraction of 2,2,4,4,6,8,8-heptamethylnonane at 400 bar and 323.15 K.

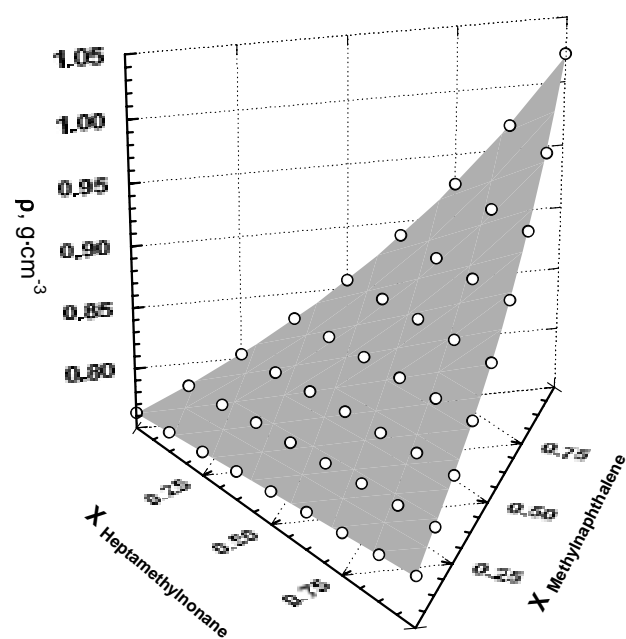


Figure II.20 Surface of the density ρ versus the mole fraction of 1-methylnaphthalene, the mole fraction of n-tridecane, and the mole fraction of 2,2,4,4,6,8,8-heptamethylnonane at 400 bar and 323.15 K.

II.4 Modeling of the Viscosity

The viscosity and density data obtained for the ternary mixtures composed of 1-methylnaphthalene + n-tridecane + 2,2,4,4,6,8,8-heptamethylnonane in the course of this investigation, combined with those obtained previously by Daugé et al. (1999), Daugé et al. (2001), and Canet et al. (2001) on the three pure compounds and the three binaries, represent the most comprehensive experimental study of this ternary system up to 1000 bar in the temperature range 293.15 K to 353.15 K at 45 different compositions. This ternary system represents some simple petroleum cuts at 510 K. Due to this and the enormous amount of measurements performed at temperature and pressure conditions normally encountered within the oil industry, these data can be used to evaluate different representative models incorporating the effects of temperature, pressure, and composition. In this way, the compositional dependent viscosity models can be evaluated for the possible extension to real petroleum fluids. Further it should be stated that most compositional dependent viscosity models have been derived based on viscosity measurements of pure compounds and binary mixtures. In the following, the viscosity of this ternary system will be used to evaluate the performance of different viscosity models. Some of these models will have a physical and theoretical background, whereas others will have a more or less semi-empirical background.

II.4.1 Classical Mixing Laws

Several mixing laws have been developed for calculating the viscosity of liquid mixtures. The objective of these mixing laws has been to predict the viscosity based on the composition, the viscosity, and the density of the pure compounds. Two of the more well-known mixing laws derived for binary mixtures are the Grunberg-Nissan mixing law (Grunberg and Nissan 1949) and the Katti-Chaudhri mixing law (Katti and Chaudhri 1964).

For a multicomponent mixture the ideal Grunberg-Nissan mixing law can be written as follows

$$\ln \eta = \sum_{i=1}^n x_i \ln \eta_i \quad (\text{II.4.1})$$

This is equivalent to the expression derived by Arrhenius (1887) for a multicomponent mixture. The Katti-Chaudhri mixing law can be expressed as

$$\ln(\eta v) = \sum_{i=1}^n x_i \ln(\eta_i v_i) \quad (\text{II.4.2})$$

where $v_i = M_{w,i}/\rho_i$ is the molar volume, $M_{w,i}$ the molecular weight, ρ_i the density, η_i the viscosity, and x_i the mole fraction of component “ i ”. For mixtures the molecular weight is defined as $M_w = \sum x_i M_{w,i}$. Both mixing laws are totally predictive in the sense that only properties of the pure compounds are required. In this work, the viscosity calculations with the Katti-Chaudhri mixing law have been performed using the experimental mixture densities in order to obtain v . The deviations obtained for the two mixing laws by comparing the predicted viscosities with the experimental values are given in Table II.1 for each of the three binary systems and the ternary. Both mixing laws overestimate the viscosity, as indicated by the Bias reported in Table II.1, which is approximately equal to the AAD. Overall, the obtained AAD is satisfactory taking into account the simplicity of the mixing laws. However, by using the experimental mixture densities in the Katti-Chaudhri mixing law additional information about the mixtures is incorporated into the viscosity calculations. Due to this, the Katti-Chaudhri mixing law

	NP	AAD%	MxD%	Bias
<u>Grunberg-Nissan</u>				
1-Methylnaphthalene + n-Tridecane	294	12.2	21.3	12.2
1-Methylnaphthalene + HMN	294	10.2	21.9	10.2
n-Tridecane + HMN	294	6.10	24.1	6.05
1-Methylnaphthalene + n-Tridecane + HMN	882	13.0	34.2	13.0
<u>Katti-Chaudhri</u>				
1-Methylnaphthalene + n-Tridecane	294	8.96	17.4	8.96
1-Methylnaphthalene + HMN	294	4.74	14.2	4.62
n-Tridecane + HMN	294	5.68	23.2	5.61
1-Methylnaphthalene + n-Tridecane + HMN	882	8.65	27.7	8.65

Table II.1 Results for viscosity predictions with the classical ideal mixing laws Eqs.(II.4.1) and (II.4.2). HMN refers to 2,2,4,4,6,8,8-heptamethylnonane.

can predict the viscosity of this ternary system better than the Grunberg-Nissan mixing law. In the Grunberg-Nissan mixing law the variation of the viscosity versus composition becomes monotonic and any interactions between the pure components influencing the total viscosity are not taken into account, such as the kind of viscosity behavior this ternary system develops, see Daugé et al. (1999), Daugé et al. (2001), Canet et al. (2001) and the experimental results presented in this work (Appendix B1).

II.4.1.1 Modified Grunberg-Nissan Mixing Laws

The Grunberg-Nissan mixing law can be modified by introducing adjustable parameters believed to be representative in some way of the interactions within the considered system. Adjustable parameters can be introduced in different ways. The following expression, which is written for ternary mixtures, shows how the Grunberg-Nissan mixing law can be modified in a simple way

$$\ln \eta = x_m \ln \eta_m + x_t \ln \eta_t + x_h \ln \eta_h + x_m x_t d_{mt} + x_m x_h d_{mh} + x_t x_h d_{th} \quad (\text{II.4.3})$$

Subscripts m , t , and h refer to 1-methylnaphthalene, n-tridecane, and 2,2,4,4,6,8,8-heptamethylnonane, respectively. The d_{ij} parameter is a quantity characteristic of the intermolecular interactions between component i and component j . In case that Eq.(II.4.3) is applied to a binary system, it reduces to the original expression proposed by Grunberg and Nissan (1949) for viscosity modeling of binary systems. The d_{ij} parameter can be evaluated from viscosity data concerning only the binary $i + j$ system. By applying Eq.(II.4.3) to each of the three binary systems Daugé (1999) determined the three d_{ij} parameters. The three parameters are $d_{mt} = -0.58110$, $d_{mh} = -0.50034$, and $d_{th} = -0.28387$. These parameters have been used in the viscosity predictions of the ternary mixtures in order to make a comparison with the experimental values. The obtained deviations from this comparison are given in Table II.2 along with the deviations obtained for each of the binary systems. The obtained results for both the binary systems and the ternary are satisfactory in the sense that the AAD is of the same order of magnitude as the experimental uncertainty ($\pm 2.0\%$). As it can be seen from Table II.2, when adjustable parameters are introduced in the Grunberg-Nissan mixing law, a significant improvement in the viscosity correlation is achieved, compared to the results presented in Table II.1 obtained with the ideal Grunberg-Nissan mixing law.

	NP	AAD%	MxD%	Bias
1-Methylnaphthalene + n-Tridecane	294	2.59	8.69	0.57
1-Methylnaphthalene + HMN	294	2.25	9.62	0.27
n-Tridecane + HMN	294	2.39	15.6	0.54
1-Methylnaphthalene + n-Tridecane + HMN	882	2.45	15.7	-0.58

Table II.2 Results for viscosity modeling with the modified Grunberg-Nissan mixing law Eq.(II.4.3). HMN refers to 2,2,4,4,6,8,8-heptamethylnonane.

Thus, when adjustable parameters are introduced, the model is no longer totally predictive. Further it can be seen from the values of the d_{ij} parameters that the largest binary interactions are obtained between 1-methylnaphthalene and n-tridecane or 2,2,4,4,6,8,8-heptamethylnonane (aromatic hydrocarbon + alkane), rather than between n-tridecane and 2,2,4,4,6,8,8-heptamethylnonane (alkane + alkane), see e.g. the viscosity behaviors shown in Figures II.4, II.5, II.17 and II.18.

II.4.1.2 The Excess Activation Energy of Viscous Flow

Another property, which can be obtained from the measured values of the viscosity and density, is the excess activation energy of viscous flow ΔG^E , which appears in

$$\ln(\eta v) = x_m \ln(\eta_m v_m) + x_t \ln(\eta_t v_t) + x_h \ln(\eta_h v_h) + \frac{\Delta G^E}{RT} \quad (\text{II.4.4})$$

where R is the gas constant and T the temperature in [K]. This relation is a modified form of the mixing law proposed by Katti and Chaudhri (1964) and is theoretically justified by Eyring's representation of the viscosity of a pure fluid (Glasstone et al. 1941). It is important to note here that the quantity ηv is also obtained from the time-correlation expression for shear viscosity (Zwanzig, 1965). Thus, the quantities ηv and ΔG^E have a theoretical background, while the corrective terms in Eqs.(II.4.3) do not. The term ΔG^E can be estimated from Eq.(II.4.4) using the experimental viscosity and density data reported in Appendix B1, and by Daugé et al. (1999), Daugé et al. (2001), and Canet et al. (2001). Figure II.21 shows the surface $\Delta G^E(x_m, x_t, x_h)$ in a ternary representation at 400 bar and 323.15 K. Generally, ΔG^E is negative and $|\Delta G^E|$ increases

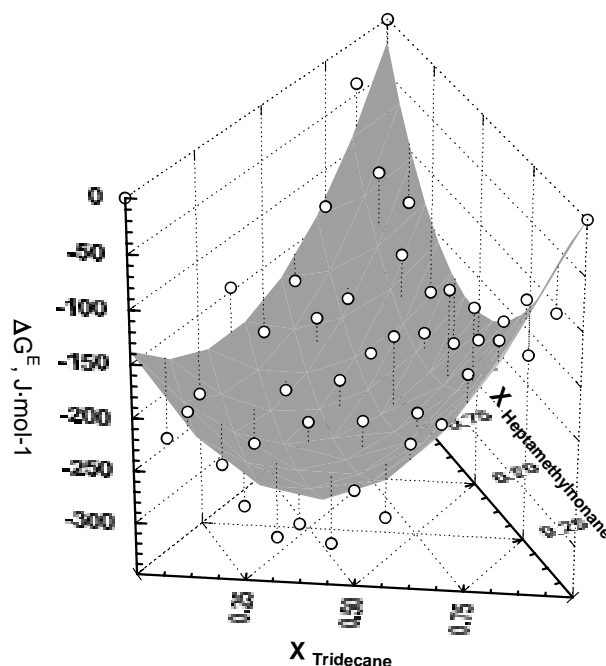


Figure II.21 Surface of the excess activation energy of viscous flow versus the mole fraction of 1-methylnaphthalene, the mole fraction of n-tridecane, and the mole fraction of 2,2,4,4,6,8,8-heptamethylnonane at 400 bar and 323.15 K.

with pressure. For some authors, such as Heric and Brewer (1967) and Cea et al. (1995), the fact that the excess activation energy of viscous flow ΔG^E is negative means that the predominant effect in the mixture is the breaking up of the ordered structure present in the pure liquids. Other authors, such as Acevedo et al. (1990) and Bravo et al. (1991), interpret the negative values of ΔG^E by the fact that the repulsive forces of interaction are the forces which predominate, corresponding to the breaking of bounds within the ordered structure. For the very associative system water + alcohol (see for instance Moha-Ouchane et al. (1998)) $|\Delta G^E|$ can reach 5000 J/mol. For the ternary system 1-methylnaphthalene + n-tridecane + 2,2,4,4,6,8,8-heptamethylnonane, the maximum value of $|\Delta G^E|$ is about 600 J/mol, which corresponds to weak interactions and consequently to a weakly interactive system.

For an ideal mixture $\Delta G^E = 0$. This will then correspond to the ideal Katti-Chaudhri mixing rule defined in Eq.(II.4.2). However, Eq.(II.4.4) can also be used to

model the viscosity of real mixtures introducing an expression for ΔG^E in order to take into account the non-ideal behavior of real mixtures. A similar expression as the one introduced in the Grunberg-Nissan mixing law (Eq.(II.4.3)) has been written below for ΔG^E

$$\Delta G^E = x_m x_t W_{mt} + x_m x_h W_{mh} + x_t x_m W_{th} \quad (\text{II.4.5})$$

where W_{ij} is a quantity characteristic of intermolecular interactions between component i and component j responsible for the excess energy of activation for viscous flow. The W_{ij} parameters can be evaluated using viscosity and density data concerning only the binary $i + j$ system. For each of the three binary systems, the following parameters have been determined; $W_{mt} = -1173.6$ J/mole, $W_{mh} = -611.55$ J/mole and $W_{th} = -726.83$ J/mole by minimizing the least squares. The estimated W_{ij} parameters are all negative, indicating that repulsive forces dominate between component i and component j . These three W_{ij} parameters have been used in the comparison of predicted viscosities using Eq.(II.4.4) incorporating Eq.(II.4.5) with the experimental values of the ternary mixtures. The resultant deviations are presented in Table II.3 along with the deviations for the binary systems. The AAD is of the same order of magnitude as the experimental uncertainty ($\pm 2.0\%$), and slightly better than the deviations obtained with the Grunberg-Nissan mixing law using binary interaction parameters, see Table II.2.

II.4.2 The Hard-Sphere Viscosity Scheme

Recently, a scheme has been introduced by Dymond and Awan (1989) and Assael et al. (1990), (1992a), and (1992b) for the simultaneous correlation of the self-diffusion, the

	NP	AAD%	MxD%	Bias
1-Methylnaphthalene + n-Tridecane	294	2.35	8.87	0.33
1-Methylnaphthalene + HMN	294	1.92	8.45	0.23
n-Tridecane + HMN	294	2.38	14.4	0.36
1-Methylnaphthalene + n-Tridecane + HMN	882	2.12	14.6	-0.51

Table II.3 Results for viscosity modeling with the modified Katti-Chaudhri mixing law Eq.(II.4.4) in conjunction with Eq.(II.4.5). HMN refers to 2,2,4,4,6,8,8-heptamethylnonane.

viscosity, and thermal conductivity coefficients of dense fluids over wide ranges of pressure and temperature. This scheme has mainly been applied to n-alkanes and their mixtures (Assael et al. 1992a, 1992c), but also to aromatic hydrocarbons (Assael et al. 1992d), n-alcohols (Assael et al. 1994), and refrigerants (Assael et al. 1995). This scheme is based on the fact that the transport properties of real dense fluids, expressed as $v_r = v/v_0$ with v the molar volume and v_0 the close packing molar volume defined as $v_0 = N_A \sigma^3/2^{1/2}$, are assumed to be proportional to the exact hard-sphere values. The best value for the molecular parameter v_0 is obtained when the self-diffusion and the viscosity are correlated simultaneously. For each reduced transport property universal curves have been determined as a function of $v_r = v/v_0$ (Assael et al. 1992b). However, in this work only the hard-sphere scheme introduced for viscosity estimation is described.

For rough spherical molecules at high densities, Chandler (1975) showed that the self-diffusion coefficient and the viscosity could be related to the smooth hard-sphere values of the transport properties. This idea has been extended by Dymond and Awan (1989) and Assael et al. (1990), (1992a), and (1992b) by assuming that a corresponding states relationship exists between the experimental transport properties of rough non-spherical molecules and the smooth hard-sphere values (subscript *shs*). Since, the experimental viscosity is proportional to the exact hard-sphere values, the following relation can be defined

$$\eta_{exp} = R_\eta \eta_{shs} \quad (\text{II.4.6})$$

where the proportionality factor R_η , described as the roughness factor, accounts for the roughness and non-spherical shape of the molecule. The exact smooth hard-sphere transport coefficient for viscosity is given by the product of the value from Enskog's theory η_E (Enskog 1922) and the computed correction from molecular simulations to Enskog's theory $(\eta/\eta_E)_{MD}$:

$$\eta_{shs} = \eta_E (\eta / \eta_E)_{MD} \quad (\text{II.4.7})$$

Enskog's theory for smooth hard spheres has been derived for dense gases and related to the concepts of the kinetic gas theory by considering only two-body collisions and taking into account that the diameter of the molecules is no longer negligible compared

to the distance between the molecules. Due to this the number of collisions in a dense system is changed by a factor $g(\sigma)$ compared to a dilute system, where $g(\sigma)$ is the radial distribution function at contact given by Carnahan and Starling (1969). Generally, the number of collisions in a dense system is increased due to the narrower distance between the molecules. However, if the molecules are close enough to shield one another from oncoming molecules, the number of collisions decreases. Further, when two rigid spheres collide, energy and momentum are transferred from one molecule to the other. The expression for viscosity based on Enskog's theory for smooth hard-spheres is defined as

$$\eta_E = \eta_0 \left(\frac{1}{g(\sigma)} + \frac{0.8b}{v} + 0.761 g(\sigma) \left(\frac{b}{v} \right)^2 \right) \quad (\text{II.4.8})$$

with $b = 2\pi N_A \sigma^3/3$, where N_A is Avogadro's constants and σ the hard-core diameter. The expression for the low-density viscosity is given to the first order approximation

$$\eta_0 = \frac{5}{16\pi\sigma^2} (\pi m k_B T)^{1/2} \quad (\text{II.4.9})$$

where m is the molecular mass, k_B Boltzmann's constant, and T the temperature. In order to avoid calculating the viscosity directly, which requires knowledge of the hard-core diameter and the roughness factor, Dymond (1973) found it convenient to express the viscosity as reduced quantities

$$\eta_{\text{exp}}^* = R_\eta \eta_{shs}^* = R_\eta \left[\frac{\eta_{shs}}{\eta_0} \right] \left[\frac{v}{v_0} \right]^{2/3} \quad (\text{II.4.10})$$

where subscript "0" refers to the low-density hard-sphere coefficient in the first order approximation. The reduced smooth hard-sphere viscosity can be obtained from experimental values after substitution of the hard-sphere expressions, which give

$$\eta_{shs}^* = \frac{\eta_{\text{exp}}^*}{R_\eta} = 6.035 \cdot 10^8 \left[\frac{1}{M_w R T} \right]^{1/2} \frac{\eta_{\text{exp}} v^{2/3}}{R_\eta} \quad (\text{II.4.11})$$

In order to determine R_η and v_0 for a given temperature a plot of $\log_{10}(\eta_{\text{exp}}^*)$ versus $\log_{10}(v)$ from the experiment is superimposed on a universal plot of $\log_{10}(\eta_{shs}^*)$ versus $\log_{10}(v/v_0)$ from the hard-sphere theory by vertical and horizontal adjustments.

The universal curve for viscosity was originally developed for n-alkanes (Assael et al. 1992a), but has also been applied to aromatic hydrocarbons (Assael et al. 1992d), alcohols (Assael et al. 1994), and refrigerants (Assael et al. 1995). The empirical expression for this curve is

$$\log_{10} \left[\frac{\eta_{\text{exp}}^*}{R_{\eta}} \right] = \sum_{k=0}^7 a_{\eta,k} (1/v_r)^k \quad (\text{II.4.12})$$

where

$$\begin{array}{ll} a_{\eta,0} = & 1.0945 & a_{\eta,4} = & 797.6900 \\ a_{\eta,1} = & -9.26324 & a_{\eta,5} = & -1221.9770 \\ a_{\eta,2} = & 71.0385 & a_{\eta,6} = & 987.5574 \\ a_{\eta,3} = & -301.9012 & a_{\eta,7} = & -319.4636 \end{array}$$

The $a_{\eta,i}$ coefficients are universal, independent of the chemical structure of the compound. This has been verified by Baylaucq et al. (1999) and Baylaucq et al. (2000), who used the hard-sphere scheme to model the viscosity of two ternary systems composed of n-heptane + methylcyclohexane + 1-methylnaphthalene and water + 2-propanol + 4-hydroxy-4-methyl-2-pentanone.

For various pure compounds it has been observed that v_0 is temperature dependent, whereas R_{η} is temperature independent for pseudo-spherical molecules, such as n-alkanes, but shows a temperature dependency for molecules that either depart too much from sphericity or have hydrogen bonds, such as alcohols (Assael et al. 1994).

For alkanes from C_5H_{12} to $\text{C}_{16}\text{H}_{34}$ the following expressions have been derived for R_{η} and v_0 (Assael 1992a)

$$R_{\eta} = 0.995 - 8.944 \cdot 10^{-4} C + 5.427 \cdot 10^{-3} C^2 \quad (\text{II.4.13})$$

and

$$\begin{aligned} 10^6 v_0 = & 117.874 + 0.15(-1)^C + 0.25275 T \\ & + 5.48 \cdot 10^{-4} T^2 - 4.246 \cdot 10^{-7} T^3 \\ & + (C - 6)(1.27 - 9 \cdot 10^{-4} T)(13.27 + 0.025C) \end{aligned} \quad (\text{II.4.14})$$

where C is the number of carbon atoms in the molecule and T the temperature in [K].

In order to evaluate the performance of the hard-sphere scheme for the pure alkanes in the ternary system (n-tridecane and 2,2,4,4,6,8,8-heptamethylnonane), a

comparison of the predicted viscosities with the experimental values (Daugé et al. 1999 and Daugé et al. 2001) have been performed. In the viscosity predictions the experimental densities have been used in order to obtain ν . For n-tridecane an AAD of 2.81% and an MxD of 8.30% are obtained, which is of the same order as the experimental uncertainty ($\pm 2.0\%$). The obtained AAD and MxD for 2,2,4,4,6,8,8-heptamethylnonane are 11.1% and 34.5%, respectively. These results can be explained by the fact that 2,2,4,4,6,8,8-heptamethylnonane is a branched alkane and that Eqs.(II.4.13) and (II.4.14) have mainly been derived for n-alkanes. Although, the hard-sphere scheme has been applied to seven aromatic hydrocarbons (Assael et al. 1992d), only an expression for ν_0 has been derived, but none for R_η . Due to this the hard-sphere scheme can not directly be applied to the viscosity prediction of 1-methylnaphthalene.

In order to apply the hard-sphere scheme to 2,2,4,4,6,8,8-heptamethylnonane and 1-methylnaphthalene a direct modeling of R_η and ν_0 has been carried out by Daugé (1999), based on the following assumptions that R_η is independent of the temperature and the $a_{\eta,i}$ parameters are universal. Based on the ν_0 values determined by Daugé (1999) the following expressions have been derived for 2,2,4,4,6,8,8-heptamethylnonane

$$10^6 \nu_0 = 272.252 - 0.2193951T + 1.54762 \cdot 10^{-4} T^2 \quad (\text{II.4.15})$$

and for 1-methylnaphthalene

$$10^6 \nu_0 = 159.263 - 0.270627T + 3.45238 \cdot 10^{-4} T^2 \quad (\text{II.4.16})$$

where T is the temperature in [K]. The estimated values for R_η by Daugé (1999) are 0.8981754 for 2,2,4,4,6,8,8-heptamethylnonane and 0.6558272 for 1-methylnaphthalene. For 2,2,4,4,6,8,8-heptamethylnonane an AAD of 3.59% and an MxD of 23.8% are obtained, whereas the obtained AAD and MxD for 1-methylnaphthalene are 2.08% and 14.8%, respectively. In spite that a direct viscosity modeling has been performed for 2,2,4,4,6,8,8-heptamethylnonane the obtained AAD still remain higher than the AAD obtained for 1-methylnaphthalene or n-tridecane. One reason can be the complex chemical structure of the compound.

In order to apply the hard-sphere scheme to mixtures, Assael et al. (1992c) introduced the following linear mixing rules

	NP	AAD%	MxD%	Bias
1-Methylnaphthalene	42	2.08	14.8	-0.59
n-Tridecane	42	2.81	8.30	-0.99
2,2,4,4,6,8,8-Heptamethylnonane (HMN)	42	3.59	23.8	-1.69
1-Methylnaphthalene + n-Tridecane	294	3.89	12.9	1.75
1-Methylnaphthalene + HMN	294	6.52	23.6	5.42
n-Tridecane + HMN	294	7.17	17.4	6.46
1-Methylnaphthalene + n-Tridecane + HMN	882	9.92	23.6	9.84

Table II.4. Results for viscosity predictions with the hard-sphere scheme.

$$v_{0,mix} = \sum_{i=1}^n x_i v_{0,i} \quad ; \quad R_{\eta,mix} = \sum_{i=1}^n x_i R_{\eta,i} \quad ; \quad M_{w,mix} = \sum_{i=1}^n x_i M_{w,i} \quad (\text{II.4.17})$$

The obtained AAD, MxD and Bias for the three binary systems and the ternary are given in Table II.4. As it can be seen from Table II.4 the highest deviations are found for mixtures containing 2,2,4,4,6,8,8-heptamethylnonane. For these mixtures the viscosity is over predicted, as indicated by the Bias. However the obtained results are satisfactory, taking into account that for mixtures the viscosity predictions are totally predictive and only based on pure component properties.

II.4.3 The Free-Volume Viscosity Model

Based on the concepts of the free-volume Allal et al. (2001a) and Allal et al. (2001b) proposed a model for accurate viscosity modeling of dense fluids over wide ranges of temperature and pressure. This model has been derived by combining the free-volume model of Doolittle (1951) using an expression for the free volume fraction derived by Allal et al. (1996) with the relation between viscosity and microstructure defined as the product of the fluid shear modulus and the mean relaxation time of the molecule.

Based on the relation between the viscosity and microstructure Allal et al. (2001a) obtained the following expression for the viscosity

$$\eta = \frac{\rho N_A L^2 \zeta}{M_w} \quad (\text{II.4.18})$$

where ρ is the density, N_A Avogadro's constant, L an average characteristic molecular quadratic length, M_w the molecular weight, and ζ the friction coefficient of a molecule related to the mobility of the molecule. The free-volume model of Doolittle (1951) is defined as

$$\eta = A \exp \left[\frac{B}{f_v} \right] \quad (\text{II.4.19})$$

where the free volume fraction $f_v = (v - v_0)/v_0$ with v the molecular volume and v_0 the hard-core volume. Allal et al. (1996) defined the free-volume fraction as

$$f_v = \left(\frac{2RT}{E} \right)^{3/2} \quad (\text{II.4.20})$$

It has been assumed (Allal et al. 2001a) that $E = E_0 + PM_w/\rho$, where the term PM_w/ρ is related to the energy necessary to form a free space available for a molecule to diffuse and E_0 is the barrier energy, which the molecule must overcome in order to diffuse. The structure of Eq.(II.4.19) led to the proposal of the following expression for the friction coefficient

$$\zeta = \zeta_0 \exp \left[\frac{B}{f_v} \right] \quad (\text{II.4.21})$$

with

$$\zeta_0 = \frac{E}{N_A b_f} \left(\frac{M_w}{3RT} \right)^{1/2} \quad (\text{II.4.22})$$

Thus, the quantity ζ_0 can be determined when $f_v \gg B$, corresponding to a dilute system. The general expression of the free-volume viscosity model is obtained by combining Eqs.(II.4.18), (II.4.20), (II.4.21), and (II.4.22) and shown below

$$\eta = \rho l \frac{\left(E_0 + \frac{P M_w}{\rho} \right)}{\sqrt{3 R T M_w}} \exp \left[B \left(\frac{E_0 + \frac{P M_w}{\rho}}{2 R T} \right)^{3/2} \right] \quad (\text{II.4.23})$$

where the energy E_0 , the coefficient B and the length $l = L^2/b_f$ are three characteristic parameters of the fluid. The unit for the viscosity is [Pa s], when all other units are kept in SI units. The following mixing rules have been proposed by Allal et al. (2001b) in

	E_0 [J/mole]	B	l [Å]
1-Methylnaphthalene	98457.01	0.041560	0.238068
n-Tridecane	119794.93	0.022007	0.493328
2,2,4,4,6,8,8-Heptamethylnonane	123054.48	0.031684	0.289637

Table II.5. Characteristic parameters for pure compounds used in the free-volume model (Daugé 1999).

order to obtain the three characteristic parameters and the molecular weight for an n component mixture

$$M_w = \sum_{i=1}^n x_i M_{w,i} \quad ; \quad E_0 = \sum_{i=1}^n \sum_{j=1}^n x_i x_j \sqrt{E_{0,i} E_{0,j}} \quad (\text{II.4.24})$$

$$B = \sum_{i=1}^n x_i B_i \quad ; \quad \frac{1}{l} = \sum_{i=1}^n \frac{x_i}{l_i} \quad (\text{II.4.25})$$

where x_i is the mole fraction of compound i . For the three studied compounds in this work, the three pure characteristic parameters have been estimated by Daugé (1999) and reported in Table II.5.

The free-volume model is related to the density of the fluid and due to this the viscosity predictions have been carried out using the experimental densities reported in Appendix B1, Daugé et al. (1999), Daugé et al. (2001), and Canet et al. (2001). A comparison between the predicted viscosities using the free-volume model and the experimental values has been performed and the obtained AAD, MxD and Bias are given in Table II.6 for the three pure compounds, their binary and ternary mixtures. As it can be seen from Table II.6 relative large deviations are obtained for the ternary and the binary mixtures, except for n-tridecane + 2,2,4,4,6,8,8-heptamethylnonane, compared to the deviations obtained for the pure compounds. A study of the mixing rules in the free-volume model has been carried out by Canet (2001). Based on this study the following modifications of the original mixing rules have been proposed in order to obtain B and l

$$\frac{1}{B} = \sum_{i=1}^n \frac{x_i}{B_i} \quad ; \quad l = \sum_{i=1}^n x_i l_i \quad (\text{II.4.26})$$

	NP	AAD%	MxD%	Bias
1-Methylnaphthalene	42	2.45	11.3	-0.40
n-Tridecane	42	2.28	9.07	0.04
2,2,4,4,6,8,8-Heptamethylnonane (HMN)	42	1.85	11.1	-0.17
1-Methylnaphthalene + n-Tridecane	294	16.2	33.1	16.2
1-Methylnaphthalene + HMN	294	10.8	21.0	10.8
n-Tridecane + HMN	294	2.77	13.8	1.60
1-Methylnaphthalene + n-Tridecane + HMN	882	13.6	34.7	13.6

Table II.6. Results for viscosity predictions with the free-volume model using experimental densities in conjunction with the mixing rules given in Eqs.(II.4.24) and (II.4.25).

Using these mixing rules along with those given for M_w and E_0 in Eq.(II.4.24) the following results reported in Table II.7 are obtained. The AAD obtained now are of the same order as the uncertainty reported for the experimental viscosities ($\pm 2.0\%$) and in agreement with the AAD obtained for the pure compounds. The overall MxD (13.1%) for the ternary system is obtained for the binary mixture composed of 75 mole% 1-methylnaphthalene and 25 mole% n-tridecane at 353.15 K and 1 bar. The obtained results are very satisfactory, especially taking into account the simple structure of the model, since only three adjustable parameters are needed for each pure compound along

	NP	AAD%	MxD%	Bias
1-Methylnaphthalene	42	2.45	11.3	-0.40
n-Tridecane	42	2.28	9.07	0.04
2,2,4,4,6,8,8-Heptamethylnonane (HMN)	42	1.85	11.1	-0.17
1-Methylnaphthalene + n-Tridecane	294	2.68	13.1	1.03
1-Methylnaphthalene + HMN	294	5.83	12.5	5.69
n-Tridecane + HMN	294	2.93	8.36	-1.43
1-Methylnaphthalene + n-Tridecane + HMN	882	2.92	9.86	1.18

Table II.7. Results for viscosity predictions with the free-volume model using experimental densities in conjunction with the mixing rules given in Eqs.(II.4.24) and (II.4.26).

with the experimental density of the fluid. By comparing the deviations obtained by the free-volume model (Table II.7) with those obtained by the hard-sphere scheme (Table II.4), it can be seen that better results are obtained with the free-volume approach.

II.4.4 The Friction Theory

Starting from basic principles of mechanics and thermodynamics Quiñones-Cisneros et al. (2000) developed the friction theory (*f-theory*) for viscosity modeling and is described in Section I.7.1. In the *f-theory* the total viscosity is separated into a dilute gas viscosity term η_0 and a residual friction term η_f

$$\eta = \eta_0 + \eta_f \quad (\text{II.4.27})$$

The dilute gas viscosity η_0 is defined as the viscosity at the zero density limit, while the residual friction contribution η_f is related to friction concepts of classical mechanics. The residual friction term can be expressed as follows

$$\eta_f = \kappa_a p_a + \kappa_r p_r + \kappa_{rr} p_r^2 \quad (\text{II.4.28})$$

where κ_a , κ_r , and κ_{rr} are temperature dependent friction coefficients, p_a and p_r are the van der Waals attractive and repulsive pressure terms. The attractive and repulsive pressure terms can be obtained from simple cubic equations of state (EOS), such as the Soave-Redlich-Kwong (SRK) EOS (Soave 1972) and the Peng-Robinson (PR) EOS (Peng and Robinson 1976). The capability of this viscosity approach has been illustrated by modeling the viscosity of primarily n-alkanes and their mixtures, representing simple petroleum fractions, over wide ranges of temperature and pressure, see Quiñones-Cisneros et al. (2000) and Section I.7. Based on this concept and a corresponding states behavior Quiñones-Cisneros et al. (2001) derived a general one-parameter *f-theory* model for hydrocarbons with a simple molecular structure. In this model the only required parameter, which has to be determined, is the characteristic critical viscosity of the pure compounds. This model is presented in Section I.7.4.

The viscosity of the ternary system has been evaluated using the general one-parameter *f-theory* model in conjunction with the PR EOS and without any binary interaction parameters. All required pure component properties (T_c , P_c , ω , and v_c) for 1-

methylnaphthalene and n-tridecane have been taken from the DIPPR Data Compilation (Daubert and Danner 1989) and given in Table II.8. The critical properties for 2,2,4,4,6,8,8-heptamethylnonane have been estimated from experimental $P\rho T$ data by a least squares fit due to the fact that these properties are not reported in the open literature. The derived critical properties for 2,2,4,4,6,8,8-heptamethylnonane are reported in Table II.8 along with the critical molar volume obtained from Eq.(I.7.43). With these properties, the PR EOS can reproduce the density of 2,2,4,4,6,8,8-heptamethylnonane with an AAD of 0.60% and an MxD of 1.63% at 293.15 K and 1000 bar.

Thus for each of the three pure compounds, the characteristic critical viscosity used in the general one-parameter f -theory model has to be estimated in order to apply this viscosity approach to the ternary system. Since, the viscosity of 2,2,4,4,6,8,8-heptamethylnonane increases rapidly with pressure due to interlinking effects, the performance of the general one-parameter PR f -theory model has been studied by modeling the viscosity of 2,2,4,4,6,8,8-heptamethylnonane. The direct modeling of 2,2,4,4,6,8,8-heptamethylnonane results in an AAD of 17.1% with an MxD of 53.2% at 293.15 K and 1000 bar. These results are relative high for a direct modeling of a pure fluid. The performance of the general one-parameter PR f -theory model is shown in Figure II.22, indicating that the viscosity is not modeled properly at high pressures or high temperatures. The reason is that the viscosity of 2,2,4,4,6,8,8-heptamethylnonane increases drastically at low temperatures due to interlinking effects when brought under pressure. Further, the temperature dependency of the viscosity of 2,2,4,4,6,8,8-heptamethylnonane is more pronounced than for simple fluids, such as n-alkanes.

	T_c [K]	P_c [bar]	ω	v_c [cm ³ /mole]
1-Methylnaphthalene*	772.04	36.6	0.3478	523
n-Tridecane*	675.80	17.225	0.6186	770
2,2,4,4,6,8,8-Heptamethylnonane	608.904	14.9819	0.580578	799.901

Table II.8. Critical properties.

* Taken from DIPPR Data Compilation (Daubert and Danner 1989).

When a fluid is brought under pressure, the distance between the molecules decreases and as a consequence the short-range repulsive forces will dominate over the long-range attractive forces. As it has been shown by Quiñones-Cisneros et al. (2000), the dominating friction contribution to the total viscosity at high pressures is related to the repulsive friction term. Based on this and in order to apply the *f-theory* models to fluids such as 2,2,4,4,6,8,8-heptamethylnonane and its mixtures, it has been found that a simple extension of the *f-theory* models from a quadratic to a third order p_r corrective

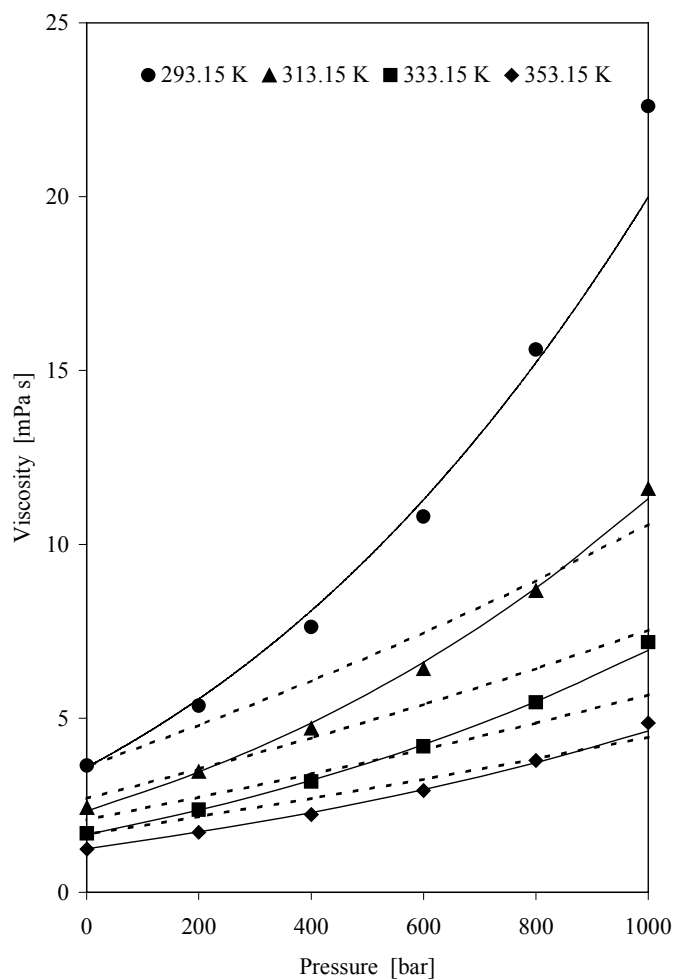


Figure II.22 Performance of the viscosity modeling of 2,2,4,4,6,8,8-heptamethylnonane using the general PR *f-theory* model (---) and the third order corrected general PR *f-theory* model (—). The points indicate the experimental values taken from Daugé et al. (2001).

term can take such dragging forces into account. Thus, a third order *f-theory* model can be written in the form

$$\eta_f = \kappa_a p_a + \kappa_r p_r + \kappa_{rr} p_r^2 + \kappa_{rrr} p_r^3 \quad (\text{II.4.29})$$

Based on this, appropriate viscosity modeling can be achieved for fluids, such as 2,2,4,4,6,8,8-heptamethylnonane, when a third order repulsive correction to the general one-parameter *f-theory* model is introduced. Thus, Eq.(II.4.29) can be written as

$$\eta_f = \eta^{GM} + \eta^{III} \quad (\text{II.4.30})$$

where η^{GM} is the friction viscosity term of the general model, defined in Section I.7.4 and η^{III} is a third order correction to the general model defined as

$$\eta^{III} = \kappa_{rrr} p_r^3 \quad (\text{II.4.31})$$

The temperature dependency for the friction coefficient κ_{rrr} can be described as follows

$$\kappa_{rrr} = d_2 (\exp(2\Gamma) - 1) (\Gamma - 1)^3 \quad (\text{II.4.32})$$

with

$$\Gamma = \frac{T_c}{T} \quad (\text{II.4.33})$$

With this approach, the modeling of the viscosity of the pure compounds requires the fitting of two parameters per compound: the characteristic critical viscosity η_c , used in the general *f-theory* model, and the d_2 constant. Thus, a least squares fit to the viscosity data of 2,2,4,4,6,8,8-heptamethylnonane results in an AAD of 2.43% and the MxD is found to be 11.6% at 293.15 K and 1000 bar. The performance of this PR *f-theory* model is shown in Figure II.22. The viscosity modeling at high pressure is significantly improved and the AAD is of the same order as the experimental uncertainty ($\pm 2\%$). The above-mentioned *f-theory* approach has also been applied to 1-methylnaphthalene and n-tridecane. The derived parameters for the three pure compounds are reported in Table II.9. The dilute gas viscosity of the pure compounds has been obtained by the Chung et al. model (Chung et al. 1988), described in Section I.2.1. The obtained AAD and MxD from the modeling of the pure compounds are reported in Table II.10. For 1-methylnaphthalene the third order corrected general PR *f-theory* model gives an AAD of 2.19% and an MxD of 12.8% at 293.15 K and 1000 bar. In the case of n-tridecane an AAD of 1.91% and an MxD of 10.2% at 293.15 K and 400 bar are obtained. These

	η_c [μP]	d_2 [$\mu\text{P}/\text{bar}^3$]
1-Methylnaphthalene	340.458	$1.05763 \cdot 10^{-9}$
n-Tridecane	240.550	$1.80168 \cdot 10^{-10}$
2,2,4,4,6,8,8-Heptamethylnonane	580.515	$2.14681 \cdot 10^{-7}$

Table II.9. Characteristic critical viscosity η_c and third order PR friction constant d_2 .

results are in agreement with the experimental uncertainty.

For the three binary systems and the ternary, the dilute gas viscosity is obtained by the mixing rule given in Eq.(I.7.25) (Quiñones-Cisneros et al. 2000). This mixing rule is based on the dilute gas viscosity of the pure components. The mixture PR general model contribution, η^{GM} , in Eq.(II.4.30) is treated according to the mixing rules given by Quiñones-Cisneros et al. (2001), and the mixture third order friction coefficient, κ_{rrr} , is obtained with an exponential mixing rule of the form

$$\ln(\kappa_{rrr}) = \sum_{i=1}^n x_i \ln(\kappa_{rrr,i}) \quad (\text{II.4.34})$$

where subscript i refers to pure component i . Further, it should be stressed that no binary interaction parameters have been used in the EOS mixing rules. A comparison of the predicted viscosities using this scheme with the experimental values has been carried out and the results are reported in Table II.10. Given the kind of viscosity behavior this ternary system develops; see e.g. Chapter II.3, Daugé et al. (1999), Daugé

	NP	AAD%	MxD%	Bias
1-Methylnaphthalene	42	2.19	12.8	-0.13
n-Tridecane	42	1.91	10.2	0.29
2,2,4,4,6,8,8-Heptamethylnonane (HMN)	42	2.43	11.6	-0.10
1-Methylnaphthalene + n-Tridecane	294	1.91	16.5	-0.18
1-Methylnaphthalene + HMN	294	5.84	12.5	4.81
n-Tridecane + HMN	294	5.85	26.7	-4.26
1-Methylnaphthalene + n-Tridecane + HMN	882	4.49	24.1	-0.55

Table II.10. Results for viscosity predictions with the friction theory using the PR EOS.

et al. (2001), and Canet et al. (2001), the obtained results for the binary and ternary mixtures are satisfactory taking into account that they have been obtained by a totally predictive method based on pure component properties and related to a cubic EOS. The overall MxD (26.7%) is obtained for the binary system composed of 25 mole% n-tridecane and 75 mole% 2,2,4,4,6,8,8-heptamethylnonane at 293.15 K and 1000 bar. A comparison of the results given in Table II.10 for the *f-theory* with those given in Table II.7 for the free-volume model using experimental densities shows that similar results are obtained, except for the binary system n-tridecane + 2,2,4,4,6,8,8-heptamethylnonane and the ternary, where the free-volume model gives slightly better results. One reason could be that the molecular structure of these mixtures may be better related to the free volume, as mentioned in Chapter II.1, than to a cubic EOS due to the possible induced interlinking between the molecules of n-tridecane and 2,2,4,4,6,8,8-heptamethylnonane, resulting in a higher viscosity.

II.4.5 The LBC Model

In addition and for comparison purposes the viscosity of the studied ternary system has also been predicted with the Lohrenz-Bray-Clark (LBC) model (Lohrenz et al. 1964). This model is widely used in the oil industry and is a sixteenth degree polynomial in the reduced density.

$$\left[(\eta - \eta_0)^\xi + 10^{-4} \right]^{1/4} = d_0 + d_1 \rho_r + d_2 \rho_r^2 + d_3 \rho_r^3 + d_4 \rho_r^4 \quad (\text{II.4.35})$$

where $\rho_r = \rho / \rho_c$ is the reduced density, η_0 the dilute gas viscosity limit and ξ the viscosity-reducing parameter. The LBC model is described in details in Section I.2.2.1. In principle, the optimal performance with the LBC model should be obtained, when the experimental densities are used. Therefore, the experimental densities reported by Daugé et al. (1999), Daugé et al. (2001), Canet et al. (2001), and in Appendix B1 have been used in conjunction with the calculation procedure originally derived for the LBC model. The necessary critical properties have been taken from Table II.8. The obtained AAD, MxD, and Bias are given in Table II.11. Thus, very large deviations are obtained with the LBC model for this ternary system representing some simple petroleum distillation cuts, although that the experimental densities have been used.

	NP	AAD%	MxD%	Bias
1-Methylnaphthalene	42	317	431	317
n-Tridecane	42	49.6	68.0	-49.6
2,2,4,4,6,8,8-Heptamethylnonane (HMN)	42	93.1	98.1	-93.1
1-Methylnaphthalene + n-Tridecane	294	69.3	284	49.3
1-Methylnaphthalene + HMN	294	67.0	124	-46.3
n-Tridecane + HMN	294	79.7	97.2	-79.7
1-Methylnaphthalene + n-Tridecane + HMN	882	56.2	95.6	-51.6

Table II.11. Results for viscosity predictions with the LBC model using experimental densities and the critical properties from Table II.8.

An important property in the LBC model is the critical molar volume v_c . Due to this, a very common procedure within the oil industry, in order to improve the viscosity calculations with the LBC model, is to tune the model with respect to the critical volume of the considered fluid. However, since mixing rules have been derived for the critical volume in the LBC model, only a tuning of the critical volumes of the pure compounds has been performed in order to improve the viscosity predictions. By minimizing the least squares the critical volume of each pure compound has been determined using the experimental densities and viscosities. For 1-methylnaphthalene $v_c = 469.114 \text{ cm}^3/\text{mole}$, while $v_c = 814.470 \text{ cm}^3/\text{mole}$ for n-tridecane and $v_c = 1018.79 \text{ cm}^3/\text{mole}$ for 2,2,4,4,6,8,8-heptamethylnonane. For the binary systems and the ternary, the resultant AAD, MxD, and Bias are given in Table II.12 using the adjusted critical volumes. All other properties have been taken from Table II.8. Although, that a tuning of the critical volumes of the pure compounds improves the performance of the LBC model significantly, the AAD and MxD obtained with the LBC model are much higher than the resultant AAD and MxD reported for the hard-sphere scheme (Table II.4), the free-volume model (Table II.7), or the friction theory (Table II.10), and even compared with the ideal mixing laws (Table II.1) (Grunberg-Nissan and Katti-Chaudhri). Further, it should be stressed that the deviations obtained with the LBC model increase significantly as the fluids become more viscous (higher viscosity). The

	NP	AAD%	MxD%	Bias
1-Methylnaphthalene	42	17.9	55.1	-7.67
n-Tridecane	42	9.20	32.4	-1.70
2,2,4,4,6,8,8-Heptamethylnonane (HMN)	42	20.5	63.5	-7.75
1-Methylnaphthalene + n-Tridecane	294	16.8	53.2	9.62
1-Methylnaphthalene + HMN	294	26.3	66.1	13.6
n-Tridecane + HMN	294	15.5	57.7	0.87
1-Methylnaphthalene + n-Tridecane + HMN	882	23.0	64.6	16.0

Table II.12. Results for viscosity predictions with the LBC model using experimental densities and tuned v_c values.

reason is that the LBC model and its constants was originally derived from experimental viscosity and density data of light fluids and hydrocarbons, which have a much lower viscosity than observed for the ternary system 1-methylnaphthalene + n-tridecane + 2,2,4,4,6,8,8-heptamethylnonane. Due to this, the LBC model will have problems calculating the viscosity of heavy hydrocarbons, as shown previously in Chapter I.5. But as Alliez et al. (1998) stated, no significant improvements of the viscosity predictions are obtained by increasing the degree of the polynomial in the LBC model.

II.4.6 The Self-Reference Model

Kanti et al. (1989) derived a self-reference model in order to calculate the viscosity of liquid petroleum fluids versus pressure and temperature using only the viscosity measured at atmospheric pressure for a selected reference temperature, generally close to room temperature. This model is based on the approach derived by Kashiwagi and Makita (1982). In the approach of Kashiwagi and Makita (1982) the liquid viscosity of a fluid versus pressure for a given temperature is related to the measured viscosity at atmospheric pressure and the corresponding temperature. In this way, it is assumed that the measured viscosity value contains within itself sufficient information about the studied fluid. The proposed model of Kashiwagi and Makita (1982) is presented below

$$\ln\left(\frac{\eta(P, T)}{\eta(0.1 \text{ MPa}, T)}\right) = E \ln \frac{D + P}{D + 0.1} \quad (\text{II.4.36})$$

where D and E are adjustable parameters dependent on the temperature and the fluid. Consequently, measurements of the viscosity at atmospheric pressure are required for each temperature. In order to avoid measuring the viscosity at atmospheric pressure for every selected temperature Kanti et al. (1989) introduced the following expression adapting the relationship by van Velzen et al. (1972)

$$\eta(0.1 \text{ MPa}, T) = \eta(0.1 \text{ MPa}, T_0) \exp\left[\alpha\left(\frac{1}{T} - \frac{1}{T_0}\right)\right] \quad (\text{II.4.37})$$

with

$$\alpha = gy_0^2 + hy_0 + i \quad (\text{II.4.38})$$

and $y_0 = \ln \eta(0.1 \text{ MPa}, T_0)$. In addition, Kanti et al. (1989) also derived expressions for the temperature dependent D and E parameters

$$\begin{aligned} D + 0.1 &= dy^2 + ey + f \\ E &= ay^2 + by + c \end{aligned} \quad (\text{II.4.39})$$

with $y = \ln \eta(0.1 \text{ MPa}, T)$. By substituting Eqs.(II.4.37), (II.4.38), and (II.4.39) into Eq.(II.4.36) the approach by Kanti et al. (1989) is obtained

$$\begin{aligned} \ln\left(\frac{\eta(P, T)}{\eta(0.1 \text{ MPa}, T)}\right) &= (ay^2 + by + c) \ln\left(1 + \frac{P - 0.1}{dy^2 + ey + f}\right) \\ &\quad + (gy_0^2 + hy_0 + i) \left(\frac{1}{T} - \frac{1}{T_0}\right) \end{aligned} \quad (\text{II.4.40})$$

with

$$y = y_0 + (gy_0^2 + hy_0 + i) \left(\frac{1}{T} - \frac{1}{T_0}\right) \quad (\text{II.4.41})$$

where T_0 is the chosen reference temperature in [K] at atmospheric pressure and P in [MPa], when the following constants are used

$a =$	0.275832	$d =$	4.059832	$g =$	6.729026
$b =$	0.533739	$e =$	23.63475	$h =$	481.5716
$c =$	1.838385	$f =$	161.0261	$i =$	1278.456

The only external property required in this viscosity approach is the measured viscosity at atmospheric pressure for a selected reference temperature T_0 . Due to this, the model is referred to as a self-referring model. This model can be applied to pure compounds, synthetic mixtures, or multicomponent mixtures, such as petroleum fluids for which Kanti et al. (1989) originally derived it. The adjustable constants in the model were determined by an analysis based on n-alkanes (C_7 , C_{10} , C_{12} , C_{14} , C_{15} , C_{16} , C_{18}) and alkyl benzenes (butyl, hexyl, octyl).

The viscosity of the three pure compounds, the binary mixtures, and the ternary mixtures has been calculated using the measured viscosity at 1 bar and 293.15 K as the reference point for each fluid. The calculated values have been compared with the experimental values and the resultant AAD, MxD and Bias are given in Table II.13, but the reference point is omitted in these results. The high deviations obtained for mixtures containing 2,2,4,4,6,8,8-heptamethylnonane can be explained by the fact that the second derivative of Eq.(II.4.40) with respect to the pressure is negative. Therefore, the model does not describe the right viscosity behavior of fluids having a rapid increase in the viscosity with pressure, such as mixtures containing 2,2,4,4,6,8,8-heptamethylnonane. This has also been stated by Kashiwagi and Makita (1982).

	NP	AAD%	MxD%	Bias
1-Methylnaphthalene	41	10.8	24.0	10.7
n-Tridecane	41	5.08	10.9	-4.44
2,2,4,4,6,8,8-Heptamethylnonane (HMN)	41	21.5	45.5	-21.5
1-Methylnaphthalene + n-Tridecane	287	4.19	17.8	1.58
1-Methylnaphthalene + HMN	287	10.3	39.4	-8.02
n-Tridecane + HMN	287	10.4	37.7	-10.1
1-Methylnaphthalene + n-Tridecane + HMN	861	8.35	43.7	-7.50

Table II.13. Results for viscosity predictions with the self-referring model using $T_0 = 293.15$ K as the reference temperature for each mixture.

II.4.7 Corresponding States Model

Viscosity models based on the corresponding states principle are common. These models are normally based on one to three reference fluids. The corresponding states model (the CS2 model) for hydrocarbon fluids proposed by Aasberg-Petersen et al. (1991) uses two reference fluids; methane and n-decane. The CS2 model is given by

$$\ln \eta_{r,x} = \ln \eta_{r,1} + K_{CS} (\ln \eta_{r,2} - \ln \eta_{r,1}) \quad (\text{II.4.42})$$

with the interpolation parameter

$$K_{CS} = \frac{M_{w,x} - M_{w,1}}{M_{w,2} - M_{w,1}} \quad (\text{II.4.43})$$

where η_r is the reduced viscosity, subscript x refers to the fluid considered whereas subscripts 1 and 2 refer to the two reference fluids, respectively methane and n-decane.

The calculated viscosities for the ternary system using the CS2 model have been compared with the experimental values and the resultant AAD, MxD and Bias are given in Table II.14. The calculation procedure is described in Section I.2.3.2. Thus, in Chapter I.6 it has been shown that the viscosity calculations of heavy hydrocarbons with the CS2 model can be improved by using the modification of the K_{CS} interpolation parameter proposed by Et-Tahir (1993)

$$K_{CS} = \frac{1}{4} \left(\frac{M_{w,x} - M_{w,1}}{M_{w,2} - M_{w,1}} + \frac{\omega_x - \omega_1}{\omega_2 - \omega_1} + \frac{P_{c,x} - P_{c,1}}{P_{c,2} - P_{c,1}} + \frac{T_{c,x} - T_{c,1}}{T_{c,2} - T_{c,1}} \right) \quad (\text{II.4.44})$$

	NP	AAD%	MxD%	Bias
1-Methylnaphthalene	42	25.8	44.5	25.4
n-Tridecane	42	14.2	29.6	14.1
2,2,4,4,6,8,8-Heptamethylnonane (HMN)	42	57.7	79.3	-57.7
1-Methylnaphthalene + n-Tridecane	294	28.0	54.2	27.9
1-Methylnaphthalene + HMN	294	27.8	74.4	-21.5
n-Tridecane + HMN	294	25.3	72.2	-24.3
1-Methylnaphthalene + n-Tridecane + HMN	882	16.7	66.1	-7.50

Table II.14 Results for viscosity predictions with the original CS2 model (Aasberg-Petersen et al. 1991).

	NP	AAD%	MxD%	Bias
1-Methylnaphthalene	42	8.98	25.0	5.92
n-Tridecane	42	5.20	16.0	3.52
2,2,4,4,6,8,8-Heptamethylnonane (HMN)	42	68.7	85.2	-68.7
1-Methylnaphthalene + n-Tridecane	294	14.9	31.9	14.3
1-Methylnaphthalene + HMN	294	37.7	81.3	-37.2
n-Tridecane + HMN	294	37.8	79.7	-37.8
1-Methylnaphthalene + n-Tridecane + HMN	882	23.6	74.6	-22.5

Table II.15 Results for viscosity predictions with the CS2 model using the modified K_{CS} interpolation parameter defined in Eq.(II.4.44).

Using this expression for the K_{CS} interpolation parameter in the CS2 model, the obtained deviations between calculated and experimental viscosities are given in Table II.15. By comparing the AAD and MxD values reported in Table II.15 and Table II.14, it can be seen that the performance of the CS2 model is significantly improved for 1-methylnaphthalene, n-tridecane, and their binary mixtures, when the modified K_{CS} interpolation parameter is used. However, for fluids containing 2,2,4,4,6,8,8-heptamethylnonane slightly better results are obtained with the original CS2 model. The present structure of the CS2 model is not capable of describing the viscosity behavior of fluids containing 2,2,4,4,6,8,8-heptamethylnonane. The viscosity of these fluids is under predicted.

II.4.8 The PRVIS Model

Based on the similarity of PvT and $T\eta P$ relationships Guo et al. (1997) and Guo (1998) developed a general viscosity model for hydrocarbon fluids related to the Peng-Robinson EOS (Peng and Robinson 1976) by interchanging the temperature T and the pressure P , replacing the molar volume v with the viscosity η , and replacing the gas constant R with the quantity r . The general structure of this model, referred to as the PRVIS model, is

	NP	AAD%	MxD%	Bias
1-Methylnaphthalene	42	59.2	83.0	-59.2
n-Tridecane	42	19.4	54.9	-17.4
2,2,4,4,6,8,8-Heptamethylnonane (HMN)	42	74.8	92.1	-74.8
1-Methylnaphthalene + n-Tridecane	294	34.9	78.9	-34.8
1-Methylnaphthalene + HMN	294	64.4	90.7	-64.4
n-Tridecane + HMN	294	49.7	89.1	-49.7
1-Methylnaphthalene + n-Tridecane + HMN	882	49.9	87.4	-49.9

Table II.16 Results for viscosity predictions with the PRVIS model.

$$T = \frac{r P}{\eta - b'} - \frac{a}{\eta(\eta + b) + b(\eta - b)} \quad (\text{II.4.45})$$

This model does not dependent on the density of the fluid.

The PRVIS model, described in Section I.2.4, has been evaluated by comparing the calculated viscosities with the experimental values of the ternary system. The viscosity calculations have been performed using the critical properties given in Table II.8 and without any binary interaction parameters. The obtained deviations are reported in Table II.16. For the studied ternary system the PRVIS model generally under predicts the viscosity, especially for fluids containing 2,2,4,4,6,8,8-heptamethylnonane. It should be mentioned that one way to improve the performance of the PRVIS model will be to carry out a direct modeling of the pure compounds in order to obtain the required pure component parameters used in the model. The reason is that the viscosity calculations with the PRVIS model are related to properties of pure compounds.

II.4.9 Comparison of Models

In addition and for comparison purposes the performance of the evaluated viscosity models is shown in Figure II.23 and Figure II.24 for all of the 1890 experimental data points of the ternary system, except in the case of the classical mixing rules (Grunberg-Nissan and Katti-Chaudhri). The plots presented in Figure II.23 show the calculated

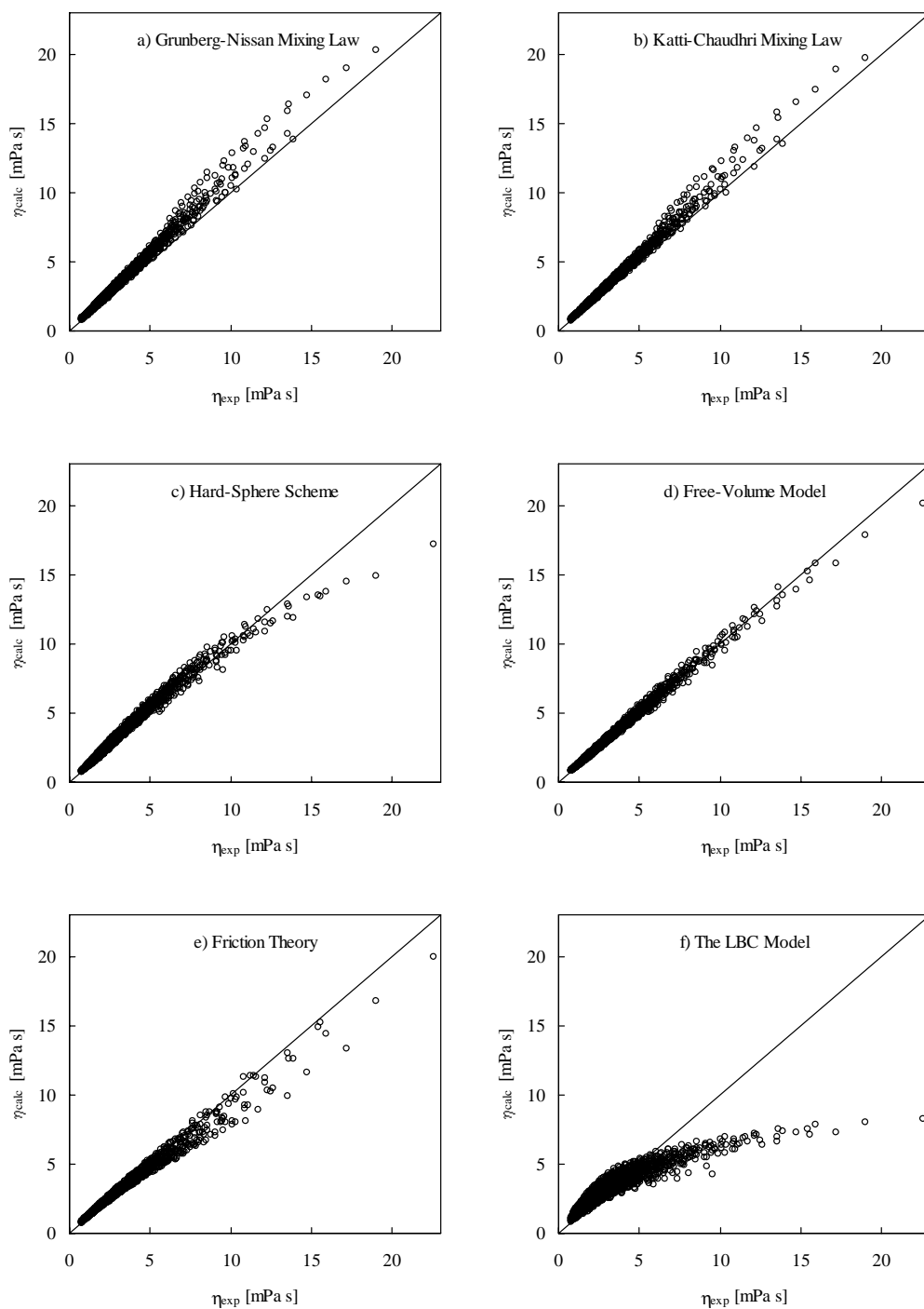


Figure II.23 Calculated viscosities versus the experimental viscosity for all measured points (1890) of the pure compounds (except in Figures a) and b)), the binary and ternary mixtures of the ternary system 1-methylnaphthalene + n-tridecane + 2,2,4,4,6,8,8-heptamethylnonane.

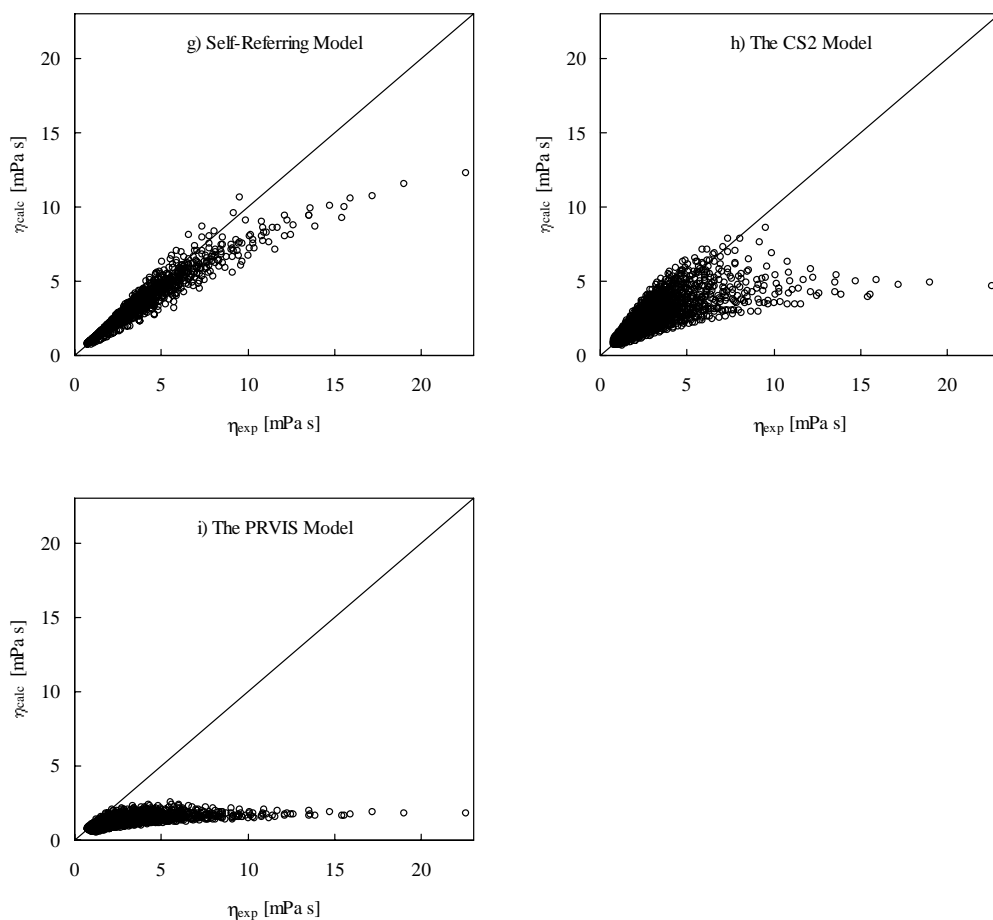


Figure II.23 Continued.

viscosities versus the experimental values. In case that the calculated viscosity is equal to the experimental value the point should lie on the diagonal line. In Figure II.24 the deviation is plotted against the experimental viscosity. From Figures II.23 and II.24 it can be seen that the free-volume model gives slightly better results than the general PR *f-theory* model. However, it should be stressed that the viscosity estimations with the free-volume model have been performed using experimental densities, whereas the viscosity estimations with the general PR *f-theory* model do not depend on the density of the considered fluid. The *f-theory* results have been obtained using a simple cubic EOS in order to estimate the attractive and repulsive pressure terms. It has already been mentioned in previous sections that viscosity approaches based on the concepts of

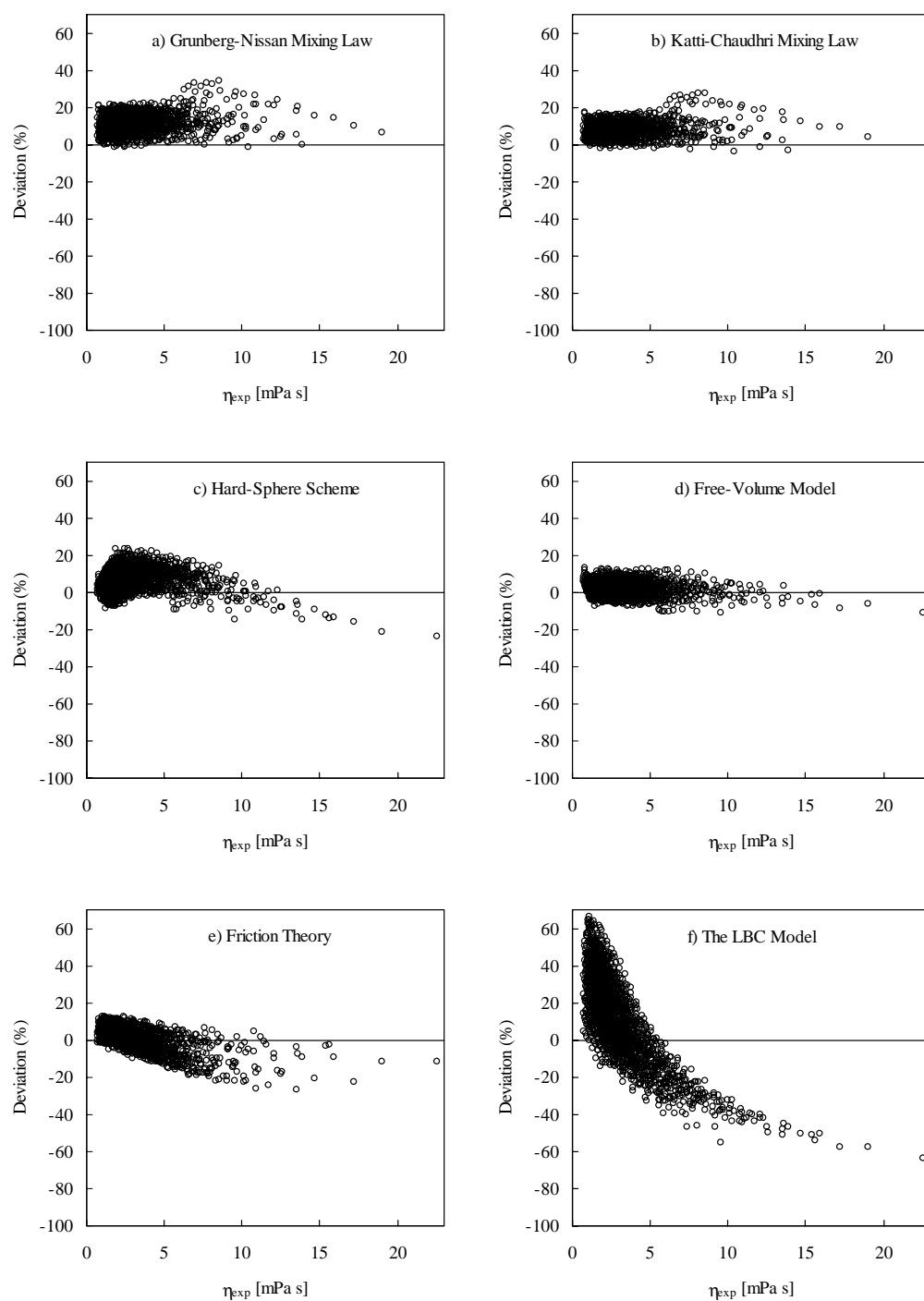


Figure II.24 Performance of viscosity models shown as the deviations versus the experimental viscosity for all measured points (1890) of the pure compounds (except in Figures a) and b)), the binary and ternary mixtures of the ternary system 1-methylnaphthalene + n-tridecane + 2,2,4,4,6,8,8-heptamethylnonane.

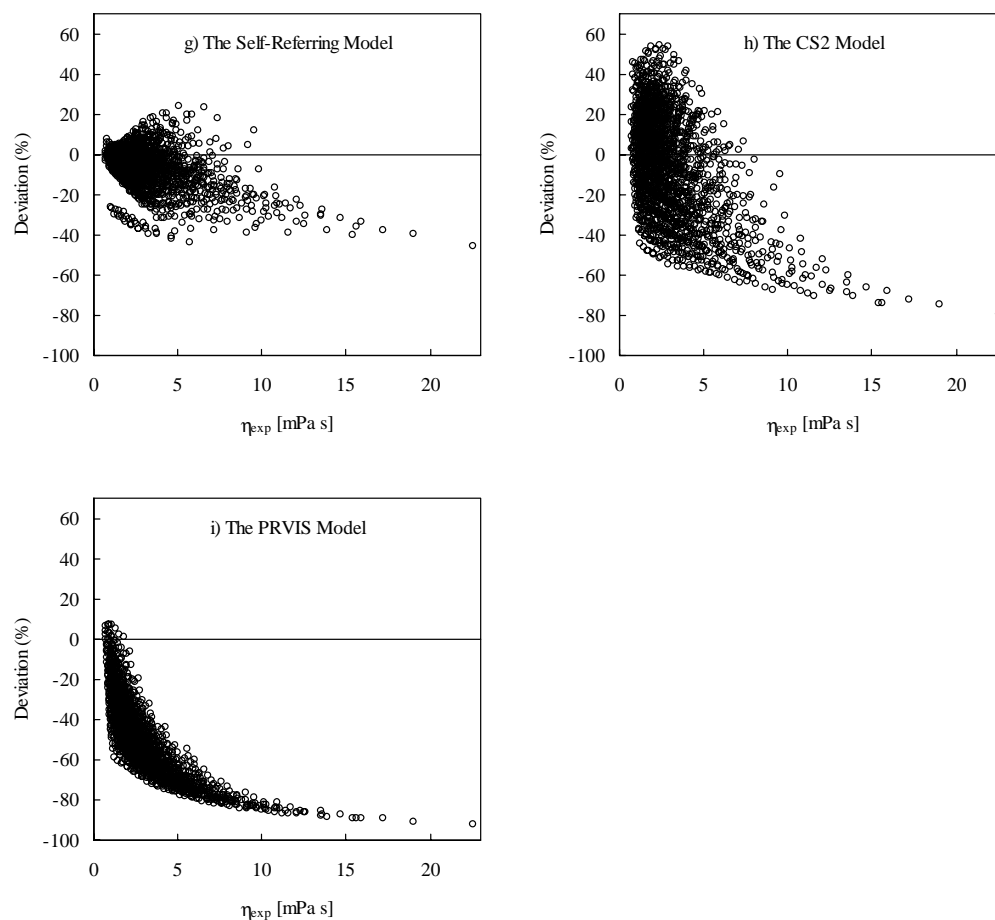


Figure II.24 *Continued.*

the free-volume may describe and represent accurately the kind of viscosity behavior this ternary system develops. Thus, the free-volume model and the *f-theory* model estimate the viscosities of this ternary system within or close to the experimental uncertainty (2%). The viscosity estimations with the hard-sphere scheme are also satisfactorily. These three models have a physical and a theoretical background and they represent three different aspects in viscosity modeling and prediction. Thus, the performance of the classical mixing laws can also be considered satisfactorily, in the sense of their simplicity. For the widely used LBC model, in spite of the optimization of the critical volume of the pure compounds, the deviations obtained are higher than those

found for the classical mixing laws and the self-referring model. For this ternary system, all models, except the classical mixing rules, under predict the viscosity of fluids having a high viscosity, corresponding to mixtures containing 2,2,4,4,6,8,8-heptamethylnonane. This under prediction is especially pronounced for the LBC model, the self-referring model, the CS2 model, and the PRVIS model, where the deviations are greater than 30%. However, most of the models, which show large deviations for fluids containing 2,2,4,4,6,8,8-heptamethylnonane, have mainly been derived based on n-alkanes and light hydrocarbons. These fluids do not show the same viscosity behavior as observed for this ternary system. Thus, it should be stressed that the performance of the evaluated viscosity models for this ternary system can be improved by introducing viscosity interaction parameters, as shown for the classical mixing laws in Section II.4.1.1 and II.4.1.2, or by modifying the models, e.g. by readjusting the parameters using experimental data for the specific ternary system, so they can exactly represent the viscosity behavior of this ternary system. In this case, the model will only be adequate for the considered system, and will no longer be considered a general model.

II.5 Conclusion

Using a falling body viscometer the dynamic viscosity of 21 ternary mixtures composed of 1-methylnaphthalene + n-tridecane + 2,2,4,4,6,8,8-heptamethylnonane has been measured up to 1000 bar and in the temperature range 293.15 – 353.15 K. The uncertainty in the measured values is 2.0%, except at 1 bar where a capillary tube viscometer has been used, reducing the uncertainty to less than 1.0%. In order to obtain the dynamic viscosity, the density has been measured at the same temperature conditions and up to 600 bar in steps of 50 bar. A Tait-type equation has been used to extrapolate the densities up to 1000 bar. The uncertainty in the tabulated densities is less than 1 kg/m³. The viscosity and density measurements reported in this work together with the viscosity and density measurements for the pure and binary systems reported by Daugé et al. (1999), Daugé et al. (2001), and Canet et al. (2001) represent the most comprehensive study for the ternary system 1-methylnaphthalene + n-tridecane + 2,2,4,4,6,8,8-heptamethylnonane (45 different composition), representing some simple petroleum distillation cuts at 510 K. For the studied ternary system it has been observed that repulsive interactions have an influencing effect on the viscosity. Further, a significantly increase in the viscosity has been observed for fluids containing 2,2,4,4,6,8,8-heptamethylnonane when brought under pressure compared to n-tridecane. This is related to the branched, inflexible molecular structure of 2,2,4,4,6,8,8-heptamethylnonane. In addition, this experimental viscosity and density study is also a fragmental part of a more general study concerning various systems (associative and non-associative mixtures, various binary systems with different compounds, ternary systems and even systems with more than three components) performed in Groupe Haute Pression, Université de Pau, France.

The experimental viscosity data for the ternary system 1-methylnaphthalene + n-tridecane + 2,2,4,4,6,8,8-heptamethylnonane have been used in order to evaluate the performance of nine different viscosity models, applicable to petroleum fluids. The evaluated models range from recently derived models, such as the free-volume model or the friction theory, to widely used models within the oil industry, such as the well-known LBC model. The conclusion of this evaluation and comparison of the different models, see Figures II.23 and II.24, is that the best results for this ternary system are

obtained with the free-volume model and the friction theory, which are simple viscosity approaches recently developed with a physical and theoretical background and related to characteristic parameters and properties of pure compounds. The AAD obtained for these two models for the pure compounds, the binaries and the ternary are within or close to the experimental uncertainty ($\pm 2\%$). Also the hard-sphere scheme predicts the viscosity of this ternary system properly. However, taking into account that these models are totally predictive and only depend on pure compound properties, the obtained viscosity predictions are satisfactory for most applications related to the petroleum industry. In spite that the studied ternary system is only a simple representation of some petroleum distillation cuts, the obtained results show the possible extension of these viscosity approaches to real petroleum fluids.

In addition, the widely used LBC model does not satisfactorily predict the viscosity of this ternary system, representing some simple distillation cuts, although that experimental densities are used along with optimized critical molar volumes for the pure compounds. The performance of the CS2 model and the PRVIS model is neither satisfactory. However, the viscosity calculations with the classical mixing laws (Grunberg-Nissan and Katti-Chaudhri) can be considered satisfactory, taking into account their simplicity. Thus, it should be stressed that the modeling of the viscosity of a fluid with a specific model can be improved if the model parameters, or the model itself, are readjusted or changed, or if viscosity interaction parameters are included. In this case, the model will only be adequate for the considered system, and will no longer be considered a general model. In spite of this, the aim of this modeling performed on this ternary system has been to evaluate some simple viscosity models for the possible extension to real petroleum fluids.

II.6 List of Symbols

Latin Letters

C	carbon number
C_e	elasticity constant
E_0	energy parameter used in Eq.(II.4.23)
f	frequency
g	gravitational acceleration
h	mean hydrostatic height
K	apparatus constant
K_{CS}	interpolation parameter in the CS2 model
k_B	Boltzmann's constant
L	length
l	characteristic molecular length
M	mass
M_w	molecular weight
N_A	Avogadro's constant
P	pressure
P_c	critical pressure
p_a	attractive pressure term
p_r	repulsive pressure term
Q	volumetric flow rate
R	gas constant
R_η	viscosity roughness factor
r	radius
T	temperature
T_c	critical temperature
t	time
V	volume
V_s	tension
v	molar volume
v_c	critical molar volume
v_r	reduced molar volume
v_0	close packing molar volume
x	mole fraction

Greek Letters

ΔG^E	excess activation energy of viscous flow
Γ	defined in Eq.(II.4.33)
η	viscosity
η_c	characteristic critical viscosity
η_f	residual friction viscosity term
η_r	reduced viscosity
η_0	dilute gas viscosity

κ_a	linear attractive friction coefficient
κ_r	linear repulsive friction coefficient
κ_{rr}	quadratic repulsive friction coefficient
κ_{rrr}	third order repulsive friction coefficient
Λ	period
ν	kinematic viscosity
ρ	density of fluid
ρ_r	reduced density
ρ_s	density of the sinker
σ	hard-core diameter
ω	acentric factor
ξ	viscosity reducing parameter
ζ	molecular friction coefficient

II.7 References

Aasberg-Petersen K., Knudsen K., and Stenby E.H.: *Prediction of Viscosities of Hydrocarbon Mixtures*. Fluid Phase Equilibria. **70** (1991) 293 – 308.

Acevedo I.L.; Postigo M.A., and Katz M.: *Excess Molar Volumes and Viscosities for 1-Propanol and 2-Propanol + Methylacetate Systems at 298.15 K*. Physics and Chemistry of Liquids. **21** (1990) 87 – 95.

Allal A., Montford J.P., and Marin G.: *Molecular Rheology: Calculation of Viscoelastic Properties from the Microstructure of Polymers*: in *Proceedings of the XIIth International Congress on Rheology*, edited by Ait Kadi A., Dealy J.M., James D.F., and Williams M.C. Canadian Rheology Group. (1996) 317.

Allal A., Moha-Ouchane M., and Boned C.: *A New Free Volume Model for Dynamic Viscosity and Density of Dense Fluids Versus Pressure and Temperature*. Physics and Chemistry of Liquids. **39** (2001a) 1 – 30.

Allal A., Boned C., and Daugé P.: *A New Free Volume Model for Dynamic Viscosity of Dense Fluids Versus Pressure and Temperature. Extension to a Predictive Model for Not Very Associative Mixtures*. Physics and Chemistry of Liquids. **39** (2001b) 607 – 624.

Alliez J., Boned C., Lagourette B., and Et-Tahir A.: *Viscosity under High-Pressure of Pure Hydrocarbons and Their Mixtures: Critical Study of a Residual Viscosity Correlation (Jossi)*. Special Publication of the Royal Society of Chemistry. **222** (1998) 75 – 80.

Arrhenius S.: *Über die Innere Reibung Verdünnter Wässeriger Lösungen*. Z. Physik. Chem. **1** (1887) 285 – 298.

Assael M.J., Dymond J.H., and Tselekidou V.: *Correlation of High-Pressure Thermal Conductivity, Viscosity, and Diffusion Coefficients for n-Alkanes*. International Journal of Thermophysics. **11** (1990) 863 – 873.

Assael M.J., Papadaki M., and Wakeham W.A.: *Measurements of the Viscosity of Benzene, Toluene, and m-Xylene at Pressure up to 80 MPa*. International Journal of Thermophysics. **12** (1991) 449 – 457.

Assael M.J., Dymond J.H., Papadaki M., and Patterson P.M.: *Correlation and Prediction of Dense Fluid Transport Coefficients. I. n-Alkanes*. International Journal of Thermophysics. **13** (1992a) 269 – 281.

Assael M.J., Dymond J.H., Papadaki M., and Patterson P.M.: *Correlation and Prediction of Dense Fluid Transport Coefficients. II. Simple Molecular Fluids*. Fluid Phase Equilibria. **75** (1992b) 245 – 255.

Assael M.J., Dymond J.H., Papadaki M., and Patterson P.M.: *Correlation and Prediction of Dense Fluid Transport Coefficients. III. n-Alkanes Mixtures*. International Journal of Thermophysics. **13** (1992c) 659 – 669.

Assael M.J., Dymond J.H., and Patterson P.M.: *Correlation and Prediction of Dense Fluid Transport Coefficients. V. Aromatic Hydrocarbons*. International Journal of Thermophysics. **13** (1992d) 895 – 905.

Assael M.J., Dymond J.H., and Polimatidou S.K.: *Correlation and Prediction of Dense Fluid Transport Coefficients. VI. n-Alcohols*. International Journal of Thermophysics. **15** (1994) 189 – 201.

Assael M.J., Dymond J.H., and Polimatidou S.K.: *Correlation and Prediction of Dense Fluid Transport Coefficients. VII. Refrigerants*. International Journal of Thermophysics. **16** (1995) 761 – 772.

Baylaucq A., Boned C., Daugé P., and Lagourette B.: *Measurements of the Viscosity and Density of Three Hydrocarbons and the Three Associated Binary Mixtures Versus Pressure and Temperature*. International Journal of Thermophysics. **18** (1997a) 3- 23.

Baylaucq A., Daugé P., and Boned C.: *Viscosity and Density of the Ternary Mixture Heptane + Methylcyclohexane + 1-Methylnaphthalene*. International Journal of Thermophysics. **18** (1997b) 1089 – 1107.

Baylaucq A., Boned C., Daugé P., and Xans P.: *Viscosity Versus Pressure, Temperature and Composition of the Ternary System Heptane + Methylcyclohexane + 1-Methylnaphthalene. Comparative Analysis of Some Models*. Physics and Chemistry of Liquids. **37** (1999) 579 – 626.

Baylaucq A., Moha-Ouchane M., and Boned C.: *A Hard-Sphere Scheme Used to Model the Viscosity of Two Ternary Mixtures up to 100 MPa*. Physics and Chemistry of Liquids. **38** (2000) 353 – 368.

Boned C., Moha-Ouchane M., Allal A., and Benseddik M.: *Viscosity and Density at High Pressures in an Associative Ternary*. International Journal of Thermophysics. **19** (1998) 1325 – 1342.

Bravo R., Pintos M., and Amigo A.: *Densities and Viscosities of the Binary Mixtures Decanol + Some n-Alkanes at 298.15 K*. Physics and Chemistry of Liquids. **22** (1991) 245 – 253.

Canet X.: *Viscosité Dynamique et Masse Volumique sous Hautes Pressions de Mélanges Binaires et Ternaires d'Hydrocarbures Lourds et Légers*. Thèse de Doctorant, Université de Pau, Pau, France. (2001).

Canet X., Daugé P., Baylaucq A., Boned C., Zéberg-Mikkelsen C.K., Quiñones-Cisneros S.E., and Stenby E.H.: *Density and Viscosity of 1-Methylnaphthalene + 2,2,4,4,6,8,8-Heptamethylnonane System from 293.15 K to 353.15 K at Pressures up to 100 MPa*. International Journal of Thermophysics. **22** (2001) 1669 - 1689

Carnahan N.F. and Starling K.E.: *Equation of State for Nonattracting Rigid Spheres*. The Journal of Chemical Physics. **51** (1969) 635 - 636

Cea P., Lafuente C., Morand J.P., Royo F.M., and Urieta J.S.: *Excess Volumes and Excess Viscosities of Binary Mixtures of 2-Chlorobutane with Isomeric Butanols at 298.15 K*. Physics and Chemistry of Liquids. **29** (1995) 69 – 77.

Chandler D.: *Rough Hard Sphere Theory of the Self-Diffusion Constant for Molecular Liquids*. The Journal of Chemical Physics. **62** (1975) 1358 – 1363.

Chung T.-H., Ajlan M., Lee L.L., and Starling K.E.: *Generalized Multiparameter Correlations for Nonpolar and Polar Fluid Transport Properties*. Industrial & Engineering Chemistry Research. **27** (1988) 671 – 679.

Daubert T.E. and Danner R.P.: *Physical and Thermodynamic Properties of Pure Chemicals Data Compilation*. DIPPR. Hemisphere Publishing Corporation, New York, USA. (1989).

Daugé P.: *Contribution à la Détermination de la Viscosité Dynamique et de la Masse Volumique d'Hydrocarbures et de Leurs Mélanges aux Hautes Pressions – Mise au Point d'un Viscomètre à Transfert Isobare*. Thèse de Doctorant. Université de Pau, Pau, France. (1999).

Daugé P., Baylaucq A., and Boned C.: *High-Pressure Viscosity Behaviour of the Tridecane + 1-Methylnaphthalene System*. High Temperatures – High Pressures. **31** (1999) 665 – 680.

Daugé P., Canet X., Baylaucq A., and Boned C.: *Measurements of the Density and Viscosity of the Tridecane + 2,2,4,4,6,8,8-Heptamethylnonane Mixtures in the Temperature Range 293.15 – 353.15 K at Pressures up to 100 MPa*. High Temperatures – High Pressures. **33** (2001) 213 - 230.

Doolittle A.K.: *Studies in Newtonian Flow. II – The Dependency of the Viscosity of Liquids on Free-Space*. Journal of Applied Physics. **22** (1951) 1471 – 1475.

Ducoulombier D., Lazarre F., Saint-Guirons H., and Xans P.: *Viscometer à Corps Chutant Permettant de Procéder à des Mesures de Viscosité de Liquides sous Hautes Pressions*. Reveu de Physique Appliqué. **20** (1985) 735 – 740.

Dymond J.H.: *Transport Properties in Dense Fluids*. Proc. 6th Symposium Thermophysical Properties. ASME, New York (1973) 143 – 157.

Dymond J.H., Robertson J., and Isdale J.D.: *(p, ρ, T) of Some Pure n -Alkanes and Binary Mixtures of n -Alkanes in the Range 298 to 373 K and 0.1 to 500 MPa*. Journal of Chemical Thermodynamics. **14** (1982) 51 – 59.

Dymond J.H. and Awan M.A.: *Correlation of High-Pressure Diffusion and Viscosity Coefficients for n -Alkanes*. International Journal of Thermophysics. **10** (1989) 941– 951.

Dymond J.H., Awan M.A., Glen N.F., and Isdale J.D.: *Transport Properties of Nonelectrolyte Liquid Mixtures. VIII. Viscosity Coefficients for Toluene and for Three Mixtures of Toluene + Hexane from 25 to 100°C at Pressures up to 500 MPa*. International Journal of Thermophysics. **12** (1991) 275 – 287.

Enskog D.: *Kinetische Theorie – Der Wärmeleitung, Reibung und Selbstdiffusion in Gewissen Verdichteten Gasen und Flüssigkeiten*. Kungliga Svenska Vetenskapsakademiens Handlingar, Stockholm, Sweden. **63(4)** (1922) 1 – 44.

Et-Tahir A.: *Determination des Variations de la Viscosité de Divers Hydrocarbures en Fonction de la Pression et de la Temperature. Etude Critique de Models Representatifs*. Thèse de Doctorant, Université de Pau, Pau, France. (1993).

Et-Tahir A., Boned C., Lagourette B., and Xans P.: *Determination of the Viscosity of Various Hydrocarbons and Mixtures of Hydrocarbons Versus Temperature and Pressure*. International Journal of Thermophysics. **16** (1995) 1309 – 1334.

Glasstone S., Laidler K.J., and Eyring H.: *The Theory of Rate Processes, the Kinetics of Chemical Reactions, Viscosity, Diffusion, and Electrochemical Phenomena*. McGraw-Hill, New York. (1941).

Grunberg L. and Nissan A.H.: *Mixture Law for Viscosity*. *Nature*. **164** (1949) 799 – 800.

Guo X.-Q., Wang L.-S., Rong S.-X. and Guo T.-M.: *Viscosity Model Based on Equations of State for Hydrocarbon Liquids and Gases*. **139** (1997) 405 – 421.

Guo -T.-M.: *Private Communication*. (1998).

Harris K.R.: *Temperature and Density Dependence of the Viscosity of Toluene*. *Journal of Chemical and Engineering Data*. **45** (2000) 893 – 897.

Heric E.L. and Brewer J.G.: *Viscosity of Some Binary Liquid Nonelectrolyte Mixtures*. *Journal of Chemical and Engineering Data*. **12** (1967) 574 – 583.

Hogenboom D.L., Webb W., and Dixon J.A.: *Viscosity of Several Liquid Hydrocarbons as a Function of Temperature, Pressure, and Free Volume*. *The Journal of Chemical Physics*. **46** (1967) 2586 – 2598.

Iglesias-Silva G.A., Estrada-Baltazar A., Hall R., and Barrufet M.A.: *Experimental Liquid Viscosity of Pentane + Octane + Decane Mixtures from 298.15 K to 373.15 K up to 25 MPa*. *Journal of Chemical and Engineering Data*. **44** (1999) 1304 – 1309.

Kanti M., Zhou H., Ye S., Boned C., Lagourette B., Saint-Guirons H., Xans P. and Montel F.: *Viscosity of Liquid Hydrocarbons, Mixtures, and Petroleum Cuts, as a Function of Pressure and Temperature*. *The Journal of Physical Chemistry*. **93** (1989) 3860 – 3864.

Kanti M., Lagourette B., Alliez J., and Boned C.: *Viscosity of Binary Heptane-Nonylbenzene as a Function of Pressure and Temperature: Application of the Flory's Theory*. *Fluid Phase Equilibria*. **65** (1991) 291 – 304.

Kashiwagi H. and Makita T.: *Viscosity of 12 Hydrocarbon Liquids in the Temperature Range 298 – 348 K at Pressures up to 110 MPa*. *International Journal of Thermophysics*. **3** (1982) 289 – 305.

Katti P.K. and Chaudhri M.M.: *Viscosities of Binary Mixtures of Benzyl Acetate with Dioxane, Aniline, and m-Cresol*. Journal of Chemical and Engineering Data. **9** (1964) 442 – 443.

Kawata M., Kurase K., Nagashima A., and Yoshida K. *Capillary Viscometers*, Chapter 3 in: *Measurements of the Transport Properties of Fluids Experimental Thermodynamic Vol. III*, edited by Wakeham W.A., Nagashima A., and Sengers J.V. IUPAC, Blackwell Scientific Publications, Oxford, England. (1991a).

Kawata M., Kurase K., Nagashima A., Yoshida K., and Isdale J.D. *Falling-Body Viscometers*, Chapter 5 in: *Measurements of the Transport Properties of Fluids Experimental Thermodynamic Vol. III*, edited by Wakeham W.A., Nagashima A., and Sengers J.V. IUPAC, Blackwell Scientific Publications, Oxford, England. (1991b).

Kell G.S. and Whalley E.: *Reanalysis of the Density of Liquid Water in the Range 0 – 150°C and 0 – 1 kbar*. Journal of Chemical Physics. **62** (1975) 3496 – 3503.

Kioupis L.I. and Maginn E.J.: *Impact of Molecular Architecture on the High-Pressure Rheology of Hydrocarbon Fluids*. The Journal of Physical Chemistry B. **104** (2000) 7774 – 7783.

Kiran E. and Sen Y.L.: *High-Pressure Viscosity and Density of n-Alkanes*. International Journal of Thermophysics. **13** (1992) 411 – 442.

Krall A.H., Sengers J.V., and Kestin J.: *Viscosity of Liquid Toluene at Temperatures from 25 to 100°C and at Pressures up to 30 MPa*. Journal of Chemical and Engineering Data. **37** (1992) 349 – 355.

Lagourette B., Boned C., Saint-Guirons H., Xans P., and Zhou H.: *Densimeter Calibration Method Versus Temperature and Pressure*. Measurement Science and Technology. **3** (1992) 699 – 703.

Lohrenz J., Bray B.G., and Clark C.R.: *Calculating Viscosities of Reservoir Fluids from Their Compositions*. Journal of Petroleum Technology. **16** (1964) 1171 – 1176.

Moha-Ouchane M., Boned C., Allal A., and Benseddik M.: *Viscosity and Excess Volume at High Pressures in Associated Binaries*. International Journal of Thermophysics. **19** 1998 161 – 189.

Oliveira C.M.B.P. and Wakeham W.A.: *The Viscosity of Five Liquid Hydrocarbons at Pressures up to 250 MPa*. International Journal of Thermophysics. **13** (1992) 773 – 790.

Pedersen K.S., Fredenslund Aa., and Thomassen P.: *Properties of Oils and Natural Gases*. Gulf Publishing Company, Houston, Texas, USA. (1989).

Peng D.-Y. and Robinson D.B.: *A New Two-Constant Equation of State*. Industrial & Engineering Chemistry Fundamentals. **15** (1976) 59 – 64.

Quiñones-Cisneros S.E., Zéberg-Mikkelsen C.K., and Stenby E.H.: *The Friction Theory (f-theory) for Viscosity Modeling*. Fluid Phase Equilibria. **169** (2000) 249 – 276.

Quiñones-Cisneros S.E., Zéberg-Mikkelsen C.K., and Stenby E.H.: *One Parameter Friction Theory Models for Viscosity*. Fluid Phase Equilibria. **178** (2001) 1 – 16.

Soave G.: *Equilibrium Constants from a Modified Redlich-Kwong Equation of State*. Chemical Engineering Science. **27** (1972) 1197 – 1203.

Tait P.G.: *Report on Some of the Physical Properties of Fresh Water and of Sea Water in: The Voyage of H.M.S. Challenger - Physics and Chemistry Vol. II*. Part IV, S.P. LXI, H.M.S.O., London, England. (1888).

van Velzen D., Cardozo R.L., and Langenkamp H.: *A Liquid Viscosity-Temperature Chemical Constitution Relation for Organic Compounds*. Industrial & Engineering Chemistry Fundamentals. **11** (1972) 20 – 25.

Vieira dos Santos F.J. and Nieto de Castro C.A.: *Viscosity of Toluene and Benzene under High Pressure*. International Journal of Thermophysics. **18** (1997) 367 – 378.

Zhang J., and Liu H.: *Determination of Viscosity under Pressure for Organic Substances and Its Correlation with Density under High Pressure*. Journal of Chemical Industry and Engineering (China). **3** (1991) 269 – 277.

Zwanzig R.: *Time-Correlation Functions and Transport Coefficients in Statistical Mechanics*. Annual Review of Physical Chemistry **16** (1965) 67 - 102.

PART III

CONCLUDING REMARKS

III.1 Concluding Overview

This work has mostly been carried out under the scope and goals of the EU project *Extended Viscosity and Density Technology* (EVIDENT). The projected main task for the EVIDENT project was to develop models for the prediction of the viscosity and density of reservoir fluids at high pressure-high temperature (HP/HT) conditions, in particular the implementation of reliable and accurate models for predicting both densities and viscosities of HP/HT fluids. Additionally, experimental data needed to be acquired on a set of selected fluids being representative of petroleum fluids. A final task for the EVIDENT project was the validation of the models developed in order to test the accuracy of the results in a wide range of industrial applications. The need for the EVIDENT project followed from the fact that in the oil as well as other industries, the viscosity is one of the weakest predicted parameters.

Thus, this Ph.D. project has been carried out as one of the main contributions of the DTU group to the EVIDENT project focusing on the friction theory for viscosity modeling. As it is widely illustrated in Part I of this thesis, the modeling results obtained with this novel approach have been validated far beyond the HP/HT conditions considered in the EVIDENT project. The *f-theory* models have shown excellent modeling capabilities, as it is broadly illustrated with the viscosity predictions of systems such as carbon dioxide + hydrocarbon mixtures, natural gas, hythane, and crude oils. In the case of crude oils, as it is illustrated in Section I.8.2, the *f-theory* models can be easily tuned to obtain a highly accurate viscosity model with excellent predictive properties under severe compositional changes – as it is the case during the producing life of an oil reservoir. Tuning an *f-theory* model only requires solving a simple linear equation against at least one experimental viscosity point. This represents a major advantage against other models commonly used in the oil industry which, in spite of undergoing more complex tuning procedures, still fail to deliver an adequate performance under compositional changes. Consequently, in contrast to the LBC model, an *f-theory* model can be safely applied in reservoir simulators for an accurate forecast of the viscosity behavior of reservoir fluids. Additionally, *f-theory* viscosity modeling of systems of industrial interest beyond the oil industry has also been carried out up to high pressure and for wide ranges of temperature. These viscosity studies include the

modeling of light gases described in Section I.7.5, or the modeling of alcohols, which is included in the list of selected articles in Appendix C.

In addition, a comprehensive viscosity and density study has been carried out for 21 ternary mixtures composed of 1-methylnaphthalene + n-tridecane + 2,2,4,4,6,8,8-heptamethylnonane up to 1000 bar and in the temperature range 293.15 – 353.15 K. These ternary mixtures should be simple representations of some petroleum distillation cuts at 510 K. The uncertainty in the measured viscosity values is 2.0%, except at 1 bar where a classical capillary viscometer has been used, reducing the uncertainty to less than 1.0%. For the measured densities the uncertainty is less than 1 kg/m³. The experimental viscosity data obtained in this work have been used in order to evaluate the performance of nine different viscosity models, applicable to petroleum fluids. The evaluated models range from recently derived models, such as the free-volume model or the friction theory, to widely used models within the oil industry, such as the well-known LBC model. The evaluation of these models shows that the best results for this ternary system are obtained with the free-volume model and the friction theory. In spite of their mathematical simplicity, these viscosity approaches have a physical and theoretical background and related to characteristic parameters and properties of pure compounds, making these models totally predictive for mixtures. The AAD obtained for these two models are within or close to the experimental uncertainty ($\pm 2\%$) for the studied ternary system. In spite the studied ternary system is only simple representation of some petroleum distillation cuts, the obtained results further show the capabilities of these viscosity approaches to real petroleum fluids.

III.1.1 Future Work

In spite the successful application of the *f-theory* in order to model and predict the viscosity of primarily hydrocarbon fluids of industrial interest over wide ranges of temperature, pressure and composition, further studies of the viscosity of fluids (non-polar as well as polar) of industrial interest with the *f-theory* have to be addressed. Some of these topics are mentioned below.

The application of the general one-parameter *f-theory* models to reservoir fluids, not only crude oils and gas condensates but also biodegradable oils, should be further investigated.

A very interesting aspect related to the tuning procedure of the general one-parameter *f-theory* model for reservoir fluids, which has to be investigated, is the possible viscosity prediction of real reservoir fluids or live fluids, based on the tuning of Kc in the general *f-theory* model, using the viscosity of the corresponding dead oil. The reason is that the tuning parameter Kc is related to the heavy fraction of the reservoir fluid, which will always be located in the liquid phase.

The extension of the concepts of the *f-theory* to other fluids such as lubricants, refrigerants, and associating fluids has also to be addressed.

In addition, experimental viscosity measurements on well-defined multicomponent mixtures covering wide ranges of temperature and up to high pressures are also of great interest in order to further evaluate the *f-theory* along with the free-volume approach, described in Section II.4.3.

Department of Chemical Engineering

June 2001

APPENDIX

**VISCOSITY STUDY OF HYDROCARBON
FLUIDS AT RESERVOIR CONDITIONS
MODELING AND MEASUREMENTS**

Claus K. Zéberg-Mikkelsen

Ph.D. Thesis, Technical University of Denmark

Table of Contents

Appendix A

A1 Density References for Methane, n-Hexane, and n-Decane.....	A1
A2 Analysis of Models.....	A3
A3 Viscosity References for Pure n-Alkanes	A4
A4 Recommended Viscosities for Pure n-Alkanes.....	A9
A5 References in Appendix A.....	A29

Appendix B

B1 Measured Viscosities and Densities of Ternary Mixtures	B1
B2 Measured Densities of Ternary Mixtures	B22

Appendix C

C1 Selected Articles in International Journals	C1
--	----

APPENDIX A

A1 Density References for Methane, n-Hexane, and n-Decane

The density data given in Table A1.1 – A1.3 are based on experimental values for the given temperature and pressure ranges. NP is the number of data points for the actual reference.

Reference	Methane		
	NP	<i>T</i> -range [K]	<i>P</i> -range [bar]
Douslin et al. (1964)	319	273 – 623	16 – 406
Händel et al. (1992)	270	100 – 260	1.8 – 81
Kleinrahm and Wagner (1986)	84*	91 – 190.53	0.1 – 46
Kleinrahm et al. (1986) (Table 1)	120*	180 – 190.53	33 – 46
Kleinrahm et al. (1986) (Table 2)	86	189 – 193	37 – 67
Kleinrahm et al. (1988)	169	273 – 323	1.0 – 80
Machado et al. (1988)	79	130 – 159	8.5 – 1111
Mollerup (1984)	51	310	1.7 – 717
Pieperbeck et al. (1991)	175	263 – 323	1.0 – 120

Table A1.1 Selected references and data for methane.

* Densities in the vicinity of the saturation line.

Reference	n-Hexane		
	NP	<i>T</i> -range [K]	<i>P</i> -range [bar]
Berstad (1989)	37	298 – 437	6.9 – 455
Brazier and Freeman (1969)	10	303	1.0 – 4500
Dymond et al. (1979)	31	298 – 373	1.0 – 5640
Isdale et al. (1979)	18	298 – 348	1.0 – 5000
Kelso and Felsing (1940)	59	373 – 548	5.7 – 316
Kiran and Sen (1992)	72	313 – 448	2.1 – 659
Kuss et al. (1976)	60	298 – 353	98 – 1961
Stewart et al. (1954)	98	311 – 511	6.5 – 664

Table A1.2. Selected references and data for n-hexane.

n-Decane			
Reference	NP	<i>T</i> -range [K]	<i>P</i> -range [bar]
Cullick and Mathis (1984)	4	303 – 311	69 – 206
Dymond et al. (1982)	19	298 – 373	1.0 – 420
Gates et al. (1986)	19	298 – 400	1.0 – 200
Gehrig and Lentz (1983)	401	298 – 673	1.5 – 3021
Goates et al. (1981)	3	283 – 313	1.0
Hutchings and van Hook (1985)	2	288 – 298	1.0
Kuss et al. (1976)	60	298 – 353	98 – 1961
Sage et al. (1940)	55	294 – 394	17 – 241

Table A1.3 Selected references and data for n-decane.

A2 Analysis of Models

To evaluate the performance of the investigated property models, the following quantities are defined

$$\text{Deviation}_i = \frac{X_{\text{calc},i} - X_{\text{exp},i}}{X_{\text{exp},i}} \quad (\text{A2.1})$$

$$\text{AAD} = \frac{1}{\text{NP}} \sum_{i=1}^{\text{NP}} |\text{Deviation}_i| \quad (\text{A2.2})$$

$$\text{MxD} = \text{Max} |\text{Deviation}_i| \quad (\text{A2.3})$$

$$\text{Bias} = \frac{1}{\text{NP}} \sum_{i=1}^{\text{NP}} \text{Deviation}_i \quad (\text{A2.4})$$

where NP is the number of experimental points, X_{exp} the experimental property and X_{calc} the calculated property of interest. The AAD (absolute average deviation) indicates how close the calculated values are to the experimental values, while the quantity Bias is an indication of how well the calculated values are distributed around the experimental values. Further the quantity MxD refers to the absolute maximum deviation.

A3 Viscosity References for Pure n-Alkanes

The data given in Table A3.1 – A3.15 are based on experimental values for the given temperature and pressure ranges. No extrapolated values have been included in these tables. NP is the number of data points for the actual reference.

Methane			
Reference	NP	<i>T</i> -range [K]	<i>P</i> -range [bar]
Baron et al. (1959)	40	325 – 408	6.9 – 552
Carmichael et al. (1965)	103	278 – 478	1.1 – 357
Chuang et al. (1976)	36	173 – 273	4.0– 506
Diller (1980)	116	100 – 300	6.4 – 331
Giddings et al. (1966)	95	283 – 411	6.9 – 551
Hellemans et al. (1970)	30	97 – 139	0.5 – 101
Huang et al. (1966)	61	153 – 273	1.0 – 345
Kestin and Yata (1968)	16	293 – 303	1.0 – 26
Knapstad (1986)	76	293 – 423	25 – 401
Kuss (1952)	48	293 – 353	1.0 - 608
Ross and Brown (1957)	21	248 – 298	70 – 690
Swift et al. (1960)	10	133 – 191	5.9 – 47
van der Gulik et al. (1992)	56	273.1	11 – 1006
van der Gulik et al. (1988)	20	298.15	1.1 – 1032

Table A3.1 Selected references and data for methane.

Ethane			
Reference	NP	<i>T</i> -range [K]	<i>P</i> -range [bar]
Baron et al. (1959)	40	325 – 408	6.9 – 552
Carmichael and Sage (1963a)	226	300 – 478	1.0 – 358
Diller and Saber (1981)	122	100 – 320	3.0 – 321
Diller and Ely (1989)	71	295 – 500	17 – 549
Eakin et al. (1962)	102	311 – 444	14 – 552
Iwasaki and Takahashi (1981)	417	298 – 348	1.0 – 129
Swift et al. (1960)	14	193 – 305	1.7 – 49

Table A3.2 Selected references and data for ethane.

Propane			
Reference	NP	<i>T</i> -range [K]	<i>P</i> -range [bar]
Baron et al. (1959)	40	325 – 408	6.9 – 552
Carmichael et al. (1964)	50	278 – 478	1.1 – 347
Diller (1982)	60	90 – 300	17 – 315
Giddings et al. (1966)	74	278 – 378	6.9 – 552
Huang et al. (1966)	30	173 – 273	69 – 343
Starling et al. (1960)	133	311 – 411	6.9 – 552
Swift et al. (1960)	14	243 – 370	3.4 – 43

Table A3.3 Selected references and data for propane.

n-Butane			
Reference	NP	<i>T</i> -range [K]	<i>P</i> -range [bar]
Abe et al. (1979)	7	298 – 468	1.0
Carmichael and Sage (1963b)	126	278 – 478	1.2 – 354
Diller and van Poolen (1985)	73	140 – 300	15 – 339
Dolan et al. (1963)	120	311 – 411	1.0 – 552
Kestin and Yata (1968)	7	293 – 303	1.1 – 2.3
Kiran and Sen (1992)	100	323 – 443	133 – 692
Sage et al. (1939)	24	311 – 361	14 – 138
Swift et al. (1960)	5	293 – 373	3.1 – 17

Table A3.4 Selected references and data for n-butane.

n-Pentane			
Reference	NP	<i>T</i> -range [K]	<i>P</i> -range [bar]
Agaev and Golubev (1963a)	315	298 – 548	1.0 – 507
Brazier and Freeman (1969)	3	303	1.0 – 1000
Collings and McLaughlin (1971)	6	303 – 323	1.0 – 981
Kiran and Sen (1992)	139	318 – 443	75 – 703
Lee and Ellington (1965a)	33	311 – 444	14 – 207
Oliveira and Wakeham (1992)	17	303 – 323	1.0 – 1027

Table A3.5 Selected references and data for n-pentane.

n-Hexane			
Reference:	NP	<i>T</i> -range [K]	<i>P</i> -range [bar]
Agaev and Golubev (1963b)	265	289 – 548	1.0 – 507
Berstad (1989)	37	294 – 437	6.9 – 455
Brazier and Freeman (1969)	9	273 – 333	1.0 – 1000
Dymond et al. (1980)	15	298 – 373	1.0 – 1022
Giller and Drickamer (1949)	1	293	1.0
Isdale et al. (1979)	12	298 – 373	1.0 – 1000
Kiran and Sen (1992)	72	313 – 448	2.1 – 659
Knapstad et al. (1989)	7	288 – 327	1.0
Kor et al. (1972)	3	303	1.0 – 981
Kuss and Pollmann (1969)	4	313	1.0 – 883
Oliveira and Wakeham (1992)	25	303 – 348	1.0 – 1001
Parisot and Johnson (1961)	11	300 – 455	1.0 – 22

Table A3.6 Selected references and data for n-hexane.

n-Heptane			
Reference	NP	<i>T</i> -range [K]	<i>P</i> -range [bar]
Agaev and Golubev (1963c)	273	298 – 548	1.0 – 507
Assael and Papadaki (1991)	28	303 – 323	1.0 – 694
Assael et al. (1992)	30	303 – 348	1.0 – 1023
Baylaucq et al. (1997)	18	303 – 343	1.0 – 1000
Knapstad et al. (1989)	8	297 – 347	1.0
Kuss and Pollmann (1969)	4	313	1.0 – 883

Table A3.7 Selected references and data for n-heptane.

n-Octane			
Reference	NP	<i>T</i> -range [K]	<i>P</i> -range [bar]
Agaev and Golubev (1963c)	237	323 – 569	1.0 – 507
Barrufet et al. (1999)	36	298 – 373	1.0 – 246
Brazier and Freeman (1969)	9	273 – 333	1.0 – 1000
Giller and Drickamer (1949)	2	273 – 293	1.0
Kiran and Sen (1992)	47	323 – 448	80 – 665
Knapstad et al. (1989)	5	294 – 370	1.0
Oliveira and Wakeham (1992)	30	303 – 348	1.0 – 1018
Tanaka et al. (1991)	16	298 – 348	1.0 – 1021

Table A3.8 Selected references and data for n-octane.

n-Decane			
Reference	NP	<i>T</i> -range [K]	<i>P</i> -range [bar]
Carmichael et al. (1969)	47	278 – 478	0.1 – 361
Ducoulombier et al. (1986)	30	293 – 373	1.0 – 1000
Estrada-Baltazar et al. (1998)	36	298 – 373	1.0 – 246
Giller and Drickamer (1949)	1	293	1.0
Knapstad et al. (1989)	11	293 – 423	1.0
Knapstad et al. (1990)	37	293 – 424	6.1 – 399
Lee and Ellington (1965b)	49	311 – 411	14 – 552
Oliveira and Wakeham (1992)	30	303 – 348	1.0 – 1019

Table A3.9 Selected references and data for n-decane.

n-Dodecane			
Reference	NP	<i>T</i> -range [K]	<i>P</i> -range [bar]
Ducoulombier et al. (1986)	30	293 – 373	1.0 – 1000
Giller and Drickamer (1949)	1	293	1.0
Hoogenboom et al. (1967)	18	311 – 408	1.0 – 800
Knapstad et al. (1989)	9	294 – 397	1.0
Tanaka et al. (1991)	17	298 – 348	1.0 – 1005

Table A3.10 Selected references and data for n-dodecane.

n-Tridecane			
Reference	NP	<i>T</i> -range [K]	<i>P</i> -range [bar]
Daugé et al. (1999)	42	293 – 353	1.0 – 1000

Table A3.11 Selected references and data for n-tridecane.

n-Tetradecane			
Reference	NP	<i>T</i> -range [K]	<i>P</i> -range [bar]
Ducoulombier et al. (1986)	30	293 – 373	1.0 – 1000
Giller and Drickamer (1949)	1	293	1.0
Knapstad et al. (1989)	8	293 – 373	1.0

Table A3.12 Selected references and data for n-tetradecane.

n-Pentadecane			
Reference	NP	<i>T</i> -range [K]	<i>P</i> -range [bar]
Ducoulombier et al. (1986)	24	313 – 373	1.0 – 1000
Hoogenboom et al. (1967)	18	311 – 408	1.0 – 800

Table A3.13 Selected references and data for n-pentadecane.

n-Hexadecane			
Reference	NP	<i>T</i> -range [K]	<i>P</i> -range [bar]
Ducoulombier et al. (1986)	24	313 – 373	1.0 – 1000
Dymond et al. (1980)	20	298 – 373	1.0 – 1034
Matthews et al. (1987)	4	323 – 371	14 – 35
Tanaka et al. (1991)	12	298 – 348	1.0 – 1023

Table A3.14 Selected references and data for n-hexadecane.

n-Octadecane			
Reference	NP	<i>T</i> -range [K]	<i>P</i> -range [bar]
Ducoulombier et al. (1986)	22	313 – 373	1.0 – 1000
Hoogenboom et al. (1967)	18	311 – 408	1.0 – 800

Table A3.15 Selected references and data for n-octadecane.

A4 Recommended Viscosities for Pure n-Alkanes

T_r P_r	0.55	0.60	0.70	0.80	0.90	1.00	1.10
0.2	1391	1115	766.9	63.82	66.82	74.21	81.15
0.4	1408	1129	777.2	556.2	69.32	75.93	82.33
0.6	1425	1143	787.3	567.1	385.6	80.03	84.86
0.8	1442	1156	797.4	577.5	402.6	89.33	89.37
0.85	1446	1160	799.9	580.0	406.5	93.50	90.93
0.9	1450	1163	802.3	582.5	410.2	99.38	92.70
0.95	1455	1166	804.8	585.0	413.7	108.9	94.72
1.0	1459	1170	807.3	587.4	417.2	156.7	97.03
1.05	1463	1173	809.8	589.9	420.6	217.8	99.66
1.1	1467	1177	812.2	592.3	423.8	235.5	102.7
1.15	1472	1180	814.7	594.6	427.0	248.2	106.1
1.2	1476	1183	817.2	597.0	430.1	258.5	110.1
1.4	1493	1197	826.9	606.2	441.8	288.6	132.8
1.6	1510	1210	836.6	615.1	452.5	310.4	165.5
1.8	1526	1224	846.3	623.6	462.5	328.0	197.2
2.0	1543	1237	855.9	632.0	471.8	343.1	222.8
2.5	1585	1270	879.7	651.1	494.6	368.4	268.9
3.0	1626	1303	903.4	671.1	515.9	395.1	303.1
4.0	1708	1368	950.3	709.8	554.9	440.4	354.6
5.0	1790	1433	997.3	747.7	591.2	479.1	394.6
6.0	1871	1498	1044	785.4	626.4	513.4	428.4
7.0	1952	1562	1092	823.2	661.3	544.3	458.1
7.5			1116	842.3	678.9	558.8	471.9
8.0						572.7	485.1
9.0						598.8	510.0
10.0						623.1	533.3
11.0						645.6	555.5
12.0							
13.0							
14.0							
15.0							
16.0							
17.0							
18.0							
19.0							
20.0							
AAD%	0.54	0.90	1.11	1.14	1.40	2.28	2.20

Table A4.1 Viscosity of Methane [μP] versus reduced pressure P_r and reduced temperature T_r .
 $T_c = 190.555 \text{ K}$ and $P_c = 45.95 \text{ bar}$.

$T_r \backslash P_r$	1.20	1.30	1.40	1.50	1.60	1.70	1.80
0.2	89.07	95.86	102.2	108.0	114.2	120.4	126.0
0.4	90.83	97.79	104.0	109.5	115.5	121.7	127.2
0.6	93.15	100.2	106.3	111.5	117.2	123.0	128.4
0.8	96.19	103.1	108.9	114.0	119.3	124.5	129.7
0.85	97.09	104.0	109.6	114.7	119.9	124.9	130.1
0.9	98.05	104.8	110.4	115.4	120.4	125.4	130.4
0.95	99.09	105.7	111.2	116.2	121.1	125.8	130.8
1.0	100.2	106.7	112.0	116.9	121.7	126.2	131.2
1.05	101.4	107.7	112.8	117.7	122.3	126.7	131.6
1.1	102.7	108.7	113.7	118.5	123.0	127.1	132.0
1.15	104.0	109.8	114.6	119.4	123.6	127.6	132.4
1.2	105.5	110.9	115.5	120.2	124.3	128.1	132.8
1.4	112.5	115.9	119.5	123.8	127.2	130.3	134.7
1.6	121.7	121.7	123.8	127.5	130.4	132.8	136.7
1.8	133.4	128.3	128.5	131.2	133.6	135.8	139.0
2.0	147.5	135.5	133.5	134.8	137.0	139.2	141.7
2.5	190.3	161.8	151.0	146.1	146.5	147.3	150.1
3.0	226.1	187.7	169.4	159.8	157.5	156.6	157.8
4.0	281.7	236.0	207.3	189.6	181.7	177.2	174.9
5.0	324.3	277.0	242.8	219.4	207.0	198.8	193.3
6.0	359.5	312.5	274.8	247.7	232.0	220.2	211.9
7.0	390.1	344.1	303.8	274.2	256.0	240.8	230.3
7.5	404.2	358.7	317.4	286.8	267.6	250.4	239.3
8.0	417.6	372.8	330.5	298.9	279.0	260.2	248.2
9.0	442.7	399.5	355.3	322.2	300.9	278.5	265.5
10.0	466.0	424.5	378.6	344.3	321.9	295.7	282.1
11.0	488.0	448.3	400.6	365.3	342.0	311.8	298.0
12.0		471.0	421.7	385.5	361.5	327.0	313.4
13.0		493.0	441.9	404.9	380.3	341.3	328.1
14.0		514.2	461.5	423.7	398.6		
15.0		534.9	480.4	442.0	416.4		
16.0		555.0	498.8	459.8	433.8		
17.0		574.8	516.8	477.2	450.9		
18.0		594.3	534.4	494.2	467.7		
19.0		613.4	551.6	510.9	484.1		
20.0		632.3	568.6	527.4	500.4		
AAD%	1.32	1.26	1.13	0.97	1.00	0.98	1.40

Table A4.1 *Continued.*

$P_r \backslash T_r$	1.90	2.00	2.10	2.20	2.30	2.40	2.50
0.2	131.6	137.1	142.6	147.8	153.0	157.9	162.9
0.4	132.9	138.4	144.0	149.1	154.2	159.1	164.1
0.6	134.3	139.7	145.5	150.4	155.6	160.3	165.4
0.8	135.8	141.2	147.0	151.9	157.0	161.6	166.7
0.85	136.2	141.6	147.4	152.2	157.3	161.9	167.1
0.9	136.6	142.0	147.8	152.6	157.7	162.3	167.4
0.95	137.0	142.4	148.3	153.0	158.1	162.6	167.7
1.0	137.5	142.8	148.7	153.3	158.4	162.9	168.1
1.05	137.9	143.2	149.1	153.7	158.8	163.3	168.4
1.1	138.3	143.7	149.5	154.1	159.2	163.6	168.8
1.15	138.8	144.1	150.0	154.5	159.5	164.0	169.1
1.2	139.3	144.5	150.4	154.9	159.9	164.3	169.5
1.4	141.2	146.3	152.2	156.5	161.5	165.8	170.9
1.6	143.3	148.2	154.1	158.2	163.0	167.3	172.3
1.8	145.4	150.3	156.0	160.0	164.7	168.8	173.8
2.0	147.7	152.4	158.0	161.8	166.4	170.4	175.3
2.5	154.0	158.0	163.4	166.5	170.7	174.4	179.2
3.0	160.8	164.2	169.0	171.6	175.3	178.7	183.2
4.0	175.8	177.6	181.3	182.4	185.0	187.7	191.5
5.0	191.9	192.1	194.3	193.8	195.2	197.2	200.1
6.0	208.6	207.1	207.8	205.8	205.8	206.9	208.9
7.0	225.2	222.3	221.4	217.9	216.6	216.6	217.7
7.5	233.5	229.9	228.3	224.0	222.0	221.5	222.1
8.0	241.7	237.5	235.2	230.1	227.4		
9.0	257.8	252.5	248.8	242.3	238.3		
10.0	273.5	267.2	262.3	254.4	249.2		
11.0	288.8	281.7	275.5	266.4	260.0		
12.0	303.6	295.8	288.6	278.2	270.7		
13.0	318.0	309.7					
14.0							
15.0							
16.0							
17.0							
18.0							
19.0							
20.0							
AAD%	1.01	0.85	0.71	0.77	0.77	0.56	0.56

Table A4.1 *Continued.*

T_r	0.35	0.40	0.50	0.60	0.70	0.80	0.90
P_r							
0.2	7079	4685	2635	1710	1190	77.66	88.64
0.4	7128	4715	2653	1723	1205	847.9	94.72
0.6	7177	4746	2670	1737	1220	864.1	585.9
0.8	7227	4776	2688	1750	1235	879.7	609.1
0.85	7239	4784	2692	1754	1239	883.5	614.4
0.9	7252	4791	2696	1757	1243	887.3	619.5
0.95	7264	4799	2701	1760	1246	891.1	624.5
1.0	7277	4807	2705	1764	1250	894.8	629.3
1.05	7289	4814	2710	1767	1253	898.5	634.0
1.1	7302	4822	2714	1771	1257	902.2	638.6
1.15	7315	4830	2718	1774	1261	905.9	643.1
1.2	7327	4837	2723	1777	1264	909.5	647.5
1.4	7378	4869	2740	1791	1278	923.8	664.0
1.6	7430	4900	2758	1804	1292	937.7	679.2
1.8	7482	4931	2776	1818	1305	951.3	693.4
2.0	7534	4963	2794	1831	1319	964.7	706.7
2.5	7668	5043	2838	1865	1351	994.1	739.6
3.0	7804	5125	2883	1899	1382	1022	769.8
4.0	8085	5292	2975	1967	1442	1075	824.5
5.0	8379	5465	3067	2035	1497	1125	874.5
6.0	8684	5643	3162	2104	1549	1173	921.9
7.0	9001	5826	3257	2173	1598	1219	967.8
8.0							1013
9.0							1058
10.0							1104
11.0							1150
11.3							
AAD%	0.53	0.55	0.56	0.95	0.63	1.09	1.40

Table A4.2 Viscosity of Ethane [μP] versus reduced pressure P_r and reduced temperature T_r .
 $T_c = 305.43 \text{ K}$ and $P_c = 48.7976 \text{ bar}$.

T_r	1.00	1.10	1.20	1.30	1.40	1.50	1.60
P_r							
0.2	95.04	104.9	115.7	124.2	132.6	140.3	147.9
0.4	96.86	106.4	118.5	126.9	135.2	142.4	149.7
0.6	102.7	109.8	121.9	130.0	138.2	144.8	151.8
0.8	117.3	115.9	126.4	133.8	141.6	147.6	154.4
0.85	124.0	118.0	127.7	134.8	142.5	148.4	155.1
0.9	133.5	120.4	129.0	135.9	143.4	149.2	155.8
0.95	149.1	123.1	130.5	137.1	144.4	150.0	156.5
1.0	226.8	126.1	132.1	138.3	145.4	150.8	157.3
1.05	321.8	129.6	133.7	139.6	146.5	151.7	158.0
1.1	348.0	133.6	135.5	140.9	147.5	152.6	158.8
1.15	366.4	138.1	137.4	142.3	148.6	153.6	159.7
1.2	381.0	143.3	139.4	143.7	149.8	154.6	160.5
1.4	422.2	171.8	148.8	150.2	154.7	158.8	164.1
1.6	450.3	212.6	161.0	157.9	160.2	163.7	168.1
1.8	471.9	254.3	176.1	166.9	166.4	169.3	172.4
2.0	489.4	288.8	194.3	177.4	173.2	175.6	177.1
2.5	534.1	365.4	254.9	211.2	194.5	190.2	190.0
3.0	574.0	416.3	304.0	246.6	218.7	208.8	204.6
4.0	639.8	493.3	383.3	314.0	269.6	249.3	237.0
5.0	694.9	553.7	445.7	372.1	318.2	290.6	271.3
6.0	743.7	605.0	498.4	422.4	362.7	330.2	305.6
7.0	788.3	650.6	544.7	466.9	403.3	367.4	339.1
8.0	830.0	692.3	586.7	507.1	440.7	402.4	371.4
9.0	869.5	731.1	625.5	544.1	475.4	435.2	402.6
10.0	907.4	767.8	662.0	578.7	508.0	466.3	432.7
11.0	944.2	802.8	696.5	611.2	538.9		
11.3	955.0	813.0	706.6	620.6	547.9		
AAD%	3.95	3.54	0.90	0.69	0.62	0.71	0.68

Table A4.2 *Continued.*

$T_r \backslash P_r$	0.30	0.40	0.50	0.60	0.70	0.80	0.90
0.2	21881	6858	3604	2298	1484	84.38	95.87
0.4	22083	6911	3628	2312	1499	1018	104.1
0.6	22287	6963	3652	2326	1514	1035	663.8
0.8	22490	7016	3676	2340	1529	1051	689.7
0.85	22541	7030	3682	2344	1533	1055	695.7
0.9	22592	7043	3688	2347	1536	1059	701.6
0.95	22643	7056	3694	2351	1540	1063	707.2
1.0	22694	7069	3700	2354	1544	1067	712.8
1.05	22745	7083	3706	2358	1547	1071	718.2
1.1	22797	7096	3712	2361	1551	1075	723.5
1.15	22848	7109	3718	2365	1555	1078	728.7
1.2	22899	7123	3724	2368	1558	1082	733.8
1.4	23104	7176	3748	2382	1573	1097	753.1
1.6	23309	7230	3772	2396	1587	1111	771.2
1.8	23515	7283	3796	2410	1602	1125	788.1
2.0	23722	7337	3820	2424	1616	1139	804.2
2.5	24239	7473	3881	2459	1651	1173	841.8
3.0	24760	7610	3942	2494	1686	1208	879.8
4.0	25810	7887	4065	2565	1754	1275	948.6
5.0	26871	8168	4190	2637	1822	1338	1011
6.0	27943	8455	4316	2710	1890	1399	1069
7.0	29027	8746	4444	2784	1957	1458	1124
8.0		9041	4573	2859	2025	1515	1177
9.0					2093	1571	1227
10.0					2161	1626	1277
11.0						1681	1325
12.0						1735	1373
13.0						1788	1419
AAD%	1.03	1.03	0.68	1.10	0.69	0.49	1.49

Table A4.3 Viscosity of Propane [μP] versus reduced pressure P_r and reduced temperature T_r .
 $T_c = 369.82$ K and $P_c = 42.4953$ bar.

$P_r \backslash T_r$	1.00	1.10	1.20	1.29
0.2	101.8	111.7	121.8	130.0
0.4	104.3	113.5	123.8	131.8
0.6	110.8	117.3	126.8	134.5
0.8	126.1	124.0	131.3	138.1
0.85	133.1	126.2	132.7	139.1
0.9	142.9	128.8	134.2	140.3
0.95	158.9	131.7	135.8	141.5
1.0	239.3	135.0	137.5	142.7
1.05	341.4	138.8	139.3	144.1
1.1	370.6	143.0	141.3	145.5
1.15	391.7	147.8	143.5	147.0
1.2	408.6	153.2	145.8	148.6
1.4	457.9	183.0	156.7	155.8
1.6	493.2	225.8	170.5	164.4
1.8	521.6	271.8	187.4	174.5
2.0	545.7	311.9	207.0	185.9
2.5	591.9	389.3	265.4	219.3
3.0	637.7	443.7	314.3	256.3
4.0	714.1	527.8	396.0	328.3
5.0	778.7	595.2	462.6	391.2
6.0	836.5	653.4	520.1	447.2
7.0	889.6	705.7	571.7	498.2
8.0	939.5	753.9	619.3	545.5
9.0	987.1	799.1	663.9	590.1
10.0	1033	841.9	706.3	632.6
11.0	1077	882.8	747.0	673.5
12.0	1121	922.3	786.3	713.1
13.0	1163	960.5	824.6	751.8
AAD%	0.87	1.14	1.04	0.70

Table A4.3 *Continued.*

T_r P_r	0.35	0.40	0.50	0.60	0.70	0.80	0.90
0.2	14565	8501	4185	2489	1608	87.29	96.36
0.4	14660	8548	4211	2509	1624	1094	101.3
0.6	14756	8595	4237	2529	1639	1111	712.7
0.8	14852	8643	4263	2548	1654	1127	737.8
0.85	14877	8656	4270	2553	1658	1131	743.6
0.9	14901	8668	4276	2558	1662	1136	749.2
0.95	14926	8680	4283	2563	1666	1140	754.7
1.0	14950	8692	4289	2568	1669	1144	760.1
1.05	14975	8704	4296	2572	1673	1147	765.3
1.1	14999	8717	4303	2577	1677	1151	770.4
1.15	15024	8729	4309	2582	1681	1155	775.4
1.2	15049	8741	4316	2587	1685	1159	780.3
1.4	15149	8791	4342	2606	1700	1174	798.8
1.6	15249	8842	4368	2625	1715	1189	816.1
1.8	15351	8893	4394	2643	1730	1204	832.2
2.0	15454	8944	4421	2662	1752	1202	847.4
2.5	15715	9076	4487	2696	1792	1241	883.9
3.0	15982	9211	4553	2742	1831	1279	923.7
4.0	16534	9491	4686	2833	1908	1352	996.4
5.0	17111	9786	4821	2924	1981	1421	1062
6.0	17711	10095	4957	3015	2053	1487	1124
7.0	18337	10418	5094	3105	2123	1550	1182
8.0	18986	10755	5233	3196	2192	1612	1238
9.0	19659	11106	5374	3287	2259	1672	1292
10.0					2326	1731	1345
11.0					2391	1789	1396
12.0					2456	1845	1446
13.0					2521	1902	1495
14.0					2584	1957	1544
15.0					2647	2012	1592
16.0					2710	2066	1639
17.0					2772	2120	1687
18.0					2834	2174	1734
AAD%	0.80	0.79	0.65	0.82	1.23	0.95	1.05

Table A4.4 Viscosity of n-Butane [μP] versus reduced pressure P_r and reduced temperature T_r .
 $T_c = 425.16 \text{ K}$ and $P_c = 37.9661 \text{ bar}$.

P_r	T_r	1.00	1.04
0.2		104.6	111.7
0.4		105.7	114.5
0.6		111.1	119.0
0.8		125.9	126.9
0.85		132.9	129.7
0.9		143.0	133.1
0.95		159.6	137.3
1.0		244.8	142.4
1.05		352.4	148.9
1.1		382.9	157.7
1.15		404.6	169.8
1.2		422.0	187.4
1.4		472.1	292.2
1.6		507.3	370.4
1.8		535.2	432.6
2.0		574.0	
2.5		631.2	
3.0		678.3	
4.0		755.9	
5.0		820.7	
6.0		877.8	
7.0		929.8	
8.0		978.0	
9.0		1024	
10.0		1067	
11.0		1109	
12.0		1150	
13.0		1189	
14.0		1228	
15.0		1266	
16.0		1304	
17.0		1341	
18.0		1379	
AAD%		1.61	1.07

Table A4.4 *Continued.*

$\begin{matrix} T_r \\ P_r \end{matrix}$	0.64	0.70	0.80	0.90	1.00	1.10	1.16
0.2	2118	1697	1136	103.0	109.9	120.2	126.9
0.4	2137	1711	1153	112.5	113.6	122.9	129.8
0.6	2156	1726	1169	757.6	121.8	127.9	134.3
0.8	2174	1740	1184	783.0	139.7	136.0	140.8
0.85	2179	1744	1188	788.9	147.6	138.7	142.8
0.9	2183	1748	1192	794.6	158.7	141.7	145.0
0.95	2188	1751	1196	800.3	176.6	145.1	147.3
1.0	2192	1755	1200	805.8	265.0	148.9	149.9
1.05	2197	1758	1203	811.1	375.4	153.1	152.6
1.1	2201	1762	1207	816.4	406.8	157.9	155.6
1.15	2206	1765	1211	821.5	429.2	163.1	158.8
1.2	2210	1769	1214	826.6	447.3	169.1	162.2
1.4	2229	1782	1229	845.8	499.6	200.2	178.6
1.6	2247	1796	1243	863.8	536.7	243.5	199.6
1.8	2265	1809	1257	880.6	566.3	290.9	224.8
2.0	2282	1823	1271	896.6	591.3	333.2	252.8
2.5	2327	1847	1307	921.5	634.0	406.0	321.4
3.0	2371	1886	1343	961.6	682.7	466.4	376.8
4.0	2458	1963	1411	1035	763.7	559.1	466.3
5.0	2543	2038	1476	1101	832.0	632.9	538.6
6.0	2628	2111	1540	1163	893.0	696.3	601.3
7.0	2712	2183	1602	1221	948.9	753.2	657.6
8.0	2796	2254	1663	1276	1001	805.5	709.5
9.0	2879	2325	1723	1330	1051	854.5	758.2
10.0	2962	2394	1783	1381	1100	901.0	804.3
11.0	3045	2463	1842	1431	1146	945.6	848.4
12.0	3127	2531	1902	1480	1192	988.5	890.8
13.0	3209	2599	1961	1529	1237	1030	931.9
14.0	3292	2667	2021	1576	1281	1071	971.9
15.0	3374	2735	2081	1622	1325	1111	1011
16.0	3457	2802	2141	1668			
17.0	3539	2869	2202	1714			
18.0	3622	2936	2263	1759			
19.0	3705	3003	2324	1804			
20.0	3788	3070	2386	1848			
25.0	4208	3406					
30.0	4637	3745					
AAD%	0.96	1.07	0.94	1.55	1.19	1.08	1.15

Table A4.5 Viscosity of n-Pentane [μP] versus reduced pressure P_r and reduced temperature T_r .
 $T_c = 469.70 \text{ K}$ and $P_c = 33.6902 \text{ bar}$.

$T_r \backslash P_r$	0.54	0.60	0.70	0.80	0.90	1.00	1.08
0.2	3756	2793	1818	1227	106.2	110.6	121.0
0.4	3781	2811	1832	1244	121.5	117.3	128.7
0.6	3805	2828	1847	1261	801.9	128.8	138.6
0.8	3830	2845	1862	1277	826.7	151.0	151.7
0.85	3836	2850	1866	1281	832.4	160.3	155.7
0.9	3842	2854	1870	1285	838.1	173.0	160.1
0.95	3848	2859	1873	1289	843.6	192.9	164.8
1.0	3854	2863	1877	1293	849.0	287.2	170.0
1.05	3860	2868	1881	1297	854.2	399.4	175.8
1.1	3866	2872	1885	1301	859.4	430.3	182.1
1.15	3872	2876	1888	1305	864.4	452.2	189.2
1.2	3878	2881	1892	1309	869.4	469.6	197.0
1.4	3903	2899	1907	1323	888.2	519.0	238.3
1.6	3927	2917	1922	1338	905.8	553.0	291.5
1.8	3952	2935	1938	1352	922.2	579.3	340.2
2.0	3976	2953	1953	1366	937.7	601.0	378.7
2.5	4037	3001	1989	1393	973.0	646.2	425.1
3.0	4098	3048	2028	1427	1000	695.2	486.4
4.0	4220	3143	2103	1494	1073	775.4	579.2
5.0	4343	3237	2177	1558	1140	842.2	652.2
6.0	4467	3331	2250	1620	1203	901.3	714.8
7.0	4591	3425	2321	1680	1263	955.4	770.8
8.0	4715	3519	2391	1739	1321	1006	822.5
9.0	4841	3612	2460	1798	1377	1055	871.2
10.0	4967	3706	2529	1856	1432	1102	917.7
11.0	5094	3801	2597	1914	1486	1148	962.7
12.0	5222	3895	2664	1972	1540	1194	1007
13.0	5352	3990	2732	2029	1594	1239	1050
14.0	5482	4085	2799	2087	1647	1284	1092
15.0	5613	4181	2865	2145	1700	1329	1135
16.0	5745	4277	2932	2204	1754	1374	1177
17.0	5879	4374	2999	2262	1807	1420	1219
18.0	6013	4471	3065	2321			
19.0	6149	4569	3131	2381			
20.0	6286	4668	3198	2441			
25.0	6988	5170	3531				
30.0	7723	5690	3868				
35.0	8490	6230	4212				
AAD%	0.76	0.80	1.23	1.44	1.38	1.25	1.85

Table A4.6 Viscosity of n-Hexane [μP] versus reduced pressure P_r and reduced temperature T_r .
 $T_c = 507.30 \text{ K}$ and $P_c = 30.1236 \text{ bar}$.

T_r P_r	0.56	0.60	0.70	0.80	0.90	1.00
0.2	3734	3028	1892	1231	103.0	108.2
0.4	3757	3047	1907	1246	115.9	113.6
0.6	3780	3067	1922	1261	790.0	123.5
0.8	3803	3086	1936	1276	814.6	143.6
0.85	3808	3091	1940	1279	820.4	152.2
0.9	3814	3096	1944	1283	826.0	164.0
0.95	3820	3101	1947	1286	831.5	182.7
1.0	3826	3106	1951	1290	836.9	273.4
1.05	3831	3110	1955	1293	842.3	384.2
1.1	3837	3115	1958	1297	847.5	415.4
1.15	3843	3120	1962	1300	852.6	437.6
1.2	3848	3125	1966	1304	857.6	455.5
1.4	3871	3144	1980	1318	876.8	506.8
1.6	3894	3163	1995	1331	894.9	542.8
1.8	3917	3182	2009	1345	912.0	571.4
2.0	3940	3201	2024	1358	928.2	595.3
2.5	3996	3258	2080	1390	952.9	636.1
3.0	4053	3306	2118	1426	991.2	684.2
4.0	4167	3401	2192	1494	1061	763.2
5.0	4281	3496	2264	1559	1125	829.0
6.0	4395	3590	2335	1622	1184	887.3
7.0	4509	3684	2405	1683	1240	940.6
8.0	4624	3779	2474	1743	1294	990.5
9.0	4740	3873	2542	1802	1347	1038
10.0	4855	3967	2610	1860	1397	1084
11.0	4972	4062	2678	1917	1447	1129
12.0	5089	4157	2745	1974	1496	1173
13.0	5207	4253	2812	2031	1544	1216
14.0	5326	4349	2879	2087	1592	1259
15.0	5445	4445	2946	2143	1639	1302
16.0	5565	4542	3013	2199	1686	1344
17.0	5686	4640	3079	2256	1733	1387
18.0	5808	4738	3146	2312	1780	1430
19.0	5931	4836	3213			
20.0	6055	4935	3280			
25.0	6688	5442	3619			
30.0	7347	5966	3965			
35.0	8032	6511	4320			
AAD%	0.45	0.42	0.41	0.62	1.33	0.78

Table A4.7 Viscosity of n-Heptane [μP] versus reduced pressure P_r and reduced temperature T_r .
 $T_c = 540.10 \text{ K}$ and $P_c = 27.3575 \text{ bar}$.

$P_r \backslash T_r$	0.50	0.60	0.70	0.80	0.90	1.00
0.2	6059	3275	1999	1276	102.8	106.9
0.4	6094	3295	2016	1294	116.3	111.8
0.6	6129	3314	2033	1311	795.2	121.0
0.8	6164	3334	2049	1328	819.1	139.5
0.85	6173	3339	2053	1332	824.8	147.5
0.9	6181	3344	2057	1336	830.3	158.5
0.95	6190	3349	2061	1341	835.8	176.0
1.0	6199	3354	2066	1345	841.1	260.8
1.05	6208	3359	2070	1349	846.3	365.2
1.1	6217	3364	2074	1353	851.5	394.7
1.15	6225	3369	2078	1357	856.5	415.9
1.2	6234	3374	2082	1361	861.5	432.9
1.4	6269	3394	2098	1376	880.6	481.8
1.6	6304	3413	2115	1392	898.6	516.5
1.8	6340	3433	2131	1407	915.6	544.1
2.0	6375	3453	2148	1422	931.9	567.4
2.5	6463	3502	2208	1460	957.1	613.1
3.0	6552	3551	2250	1499	998.3	660.2
4.0	6730	3648	2332	1574	1074	739.0
5.0	6910	3745	2413	1645	1143	805.6
6.0	7091	3842	2492	1713	1207	865.0
7.0	7274	3938	2570	1778	1267	919.5
8.0	7459	4035	2647	1841	1324	970.6
9.0	7644	4132	2723	1903	1379	1019
10.0	7832	4229	2798	1962	1431	1066
11.0	8021	4327	2873	2021	1482	1111
12.0	8212	4424	2947	2078	1531	1155
13.0	8405	4522	3021	2134	1578	1198
14.0	8600	4621	3094	2188	1625	1240
15.0	8796	4720	3167	2243	1670	1282
16.0	8995	4819	3240	2296	1714	1323
17.0	9195	4919	3313	2348	1757	1364
18.0	9397	5020	3386	2400	1799	1405
19.0	9601	5121	3458	2451	1841	1445
20.0	9807	5223	3530	2501	1881	1486
25.0	10867	5742	3893	2746	2074	
30.0	11978	6280	4257			
35.0	13140	6838	4625			
40.0	14356	7416	4999			
AAD%	0.99	0.85	0.69	0.59	1.17	0.85

Table A4.8 Viscosity of n-Octane [μP] versus reduced pressure P_r and reduced temperature T_r .
 $T_c = 568.76 \text{ K}$ and $P_c = 24.8649 \text{ bar}$.

T_r P_r	0.45	0.50	0.55	0.60	0.65	0.70	0.76
0.2	11978	7402	5118	3785	2898	2269	1732
0.4	12046	7441	5146	3806	2920	2287	1749
0.6	12113	7480	5175	3826	2941	2305	1766
0.8	12181	7519	5204	3847	2962	2323	1783
0.85	12198	7528	5212	3852	2967	2327	1787
0.9	12215	7538	5219	3857	2972	2332	1791
0.95	12232	7548	5226	3862	2978	2336	1795
1.0	12249	7557	5233	3867	2983	2340	1799
1.05	12266	7567	5241	3872	2988	2345	1803
1.1	12283	7577	5248	3877	2993	2349	1807
1.15	12300	7587	5255	3882	2998	2354	1812
1.2	12317	7596	5262	3887	3003	2358	1816
1.4	12385	7635	5291	3908	3024	2375	1832
1.6	12453	7674	5320	3928	3044	2393	1848
1.8	12521	7714	5349	3948	3065	2410	1863
2.0	12590	7753	5377	3969	3085	2427	1879
2.5	12761	7851	5449	4019	3134	2468	1917
3.0	12933	7949	5521	4070	3183	2509	1954
4.0	13278	8147	5665	4171	3279	2589	2025
5.0	13627	8346	5808	4271	3371	2667	2094
6.0	13977	8546	5951	4372	3461	2742	2160
7.0	14331	8748	6094	4473	3549	2816	2225
8.0	14687	8951	6237	4573	3634	2887	2287
9.0	15047	9156	6380	4674	3718	2958	2349
10.0	15409	9362	6523	4776	3799	3026	2409
11.0	15774	9570	6667	4877	3878	3094	2468
12.0	16142	9780	6811	4979	3956	3160	2526
13.0	16512	9992	6955	5082	4032	3225	2584
14.0	16886	10205	7100	5185	4106	3289	2641
15.0	17263	10420	7245	5288	4179	3353	2697
16.0	17643	10637	7390	5392	4251	3415	2753
17.0	18026	10855	7536	5497	4320	3476	2808
18.0	18412	11075	7682	5602	4389	3537	2862
19.0	18801	11298	7829	5708	4456	3597	2917
20.0	19193	11522	7977	5815			
25.0	21202	12671	8723	6360			
30.0	23290	13869	9485	6925			
35.0	25460	15117	10265	7511			
40.0	27712	16417	11065	8120			
45.0	30047	17768	11884	8753			
48.0	31488	18604	12385	9144			
AAD%	1.17	1.47	1.21	1.09	1.09	1.15	1.37

Table A4.9 Viscosity of n-Decane [μP] versus reduced pressure P_r and reduced temperature T_r .
 $T_c = 617.50 \text{ K}$ and $P_c = 21.0349 \text{ bar}$.

$T_r \backslash P_r$	0.45	0.50	0.55	0.60
0.2	14097	8545	5737	4090
0.4	14164	8579	5763	4112
0.6	14231	8613	5789	4134
0.8	14299	8647	5815	4156
0.85	14315	8664	5821	4162
0.9	14332	8673	5828	4167
0.95	14349	8681	5834	4173
1.0	14366	8681	5841	4178
1.05	14383	8690	5847	4184
1.1	14400	8698	5854	4189
1.15	14417	8707	5860	4195
1.2	14434	8716	5867	4200
1.4	14502	8750	5893	4222
1.6	14570	8784	5918	4244
1.8	14638	8819	5944	4266
2.0	14706	8853	5970	4288
2.5	14878	8940	6035	4342
3.0	15050	9027	6100	4396
4.0	15398	9203	6229	4505
5.0	15750	9381	6360	4613
6.0	16106	9561	6490	4721
7.0	16466	9744	6621	4829
8.0	16830	9928	6753	4937
9.0	17199	10115	6885	5045
10.0	17571	10305	7018	5153
11.0	17948	10497	7152	5261
12.0	18329	10691	7286	5370
13.0	18715	10888	7421	5479
14.0	19104	11087	7557	5588
15.0	19498	11289	7694	5698
16.0	19897	11493	7832	5808
17.0	20299	11700	7971	5918
18.0	20707	11909	8111	6029
19.0	21118	12121	8252	6141
20.0	21534	12335	8393	6253
25.0	23680	13447	9118	6821
30.0	25938	14626	9870	7406
35.0	28309	15872	10650	8008
40.0	30793	17186	11461	8628
45.0	33392	18570	12301	9267
50.0	36105	20023	13173	9927
55.0	38933	21546	14077	10606
AAD%	0.87	1.07	1.08	0.90

Table A4.10 Viscosity of n-Dodecane [μP] versus reduced pressure P_r and reduced temperature T_r .
 $T_c = 658.2 \text{ K}$ and $P_c = 18.2383 \text{ bar}$.

$T_r \backslash P_r$	0.44	0.47	0.50	0.525
0.2	16669	12182	9163	7320
0.4	16748	12237	9206	7356
0.6	16827	12292	9248	7392
0.8	16906	12347	9290	7427
0.85	16926	12360	9301	7436
0.9	16946	12374	9312	7445
0.95	16966	12388	9322	7454
1.0	16985	12402	9333	7463
1.05	17005	12416	9343	7472
1.1	17025	12429	9354	7481
1.15	17045	12443	9365	7490
1.2	17065	12457	9375	7498
1.4	17144	12512	9417	7534
1.6	17224	12567	9460	7570
1.8	17304	12623	9502	7605
2.0	17384	12678	9545	7641
2.5	17584	12817	9651	7729
3.0	17785	12956	9757	7818
4.0	18189	13235	9970	7996
5.0	18597	13516	10183	8173
6.0	19007	13799	10397	8351
7.0	19421	14084	10612	8529
8.0	19838	14370	10827	8707
9.0	20258	14659	11043	8885
10.0	20681	14949	11260	9064
11.0	21108	15241	11478	9243
12.0	21538	15535	11696	9423
13.0	21971	15832	11916	9602
14.0	22408	16130	12136	9783
15.0	22848	16430	12358	9964
16.0	23292	16733	12580	10145
17.0	23739	17037	12803	10327
18.0	24189	17344	13028	10510
19.0	24643	17653	13253	10693
20.0	25101	17964	13480	10877
25.0	27441	19552	14630	11806
30.0	29871	21197	15810	12754
35.0	32391	22900	17021	13722
40.0	35004	24661	18264	14710
45.0	37709	26482	19540	15720
50.0	40507	28363	20850	16753
60.0	46384	32309	23572	18888
AAD%	0.20	0.52	0.38	0.24

Table A4.11 Viscosity of n-Tridecane [μP] versus reduced pressure P_r and reduced temperature T_r .
 $T_c = 675.8 \text{ K}$ and $P_c = 17.2251 \text{ bar}$.

T_r P_r	0.425	0.45	0.48	0.51	0.54
0.2	22680	16293	11642	8689	6977
0.4	22788	16354	11683	8720	7002
0.6	22897	16416	11724	8752	7028
0.8	23006	16478	11766	8783	7054
0.85	23033	16494	11776	8791	7060
0.9	23060	16509	11786	8799	7067
0.95	23088	16525	11797	8807	7073
1.0	23115	16540	11807	8815	7079
1.05	23142	16556	11817	8823	7086
1.1	23170	16571	11828	8831	7092
1.15	23197	16587	11838	8839	7099
1.2	23224	16603	11848	8847	7105
1.4	23334	16665	11890	8878	7131
1.6	23443	16728	11931	8910	7157
1.8	23553	16790	11973	8942	7182
2.0	23663	16853	12015	8974	7208
2.5	23940	17011	12120	9053	7272
3.0	24217	17170	12225	9133	7337
4.0	24775	17490	12437	9294	7467
5.0	25338	17813	12652	9455	7597
6.0	25907	18141	12869	9618	7727
7.0	26480	18472	13088	9782	7859
8.0	27058	18806	13310	9947	7991
9.0	27641	19145	13534	10113	8124
10.0	28230	19487	13760	10281	8258
11.0	28823	19834	13989	10450	8393
12.0	29422	20184	14221	10620	8529
13.0	30026	20538	14455	10792	8665
14.0	30635	20896	14692	10965	8803
15.0	31250	21257	14931	11139	8942
16.0	31870	21623	15173	11315	9082
17.0	32494	21993	15418	11493	9223
18.0	33125	22367	15665	11672	9365
19.0	33760	22744	15915	11852	9508
20.0	34401	23126	16167	12034	9653
25.0	37686	25096	17471	12968	10392
30.0	41106	27168	18843	13943	11163
35.0	44662	29343	20286	14960	11966
40.0		31622	21800	16019	12803
45.0		34006	23385	17122	13674
50.0		36495	25042	18269	14579
60.0		41791	28575	20698	16496
AAD%	0.68	0.68	0.64	0.98	0.98

Table A4.12 Viscosity of n-Tetradecane [μP] versus reduced pressure P_r and reduced temperature T_r .
 $T_c = 691.8 \text{ K}$ and $P_c = 16.2118 \text{ bar}$.

T_r P_r	0.44	0.47	0.50	0.525	0.55	0.575
0.2	19711	13811	10133	8196	6687	5579
0.4	19793	13859	10170	8225	6714	5603
0.6	19876	13907	10207	8254	6740	5627
0.8	19959	13956	10244	8283	6767	5651
0.85	19979	13968	10253	8290	6774	5657
0.9	20000	13980	10262	8297	6780	5663
0.95	20021	13993	10271	8305	6787	5669
1.0	20042	14005	10281	8312	6793	5675
1.05	20062	14017	10290	8319	6800	5681
1.1	20083	14029	10299	8326	6807	5687
1.15	20104	14041	10308	8334	6813	5693
1.2	20125	14054	10318	8341	6820	5699
1.4	20208	14103	10355	8370	6847	5722
1.6	20291	14152	10392	8399	6873	5746
1.8	20375	14201	10429	8428	6900	5770
2.0	20459	14250	10466	8457	6926	5794
2.5	20669	14374	10560	8530	6993	5853
3.0	20880	14499	10653	8604	7059	5913
4.0	21306	14751	10842	8751	7193	6031
5.0	21737	15006	11032	8899	7326	6150
6.0	22172	15264	11223	9049	7460	6269
7.0	22612	15526	11416	9199	7594	6388
8.0	23057	15791	11611	9351	7728	6507
9.0	23506	16059	11807	9503	7863	6626
10.0	23960	16331	12005	9657	7999	6746
11.0	24419	16607	12204	9813	8135	6866
12.0	24882	16885	12405	9969	8272	6987
13.0	25351	17168	12608	10127	8409	7108
14.0	25824	17453	12813	10287	8547	7229
15.0	26302	17743	13019	10447	8686	7351
16.0	26785	18036	13227	10609	8825	7473
17.0	27272	18332	13437	10773	8966	7597
18.0	27765	18632	13649	10938	9107	7720
19.0	28263	18936	13863	11104	9248	7845
20.0	28765	19243	14079	11272	9391	7969
25.0	31352	20834	15186	12135	10117	8604
30.0	34063	22516	16342	13036	10866	9257
35.0	36899	24291	17548	13979	11639	9930
40.0	39862	26160	18806	14962	12438	10624
45.0	42952	28123	20115	15988	13262	11340
50.0	46170	30181	21477	17057	14113	12077
60.0	52989	34581	24360	19324	15897	13621
65.0	56592	36925	25882	20523	16830	14428
AAD%	0.90	0.90	0.79	0.79	0.64	0.64

Table A4.13 Viscosity of n-Pentadecane [μP] versus reduced pressure P_r and reduced temperature T_r .
 $T_c = 706.8 \text{ K}$ and $P_c = 15.1986 \text{ bar}$.

T_r P_r	0.415	0.435	0.46	0.49	0.52
0.2	30061	21685	16306	11589	8861
0.4	30178	21771	16358	11628	8892
0.6	30294	21856	16411	11668	8923
0.8	30411	21942	16463	11708	8954
0.85	30440	21964	16476	11718	8962
0.9	30470	21985	16490	11728	8970
0.95	30499	22007	16503	11738	8977
1.0	30528	22029	16516	11748	8985
1.05	30558	22050	16529	11758	8993
1.1	30587	22072	16542	11768	9000
1.15	30616	22093	16556	11778	9008
1.2	30646	22115	16569	11788	9016
1.4	30764	22202	16622	11828	9047
1.6	30882	22289	16675	11868	9078
1.8	31000	22376	16728	11908	9109
2.0	31119	22463	16781	11949	9140
2.5	31417	22683	16915	12050	9218
3.0	31717	22904	17050	12151	9296
4.0	32323	23351	17321	12355	9452
5.0	32936	23804	17596	12560	9610
6.0	33558	24263	17874	12768	9768
7.0	34186	24729	18155	12977	9927
8.0	34823	25200	18440	13188	10087
9.0	35467	25678	18728	13401	10248
10.0	36119	26163	19020	13615	10410
11.0	36779	26654	19315	13832	10573
12.0	37447	27151	19614	14051	10737
13.0	38122	27654	19916	14271	10903
14.0	38805	28164	20221	14494	11069
15.0	39496	28680	20530	14719	11237
16.0	40196	29202	20843	14945	11406
17.0	40902	29731	21159	15174	11576
18.0	41617	30266	21479	15405	11748
19.0	42340	30808	21802	15638	11921
20.0	43071	31356	22129	15874	12095
25.0		34194	23819	17082	12985
30.0		37194	25601	18345	13909
35.0		40357	27476	19665	14870
40.0		43683	29445	21042	15867
45.0		47173	31508	22476	16901
50.0		50827	33667	23969	17973
60.0		58628	38271	27132	20234
70.0		67088	43260	30532	22650
AAD%	0.74	1.05	0.83	0.99	0.72

Table A4.14 Viscosity of n-Hexadecane [μP] versus reduced pressure P_r and reduced temperature T_r .
 $T_c = 720.6 \text{ K}$ and $P_c = 14.1854 \text{ bar}$.

$\begin{matrix} T_r \\ P_r \end{matrix}$	0.42	0.45	0.48	0.51	0.55
0.2	31561	19965	14199	10490	7387
0.4	31705	20038	14246	10525	7413
0.6	31849	20111	14292	10560	7438
0.8	31994	20184	14338	10595	7463
0.85	32030	20203	14350	10604	7470
0.9	32066	20221	14361	10613	7476
0.95	32102	20239	14373	10622	7482
1.0	32138	20258	14385	10630	7489
1.05	32174	20276	14396	10639	7495
1.1	32210	20294	14408	10648	7502
1.15	32246	20313	14419	10657	7508
1.2	32282	20331	14431	10665	7514
1.4	32427	20405	14477	10700	7540
1.6	32571	20478	14524	10736	7565
1.8	32716	20552	14570	10771	7590
2.0	32861	20625	14617	10806	7616
2.5	33223	20810	14733	10893	7679
3.0	33586	20995	14850	10981	7742
4.0	34314	21366	15084	11157	7869
5.0	35044	21738	15320	11333	7995
6.0	35777	22113	15556	11509	8121
7.0	36512	22489	15793	11685	8247
8.0	37251	22867	16032	11862	8373
9.0	37992	23247	16272	12039	8500
10.0	38735	23629	16513	12217	8626
11.0	39482	24013	16755	12395	8753
12.0	40231	24399	16999	12574	8880
13.0	40983	24787	17244	12753	9007
14.0	41738	25177	17490	12933	9135
15.0	42496	25569	17738	13113	9262
16.0	43257	25964	17987	13294	9391
17.0	44021	26360	18238	13475	9519
18.0	44788	26758	18490	13658	9648
19.0	45558	27159	18743	13841	9778
20.0	46331	27561	18998	14024	9907
25.0	50242	29608	20296	14954	10564
30.0	54231	31711	21633	15903	11233
35.0	58300	33872	23011	16874	11918
40.0	62451	36091	24430	17867	12618
45.0	66685	38370	25892	18883	13334
50.0	71002	40710	27397	19923	14068
60.0		45572	30538	22078	15589
70.0		50683	33858	24333	17185
80.0		56043	37357	26692	18856
AAD%	0.85	0.85	0.94	0.72	0.72

Table A4.15 Viscosity of n-Octadecane [μP] versus reduced pressure P_r and reduced temperature T_r .
 $T_c = 745.2 \text{ K}$ and $P_c = 12.1589 \text{ bar}$.

A5 References in Appendix A

Abe Y., Kestin J., Khalifa H.E., and Wakeham W.A.: *The Viscosity of Normal Butane, Isobutane, and Their Mixtures*. Physica. **97A** (1979) 296 – 305.

Agaev N.A. and Golubev I.F.: *The Viscosities of Liquid and Gaseous n-Pentane at High Pressures and Different Temperatures*. Gazovaja Promyslennost'. **8(5)** (1963a) 45 – 50.

Agaev N.A. and Golubev I.F.: *The Viscosity of n-Hexane in the Liquid and Gaseous State at High Pressures and Different Temperatures*. Doklady Physical Chemistry Proceedings of the Academy of Sciences of the USSR. **151** (1963b) 635 – 640.

Agaev N.A. and Golubev I.F.: *Viscosities of Liquid and Gaseous n-Heptane and n-Octane at High Pressures and Different Temperatures*. Gazovaja Promyslennost'. **8(7)** (1963c) 50 – 53.

Assael M.J. and Papadaki M.: *Measurements of the Viscosity of n-Heptane, n-Nonane, and n-Undecane at Pressures up to 70 MPa*. International Journal of Thermophysics. **12** (1991) 801 – 810.

Assael M.J., Oliveira C.P., Papadaki M., and Wakeham W.A.: *Vibrating-Wire Viscometers for Liquids at High Pressures*. International Journal of Thermophysics. **13** (1992) 593 – 615.

Baron J.D., Roof J.G., and Wells F.W.: *Viscosity of Nitrogen, Methane, Ethane, and Propane at Elevated Temperature and Pressure*. Journal of Chemical and Engineering Data. **4** (1959) 283 – 288.

Barrufet M.A., Hall K.R., Estrada-Baltazar A., and Iglesias-Silva G.A.: *Liquid Viscosity of Octane and Pentane + Octane Mixtures from 298.15 K to 373.15 K up to 25 MPa*. Journal of Chemical and Engineering Data. **44** (1999) 1310 – 1314.

Baylaucq A., Boned C., Daugé P., and Lagourette B.: *Measurements of the Viscosity and Density of Three Hydrocarbons and the Three Associated Binary Mixtures Versus Pressure and Temperature*. International Journal of Thermophysics. **18** (1997) 3 – 23.

Berstad D.A.: *Viscosity and Density of n-Hexane, Cyclohexane and Benzene, and Their Mixtures with Methane*. Ph.D. Thesis, (IUK-Thesis 55), Insititutt for Uorganisk Kjemi, Universitetet i Trondheim, Norges Tekniske Høgskole, Trondheim, Norway. (1989).

Brazier D.W. and Freeman G.R.: *The Effects of Pressure on the Density, Dielectric Constant, and Viscosity of Several Hydrocarbons and Other Organic Liquids*. Canadian Journal of Chemistry. **47** (1969) 893 – 899.

Carmichael L.T. and Sage B.H.: *Viscosity of Ethane at High Pressures*. Journal of Chemical and Engineering Data. **8** (1963a) 94 – 98.

Carmichael L.T. and Sage B.H.: *Viscosity of Hydrocarbons. n-Butane*. Journal of Chemical and Engineering Data. **8** (1963b) 612 – 616.

Carmichael L.T., Berry V.M., and Sage B.H.: *Viscosity of Hydrocarbons. Propane*. Journal of Chemical and Engineering Data. **9** (1964) 411 – 415.

Carmichael L.T., Berry V., and Sage B.H.: *Viscosity of Hydrocarbons. Methane*. Journal of Chemical and Engineering Data. **10** (1965) 57 – 61.

Carmichael L.T., Berry V.M., and Sage B.H.: *Viscosity of Hydrocarbons. n-Decane*. Journal of Chemical and Engineering Data. **14** (1969) 27 – 31.

Chuang S.-Y., Chapple P.S., and Kobayashi R.: *Viscosity of Methane, Hydrogen, and Four Mixtures of Methane and Hydrogen from –100°C to 0°C at High Pressures*. Journal of Chemical and Engineering Data. **21** (1976) 403 – 411.

Collings A.F. and McLaughlin E.: *Torsional Crystal Technique for the Measurement of Viscosities of Liquids at High Pressure*. Transaction Faraday Society. **67** (1971) 340 – 352.

Cullick A.S. and Mathis M.L.: *Densities and Viscosities of Mixtures of Carbon Dioxide and n-Decane from 310 K to 403 K and 7 to 30 MPa*. Journal of Chemical and Engineering Data. **29** (1984) 393 – 396.

Daugé P., Baylaucq A., and Boned C.: *High-Pressure Viscosity Behaviour of the Tridecane + 1-Methylnaphthalene System*. High Temperatures – High Pressures. **31** (1999) 665 – 680.

Diller D.E.: *Measurements of the Viscosity of Compressed Gaseous and Liquid Methane*. Physica. **104A** (1980) 417 – 426.

Diller D.E. and Saber J.M.: *Measurements of the Viscosity of Compressed Gaseous and Liquid Ethane*. Physica. **108A** (1981) 143 – 152.

Diller D.E.: *Measurements of the Viscosity of Saturated and Compressed Liquid Propane*. Journal of Chemical and Engineering Data. **27** (1982) 240 – 243.

Diller D.E. and van Poolen L.J.: *Measurements of the Viscosities of Saturated and Compressed Liquid Normal Butane and Isobutane*. International Journal of Thermophysics. **6** (1985) 43 – 62.

Diller D.E. and Ely J.F.: *Measurements of the Viscosities of Compressed Gaseous Carbon Dioxide, Ethane, and Their Mixtures at Temperatures up to 500 K. High-Temperatures – High Pressures*. **21** (1989) 613 – 620.

Dolan J.P., Starling K.E., Lee A.L., Eakin B.E., and Ellington R.T.: *Liquid, Gas, and Dense Fluid Viscosity of n-Butane*. Journal of Chemical and Engineering Data. **8** (1963) 396 – 399.

Douslin D.P., Harrison R.H., Moore R.T., and McCullough J.P.: *P-V-T Relations for Methane*. Journal of Chemical and Engineering Data. **9** (1964) 358 – 363.

Ducoulombier D., Zhou H., Boned C., Peyrelasse J., Saint-Guirons H., and Xans P.: *Condensed Phases and Macromolecules. Pressures (1 – 1000 bars) and Temperatures (20 – 100°C) Dependence of the Viscosity of Liquid Hydrocarbons*. Journal of Physical Chemistry. **90** (1986) 1692 – 1700.

Dymond J.H., Young K.J., and Isdale J.D.: *P, ρ , T Behavior for n-Hexane + n-Hexadecane in the Range 298 to 373 K and 0.1 to 500 MPa*. Journal of Chemical Thermodynamics. **11** (1979) 887 – 895.

Dymond J.H., Young K.J., and Isdale J.D.: *Transport Properties of Nonelectrolyte Liquid Mixtures – II. Viscosity Coefficients for the n-Hexane + n-Hexadecane System at Temperatures from 25 to 100°C at Pressures up to the Freezing Pressure or 500 MPa*. International Journal of Thermophysics. **1** (1980) 345 – 373.

Dymond J.H., Robertson J., and Isdale J.D.: *(P, ρ , T) of Some Pure n-Alkanes and Binary Mixtures of n-Alkanes in the Range 298 to 373 K and 0.1 to 500 MPa*. Journal of Chemical Thermodynamics. **14** (1982) 51 – 59.

Eakin B.E., Starling K.E., Dolan J.P., and Ellington R.T.: *Liquid, Gas, and Dense Fluid Viscosity of Ethane*. Journal of Chemical and Engineering Data. **7** (1962) 33 – 36.

Estrada-Baltazar A., Alvarado J.F.J., Iglesias-Silva G.A., and Barrufet M. A.: *Experimental Liquid Viscosities of Decane and Octane + Decane from 298.15 K to 373.15 K and up to 25 MPa*. Journal of Chemical and Engineering Data. **43** (1998) 441 – 446.

Gates J.A., Wood R.H., Cobos J.C., Casanova C., Roux A.H., Roux-Desgranges G., and Grolier J.-P.E.: *Densities and Heat Capacities of 1-Butanol + n-Decane from 298 K to 400 K*. Fluid Phase Equilibria. **27** (1986) 137 – 151.

Gehrig M. and Lentz H.: *Values of $P(V_m, T)$ for n-Decane up to 300 MPa and 673 K*. Journal of Chemical Thermodynamics. **15** (1983) 1159 – 1167.

Giddings J.G., Kao J.T.F., and Kobayashi R.: *Development of a High-Pressure Capillary-Tube Viscometer and Its Application to Methane, Propane, and Their Mixtures in the Gaseous and Liquid Regions*. The Journal of Chemical Physics. **45** (1966) 578 – 586.

Giller E.B. and Drickamer H.G.: *Viscosity of Normal Paraffins Near the Freezing Point*. Industrial and Engineering Chemistry. **41** (1949) 2067 – 2069.

Goates J.R., Ott J.B., and Grigg R.B.: *Excess Volumes of n-Hexane + n-Heptane, + n-Octane, + n-Nonane, and + n-Decane at 283.15, 298.15, and 313.15 K*. Journal of Chemical Thermodynamics. **13** (1981) 908 – 913.

Händel G., Kleinrahm R., and Wagner W.: *Measurements of the (Pressure, Density, Temperature) Relation of Methane in the Homogeneous Gas and Liquid Regions in the Temperature Range from 100 K to 260 K and at Pressures up to 8 MPa*. Journal of Chemical Thermodynamics. **24** (1992) 685 – 695.

Hellemans J., Zink H., and van Paemel O.: *The Viscosity of Liquid Argon and Liquid Methane along Isotherms as a Function of Pressure*. Physica. **46** (1970) 395 – 410.

Hogenboom D.L., Webb W., and Dixon J.A.: *Viscosity of Several Liquid Hydrocarbons as a Function of Temperature, Pressure, and Free Volume*. The Journal of Chemical Physics. **46** (1967) 2586 – 2598.

Huang E.T.S., Swift G.W., and Kurata F.: *Viscosities of Methane and Propane at Low Temperatures and High Pressures*. AIChE Journal. **12** (1966) 932 – 936.

Hutchings R. and van Hook W.A.: *Molar Volumes in the Homologous Series of Normal Alkanes at Two Temperatures*. Fluid Phase Equilibria. **21** (1985) 165 – 170.

Isdale J.D., Dymond J.H., and Brawn T.A.: *Viscosity and Density of n-Hexane - Cyclohexane Mixtures between 25 and 100 °C up to 500 MPa*. High Temperatures - High Pressures. **11** (1979) 571 – 580.

Iwasaki H. and Takahashi M.: *Viscosity of Carbon Dioxide and Ethane*. Journal of Chemical Physics. **74** (1981) 1930 – 1943.

Kelso E.A. and Felsing W.A.: *The Pressure-Volume-Temperature Relations of n-Hexane and of 2-Methylpentane*. Journal of the American Chemical Society. **62** (1940) 3132 – 3134.

Kestin J. and Yata J.: *Viscosity and Diffusion Coefficient of Six Binary Mixtures*. The Journal of Chemical Physics. **49** (1968) 4780 – 4791.

Kiran E. and Sen Y.L.: *High-Pressure Viscosity and Density of n-Alkanes*. International Journal of Thermophysics. **13** (1992) 411 – 442.

Kleinrahm R. and Wagner W.: *Measurement and Correlation of the Equilibrium Liquid and Vapour Densities and the Vapour Pressure along the Coexistence Curve of Methane*. Journal of Chemical Thermodynamics. **18** (1986) 739 – 760.

Kleinrahm R., Duschek W., and Wagner W.: *(Pressure, Density, Temperature) Measurements in the Critical Region of Methane*. Journal of Chemical Thermodynamics. **18** (1986) 1103 – 1114.

Kleinrahm R., Duschek W., and Wagner W.: *Measurement and Correlation of the (Pressure, Density, Temperature) Relation of Methane in the Temperature Range from 273.15 K to 323.15 K at Pressures up to 8 MPa*. Journal of Chemical Thermodynamics. **20** (1988) 621 – 631.

Knapstad B.: *Viscosity of n-Decane – Methane at Elevated Pressure and Temperature*. Ph.D. Thesis (IUK-Thesis 48), Institutt for Uorganisk Kjemi, Universitetet i Trondheim, Norges Tekniske Høgskole, Trondheim, Norway. (1986).

Knapstad B., Skjølsvik P.A., and Øye H.A.: *Viscosity of Pure Hydrocarbons*. Journal of Chemical and Engineering Data. **34** (1989) 37 – 43.

Knapstad B., Skjølsvik P.A., and Øye H.A.: *Viscosity of the n-Decane – Methane System in the Liquid Phase*. Berichte der Bunsengesellschaft für Physikalische Chemie. **94** (1990) 1156 – 1165.

Kor S.K., Singh B.K., and Rai G.: *Pressure Dependence of Ultrasonic Absorption and Compressional Viscosity due to Structural Rearrangement in Hexane and Toluene*. II Nouovo Cimento. **12B** (1972) 205 – 214.

Kuss E.: *Hochdruckuntersuchungen II: Die Viskosität von Komprimierten Gasen*. Zeitschrift für Angewandte Physik. **4** (1952) 203 – 207.

Kuss E. and Pollmann P.: *Viskositäts-Druckabhängigkeit und Verzweigungsgrad Flüssiger Alkane*. Zeitschrift für Physikalische Chemie Neue Folge. **68** (1969) 205 – 227.

Kuss E., Oelert, Deininger, Hugo, Miessner, and Wisken.: *PVT-Daten bei Hohen Drücken*, DGMK-Projekt 4510. Deutsche Gesellschaft für Mineralölwissenschaft und Kohlechemie E. V. (1976).

Lee A.L. and Ellington R.T.: *Viscosity of n-Pentane*. Journal of Chemical and Engineering Data. **10** (1965a) 101 – 104.

Lee A.L. and Ellington R.T.: *Viscosity of n-Decane in the Liquid Phase*. Journal of Chemical and Engineering Data. **10** (1965b) 346 – 348.

Machado J.R.S., Streett W.B., and Dieters U.: *PVT Measurements of Hydrogen/Methane Mixtures at High Pressures*. Journal of Chemical and Engineering Data. **33** (1988) 148 – 152.

Matthews M.A., Rodden J.B., and Akgerman A.: *High-Temperature Diffusion, Viscosity, and Density Measurements in n-Hexadecane*. Journal of Chemical and Engineering Data. **32** (1987) 317 – 319.

Mollerup J.: *Measurement of the Volumetric Properties of Methane and Ethylene at 310 K at Pressures to 70 MPa*. SEP 8404, (IVC-SEP), Department of Chemical Engineering, Technical University of Denmark, Lyngby, Denmark. (1984).

Oliveira C.M.B.P. and Wakeham W.A.: *The Viscosity of Five Liquid Hydrocarbons at Pressures up to 250 MPa*. International Journal of Thermophysics. **13** (1992) 773 – 790.

Parisot P.E. and Johnson E.F.: *Liquid Viscosity above the Normal Boiling Point*. Journal of Chemical Engineering Data. **6** (1961) 263 – 267.

Pieperbeck N., Kleinrahm R., Wagner W., and Jaeschke M.: *Results of (Pressure, Density, Temperature) Measurements on Methane and on Nitrogen in the Temperature Range from 273.15 K to 323.15 K at Pressures up to 12 MPa using a New Apparatus for Accurate Gas-Density Measurements*. Journal of Chemical Thermodynamics. **23** (1991) 175 – 194.

Roos J.F. and Brown G.M.: *Viscosities of Gases at High Pressures*. Industrial and Engineering Chemistry. **49** (1957) 2026 – 2034.

Sage B.H., Yale W.D., and Lacey W.N.: *Effect of Pressure on Viscosity of n-Butane and Isobutane* Industrial and Engineering Chemistry. **31** (1939) 223 – 226.

Sage B.H., Lavender H.M., and Lacey W.N.: *Phase Equilibria in Hydrocarbon Systems. Methane – Decane System*. Industrial and Engineering Chemistry. **32** (1940) 743 – 747.

Starling K.E., Eakin B.E., and Ellington R.T.: *Liquid, Gas, and Dense-Fluid Viscosity of Propane*. AIChE Journal. **6** (1960) 438 – 442.

Stewart D.E., Sage B.H., and Lacey W.N.: *Volumetric Behavior of n-Hexane in Liquid Phase*. Industrial and Engineering Chemistry. **46** (1954) 2529 – 2531.

Swift G.W., Lohrenz J., and Kurata F.: *Liquid Viscosities above the Normal Boiling Point for Methane, Ethane, Propane, and n-Butane*. AIChE Journal. **6** (1960) 415 – 419.

Tanaka Y., Hosokawa H., Kubota H., and Makita T.: *Viscosity and Density of Binary Mixtures of Cyclohexane with n-Octane, n-Dodecane, and n-Hexadecane under High Pressure*. International Journal of Thermophysics. **12** (1991) 245 – 264.

van der Gulik P.S., Mostert R., and van den Berg H.R.: *The Viscosity of Methane at 25°C up to 10 kbar*. Physica. **151A** (1988) 153 – 166.

van der Gulik P.S., Mostert R., and van den Berg H.R.: *The Viscosity of Methane at 273 K up to 1 GPa*. Fluid Phase Equilibria. **79** (1992) 301 – 311.

APPENDIX B

B1 Measured Viscosities and Densities of Ternary Mixtures

x_m	x_t	x_h	T [K]	P [MPa]	ρ [g/cm ³]	η [mPa s]
0.125	0.125	0.750	293.15	0.1	0.7964	3.130
0.125	0.125	0.750	293.15	20	0.8089	4.380
0.125	0.125	0.750	293.15	40	0.8197	6.070
0.125	0.125	0.750	293.15	60	0.8292	8.153
0.125	0.125	0.750	293.15	80	0.8377	11.055
0.125	0.125	0.750	293.15	100	0.8454	14.696
0.125	0.125	0.750	303.15	0.1	0.7895	2.504
0.125	0.125	0.750	303.15	20	0.8027	3.481
0.125	0.125	0.750	303.15	40	0.8139	4.661
0.125	0.125	0.750	303.15	60	0.8238	6.221
0.125	0.125	0.750	303.15	80	0.8325	8.258
0.125	0.125	0.750	303.15	100	0.8403	10.896
0.125	0.125	0.750	313.15	0.1	0.7827	2.049
0.125	0.125	0.750	313.15	20	0.7965	2.801
0.125	0.125	0.750	313.15	40	0.8083	3.718
0.125	0.125	0.750	313.15	60	0.8184	4.903
0.125	0.125	0.750	313.15	80	0.8272	6.411
0.125	0.125	0.750	313.15	100	0.8351	8.314
0.125	0.125	0.750	323.15	0.1	0.7759	1.708
0.125	0.125	0.750	323.15	20	0.7905	2.386
0.125	0.125	0.750	323.15	40	0.8027	3.127
0.125	0.125	0.750	323.15	60	0.8133	4.020
0.125	0.125	0.750	323.15	80	0.8226	5.132
0.125	0.125	0.750	323.15	100	0.8310	6.588
0.125	0.125	0.750	333.15	0.1	0.7691	1.447
0.125	0.125	0.750	333.15	20	0.7844	2.002
0.125	0.125	0.750	333.15	40	0.7972	2.585
0.125	0.125	0.750	333.15	60	0.8081	3.287
0.125	0.125	0.750	333.15	80	0.8177	4.127
0.125	0.125	0.750	333.15	100	0.8263	5.179
0.125	0.125	0.750	343.15	0.1	0.7621	1.248
0.125	0.125	0.750	343.15	20	0.7783	1.740
0.125	0.125	0.750	343.15	40	0.7915	2.250
0.125	0.125	0.750	343.15	60	0.8029	2.856
0.125	0.125	0.750	343.15	80	0.8127	3.567
0.125	0.125	0.750	343.15	100	0.8216	4.389
0.125	0.125	0.750	353.15	0.1	0.7552	1.083
0.125	0.125	0.750	353.15	20	0.7721	1.500
0.125	0.125	0.750	353.15	40	0.7860	1.920
0.125	0.125	0.750	353.15	60	0.7977	2.434
0.125	0.125	0.750	353.15	80	0.8079	3.054
0.125	0.125	0.750	353.15	100	0.8169	3.721

Table B1.1 Density ρ and dynamic viscosity η versus temperature T , pressure P , and mole fraction x_i for ternary mixtures of 1-methylnaphthalene (m) + n-tridecane (t) + 2,2,4,4,6,8,8-heptamethylnonane (h).

x_m	x_t	x_h	T [K]	P [MPa]	ρ [g/cm ³]	η [mPa s]
0.125	0.250	0.625	293.15	0.1	0.7936	2.775
0.125	0.250	0.625	293.15	20	0.8061	3.894
0.125	0.250	0.625	293.15	40	0.8169	5.210
0.125	0.250	0.625	293.15	60	0.8264	6.900
0.125	0.250	0.625	293.15	80	0.8349	9.042
0.125	0.250	0.625	293.15	100	0.8427	11.735
0.125	0.250	0.625	303.15	0.1	0.7870	2.241
0.125	0.250	0.625	303.15	20	0.8002	3.113
0.125	0.250	0.625	303.15	40	0.8114	4.120
0.125	0.250	0.625	303.15	60	0.8213	5.376
0.125	0.250	0.625	303.15	80	0.8301	6.920
0.125	0.250	0.625	303.15	100	0.8381	8.799
0.125	0.250	0.625	313.15	0.1	0.7802	1.846
0.125	0.250	0.625	313.15	20	0.7940	2.550
0.125	0.250	0.625	313.15	40	0.8057	3.364
0.125	0.250	0.625	313.15	60	0.8159	4.354
0.125	0.250	0.625	313.15	80	0.8249	5.540
0.125	0.250	0.625	313.15	100	0.8330	6.944
0.125	0.250	0.625	323.15	0.1	0.7732	1.550
0.125	0.250	0.625	323.15	20	0.7877	2.128
0.125	0.250	0.625	323.15	40	0.7999	2.781
0.125	0.250	0.625	323.15	60	0.8105	3.568
0.125	0.250	0.625	323.15	80	0.8199	4.501
0.125	0.250	0.625	323.15	100	0.8283	5.594
0.125	0.250	0.625	333.15	0.1	0.7663	1.326
0.125	0.250	0.625	333.15	20	0.7816	1.815
0.125	0.250	0.625	333.15	40	0.7943	2.331
0.125	0.250	0.625	333.15	60	0.8053	2.945
0.125	0.250	0.625	333.15	80	0.8148	3.662
0.125	0.250	0.625	333.15	100	0.8233	4.493
0.125	0.250	0.625	343.15	0.1	0.7593	1.144
0.125	0.250	0.625	343.15	20	0.7755	1.561
0.125	0.250	0.625	343.15	40	0.7887	1.983
0.125	0.250	0.625	343.15	60	0.8000	2.489
0.125	0.250	0.625	343.15	80	0.8099	3.083
0.125	0.250	0.625	343.15	100	0.8187	3.774
0.125	0.250	0.625	353.15	0.1	0.7523	0.999
0.125	0.250	0.625	353.15	20	0.7692	1.375
0.125	0.250	0.625	353.15	40	0.7830	1.740
0.125	0.250	0.625	353.15	60	0.7948	2.167
0.125	0.250	0.625	353.15	80	0.8050	2.658
0.125	0.250	0.625	353.15	100	0.8140	3.216

Table B1.1 *Continued.*

x_m	x_t	x_h	T [K]	P [MPa]	ρ [g/cm ³]	η [mPa s]
0.125	0.375	0.500	293.15	0.1	0.7903	2.524
0.125	0.375	0.500	293.15	20	0.8027	3.436
0.125	0.375	0.500	293.15	40	0.8135	4.526
0.125	0.375	0.500	293.15	60	0.8230	5.871
0.125	0.375	0.500	293.15	80	0.8315	7.506
0.125	0.375	0.500	293.15	100	0.8392	9.519
0.125	0.375	0.500	303.15	0.1	0.7833	2.052
0.125	0.375	0.500	303.15	20	0.7965	2.765
0.125	0.375	0.500	303.15	40	0.8076	3.614
0.125	0.375	0.500	303.15	60	0.8176	4.644
0.125	0.375	0.500	303.15	80	0.8263	5.875
0.125	0.375	0.500	303.15	100	0.8343	7.284
0.125	0.375	0.500	313.15	0.1	0.7764	1.702
0.125	0.375	0.500	313.15	20	0.7902	2.306
0.125	0.375	0.500	313.15	40	0.8019	2.990
0.125	0.375	0.500	313.15	60	0.8121	3.801
0.125	0.375	0.500	313.15	80	0.8211	4.749
0.125	0.375	0.500	313.15	100	0.8293	5.819
0.125	0.375	0.500	323.15	0.1	0.7695	1.434
0.125	0.375	0.500	323.15	20	0.7840	1.930
0.125	0.375	0.500	323.15	40	0.7961	2.475
0.125	0.375	0.500	323.15	60	0.8068	3.114
0.125	0.375	0.500	323.15	80	0.8161	3.854
0.125	0.375	0.500	323.15	100	0.8246	4.704
0.125	0.375	0.500	333.15	0.1	0.7625	1.229
0.125	0.375	0.500	333.15	20	0.7778	1.650
0.125	0.375	0.500	333.15	40	0.7905	2.097
0.125	0.375	0.500	333.15	60	0.8014	2.613
0.125	0.375	0.500	333.15	80	0.8110	3.199
0.125	0.375	0.500	333.15	100	0.8196	3.877
0.125	0.375	0.500	343.15	0.1	0.7554	1.066
0.125	0.375	0.500	343.15	20	0.7716	1.414
0.125	0.375	0.500	343.15	40	0.7848	1.783
0.125	0.375	0.500	343.15	60	0.7961	2.213
0.125	0.375	0.500	343.15	80	0.8060	2.706
0.125	0.375	0.500	343.15	100	0.8148	3.279
0.125	0.375	0.500	353.15	0.1	0.7484	0.934
0.125	0.375	0.500	353.15	20	0.7654	1.245
0.125	0.375	0.500	353.15	40	0.7792	1.568
0.125	0.375	0.500	353.15	60	0.7910	1.944
0.125	0.375	0.500	353.15	80	0.8011	2.376
0.125	0.375	0.500	353.15	100	0.8101	2.859

Table B1.1 *Continued.*

x_m	x_t	x_h	T [K]	P [MPa]	ρ [g/cm ³]	η [mPa s]
0.125	0.500	0.375	293.15	0.1	0.7872	2.319
0.125	0.500	0.375	293.15	20	0.7997	3.083
0.125	0.500	0.375	293.15	40	0.8105	3.978
0.125	0.500	0.375	293.15	60	0.8201	5.073
0.125	0.500	0.375	293.15	80	0.8286	6.390
0.125	0.500	0.375	293.15	100	0.8363	7.962
0.125	0.500	0.375	303.15	0.1	0.7805	1.889
0.125	0.500	0.375	303.15	20	0.7936	2.551
0.125	0.500	0.375	303.15	40	0.8048	3.259
0.125	0.500	0.375	303.15	60	0.8148	4.092
0.125	0.500	0.375	303.15	80	0.8236	5.056
0.125	0.500	0.375	303.15	100	0.8316	6.158
0.125	0.500	0.375	313.15	0.1	0.7736	1.573
0.125	0.500	0.375	313.15	20	0.7874	2.129
0.125	0.500	0.375	313.15	40	0.7990	2.715
0.125	0.500	0.375	313.15	60	0.8093	3.396
0.125	0.500	0.375	313.15	80	0.8183	4.173
0.125	0.500	0.375	313.15	100	0.8265	5.050
0.125	0.500	0.375	323.15	0.1	0.7666	1.333
0.125	0.500	0.375	323.15	20	0.7811	1.814
0.125	0.500	0.375	323.15	40	0.7932	2.304
0.125	0.500	0.375	323.15	60	0.8038	2.859
0.125	0.500	0.375	323.15	80	0.8131	3.477
0.125	0.500	0.375	323.15	100	0.8215	4.153
0.125	0.500	0.375	333.15	0.1	0.7595	1.149
0.125	0.500	0.375	333.15	20	0.7748	1.544
0.125	0.500	0.375	333.15	40	0.7875	1.936
0.125	0.500	0.375	333.15	60	0.7985	2.387
0.125	0.500	0.375	333.15	80	0.8080	2.896
0.125	0.500	0.375	333.15	100	0.8166	3.465
0.125	0.500	0.375	343.15	0.1	0.7524	0.998
0.125	0.500	0.375	343.15	20	0.7685	1.340
0.125	0.500	0.375	343.15	40	0.7817	1.666
0.125	0.500	0.375	343.15	60	0.7930	2.034
0.125	0.500	0.375	343.15	80	0.8030	2.440
0.125	0.500	0.375	343.15	100	0.8119	2.884
0.125	0.500	0.375	353.15	0.1	0.7453	0.882
0.125	0.500	0.375	353.15	20	0.7622	1.177
0.125	0.500	0.375	353.15	40	0.7759	1.461
0.125	0.500	0.375	353.15	60	0.7877	1.777
0.125	0.500	0.375	353.15	80	0.7979	2.123
0.125	0.500	0.375	353.15	100	0.8070	2.497

Table B1.1 *Continued.*

x_m	x_t	x_h	T [K]	P [MPa]	ρ [g/cm ³]	η [mPa s]
0.125	0.625	0.250	293.15	0.1	0.7839	2.141
0.125	0.625	0.250	293.15	20	0.7963	2.841
0.125	0.625	0.250	293.15	40	0.8071	3.606
0.125	0.625	0.250	293.15	60	0.8166	4.518
0.125	0.625	0.250	293.15	80	0.8252	5.587
0.125	0.625	0.250	293.15	100	0.8329	6.829
0.125	0.625	0.250	303.15	0.1	0.7769	1.758
0.125	0.625	0.250	303.15	20	0.7901	2.326
0.125	0.625	0.250	303.15	40	0.8013	2.939
0.125	0.625	0.250	303.15	60	0.8112	3.649
0.125	0.625	0.250	303.15	80	0.8200	4.458
0.125	0.625	0.250	303.15	100	0.8280	5.368
0.125	0.625	0.250	313.15	0.1	0.7700	1.469
0.125	0.625	0.250	313.15	20	0.7838	1.942
0.125	0.625	0.250	313.15	40	0.7954	2.445
0.125	0.625	0.250	313.15	60	0.8057	3.028
0.125	0.625	0.250	313.15	80	0.8147	3.618
0.125	0.625	0.250	313.15	100	0.8229	4.347
0.125	0.625	0.250	323.15	0.1	0.7629	1.249
0.125	0.625	0.250	323.15	20	0.7774	1.668
0.125	0.625	0.250	323.15	40	0.7896	2.099
0.125	0.625	0.250	323.15	60	0.8002	2.590
0.125	0.625	0.250	323.15	80	0.8097	3.077
0.125	0.625	0.250	323.15	100	0.8182	3.600
0.125	0.625	0.250	333.15	0.1	0.7557	1.077
0.125	0.625	0.250	333.15	20	0.7710	1.437
0.125	0.625	0.250	333.15	40	0.7837	1.789
0.125	0.625	0.250	333.15	60	0.7947	2.186
0.125	0.625	0.250	333.15	80	0.8043	2.622
0.125	0.625	0.250	333.15	100	0.8129	3.092
0.125	0.625	0.250	343.15	0.1	0.7486	0.942
0.125	0.625	0.250	343.15	20	0.7646	1.237
0.125	0.625	0.250	343.15	40	0.7779	1.527
0.125	0.625	0.250	343.15	60	0.7893	1.857
0.125	0.625	0.250	343.15	80	0.7993	2.226
0.125	0.625	0.250	343.15	100	0.8082	2.633
0.125	0.625	0.250	353.15	0.1	0.7414	0.837
0.125	0.625	0.250	353.15	20	0.7583	1.096
0.125	0.625	0.250	353.15	40	0.7721	1.353
0.125	0.625	0.250	353.15	60	0.7840	1.642
0.125	0.625	0.250	353.15	80	0.7943	1.961
0.125	0.625	0.250	353.15	100	0.8035	2.309

Table B1.1 *Continued.*

x_m	x_t	x_h	T [K]	P [MPa]	ρ [g/cm ³]	η [mPa s]
0.125	0.750	0.125	293.15	0.1	0.7800	1.990
0.125	0.750	0.125	293.15	20	0.7924	2.582
0.125	0.750	0.125	293.15	40	0.8032	3.245
0.125	0.750	0.125	293.15	60	0.8127	4.014
0.125	0.750	0.125	293.15	80	0.8213	4.988
0.125	0.750	0.125	293.15	100	0.8291	6.017
0.125	0.750	0.125	303.15	0.1	0.7728	1.642
0.125	0.750	0.125	303.15	20	0.7859	2.159
0.125	0.750	0.125	303.15	40	0.7971	2.685
0.125	0.750	0.125	303.15	60	0.8070	3.288
0.125	0.750	0.125	303.15	80	0.8158	3.966
0.125	0.750	0.125	303.15	100	0.8237	4.690
0.125	0.750	0.125	313.15	0.1	0.7658	1.381
0.125	0.750	0.125	313.15	20	0.7795	1.805
0.125	0.750	0.125	313.15	40	0.7912	2.227
0.125	0.750	0.125	313.15	60	0.8014	2.711
0.125	0.750	0.125	313.15	80	0.8105	3.257
0.125	0.750	0.125	313.15	100	0.8187	3.848
0.125	0.750	0.125	323.15	0.1	0.7586	1.178
0.125	0.750	0.125	323.15	20	0.7730	1.544
0.125	0.750	0.125	323.15	40	0.7852	1.902
0.125	0.750	0.125	323.15	60	0.7958	2.307
0.125	0.750	0.125	323.15	80	0.8053	2.757
0.125	0.750	0.125	323.15	100	0.8138	3.252
0.125	0.750	0.125	333.15	0.1	0.7514	1.017
0.125	0.750	0.125	333.15	20	0.7666	1.311
0.125	0.750	0.125	333.15	40	0.7794	1.617
0.125	0.750	0.125	333.15	60	0.7903	1.966
0.125	0.750	0.125	333.15	80	0.8000	2.356
0.125	0.750	0.125	333.15	100	0.8087	2.801
0.125	0.750	0.125	343.15	0.1	0.7442	0.893
0.125	0.750	0.125	343.15	20	0.7602	1.153
0.125	0.750	0.125	343.15	40	0.7735	1.415
0.125	0.750	0.125	343.15	60	0.7849	1.715
0.125	0.750	0.125	343.15	80	0.7949	2.052
0.125	0.750	0.125	343.15	100	0.8039	2.437
0.125	0.750	0.125	353.15	0.1	0.7370	0.789
0.125	0.750	0.125	353.15	20	0.7538	0.999
0.125	0.750	0.125	353.15	40	0.7677	1.221
0.125	0.750	0.125	353.15	60	0.7795	1.478
0.125	0.750	0.125	353.15	80	0.7899	1.769
0.125	0.750	0.125	353.15	100	0.7991	2.088

Table B1.1 *Continued.*

x_m	x_t	x_h	T [K]	P [MPa]	ρ [g/cm ³]	η [mPa s]
0.250	0.125	0.625	293.15	0.1	0.8146	2.903
0.250	0.125	0.625	293.15	20	0.8269	4.016
0.250	0.125	0.625	293.15	40	0.8376	5.412
0.250	0.125	0.625	293.15	60	0.8470	7.194
0.250	0.125	0.625	293.15	80	0.8555	9.440
0.250	0.125	0.625	293.15	100	0.8631	12.299
0.250	0.125	0.625	303.15	0.1	0.8078	2.333
0.250	0.125	0.625	303.15	20	0.8207	3.197
0.250	0.125	0.625	303.15	40	0.8318	4.254
0.250	0.125	0.625	303.15	60	0.8416	5.608
0.250	0.125	0.625	303.15	80	0.8503	7.320
0.250	0.125	0.625	303.15	100	0.8581	9.405
0.250	0.125	0.625	313.15	0.1	0.8009	1.925
0.250	0.125	0.625	313.15	20	0.8145	2.606
0.250	0.125	0.625	313.15	40	0.8260	3.423
0.250	0.125	0.625	313.15	60	0.8362	4.444
0.250	0.125	0.625	313.15	80	0.8452	5.702
0.250	0.125	0.625	313.15	100	0.8533	7.207
0.250	0.125	0.625	323.15	0.1	0.7940	1.612
0.250	0.125	0.625	323.15	20	0.8083	2.161
0.250	0.125	0.625	323.15	40	0.8203	2.821
0.250	0.125	0.625	323.15	60	0.8308	3.627
0.250	0.125	0.625	323.15	80	0.8401	4.598
0.250	0.125	0.625	323.15	100	0.8485	5.764
0.250	0.125	0.625	333.15	0.1	0.7871	1.376
0.250	0.125	0.625	333.15	20	0.8021	1.861
0.250	0.125	0.625	333.15	40	0.8146	2.388
0.250	0.125	0.625	333.15	60	0.8254	3.028
0.250	0.125	0.625	333.15	80	0.8349	3.795
0.250	0.125	0.625	333.15	100	0.8435	4.728
0.250	0.125	0.625	343.15	0.1	0.7803	1.187
0.250	0.125	0.625	343.15	20	0.7959	1.594
0.250	0.125	0.625	343.15	40	0.8089	2.042
0.250	0.125	0.625	343.15	60	0.8202	2.579
0.250	0.125	0.625	343.15	80	0.8301	3.215
0.250	0.125	0.625	343.15	100	0.8390	3.975
0.250	0.125	0.625	353.15	0.1	0.7732	1.037
0.250	0.125	0.625	353.15	20	0.7897	1.398
0.250	0.125	0.625	353.15	40	0.8033	1.787
0.250	0.125	0.625	353.15	60	0.8150	2.245
0.250	0.125	0.625	353.15	80	0.8252	2.777
0.250	0.125	0.625	353.15	100	0.8343	3.380

Table B1.1 *Continued.*

x_m	x_t	x_h	T [K]	P [MPa]	ρ [g/cm ³]	η [mPa s]
0.250	0.250	0.500	293.15	0.1	0.8110	2.621
0.250	0.250	0.500	293.15	20	0.8233	3.545
0.250	0.250	0.500	293.15	40	0.8340	4.728
0.250	0.250	0.500	293.15	60	0.8435	6.130
0.250	0.250	0.500	293.15	80	0.8520	7.920
0.250	0.250	0.500	293.15	100	0.8597	10.100
0.250	0.250	0.500	303.15	0.1	0.8043	2.122
0.250	0.250	0.500	303.15	20	0.8172	2.867
0.250	0.250	0.500	303.15	40	0.8283	3.730
0.250	0.250	0.500	303.15	60	0.8381	4.799
0.250	0.250	0.500	303.15	80	0.8468	6.102
0.250	0.250	0.500	303.15	100	0.8546	7.674
0.250	0.250	0.500	313.15	0.1	0.7974	1.757
0.250	0.250	0.500	313.15	20	0.8110	2.362
0.250	0.250	0.500	313.15	40	0.8225	3.082
0.250	0.250	0.500	313.15	60	0.8327	3.922
0.250	0.250	0.500	313.15	80	0.8417	4.882
0.250	0.250	0.500	313.15	100	0.8498	5.966
0.250	0.250	0.500	323.15	0.1	0.7904	1.486
0.250	0.250	0.500	323.15	20	0.8047	1.989
0.250	0.250	0.500	323.15	40	0.8168	2.535
0.250	0.250	0.500	323.15	60	0.8273	3.182
0.250	0.250	0.500	323.15	80	0.8365	3.935
0.250	0.250	0.500	323.15	100	0.8449	4.800
0.250	0.250	0.500	333.15	0.1	0.7834	1.272
0.250	0.250	0.500	333.15	20	0.7984	1.701
0.250	0.250	0.500	333.15	40	0.8110	2.161
0.250	0.250	0.500	333.15	60	0.8218	2.703
0.250	0.250	0.500	333.15	80	0.8313	3.331
0.250	0.250	0.500	333.15	100	0.8399	4.051
0.250	0.250	0.500	343.15	0.1	0.7764	1.109
0.250	0.250	0.500	343.15	20	0.7922	1.473
0.250	0.250	0.500	343.15	40	0.8052	1.859
0.250	0.250	0.500	343.15	60	0.8165	2.274
0.250	0.250	0.500	343.15	80	0.8262	2.777
0.250	0.250	0.500	343.15	100	0.8349	3.390
0.250	0.250	0.500	353.15	0.1	0.7693	0.969
0.250	0.250	0.500	353.15	20	0.7858	1.304
0.250	0.250	0.500	353.15	40	0.7995	1.622
0.250	0.250	0.500	353.15	60	0.8112	1.996
0.250	0.250	0.500	353.15	80	0.8213	2.427
0.250	0.250	0.500	353.15	100	0.8303	2.918

Table B1.1 *Continued.*

x_m	x_t	x_h	T [K]	P [MPa]	ρ [g/cm ³]	η [mPa s]
0.250	0.375	0.375	293.15	0.1	0.8089	2.396
0.250	0.375	0.375	293.15	20	0.8212	3.161
0.250	0.375	0.375	293.15	40	0.8319	4.063
0.250	0.375	0.375	293.15	60	0.8414	5.159
0.250	0.375	0.375	293.15	80	0.8498	6.470
0.250	0.375	0.375	293.15	100	0.8575	8.102
0.250	0.375	0.375	303.15	0.1	0.8019	1.959
0.250	0.375	0.375	303.15	20	0.8148	2.622
0.250	0.375	0.375	303.15	40	0.8259	3.358
0.250	0.375	0.375	303.15	60	0.8358	4.239
0.250	0.375	0.375	303.15	80	0.8445	5.277
0.250	0.375	0.375	303.15	100	0.8525	6.487
0.250	0.375	0.375	313.15	0.1	0.7950	1.625
0.250	0.375	0.375	313.15	20	0.8085	2.154
0.250	0.375	0.375	313.15	40	0.8200	2.756
0.250	0.375	0.375	313.15	60	0.8302	3.471
0.250	0.375	0.375	313.15	80	0.8392	4.305
0.250	0.375	0.375	313.15	100	0.8474	5.266
0.250	0.375	0.375	323.15	0.1	0.7879	1.376
0.250	0.375	0.375	323.15	20	0.8021	1.842
0.250	0.375	0.375	323.15	40	0.8142	2.341
0.250	0.375	0.375	323.15	60	0.8247	2.915
0.250	0.375	0.375	323.15	80	0.8339	3.566
0.250	0.375	0.375	323.15	100	0.8422	4.291
0.250	0.375	0.375	333.15	0.1	0.7808	1.182
0.250	0.375	0.375	333.15	20	0.7958	1.560
0.250	0.375	0.375	333.15	40	0.8083	1.967
0.250	0.375	0.375	333.15	60	0.8192	2.433
0.250	0.375	0.375	333.15	80	0.8288	2.958
0.250	0.375	0.375	333.15	100	0.8373	3.542
0.250	0.375	0.375	343.15	0.1	0.7738	1.029
0.250	0.375	0.375	343.15	20	0.7895	1.352
0.250	0.375	0.375	343.15	40	0.8026	1.683
0.250	0.375	0.375	343.15	60	0.8139	2.063
0.250	0.375	0.375	343.15	80	0.8236	2.491
0.250	0.375	0.375	343.15	100	0.8325	2.968
0.250	0.375	0.375	353.15	0.1	0.7666	0.905
0.250	0.375	0.375	353.15	20	0.7831	1.199
0.250	0.375	0.375	353.15	40	0.7968	1.480
0.250	0.375	0.375	353.15	60	0.8085	1.809
0.250	0.375	0.375	353.15	80	0.8187	2.186
0.250	0.375	0.375	353.15	100	0.8278	2.612

Table B1.1 *Continued.*

x_m	x_t	x_h	T [K]	P [MPa]	ρ [g/cm ³]	η [mPa s]
0.250	0.500	0.250	293.15	0.1	0.8059	2.203
0.250	0.500	0.250	293.15	20	0.8182	2.877
0.250	0.500	0.250	293.15	40	0.8289	3.666
0.250	0.500	0.250	293.15	60	0.8384	4.610
0.250	0.500	0.250	293.15	80	0.8468	5.720
0.250	0.500	0.250	293.15	100	0.8545	7.013
0.250	0.500	0.250	303.15	0.1	0.7990	1.805
0.250	0.500	0.250	303.15	20	0.8118	2.357
0.250	0.500	0.250	303.15	40	0.8229	2.980
0.250	0.500	0.250	303.15	60	0.8328	3.710
0.250	0.500	0.250	303.15	80	0.8415	4.550
0.250	0.500	0.250	303.15	100	0.8495	5.505
0.250	0.500	0.250	313.15	0.1	0.7918	1.506
0.250	0.500	0.250	313.15	20	0.8054	1.988
0.250	0.500	0.250	313.15	40	0.8169	2.499
0.250	0.500	0.250	313.15	60	0.8270	3.075
0.250	0.500	0.250	313.15	80	0.8360	3.712
0.250	0.500	0.250	313.15	100	0.8442	4.404
0.250	0.500	0.250	323.15	0.1	0.7847	1.281
0.250	0.500	0.250	323.15	20	0.7989	1.686
0.250	0.500	0.250	323.15	40	0.8110	2.092
0.250	0.500	0.250	323.15	60	0.8216	2.591
0.250	0.500	0.250	323.15	80	0.8309	3.126
0.250	0.500	0.250	323.15	100	0.8394	3.678
0.250	0.500	0.250	333.15	0.1	0.7775	1.107
0.250	0.500	0.250	333.15	20	0.7925	1.449
0.250	0.500	0.250	333.15	40	0.8050	1.783
0.250	0.500	0.250	333.15	60	0.8159	2.167
0.250	0.500	0.250	333.15	80	0.8255	2.600
0.250	0.500	0.250	333.15	100	0.8342	3.082
0.250	0.500	0.250	343.15	0.1	0.7704	0.967
0.250	0.500	0.250	343.15	20	0.7861	1.268
0.250	0.500	0.250	343.15	40	0.7992	1.561
0.250	0.500	0.250	343.15	60	0.8104	1.897
0.250	0.500	0.250	343.15	80	0.8203	2.275
0.250	0.500	0.250	343.15	100	0.8292	2.696
0.250	0.500	0.250	353.15	0.1	0.7631	0.849
0.250	0.500	0.250	353.15	20	0.7797	1.126
0.250	0.500	0.250	353.15	40	0.7933	1.373
0.250	0.500	0.250	353.15	60	0.8051	1.656
0.250	0.500	0.250	353.15	80	0.8152	1.973
0.250	0.500	0.250	353.15	100	0.8243	2.325

Table B1.1 *Continued.*

x_m	x_t	x_h	T [K]	P [MPa]	ρ [g/cm ³]	η [mPa s]
0.250	0.625	0.125	293.15	0.1	0.8033	2.068
0.250	0.625	0.125	293.15	20	0.8155	2.627
0.250	0.625	0.125	293.15	40	0.8261	3.295
0.250	0.625	0.125	293.15	60	0.8356	4.083
0.250	0.625	0.125	293.15	80	0.8441	4.998
0.250	0.625	0.125	293.15	100	0.8519	6.076
0.250	0.625	0.125	303.15	0.1	0.7961	1.728
0.250	0.625	0.125	303.15	20	0.8088	2.150
0.250	0.625	0.125	303.15	40	0.8200	2.668
0.250	0.625	0.125	303.15	60	0.8298	3.267
0.250	0.625	0.125	303.15	80	0.8386	3.949
0.250	0.625	0.125	303.15	100	0.8467	4.685
0.250	0.625	0.125	313.15	0.1	0.7887	1.442
0.250	0.625	0.125	313.15	20	0.8022	1.807
0.250	0.625	0.125	313.15	40	0.8138	2.227
0.250	0.625	0.125	313.15	60	0.8239	2.713
0.250	0.625	0.125	313.15	80	0.8330	3.266
0.250	0.625	0.125	313.15	100	0.8412	3.871
0.250	0.625	0.125	323.15	0.1	0.7814	1.224
0.250	0.625	0.125	323.15	20	0.7956	1.558
0.250	0.625	0.125	323.15	40	0.8077	1.915
0.250	0.625	0.125	323.15	60	0.8183	2.323
0.250	0.625	0.125	323.15	80	0.8276	2.780
0.250	0.625	0.125	323.15	100	0.8360	3.289
0.250	0.625	0.125	333.15	0.1	0.7743	1.052
0.250	0.625	0.125	333.15	20	0.7891	1.346
0.250	0.625	0.125	333.15	40	0.8017	1.651
0.250	0.625	0.125	333.15	60	0.8126	1.998
0.250	0.625	0.125	333.15	80	0.8223	2.385
0.250	0.625	0.125	333.15	100	0.8310	2.825
0.250	0.625	0.125	343.15	0.1	0.7670	0.911
0.250	0.625	0.125	343.15	20	0.7827	1.168
0.250	0.625	0.125	343.15	40	0.7957	1.421
0.250	0.625	0.125	343.15	60	0.8071	1.725
0.250	0.625	0.125	343.15	80	0.8171	2.062
0.250	0.625	0.125	343.15	100	0.8261	2.437
0.250	0.625	0.125	353.15	0.1	0.7597	0.806
0.250	0.625	0.125	353.15	20	0.7762	1.025
0.250	0.625	0.125	353.15	40	0.7899	1.248
0.250	0.625	0.125	353.15	60	0.8016	1.492
0.250	0.625	0.125	353.15	80	0.8118	1.773
0.250	0.625	0.125	353.15	100	0.8210	2.070

Table B1.1 *Continued.*

x_m	x_t	x_h	T [K]	P [MPa]	ρ [g/cm ³]	η [mPa s]
0.375	0.125	0.500	293.15	0.1	0.8353	2.770
0.375	0.125	0.500	293.15	20	0.8473	3.725
0.375	0.125	0.500	293.15	40	0.8579	4.939
0.375	0.125	0.500	293.15	60	0.8672	6.481
0.375	0.125	0.500	293.15	80	0.8756	8.410
0.375	0.125	0.500	293.15	100	0.8832	10.852
0.375	0.125	0.500	303.15	0.1	0.8284	2.232
0.375	0.125	0.500	303.15	20	0.8410	2.995
0.375	0.125	0.500	303.15	40	0.8518	3.892
0.375	0.125	0.500	303.15	60	0.8616	5.019
0.375	0.125	0.500	303.15	80	0.8702	6.416
0.375	0.125	0.500	303.15	100	0.8781	8.077
0.375	0.125	0.500	313.15	0.1	0.8213	1.841
0.375	0.125	0.500	313.15	20	0.8346	2.453
0.375	0.125	0.500	313.15	40	0.8460	3.171
0.375	0.125	0.500	313.15	60	0.8560	4.053
0.375	0.125	0.500	313.15	80	0.8649	5.120
0.375	0.125	0.500	313.15	100	0.8730	6.371
0.375	0.125	0.500	323.15	0.1	0.8143	1.550
0.375	0.125	0.500	323.15	20	0.8283	2.078
0.375	0.125	0.500	323.15	40	0.8402	2.657
0.375	0.125	0.500	323.15	60	0.8506	3.347
0.375	0.125	0.500	323.15	80	0.8598	4.155
0.375	0.125	0.500	323.15	100	0.8681	5.097
0.375	0.125	0.500	333.15	0.1	0.8074	1.325
0.375	0.125	0.500	333.15	20	0.8220	1.745
0.375	0.125	0.500	333.15	40	0.8344	2.218
0.375	0.125	0.500	333.15	60	0.8451	2.771
0.375	0.125	0.500	333.15	80	0.8547	3.408
0.375	0.125	0.500	333.15	100	0.8633	4.155
0.375	0.125	0.500	343.15	0.1	0.8003	1.146
0.375	0.125	0.500	343.15	20	0.8157	1.508
0.375	0.125	0.500	343.15	40	0.8286	1.886
0.375	0.125	0.500	343.15	60	0.8397	2.335
0.375	0.125	0.500	343.15	80	0.8495	2.887
0.375	0.125	0.500	343.15	100	0.8583	3.512
0.375	0.125	0.500	353.15	0.1	0.7933	1.004
0.375	0.125	0.500	353.15	20	0.8095	1.324
0.375	0.125	0.500	353.15	40	0.8229	1.649
0.375	0.125	0.500	353.15	60	0.8344	2.038
0.375	0.125	0.500	353.15	80	0.8444	2.496
0.375	0.125	0.500	353.15	100	0.8534	3.021

Table B1.1 *Continued.*

x_m	x_t	x_h	T [K]	P [MPa]	ρ [g/cm ³]	η [mPa s]
0.375	0.250	0.375	293.15	0.1	0.8331	2.495
0.375	0.250	0.375	293.15	20	0.8451	3.308
0.375	0.250	0.375	293.15	40	0.8557	4.227
0.375	0.250	0.375	293.15	60	0.8650	5.446
0.375	0.250	0.375	293.15	80	0.8734	6.867
0.375	0.250	0.375	293.15	100	0.8811	8.567
0.375	0.250	0.375	303.15	0.1	0.8261	2.028
0.375	0.250	0.375	303.15	20	0.8387	2.680
0.375	0.250	0.375	303.15	40	0.8496	3.436
0.375	0.250	0.375	303.15	60	0.8593	4.336
0.375	0.250	0.375	303.15	80	0.8680	5.391
0.375	0.250	0.375	303.15	100	0.8760	6.612
0.375	0.250	0.375	313.15	0.1	0.8190	1.684
0.375	0.250	0.375	313.15	20	0.8322	2.231
0.375	0.250	0.375	313.15	40	0.8436	2.823
0.375	0.250	0.375	313.15	60	0.8537	3.529
0.375	0.250	0.375	313.15	80	0.8626	4.354
0.375	0.250	0.375	313.15	100	0.8707	5.308
0.375	0.250	0.375	323.15	0.1	0.8119	1.423
0.375	0.250	0.375	323.15	20	0.8258	1.869
0.375	0.250	0.375	323.15	40	0.8377	2.388
0.375	0.250	0.375	323.15	60	0.8480	2.952
0.375	0.250	0.375	323.15	80	0.8573	3.634
0.375	0.250	0.375	323.15	100	0.8656	4.374
0.375	0.250	0.375	333.15	0.1	0.8048	1.221
0.375	0.250	0.375	333.15	20	0.8194	1.597
0.375	0.250	0.375	333.15	40	0.8318	1.986
0.375	0.250	0.375	333.15	60	0.8426	2.440
0.375	0.250	0.375	333.15	80	0.8520	2.961
0.375	0.250	0.375	333.15	100	0.8606	3.552
0.375	0.250	0.375	343.15	0.1	0.7977	1.065
0.375	0.250	0.375	343.15	20	0.8130	1.381
0.375	0.250	0.375	343.15	40	0.8259	1.723
0.375	0.250	0.375	343.15	60	0.8371	2.122
0.375	0.250	0.375	343.15	80	0.8468	2.579
0.375	0.250	0.375	343.15	100	0.8556	3.096
0.375	0.250	0.375	353.15	0.1	0.7905	0.938
0.375	0.250	0.375	353.15	20	0.8066	1.214
0.375	0.250	0.375	353.15	40	0.8200	1.496
0.375	0.250	0.375	353.15	60	0.8316	1.820
0.375	0.250	0.375	353.15	80	0.8418	2.187
0.375	0.250	0.375	353.15	100	0.8508	2.597

Table B1.1 *Continued.*

x_m	x_t	x_h	T [K]	P [MPa]	ρ [g/cm ³]	η [mPa s]
0.375	0.375	0.250	293.15	0.1	0.8307	2.314
0.375	0.375	0.250	293.15	20	0.8427	3.032
0.375	0.375	0.250	293.15	40	0.8532	3.853
0.375	0.375	0.250	293.15	60	0.8626	4.838
0.375	0.375	0.250	293.15	80	0.8710	6.002
0.375	0.375	0.250	293.15	100	0.8786	7.363
0.375	0.375	0.250	303.15	0.1	0.8236	1.886
0.375	0.375	0.250	303.15	20	0.8362	2.477
0.375	0.375	0.250	303.15	40	0.8471	3.110
0.375	0.375	0.250	303.15	60	0.8569	3.866
0.375	0.375	0.250	303.15	80	0.8656	4.752
0.375	0.375	0.250	303.15	100	0.8736	5.780
0.375	0.375	0.250	313.15	0.1	0.8165	1.574
0.375	0.375	0.250	313.15	20	0.8298	2.051
0.375	0.375	0.250	313.15	40	0.8411	2.578
0.375	0.375	0.250	313.15	60	0.8512	3.192
0.375	0.375	0.250	313.15	80	0.8602	3.814
0.375	0.375	0.250	313.15	100	0.8684	4.589
0.375	0.375	0.250	323.15	0.1	0.8093	1.332
0.375	0.375	0.250	323.15	20	0.8232	1.747
0.375	0.375	0.250	323.15	40	0.8351	2.165
0.375	0.375	0.250	323.15	60	0.8456	2.648
0.375	0.375	0.250	323.15	80	0.8548	3.198
0.375	0.375	0.250	323.15	100	0.8632	3.813
0.375	0.375	0.250	333.15	0.1	0.8021	1.149
0.375	0.375	0.250	333.15	20	0.8168	1.490
0.375	0.375	0.250	333.15	40	0.8292	1.836
0.375	0.375	0.250	333.15	60	0.8399	2.238
0.375	0.375	0.250	333.15	80	0.8495	2.696
0.375	0.375	0.250	333.15	100	0.8580	3.211
0.375	0.375	0.250	343.15	0.1	0.7949	1.002
0.375	0.375	0.250	343.15	20	0.8103	1.295
0.375	0.375	0.250	343.15	40	0.8232	1.583
0.375	0.375	0.250	343.15	60	0.8344	1.916
0.375	0.375	0.250	343.15	80	0.8441	2.294
0.375	0.375	0.250	343.15	100	0.8528	2.717
0.375	0.375	0.250	353.15	0.1	0.7878	0.884
0.375	0.375	0.250	353.15	20	0.8039	1.142
0.375	0.375	0.250	353.15	40	0.8173	1.382
0.375	0.375	0.250	353.15	60	0.8289	1.659
0.375	0.375	0.250	353.15	80	0.8391	1.972
0.375	0.375	0.250	353.15	100	0.8482	2.323

Table B1.1 *Continued.*

x_m	x_t	x_h	T [K]	P [MPa]	ρ [g/cm ³]	η [mPa s]
0.375	0.500	0.125	293.15	0.1	0.8287	2.120
0.375	0.500	0.125	293.15	20	0.8408	2.717
0.375	0.500	0.125	293.15	40	0.8512	3.406
0.375	0.500	0.125	293.15	60	0.8606	4.217
0.375	0.500	0.125	293.15	80	0.8691	5.158
0.375	0.500	0.125	293.15	100	0.8769	6.263
0.375	0.500	0.125	303.15	0.1	0.8215	1.741
0.375	0.500	0.125	303.15	20	0.8340	2.212
0.375	0.500	0.125	303.15	40	0.8451	2.740
0.375	0.500	0.125	303.15	60	0.8548	3.348
0.375	0.500	0.125	303.15	80	0.8636	4.035
0.375	0.500	0.125	303.15	100	0.8716	4.771
0.375	0.500	0.125	313.15	0.1	0.8142	1.459
0.375	0.500	0.125	313.15	20	0.8274	1.859
0.375	0.500	0.125	313.15	40	0.8388	2.287
0.375	0.500	0.125	313.15	60	0.8489	2.768
0.375	0.500	0.125	313.15	80	0.8580	3.297
0.375	0.500	0.125	313.15	100	0.8662	3.856
0.375	0.500	0.125	323.15	0.1	0.8068	1.243
0.375	0.500	0.125	323.15	20	0.8207	1.578
0.375	0.500	0.125	323.15	40	0.8326	1.926
0.375	0.500	0.125	323.15	60	0.8431	2.325
0.375	0.500	0.125	323.15	80	0.8525	2.772
0.375	0.500	0.125	323.15	100	0.8609	3.271
0.375	0.500	0.125	333.15	0.1	0.7996	1.078
0.375	0.500	0.125	333.15	20	0.8141	1.374
0.375	0.500	0.125	333.15	40	0.8266	1.676
0.375	0.500	0.125	333.15	60	0.8374	2.024
0.375	0.500	0.125	333.15	80	0.8470	2.416
0.375	0.500	0.125	333.15	100	0.8557	2.867
0.375	0.500	0.125	343.15	0.1	0.7924	0.947
0.375	0.500	0.125	343.15	20	0.8076	1.197
0.375	0.500	0.125	343.15	40	0.8204	1.454
0.375	0.500	0.125	343.15	60	0.8318	1.746
0.375	0.500	0.125	343.15	80	0.8418	2.071
0.375	0.500	0.125	343.15	100	0.8509	2.437
0.375	0.500	0.125	353.15	0.1	0.7849	0.834
0.375	0.500	0.125	353.15	20	0.8011	1.040
0.375	0.500	0.125	353.15	40	0.8145	1.268
0.375	0.500	0.125	353.15	60	0.8262	1.517
0.375	0.500	0.125	353.15	80	0.8363	1.784
0.375	0.500	0.125	353.15	100	0.8454	2.061

Table B1.1 *Continued.*

x_m	x_t	x_h	T [K]	P [MPa]	ρ [g/cm ³]	η [mPa s]
0.500	0.125	0.375	293.15	0.1	0.8602	2.677
0.500	0.125	0.375	293.15	20	0.8719	3.539
0.500	0.125	0.375	293.15	40	0.8823	4.577
0.500	0.125	0.375	293.15	60	0.8915	5.890
0.500	0.125	0.375	293.15	80	0.8999	7.526
0.500	0.125	0.375	293.15	100	0.9075	9.590
0.500	0.125	0.375	303.15	0.1	0.8531	2.161
0.500	0.125	0.375	303.15	20	0.8654	2.840
0.500	0.125	0.375	303.15	40	0.8761	3.637
0.500	0.125	0.375	303.15	60	0.8857	4.618
0.500	0.125	0.375	303.15	80	0.8943	5.807
0.500	0.125	0.375	303.15	100	0.9022	7.187
0.500	0.125	0.375	313.15	0.1	0.8460	1.786
0.500	0.125	0.375	313.15	20	0.8589	2.333
0.500	0.125	0.375	313.15	40	0.8701	2.949
0.500	0.125	0.375	313.15	60	0.8800	3.709
0.500	0.125	0.375	313.15	80	0.8890	4.633
0.500	0.125	0.375	313.15	100	0.8971	5.719
0.500	0.125	0.375	323.15	0.1	0.8389	1.510
0.500	0.125	0.375	323.15	20	0.8525	1.969
0.500	0.125	0.375	323.15	40	0.8641	2.474
0.500	0.125	0.375	323.15	60	0.8744	3.077
0.500	0.125	0.375	323.15	80	0.8836	3.786
0.500	0.125	0.375	323.15	100	0.8920	4.616
0.500	0.125	0.375	333.15	0.1	0.8319	1.294
0.500	0.125	0.375	333.15	20	0.8461	1.673
0.500	0.125	0.375	333.15	40	0.8582	2.081
0.500	0.125	0.375	333.15	60	0.8688	2.561
0.500	0.125	0.375	333.15	80	0.8783	3.115
0.500	0.125	0.375	333.15	100	0.8868	3.767
0.500	0.125	0.375	343.15	0.1	0.8247	1.120
0.500	0.125	0.375	343.15	20	0.8397	1.449
0.500	0.125	0.375	343.15	40	0.8523	1.800
0.500	0.125	0.375	343.15	60	0.8633	2.211
0.500	0.125	0.375	343.15	80	0.8731	2.681
0.500	0.125	0.375	343.15	100	0.8818	3.227
0.500	0.125	0.375	353.15	0.1	0.8176	0.983
0.500	0.125	0.375	353.15	20	0.8332	1.261
0.500	0.125	0.375	353.15	40	0.8464	1.553
0.500	0.125	0.375	353.15	60	0.8577	1.890
0.500	0.125	0.375	353.15	80	0.8677	2.272
0.500	0.125	0.375	353.15	100	0.8767	2.694

Table B1.1 *Continued.*

x_m	x_t	x_h	T [K]	P [MPa]	ρ [g/cm ³]	η [mPa s]
0.500	0.250	0.250	293.15	0.1	0.8581	2.421
0.500	0.250	0.250	293.15	20	0.8699	3.200
0.500	0.250	0.250	293.15	40	0.8802	4.050
0.500	0.250	0.250	293.15	60	0.8895	5.081
0.500	0.250	0.250	293.15	80	0.8978	6.310
0.500	0.250	0.250	293.15	100	0.9055	7.761
0.500	0.250	0.250	303.15	0.1	0.8511	1.977
0.500	0.250	0.250	303.15	20	0.8633	2.596
0.500	0.250	0.250	303.15	40	0.8740	3.261
0.500	0.250	0.250	303.15	60	0.8837	4.047
0.500	0.250	0.250	303.15	80	0.8924	4.959
0.500	0.250	0.250	303.15	100	0.9004	6.005
0.500	0.250	0.250	313.15	0.1	0.8439	1.639
0.500	0.250	0.250	313.15	20	0.8568	2.131
0.500	0.250	0.250	313.15	40	0.8680	2.676
0.500	0.250	0.250	313.15	60	0.8780	3.303
0.500	0.250	0.250	313.15	80	0.8868	4.010
0.500	0.250	0.250	313.15	100	0.8948	4.798
0.500	0.250	0.250	323.15	0.1	0.8368	1.392
0.500	0.250	0.250	323.15	20	0.8503	1.820
0.500	0.250	0.250	323.15	40	0.8619	2.253
0.500	0.250	0.250	323.15	60	0.8723	2.748
0.500	0.250	0.250	323.15	80	0.8815	3.305
0.500	0.250	0.250	323.15	100	0.8899	3.922
0.500	0.250	0.250	333.15	0.1	0.8296	1.195
0.500	0.250	0.250	333.15	20	0.8437	1.545
0.500	0.250	0.250	333.15	40	0.8559	1.897
0.500	0.250	0.250	333.15	60	0.8666	2.298
0.500	0.250	0.250	333.15	80	0.8761	2.747
0.500	0.250	0.250	333.15	100	0.8847	3.243
0.500	0.250	0.250	343.15	0.1	0.8223	1.043
0.500	0.250	0.250	343.15	20	0.8373	1.341
0.500	0.250	0.250	343.15	40	0.8499	1.632
0.500	0.250	0.250	343.15	60	0.8609	1.967
0.500	0.250	0.250	343.15	80	0.8707	2.344
0.500	0.250	0.250	343.15	100	0.8794	2.764
0.500	0.250	0.250	353.15	0.1	0.8152	0.918
0.500	0.250	0.250	353.15	20	0.8307	1.185
0.500	0.250	0.250	353.15	40	0.8439	1.438
0.500	0.250	0.250	353.15	60	0.8554	1.725
0.500	0.250	0.250	353.15	80	0.8655	2.045
0.500	0.250	0.250	353.15	100	0.8746	2.397

Table B1.1 *Continued.*

x_m	x_t	x_h	T [K]	P [MPa]	ρ [g/cm ³]	η [mPa s]
0.500	0.375	0.125	293.15	0.1	0.8565	2.222
0.500	0.375	0.125	293.15	20	0.8682	2.838
0.500	0.375	0.125	293.15	40	0.8786	3.538
0.500	0.375	0.125	293.15	60	0.8879	4.382
0.500	0.375	0.125	293.15	80	0.8963	5.382
0.500	0.375	0.125	293.15	100	0.9041	6.584
0.500	0.375	0.125	303.15	0.1	0.8493	1.818
0.500	0.375	0.125	303.15	20	0.8616	2.285
0.500	0.375	0.125	303.15	40	0.8724	2.826
0.500	0.375	0.125	303.15	60	0.8821	3.456
0.500	0.375	0.125	303.15	80	0.8908	4.176
0.500	0.375	0.125	303.15	100	0.8989	4.958
0.500	0.375	0.125	313.15	0.1	0.8421	1.519
0.500	0.375	0.125	313.15	20	0.8548	1.889
0.500	0.375	0.125	313.15	40	0.8660	2.344
0.500	0.375	0.125	313.15	60	0.8760	2.864
0.500	0.375	0.125	313.15	80	0.8850	3.423
0.500	0.375	0.125	313.15	100	0.8933	3.988
0.500	0.375	0.125	323.15	0.1	0.8347	1.293
0.500	0.375	0.125	323.15	20	0.8481	1.626
0.500	0.375	0.125	323.15	40	0.8598	1.989
0.500	0.375	0.125	323.15	60	0.8702	2.398
0.500	0.375	0.125	323.15	80	0.8794	2.850
0.500	0.375	0.125	323.15	100	0.8879	3.347
0.500	0.375	0.125	333.15	0.1	0.8273	1.115
0.500	0.375	0.125	333.15	20	0.8415	1.415
0.500	0.375	0.125	333.15	40	0.8536	1.721
0.500	0.375	0.125	333.15	60	0.8643	2.068
0.500	0.375	0.125	333.15	80	0.8739	2.455
0.500	0.375	0.125	333.15	100	0.8826	2.895
0.500	0.375	0.125	343.15	0.1	0.8200	0.979
0.500	0.375	0.125	343.15	20	0.8348	1.224
0.500	0.375	0.125	343.15	40	0.8474	1.480
0.500	0.375	0.125	343.15	60	0.8585	1.771
0.500	0.375	0.125	343.15	80	0.8683	2.095
0.500	0.375	0.125	343.15	100	0.8772	2.460
0.500	0.375	0.125	353.15	0.1	0.8125	0.865
0.500	0.375	0.125	353.15	20	0.8283	1.074
0.500	0.375	0.125	353.15	40	0.8414	1.304
0.500	0.375	0.125	353.15	60	0.8528	1.559
0.500	0.375	0.125	353.15	80	0.8629	1.836
0.500	0.375	0.125	353.15	100	0.8720	2.127

Table B1.1 *Continued.*

x_m	x_t	x_h	T [K]	P [MPa]	ρ [g/cm ³]	η [mPa s]
0.625	0.125	0.250	293.15	0.1	0.8873	2.615
0.625	0.125	0.250	293.15	20	0.8986	3.392
0.625	0.125	0.250	293.15	40	0.9088	4.301
0.625	0.125	0.250	293.15	60	0.9178	5.438
0.625	0.125	0.250	293.15	80	0.9261	6.839
0.625	0.125	0.250	293.15	100	0.9337	8.588
0.625	0.125	0.250	303.15	0.1	0.8801	2.113
0.625	0.125	0.250	303.15	20	0.8920	2.724
0.625	0.125	0.250	303.15	40	0.9024	3.434
0.625	0.125	0.250	303.15	60	0.9119	4.285
0.625	0.125	0.250	303.15	80	0.9205	5.286
0.625	0.125	0.250	303.15	100	0.9284	6.410
0.625	0.125	0.250	313.15	0.1	0.8729	1.751
0.625	0.125	0.250	313.15	20	0.8854	2.247
0.625	0.125	0.250	313.15	40	0.8963	2.794
0.625	0.125	0.250	313.15	60	0.9061	3.449
0.625	0.125	0.250	313.15	80	0.9149	4.219
0.625	0.125	0.250	313.15	100	0.9230	5.095
0.625	0.125	0.250	323.15	0.1	0.8657	1.482
0.625	0.125	0.250	323.15	20	0.8788	1.890
0.625	0.125	0.250	323.15	40	0.8902	2.331
0.625	0.125	0.250	323.15	60	0.9003	2.848
0.625	0.125	0.250	323.15	80	0.9094	3.446
0.625	0.125	0.250	323.15	100	0.9177	4.134
0.625	0.125	0.250	333.15	0.1	0.8585	1.268
0.625	0.125	0.250	333.15	20	0.8723	1.622
0.625	0.125	0.250	333.15	40	0.8841	1.990
0.625	0.125	0.250	333.15	60	0.8945	2.417
0.625	0.125	0.250	333.15	80	0.9039	2.903
0.625	0.125	0.250	333.15	100	0.9123	3.466
0.625	0.125	0.250	343.15	0.1	0.8516	1.100
0.625	0.125	0.250	343.15	20	0.8659	1.389
0.625	0.125	0.250	343.15	40	0.8783	1.693
0.625	0.125	0.250	343.15	60	0.8891	2.042
0.625	0.125	0.250	343.15	80	0.8988	2.435
0.625	0.125	0.250	343.15	100	0.9076	2.885
0.625	0.125	0.250	353.15	0.1	0.8443	0.967
0.625	0.125	0.250	353.15	20	0.8595	1.216
0.625	0.125	0.250	353.15	40	0.8723	1.483
0.625	0.125	0.250	353.15	60	0.8835	1.775
0.625	0.125	0.250	353.15	80	0.8934	2.088
0.625	0.125	0.250	353.15	100	0.9024	2.412

Table B1.1 *Continued.*

x_m	x_t	x_h	T [K]	P [MPa]	ρ [g/cm ³]	η [mPa s]
0.625	0.250	0.125	293.15	0.1	0.8862	2.381
0.625	0.250	0.125	293.15	20	0.8976	3.027
0.625	0.250	0.125	293.15	40	0.9077	3.766
0.625	0.250	0.125	293.15	60	0.9168	4.638
0.625	0.250	0.125	293.15	80	0.9251	5.647
0.625	0.250	0.125	293.15	100	0.9328	6.971
0.625	0.250	0.125	303.15	0.1	0.8789	1.938
0.625	0.250	0.125	303.15	20	0.8908	2.440
0.625	0.250	0.125	303.15	40	0.9012	3.002
0.625	0.250	0.125	303.15	60	0.9107	3.668
0.625	0.250	0.125	303.15	80	0.9193	4.442
0.625	0.250	0.125	303.15	100	0.9272	5.298
0.625	0.250	0.125	313.15	0.1	0.8716	1.646
0.625	0.250	0.125	313.15	20	0.8841	2.029
0.625	0.250	0.125	313.15	40	0.8950	2.485
0.625	0.250	0.125	313.15	60	0.9047	3.016
0.625	0.250	0.125	313.15	80	0.9136	3.621
0.625	0.250	0.125	313.15	100	0.9216	4.284
0.625	0.250	0.125	323.15	0.1	0.8643	1.374
0.625	0.250	0.125	323.15	20	0.8774	1.712
0.625	0.250	0.125	323.15	40	0.8887	2.082
0.625	0.250	0.125	323.15	60	0.8989	2.512
0.625	0.250	0.125	323.15	80	0.9080	3.005
0.625	0.250	0.125	323.15	100	0.9164	3.566
0.625	0.250	0.125	333.15	0.1	0.8569	1.178
0.625	0.250	0.125	333.15	20	0.8706	1.466
0.625	0.250	0.125	333.15	40	0.8825	1.774
0.625	0.250	0.125	333.15	60	0.8930	2.131
0.625	0.250	0.125	333.15	80	0.9023	2.537
0.625	0.250	0.125	333.15	100	0.9108	3.008
0.625	0.250	0.125	343.15	0.1	0.8496	1.029
0.625	0.250	0.125	343.15	20	0.8640	1.256
0.625	0.250	0.125	343.15	40	0.8763	1.509
0.625	0.250	0.125	343.15	60	0.8872	1.799
0.625	0.250	0.125	343.15	80	0.8968	2.123
0.625	0.250	0.125	343.15	100	0.9056	2.490
0.625	0.250	0.125	353.15	0.1	0.8422	0.907
0.625	0.250	0.125	353.15	20	0.8573	1.109
0.625	0.250	0.125	353.15	40	0.8702	1.339
0.625	0.250	0.125	353.15	60	0.8814	1.594
0.625	0.250	0.125	353.15	80	0.8915	1.871
0.625	0.250	0.125	353.15	100	0.9005	2.161

Table B1.1 *Continued.*

x_m	x_t	x_h	T [K]	P [MPa]	ρ [g/cm ³]	η [mPa s]
0.750	0.125	0.125	293.15	0.1	0.9222	2.624
0.750	0.125	0.125	293.15	20	0.9332	3.321
0.750	0.125	0.125	293.15	40	0.9431	4.127
0.750	0.125	0.125	293.15	60	0.9520	5.108
0.750	0.125	0.125	293.15	80	0.9601	6.283
0.750	0.125	0.125	293.15	100	0.9677	7.774
0.750	0.125	0.125	303.15	0.1	0.9149	2.135
0.750	0.125	0.125	303.15	20	0.9264	2.663
0.750	0.125	0.125	303.15	40	0.9366	3.254
0.750	0.125	0.125	303.15	60	0.9459	3.980
0.750	0.125	0.125	303.15	80	0.9543	4.855
0.750	0.125	0.125	303.15	100	0.9621	5.899
0.750	0.125	0.125	313.15	0.1	0.9076	1.765
0.750	0.125	0.125	313.15	20	0.9196	2.192
0.750	0.125	0.125	313.15	40	0.9302	2.667
0.750	0.125	0.125	313.15	60	0.9398	3.228
0.750	0.125	0.125	313.15	80	0.9485	3.876
0.750	0.125	0.125	313.15	100	0.9564	4.618
0.750	0.125	0.125	323.15	0.1	0.9003	1.490
0.750	0.125	0.125	323.15	20	0.9128	1.864
0.750	0.125	0.125	323.15	40	0.9239	2.248
0.750	0.125	0.125	323.15	60	0.9339	2.700
0.750	0.125	0.125	323.15	80	0.9428	3.186
0.750	0.125	0.125	323.15	100	0.9511	3.768
0.750	0.125	0.125	333.15	0.1	0.8930	1.273
0.750	0.125	0.125	333.15	20	0.9061	1.569
0.750	0.125	0.125	333.15	40	0.9176	1.901
0.750	0.125	0.125	333.15	60	0.9279	2.254
0.750	0.125	0.125	333.15	80	0.9371	2.705
0.750	0.125	0.125	333.15	100	0.9456	3.200
0.750	0.125	0.125	343.15	0.1	0.8856	1.106
0.750	0.125	0.125	343.15	20	0.8994	1.383
0.750	0.125	0.125	343.15	40	0.9113	1.668
0.750	0.125	0.125	343.15	60	0.9220	1.971
0.750	0.125	0.125	343.15	80	0.9315	2.284
0.750	0.125	0.125	343.15	100	0.9402	2.629
0.750	0.125	0.125	353.15	0.1	0.8782	0.965
0.750	0.125	0.125	353.15	20	0.8926	1.220
0.750	0.125	0.125	353.15	40	0.9051	1.447
0.750	0.125	0.125	353.15	60	0.9161	1.696
0.750	0.125	0.125	353.15	80	0.9259	1.964
0.750	0.125	0.125	353.15	100	0.9349	2.248

Table B1.1 *Continued.*

B2 Measured Densities of Ternary Mixtures

Density		T [K]						
[g/cm ³]		293.15	303.15	313.15	323.15	333.15	343.15	353.15
P [MPa]	0.1	0.7964	0.7895	0.7827	0.7759	0.7691	0.7621	0.7552
	5	0.7997	0.7930	0.7863	0.7798	0.7732	0.7665	0.7598
	10	0.8030	0.7964	0.7900	0.7835	0.7772	0.7707	0.7642
	15	0.8060	0.7996	0.7933	0.7871	0.7809	0.7746	0.7683
	20	0.8089	0.8027	0.7965	0.7905	0.7844	0.7783	0.7721
	25	0.8118	0.8056	0.7996	0.7937	0.7878	0.7818	0.7759
	30	0.8145	0.8085	0.8026	0.7968	0.7911	0.7851	0.7794
	35	0.8172	0.8113	0.8055	0.7998	0.7942	0.7884	0.7828
	40	0.8197	0.8139	0.8083	0.8027	0.7972	0.7915	0.7860
	45	0.8222	0.8166	0.8109	0.8055	0.8000	0.7945	0.7891
	50	0.8246	0.8189	0.8135	0.8081	0.8028	0.7973	0.7921
	55	0.8270	0.8214	0.8160	0.8108	0.8055	0.8002	0.7950
	60	0.8292	0.8238	0.8184	0.8133	0.8081	0.8029	0.7977

Table B2.1 Density versus temperature T and pressure P for the ternary mixture 1-methylnaphthalene (m) + n-tridecane (t) + 2,2,4,4,6,8,8-heptamethylnonane (h) with the mole fraction: $x_m = 0.125$, $x_t = 0.125$, and $x_h = 0.750$.

Density		T [K]						
[g/cm ³]		293.15	303.15	313.15	323.15	333.15	343.15	353.15
P [MPa]	0.1	0.7936	0.7870	0.7802	0.7732	0.7663	0.7593	0.7523
	5	0.7969	0.7904	0.7839	0.7771	0.7704	0.7636	0.7569
	10	0.8001	0.7938	0.7874	0.7808	0.7744	0.7678	0.7613
	15	0.8032	0.7970	0.7907	0.7843	0.7781	0.7717	0.7654
	20	0.8061	0.8002	0.7940	0.7877	0.7816	0.7755	0.7692
	25	0.8090	0.8031	0.7971	0.7909	0.7850	0.7790	0.7730
	30	0.8117	0.8059	0.8001	0.7941	0.7883	0.7823	0.7764
	35	0.8144	0.8087	0.8029	0.7970	0.7914	0.7856	0.7798
	40	0.8169	0.8114	0.8057	0.7999	0.7943	0.7887	0.7830
	45	0.8194	0.8140	0.8083	0.8027	0.7972	0.7916	0.7861
	50	0.8218	0.8164	0.8110	0.8054	0.8000	0.7945	0.7891
	55	0.8242	0.8189	0.8135	0.8080	0.8027	0.7973	0.7920
	60	0.8264	0.8213	0.8159	0.8105	0.8053	0.8000	0.7948

Table B2.2 Density versus temperature T and pressure P for the ternary mixture 1-methylnaphthalene (m) + n-tridecane (t) + 2,2,4,4,6,8,8-heptamethylnonane (h) with the mole fraction: $x_m = 0.125$, $x_t = 0.250$, and $x_h = 0.625$.

Density		T [K]						
[g/cm ³]		293.15	303.15	313.15	323.15	333.15	343.15	353.15
P [MPa]	0.1	0.7903	0.7833	0.7764	0.7695	0.7625	0.7554	0.7484
	5	0.7936	0.7868	0.7800	0.7733	0.7666	0.7598	0.7531
	10	0.7968	0.7902	0.7836	0.7770	0.7705	0.7639	0.7574
	15	0.7998	0.7934	0.7870	0.7806	0.7743	0.7678	0.7615
	20	0.8027	0.7965	0.7902	0.7840	0.7778	0.7716	0.7654
	25	0.8056	0.7994	0.7933	0.7871	0.7811	0.7751	0.7691
	30	0.8083	0.8023	0.7963	0.7903	0.7844	0.7784	0.7726
	35	0.8110	0.8050	0.7992	0.7933	0.7875	0.7817	0.7759
	40	0.8135	0.8076	0.8019	0.7961	0.7905	0.7848	0.7792
	45	0.8160	0.8103	0.8046	0.7990	0.7933	0.7877	0.7823
	50	0.8184	0.8127	0.8072	0.8016	0.7961	0.7906	0.7853
	55	0.8207	0.8152	0.8097	0.8043	0.7988	0.7935	0.7882
	60	0.8230	0.8176	0.8121	0.8068	0.8014	0.7961	0.7910

Table B2.3 Density versus temperature T and pressure P for the ternary mixture 1-methylnaphthalene (m) + n-tridecane (t) + 2,2,4,4,6,8,8-heptamethylnonane (h) with the mole fraction: $x_m = 0.125$, $x_t = 0.375$, and $x_h = 0.500$.

Density		T [K]						
[g/cm ³]		293.15	303.15	313.15	323.15	333.15	343.15	353.15
P [MPa]	0.1	0.7872	0.7805	0.7736	0.7666	0.7595	0.7524	0.7453
	5	0.7906	0.7839	0.7772	0.7704	0.7636	0.7567	0.7498
	10	0.7937	0.7873	0.7807	0.7741	0.7675	0.7609	0.7542
	15	0.7967	0.7905	0.7841	0.7777	0.7713	0.7647	0.7583
	20	0.7997	0.7936	0.7874	0.7811	0.7748	0.7685	0.7622
	25	0.8026	0.7966	0.7905	0.7842	0.7782	0.7720	0.7659
	30	0.8053	0.7994	0.7934	0.7873	0.7814	0.7754	0.7694
	35	0.8079	0.8022	0.7963	0.7903	0.7845	0.7786	0.7727
	40	0.8105	0.8048	0.7990	0.7932	0.7875	0.7817	0.7759
	45	0.8130	0.8075	0.8017	0.7960	0.7904	0.7847	0.7790
	50	0.8155	0.8099	0.8043	0.7986	0.7932	0.7875	0.7821
	55	0.8178	0.8124	0.8068	0.8012	0.7958	0.7904	0.7849
	60	0.8201	0.8148	0.8093	0.8038	0.7985	0.7930	0.7877

Table B2.4 Density versus temperature T and pressure P for the ternary mixture 1-methylnaphthalene (m) + n-tridecane (t) + 2,2,4,4,6,8,8-heptamethylnonane (h) with the mole fraction: $x_m = 0.125$, $x_t = 0.500$, and $x_h = 0.375$.

Density		<i>T</i> [K]						
[g/cm ³]		293.15	303.15	313.15	323.15	333.15	343.15	353.15
<i>P</i> [MPa]	0.1	0.7839	0.7769	0.7700	0.7629	0.7557	0.7486	0.7414
	5	0.7871	0.7804	0.7736	0.7668	0.7598	0.7529	0.7459
	10	0.7903	0.7838	0.7771	0.7705	0.7637	0.7570	0.7503
	15	0.7933	0.7870	0.7804	0.7740	0.7674	0.7609	0.7543
	20	0.7963	0.7901	0.7838	0.7774	0.7710	0.7646	0.7583
	25	0.7992	0.7930	0.7868	0.7806	0.7744	0.7682	0.7620
	30	0.8019	0.7959	0.7898	0.7837	0.7776	0.7715	0.7655
	35	0.8046	0.7986	0.7927	0.7867	0.7807	0.7747	0.7688
	40	0.8071	0.8013	0.7954	0.7896	0.7837	0.7779	0.7721
	45	0.8096	0.8040	0.7981	0.7924	0.7866	0.7808	0.7752
	50	0.8120	0.8064	0.8007	0.7950	0.7894	0.7838	0.7783
	55	0.8143	0.8089	0.8032	0.7977	0.7921	0.7866	0.7811
	60	0.8166	0.8112	0.8057	0.8002	0.7947	0.7893	0.7840

Table B2.5 Density versus temperature *T* and pressure *P* for the ternary mixture 1-methylnaphthalene (m) + n-tridecane (t) + 2,2,4,4,6,8,8-heptamethylnonane (h) with the mole fraction: $x_m = 0.125$, $x_t = 0.625$, and $x_h = 0.250$.

Density		<i>T</i> [K]						
[g/cm ³]		293.15	303.15	313.15	323.15	333.15	343.15	353.15
<i>P</i> [MPa]	0.1	0.7800	0.7728	0.7658	0.7586	0.7514	0.7442	0.7370
	5	0.7833	0.7763	0.7693	0.7624	0.7555	0.7484	0.7415
	10	0.7864	0.7797	0.7729	0.7661	0.7594	0.7526	0.7458
	15	0.7895	0.7829	0.7762	0.7696	0.7631	0.7565	0.7499
	20	0.7924	0.7859	0.7795	0.7730	0.7666	0.7602	0.7538
	25	0.7952	0.7888	0.7825	0.7762	0.7700	0.7637	0.7576
	30	0.7980	0.7917	0.7855	0.7793	0.7733	0.7670	0.7611
	35	0.8006	0.7944	0.7884	0.7823	0.7764	0.7704	0.7644
	40	0.8032	0.7971	0.7912	0.7852	0.7794	0.7735	0.7677
	45	0.8057	0.7997	0.7938	0.7880	0.7822	0.7765	0.7708
	50	0.8081	0.8022	0.7964	0.7907	0.7851	0.7793	0.7738
	55	0.8104	0.8046	0.7989	0.7934	0.7878	0.7822	0.7767
	60	0.8127	0.8070	0.8014	0.7958	0.7903	0.7849	0.7795

Table B2.6 Density versus temperature *T* and pressure *P* for the ternary mixture 1-methylnaphthalene (m) + n-tridecane (t) + 2,2,4,4,6,8,8-heptamethylnonane (h) with the mole fraction: $x_m = 0.125$, $x_t = 0.750$, and $x_h = 0.125$.

Density		<i>T</i> [K]						
[g/cm ³]		293.15	303.15	313.15	323.15	333.15	343.15	353.15
<i>P</i> [MPa]	0.1	0.8146	0.8078	0.8009	0.7940	0.7871	0.7803	0.7732
	5	0.8179	0.8112	0.8046	0.7978	0.7911	0.7843	0.7776
	10	0.8210	0.8145	0.8080	0.8014	0.7949	0.7884	0.7819
	15	0.8240	0.8176	0.8113	0.8049	0.7986	0.7922	0.7859
	20	0.8269	0.8207	0.8145	0.8083	0.8021	0.7959	0.7897
	25	0.8298	0.8236	0.8176	0.8114	0.8054	0.7994	0.7934
	30	0.8324	0.8265	0.8205	0.8145	0.8086	0.8027	0.7968
	35	0.8351	0.8292	0.8233	0.8174	0.8116	0.8059	0.8001
	40	0.8376	0.8318	0.8260	0.8203	0.8146	0.8089	0.8033
	45	0.8400	0.8344	0.8287	0.8231	0.8175	0.8119	0.8064
	50	0.8425	0.8368	0.8313	0.8257	0.8202	0.8147	0.8094
	55	0.8448	0.8392	0.8337	0.8283	0.8228	0.8176	0.8122
	60	0.8470	0.8416	0.8362	0.8308	0.8254	0.8202	0.8150

Table B2.7 Density versus temperature *T* and pressure *P* for the ternary mixture 1-methylnaphthalene (m) + n-tridecane (t) + 2,2,4,4,6,8,8-heptamethylnonane (h) with the mole fraction: $x_m = 0.250$, $x_t = 0.125$, and $x_h = 0.625$.

Density		<i>T</i> [K]						
[g/cm ³]		293.15	303.15	313.15	323.15	333.15	343.15	353.15
<i>P</i> [MPa]	0.1	0.8110	0.8043	0.7974	0.7904	0.7834	0.7764	0.7693
	5	0.8143	0.8077	0.8010	0.7942	0.7874	0.7806	0.7738
	10	0.8174	0.8110	0.8045	0.7979	0.7913	0.7847	0.7781
	15	0.8204	0.8142	0.8077	0.8014	0.7950	0.7885	0.7820
	20	0.8233	0.8172	0.8110	0.8047	0.7984	0.7922	0.7858
	25	0.8262	0.8201	0.8140	0.8079	0.8017	0.7956	0.7895
	30	0.8288	0.8230	0.8169	0.8109	0.8049	0.7989	0.7930
	35	0.8315	0.8256	0.8198	0.8139	0.8080	0.8021	0.7962
	40	0.8340	0.8283	0.8225	0.8168	0.8110	0.8052	0.7995
	45	0.8364	0.8309	0.8252	0.8195	0.8139	0.8081	0.8025
	50	0.8389	0.8333	0.8277	0.8221	0.8166	0.8110	0.8055
	55	0.8412	0.8357	0.8302	0.8247	0.8192	0.8138	0.8084
	60	0.8435	0.8381	0.8327	0.8273	0.8218	0.8165	0.8112

Table B2.8 Density versus temperature *T* and pressure *P* for the ternary mixture 1-methylnaphthalene (m) + n-tridecane (t) + 2,2,4,4,6,8,8-heptamethylnonane (h) with the mole fraction: $x_m = 0.250$, $x_t = 0.250$, and $x_h = 0.500$.

Density		<i>T</i> [K]						
[g/cm ³]		293.15	303.15	313.15	323.15	333.15	343.15	353.15
<i>P</i> [MPa]	0.1	0.8089	0.8019	0.7950	0.7879	0.7808	0.7738	0.7666
	5	0.8122	0.8053	0.7985	0.7917	0.7849	0.7780	0.7711
	10	0.8153	0.8087	0.8020	0.7953	0.7887	0.7820	0.7753
	15	0.8183	0.8118	0.8053	0.7988	0.7923	0.7859	0.7794
	20	0.8212	0.8148	0.8085	0.8021	0.7958	0.7895	0.7831
	25	0.8240	0.8177	0.8116	0.8053	0.7991	0.7930	0.7868
	30	0.8267	0.8206	0.8145	0.8084	0.8023	0.7963	0.7903
	35	0.8293	0.8233	0.8173	0.8113	0.8054	0.7995	0.7936
	40	0.8319	0.8259	0.8200	0.8142	0.8083	0.8026	0.7968
	45	0.8343	0.8285	0.8227	0.8169	0.8112	0.8055	0.7998
	50	0.8368	0.8309	0.8253	0.8196	0.8140	0.8084	0.8028
	55	0.8391	0.8334	0.8278	0.8222	0.8166	0.8112	0.8057
	60	0.8414	0.8358	0.8302	0.8247	0.8192	0.8139	0.8085

Table B2.9 Density versus temperature *T* and pressure *P* for the ternary mixture 1-methylnaphthalene (m) + n-tridecane (t) + 2,2,4,4,6,8,8-heptamethylnonane (h) with the mole fraction: $x_m = 0.250$, $x_t = 0.375$, and $x_h = 0.375$.

Density		<i>T</i> [K]						
[g/cm ³]		293.15	303.15	313.15	323.15	333.15	343.15	353.15
<i>P</i> [MPa]	0.1	0.8059	0.7990	0.7918	0.7847	0.7775	0.7704	0.7631
	5	0.8092	0.8023	0.7955	0.7885	0.7815	0.7745	0.7676
	10	0.8123	0.8056	0.7989	0.7921	0.7853	0.7786	0.7718
	15	0.8153	0.8087	0.8021	0.7956	0.7890	0.7824	0.7759
	20	0.8182	0.8118	0.8054	0.7989	0.7925	0.7861	0.7797
	25	0.8210	0.8147	0.8084	0.8021	0.7957	0.7895	0.7834
	30	0.8237	0.8175	0.8114	0.8052	0.7990	0.7929	0.7868
	35	0.8263	0.8203	0.8142	0.8081	0.8021	0.7961	0.7901
	40	0.8289	0.8229	0.8169	0.8110	0.8050	0.7992	0.7933
	45	0.8313	0.8255	0.8196	0.8138	0.8079	0.8021	0.7964
	50	0.8338	0.8279	0.8221	0.8165	0.8107	0.8049	0.7994
	55	0.8361	0.8303	0.8246	0.8191	0.8133	0.8078	0.8023
	60	0.8384	0.8328	0.8270	0.8216	0.8159	0.8104	0.8051

Table B2.10 Density versus temperature *T* and pressure *P* for the ternary mixture 1-methylnaphthalene (m) + n-tridecane (t) + 2,2,4,4,6,8,8-heptamethylnonane (h) with the mole fraction: $x_m = 0.250$, $x_t = 0.500$, and $x_h = 0.250$.

Density		T [K]						
[g/cm ³]		293.15	303.15	313.15	323.15	333.15	343.15	353.15
P [MPa]	0.1	0.8033	0.7961	0.7887	0.7814	0.7743	0.7670	0.7597
	5	0.8065	0.7994	0.7923	0.7852	0.7782	0.7711	0.7642
	10	0.8096	0.8027	0.7957	0.7889	0.7820	0.7752	0.7684
	15	0.8126	0.8058	0.7990	0.7923	0.7857	0.7791	0.7724
	20	0.8155	0.8088	0.8022	0.7956	0.7891	0.7827	0.7762
	25	0.8182	0.8118	0.8052	0.7988	0.7925	0.7861	0.7799
	30	0.8210	0.8146	0.8082	0.8019	0.7957	0.7895	0.7834
	35	0.8236	0.8173	0.8111	0.8049	0.7987	0.7927	0.7867
	40	0.8261	0.8200	0.8138	0.8077	0.8017	0.7957	0.7899
	45	0.8286	0.8226	0.8165	0.8105	0.8046	0.7987	0.7929
	50	0.8310	0.8250	0.8190	0.8132	0.8074	0.8016	0.7960
	55	0.8333	0.8274	0.8215	0.8158	0.8100	0.8044	0.7988
	60	0.8356	0.8298	0.8239	0.8183	0.8126	0.8071	0.8016

Table B2.11 Density versus temperature T and pressure P for the ternary mixture 1-methylnaphthalene (m) + n-tridecane (t) + 2,2,4,4,6,8,8-heptamethylnonane (h) with the mole fraction: $x_m = 0.250$, $x_t = 0.625$, and $x_h = 0.125$.

Density		T [K]						
[g/cm ³]		293.15	303.15	313.15	323.15	333.15	343.15	353.15
P [MPa]	0.1	0.8353	0.8284	0.8213	0.8143	0.8074	0.8003	0.7933
	5	0.8385	0.8316	0.8248	0.8181	0.8113	0.8044	0.7976
	10	0.8415	0.8349	0.8283	0.8216	0.8150	0.8084	0.8018
	15	0.8445	0.8380	0.8315	0.8250	0.8186	0.8121	0.8057
	20	0.8473	0.8410	0.8346	0.8283	0.8220	0.8157	0.8095
	25	0.8501	0.8438	0.8376	0.8314	0.8252	0.8191	0.8131
	30	0.8527	0.8466	0.8405	0.8344	0.8284	0.8224	0.8165
	35	0.8553	0.8492	0.8433	0.8373	0.8314	0.8255	0.8197
	40	0.8579	0.8518	0.8460	0.8402	0.8344	0.8286	0.8229
	45	0.8603	0.8544	0.8486	0.8429	0.8372	0.8315	0.8259
	50	0.8627	0.8568	0.8511	0.8455	0.8399	0.8343	0.8288
	55	0.8649	0.8592	0.8536	0.8481	0.8425	0.8371	0.8316
	60	0.8672	0.8616	0.8560	0.8506	0.8451	0.8397	0.8344

Table B2.12 Density versus temperature T and pressure P for the ternary mixture 1-methylnaphthalene (m) + n-tridecane (t) + 2,2,4,4,6,8,8-heptamethylnonane (h) with the mole fraction: $x_m = 0.375$, $x_t = 0.125$, and $x_h = 0.500$.

Density		T [K]						
[g/cm ³]		293.15	303.15	313.15	323.15	333.15	343.15	353.15
P [MPa]	0.1	0.8331	0.8261	0.8190	0.8119	0.8048	0.7977	0.7905
	5	0.8363	0.8294	0.8225	0.8156	0.8087	0.8018	0.7949
	10	0.8393	0.8326	0.8259	0.8191	0.8124	0.8057	0.7990
	15	0.8423	0.8356	0.8291	0.8225	0.8160	0.8095	0.8029
	20	0.8451	0.8387	0.8322	0.8258	0.8194	0.8130	0.8066
	25	0.8479	0.8415	0.8352	0.8289	0.8227	0.8164	0.8103
	30	0.8506	0.8443	0.8381	0.8319	0.8258	0.8197	0.8136
	35	0.8531	0.8470	0.8409	0.8348	0.8288	0.8229	0.8169
	40	0.8557	0.8496	0.8436	0.8377	0.8318	0.8259	0.8200
	45	0.8581	0.8522	0.8462	0.8404	0.8346	0.8288	0.8231
	50	0.8605	0.8545	0.8488	0.8430	0.8373	0.8317	0.8260
	55	0.8628	0.8570	0.8512	0.8456	0.8400	0.8344	0.8289
	60	0.8650	0.8593	0.8537	0.8480	0.8426	0.8371	0.8316

Table B2.13 Density versus temperature T and pressure P for the ternary mixture 1-methylnaphthalene (m) + n-tridecane (t) + 2,2,4,4,6,8,8-heptamethylnonane (h) with the mole fraction: $x_m = 0.375$, $x_t = 0.250$, and $x_h = 0.375$.

Density		T [K]						
[g/cm ³]		293.15	303.15	313.15	323.15	333.15	343.15	353.15
P [MPa]	0.1	0.8307	0.8236	0.8165	0.8093	0.8021	0.7949	0.7878
	5	0.8339	0.8269	0.8200	0.8130	0.8061	0.7990	0.7921
	10	0.8369	0.8301	0.8234	0.8165	0.8098	0.8030	0.7963
	15	0.8398	0.8332	0.8266	0.8200	0.8134	0.8067	0.8001
	20	0.8427	0.8362	0.8298	0.8232	0.8168	0.8103	0.8039
	25	0.8455	0.8391	0.8327	0.8263	0.8201	0.8137	0.8075
	30	0.8481	0.8418	0.8356	0.8294	0.8232	0.8170	0.8108
	35	0.8507	0.8445	0.8384	0.8323	0.8262	0.8201	0.8141
	40	0.8532	0.8471	0.8411	0.8351	0.8292	0.8232	0.8173
	45	0.8556	0.8497	0.8438	0.8379	0.8320	0.8261	0.8203
	50	0.8580	0.8522	0.8463	0.8405	0.8347	0.8289	0.8233
	55	0.8603	0.8545	0.8488	0.8431	0.8374	0.8318	0.8261
	60	0.8626	0.8569	0.8512	0.8456	0.8399	0.8344	0.8289

Table B2.14 Density versus temperature T and pressure P for the ternary mixture 1-methylnaphthalene (m) + n-tridecane (t) + 2,2,4,4,6,8,8-heptamethylnonane (h) with the mole fraction: $x_m = 0.375$, $x_t = 0.375$, and $x_h = 0.250$.

Density		T [K]						
[g/cm ³]		293.15	303.15	313.15	323.15	333.15	343.15	353.15
P [MPa]	0.1	0.8287	0.8215	0.8142	0.8068	0.7996	0.7924	0.7849
	5	0.8318	0.8248	0.8176	0.8105	0.8035	0.7964	0.7893
	10	0.8349	0.8280	0.8210	0.8141	0.8072	0.8003	0.7934
	15	0.8379	0.8310	0.8243	0.8174	0.8107	0.8041	0.7973
	20	0.8408	0.8340	0.8274	0.8207	0.8141	0.8076	0.8011
	25	0.8435	0.8370	0.8304	0.8238	0.8174	0.8110	0.8047
	30	0.8462	0.8397	0.8333	0.8269	0.8206	0.8143	0.8082
	35	0.8487	0.8424	0.8361	0.8298	0.8236	0.8175	0.8114
	40	0.8512	0.8451	0.8388	0.8326	0.8266	0.8204	0.8145
	45	0.8537	0.8476	0.8414	0.8354	0.8293	0.8234	0.8176
	50	0.8561	0.8500	0.8440	0.8380	0.8322	0.8263	0.8206
	55	0.8584	0.8524	0.8464	0.8406	0.8348	0.8291	0.8234
	60	0.8606	0.8548	0.8489	0.8431	0.8374	0.8318	0.8262

Table B2.15 Density versus temperature T and pressure P for the ternary mixture 1-methylnaphthalene (m) + n-tridecane (t) + 2,2,4,4,6,8,8-heptamethylnonane (h) with the mole fraction: $x_m = 0.375$, $x_t = 0.500$, and $x_h = 0.125$.

Density		T [K]						
[g/cm ³]		293.15	303.15	313.15	323.15	333.15	343.15	353.15
P [MPa]	0.1	0.8602	0.8531	0.8460	0.8389	0.8319	0.8247	0.8176
	5	0.8633	0.8563	0.8494	0.8426	0.8357	0.8287	0.8217
	10	0.8662	0.8594	0.8527	0.8460	0.8393	0.8325	0.8258
	15	0.8691	0.8625	0.8558	0.8493	0.8428	0.8362	0.8296
	20	0.8719	0.8654	0.8589	0.8525	0.8461	0.8397	0.8332
	25	0.8746	0.8682	0.8618	0.8555	0.8493	0.8430	0.8367
	30	0.8772	0.8709	0.8647	0.8585	0.8524	0.8462	0.8401
	35	0.8798	0.8736	0.8674	0.8614	0.8553	0.8493	0.8433
	40	0.8823	0.8761	0.8701	0.8641	0.8582	0.8523	0.8464
	45	0.8846	0.8787	0.8727	0.8668	0.8610	0.8551	0.8493
	50	0.8870	0.8810	0.8752	0.8694	0.8637	0.8579	0.8522
	55	0.8893	0.8834	0.8776	0.8720	0.8663	0.8607	0.8550
	60	0.8915	0.8857	0.8800	0.8744	0.8688	0.8633	0.8577

Table B2.16 Density versus temperature T and pressure P for the ternary mixture 1-methylnaphthalene (m) + n-tridecane (t) + 2,2,4,4,6,8,8-heptamethylnonane (h) with the mole fraction: $x_m = 0.500$, $x_t = 0.125$, and $x_h = 0.375$.

Density		T [K]						
[g/cm ³]		293.15	303.15	313.15	323.15	333.15	343.15	353.15
P [MPa]	0.1	0.8581	0.8511	0.8439	0.8368	0.8296	0.8223	0.8152
	5	0.8612	0.8542	0.8473	0.8403	0.8333	0.8263	0.8193
	10	0.8642	0.8574	0.8506	0.8438	0.8370	0.8301	0.8233
	15	0.8670	0.8604	0.8537	0.8471	0.8404	0.8338	0.8271
	20	0.8699	0.8633	0.8568	0.8503	0.8437	0.8373	0.8307
	25	0.8726	0.8661	0.8597	0.8533	0.8469	0.8406	0.8342
	30	0.8752	0.8689	0.8626	0.8563	0.8501	0.8438	0.8376
	35	0.8777	0.8714	0.8654	0.8592	0.8530	0.8469	0.8408
	40	0.8802	0.8740	0.8680	0.8619	0.8559	0.8499	0.8439
	45	0.8826	0.8766	0.8706	0.8647	0.8587	0.8528	0.8469
	50	0.8850	0.8790	0.8731	0.8673	0.8614	0.8555	0.8498
	55	0.8873	0.8814	0.8755	0.8698	0.8640	0.8583	0.8527
	60	0.8895	0.8837	0.8780	0.8723	0.8666	0.8609	0.8554

Table B2.17 Density versus temperature T and pressure P for the ternary mixture 1-methylnaphthalene (m) + n-tridecane (t) + 2,2,4,4,6,8,8-heptamethylnonane (h) with the mole fraction: $x_m = 0.500$, $x_t = 0.250$, and $x_h = 0.250$.

Density		T [K]						
[g/cm ³]		293.15	303.15	313.15	323.15	333.15	343.15	353.15
P [MPa]	0.1	0.8565	0.8493	0.8421	0.8347	0.8273	0.8200	0.8125
	5	0.8595	0.8525	0.8454	0.8382	0.8310	0.8239	0.8168
	10	0.8625	0.8556	0.8486	0.8417	0.8347	0.8277	0.8208
	15	0.8654	0.8586	0.8518	0.8450	0.8381	0.8314	0.8245
	20	0.8682	0.8616	0.8548	0.8481	0.8415	0.8348	0.8283
	25	0.8708	0.8644	0.8577	0.8512	0.8447	0.8381	0.8317
	30	0.8736	0.8671	0.8607	0.8542	0.8478	0.8414	0.8351
	35	0.8760	0.8698	0.8633	0.8571	0.8508	0.8445	0.8383
	40	0.8786	0.8724	0.8660	0.8598	0.8536	0.8474	0.8414
	45	0.8810	0.8749	0.8686	0.8625	0.8564	0.8503	0.8444
	50	0.8833	0.8773	0.8712	0.8652	0.8591	0.8531	0.8473
	55	0.8857	0.8797	0.8736	0.8677	0.8618	0.8558	0.8501
	60	0.8879	0.8821	0.8760	0.8702	0.8643	0.8585	0.8528

Table B2.18 Density versus temperature T and pressure P for the ternary mixture 1-methylnaphthalene (m) + n-tridecane (t) + 2,2,4,4,6,8,8-heptamethylnonane (h) with the mole fraction: $x_m = 0.500$, $x_t = 0.375$, and $x_h = 0.125$.

Density		<i>T</i> [K]						
[g/cm ³]		293.15	303.15	313.15	323.15	333.15	343.15	353.15
<i>P</i> [MPa]	0.1	0.8873	0.8801	0.8729	0.8657	0.8585	0.8516	0.8443
	5	0.8902	0.8832	0.8762	0.8691	0.8622	0.8553	0.8484
	10	0.8931	0.8862	0.8794	0.8725	0.8657	0.8591	0.8522
	15	0.8959	0.8892	0.8824	0.8757	0.8691	0.8626	0.8559
	20	0.8986	0.8920	0.8854	0.8788	0.8723	0.8659	0.8595
	25	0.9013	0.8947	0.8883	0.8818	0.8754	0.8691	0.8629
	30	0.9038	0.8974	0.8910	0.8846	0.8784	0.8723	0.8661
	35	0.9063	0.8999	0.8937	0.8875	0.8813	0.8753	0.8693
	40	0.9088	0.9024	0.8963	0.8902	0.8841	0.8783	0.8723
	45	0.9111	0.9050	0.8989	0.8928	0.8868	0.8810	0.8753
	50	0.9134	0.9073	0.9013	0.8953	0.8895	0.8838	0.8781
	55	0.9157	0.9097	0.9037	0.8979	0.8920	0.8865	0.8809
	60	0.9178	0.9119	0.9061	0.9003	0.8945	0.8891	0.8835

Table B2.19 Density versus temperature *T* and pressure *P* for the ternary mixture 1-methylnaphthalene (m) + n-tridecane (t) + 2,2,4,4,6,8,8-heptamethylnonane (h) with the mole fraction: $x_m = 0.625$, $x_t = 0.125$, and $x_h = 0.250$.

Density		<i>T</i> [K]						
[g/cm ³]		293.15	303.15	313.15	323.15	333.15	343.15	353.15
<i>P</i> [MPa]	0.1	0.8862	0.8789	0.8716	0.8643	0.8569	0.8496	0.8422
	5	0.8892	0.8820	0.8748	0.8677	0.8605	0.8534	0.8462
	10	0.8921	0.8850	0.8780	0.8710	0.8640	0.8571	0.8501
	15	0.8949	0.8880	0.8811	0.8742	0.8674	0.8606	0.8537
	20	0.8976	0.8908	0.8841	0.8774	0.8706	0.8640	0.8573
	25	0.9002	0.8935	0.8869	0.8803	0.8737	0.8672	0.8607
	30	0.9028	0.8962	0.8897	0.8832	0.8768	0.8703	0.8640
	35	0.9053	0.8987	0.8924	0.8860	0.8797	0.8733	0.8671
	40	0.9077	0.9012	0.8950	0.8887	0.8825	0.8763	0.8702
	45	0.9100	0.9037	0.8976	0.8914	0.8852	0.8791	0.8731
	50	0.9124	0.9061	0.9000	0.8939	0.8879	0.8819	0.8760
	55	0.9146	0.9085	0.9024	0.8965	0.8905	0.8846	0.8787
	60	0.9168	0.9107	0.9047	0.8989	0.8930	0.8872	0.8814

Table B2.20 Density versus temperature *T* and pressure *P* for the ternary mixture 1-methylnaphthalene (m) + n-tridecane (t) + 2,2,4,4,6,8,8-heptamethylnonane (h) with the mole fraction: $x_m = 0.625$, $x_t = 0.250$, and $x_h = 0.125$.

Density		T [K]						
[g/cm ³]		293.15	303.15	313.15	323.15	333.15	343.15	353.15
P [MPa]	0.1	0.9222	0.9149	0.9076	0.9003	0.8930	0.8856	0.8782
	5	0.9251	0.9179	0.9107	0.9036	0.8965	0.8892	0.8820
	10	0.9279	0.9208	0.9138	0.9067	0.8998	0.8927	0.8857
	15	0.9306	0.9236	0.9167	0.9098	0.9030	0.8961	0.8892
	20	0.9332	0.9264	0.9196	0.9128	0.9061	0.8994	0.8926
	25	0.9358	0.9290	0.9224	0.9157	0.9091	0.9025	0.8959
	30	0.9383	0.9316	0.9251	0.9185	0.9120	0.9055	0.8991
	35	0.9407	0.9342	0.9277	0.9212	0.9149	0.9084	0.9021
	40	0.9431	0.9366	0.9302	0.9239	0.9176	0.9113	0.9051
	45	0.9454	0.9391	0.9327	0.9265	0.9203	0.9140	0.9080
	50	0.9477	0.9413	0.9351	0.9290	0.9229	0.9168	0.9108
	55	0.9499	0.9436	0.9375	0.9314	0.9254	0.9194	0.9135
	60	0.9520	0.9459	0.9398	0.9339	0.9279	0.9220	0.9161

Table B2.21 Density versus temperature T and pressure P for the ternary mixture 1-methylnaphthalene (m) + n-tridecane (t) + 2,2,4,4,6,8,8-heptamethylnonane (h) with the mole fraction: $x_m = 0.750$, $x_t = 0.125$, and $x_h = 0.125$.

APPENDIX C

C1 Selected Articles in International Journals

Canet X, Daugé P., Baylaucq A., Boned C., Zéberg-Mikkelsen C.K., Quiñones-Cisneros S.E., and Stenby E.H.: *Density and Viscosity of the 1-Methylnaphthalene + 2,2,4,4,6,8,8-Heptamethylnonane System up to 100 MPa*. International Journal of Thermophysics. **22** (2001) 1669 – 1689.

Quiñones-Cisneros S.E., Zéberg-Mikkelsen C.K., and Stenby E.H.: *The Friction Theory (f-theory) for Viscosity Modeling*. Fluid Phase Equilibria. **169** (2000) 249 – 276.

Quiñones-Cisneros S.E., Zéberg-Mikkelsen C.K., and Stenby E.H.: *One Parameter Friction Theory Models for Viscosity*. Fluid Phase Equilibria. **178** (2001) 1 – 16.

Quiñones-Cisneros S.E., Zéberg-Mikkelsen C.K., and Stenby E.H.: *The Friction Theory for Viscosity Modeling: Extension to Crude Oil Systems*. Chemical Engineering Science. **56** (2001) 7007 – 7015.

Quiñones-Cisneros S.E., Zéberg-Mikkelsen C.K., and Stenby E.H.: *Accurate Density and Viscosity Modeling of Non-Polar Fluids Based on the “f-theory” and a Non-Cubic EOS*. Paper presented at the Fourteenth Symposium on Thermophysical Properties, (June 25 – 30, 2000), Boulder, Colorado, USA. International Journal of Thermophysics. **23** (2002) 41 – 55.

Zéberg-Mikkelsen C.K., Quiñones-Cisneros S.E., and Stenby E.H.: *Viscosity Prediction of Hydrogen + Natural Gas Mixtures (Hythane)*. Industrial & Engineering Chemistry Research. **40** (2001) 2966 - 2970.

Zéberg-Mikkelsen C.K., Quiñones-Cisneros S.E., and Stenby E.H.: *Viscosity Modeling of Light Gases at Supercritical Conditions Using the Friction Theory*. Industrial & Engineering Chemistry Research. **40** (2001) 3848 – 3854.

Zéberg-Mikkelsen C.K., Quiñones-Cisneros S.E., and Stenby E.H.: *Viscosity Prediction of Hydrocarbon Mixtures Based on the Friction Theory*. Petroleum Science and Technology. **19** (2001) 899 – 909.

Zéberg-Mikkelsen C.K., Canet X., Baylaucq A., Quiñones-Cisneros S.E., Boned C., and Stenby E.H.: *High Pressure Viscosity and Density Behavior of Ternary Mixtures: 1-Methylnaphthalene + n-Tridecane + 2,2,4,4,6,8,8-Heptamethylnonane*. International Journal of Thermophysics. **22** (2001) 1691 – 1726.

Zéberg-Mikkelsen C.K., Canet X., Quinones-Cisneros S.E., Baylaucq A., Allal A., Boned C., and Stenby E.H.: *Viscosity Modeling of the Ternary System 1-Methylnaphthalene + n-Tridecane + 2,2,4,4,6,8,8-Heptamethylnonane up to 100 MPa*. High Pressure Research. **21** (2001) 281 – 303.

Zéberg-Mikkelsen C.K., Quiñones-Cisneros S.E., and Stenby E.H.: *Viscosity Prediction of Carbon Dioxide + Hydrocarbon Mixtures Using the Friction Theory*. Petroleum Science and Technology. **20** (2002) 27 – 42.

Zéberg-Mikkelsen C.K., Quiñones-Cisneros S.E., and Stenby E.H.: *Viscosity Modeling of Associating Fluids Based on the Friction Theory: Pure Alcohols*. Presented at PPEPPD 2001, Ninth International Conference on Properties and Phase Equilibria for Product and Process Design, (May 20 – 25, 2001), Kurashiki, Japan. Fluid Phase Equilibria **194-197** (2002) 1191 – 1203.

Zéberg-Mikkelsen C.K., Quiñones-Cisneros S.E., and Stenby E.H.: *Viscosity Prediction of Natural Gas Using the Friction Theory*. International Journal of Thermophysics. **23** (2002) 437 – 454.